



**FRANCISCO ANTONIO MARTINS**

**FLUORINE EFFECTS ON STRUCTURAL, PHYSICAL,  
BIOLOGICAL, AND AGROCHEMICAL PROPERTIES OF  
ORGANOFLUORINE COMPOUNDS**

**LAVRAS-MG  
2022**

**FRANCISCO ANTONIO MARTINS**

**FLUORINE EFFECTS ON STRUCTURAL, PHYSICAL, BIOLOGICAL, AND  
AGROCHEMICAL PROPERTIES OF ORGANOFLUORINE COMPOUNDS**

Tese apresentada à Universidade Federal de Lavras, como parte das exigências do Programa de Pós-Graduação em Agroquímica, área de concentração em Química/Bioquímica, para obter o título de doutor.

Prof. Dr. Matheus Puggina de Freitas

Orientador

**LAVRAS-MG  
2022**

**Ficha catalográfica elaborada pelo Sistema de Geração de Ficha Catalográfica da Biblioteca Universitária da UFLA, com dados informados pelo(a) próprio(a) autor(a).**

Martins, Francisco Antonio.

Fluorine Effects on Structural, Physical, Biological, and Agrochemical Properties of Organofluorine Compounds / Francisco Antonio Martins. - 2022.

245 p.: il.

Orientador: Matheus Puggina Freitas.

Tese (doutorado) - Universidade Federal de Lavras, 2022.  
Bibliografia.

1. Organofluorados. 2. Modelagem Molecular. 3.  
Estereoquímica. I. Freitas, Matheus Puggina. II. Título.

**FRANCISCO ANTONIO MARTINS**

**FLUORINE EFFECTS ON STRUCTURAL, PHYSICAL, BIOLOGICAL, AND AGROCHEMICAL PROPERTIES OF ORGANOFLUORINE COMPOUNDS**

**EFEITOS DO FLÚOR SOBRE PROPRIEDADES ESTRUTURAIS, FÍSICAS, BIOLÓGICAS E AGROQUÍMICAS DE COMPOSTOS ORGANOFLUORADOS**

Tese apresentada à Universidade Federal de Lavras, como parte das exigências do Programa de Pós-Graduação em Agroquímica, área de concentração em Química/Bioquímica, para obter o título de doutor.

APROVADA em 21 de julho de 2022.

Dr. Cláudio Francisco Tormena

UNICAMP

Dr. Daniel Henriques Soares Leal

UNIFEI

Dr. Sérgio Scherrer Thomasi

UFLA

Dr. Teodorico de Castro Ramalho

UFLA

Prof. Dr. Matheus Puggina de Freitas

Orientador

**LAVRAS-MG  
2022**

## **AGRADECIMENTOS**

À Universidade Federal de Lavras, em especial ao Departamento de Química (DQI), pela oportunidade.

À Coordenação de Aperfeiçoamento de Pessoal de Nível Superior – CAPES (código de financiamento: 001), pela concessão da bolsa de doutorado. À FAPEMIG e ao CNPq, pelo apoio financeiro.

Ao professor doutor Matheus Puggina de Freitas, pela valiosa orientação, paciência e grande disposição e por ser uma pessoa incrível tanto profissional quanto pessoal.

A todos os funcionários do Departamento de Química e da UFLA.

A todos os meus amigos, em especial ao Douglas, Denissander, Caio, Gabriel, Wallace, Joyce e Felipe pelo grande apoio e disposição durante vários anos.

Aos meus pais, Rogério e Ana Paula, pelo suporte de todos esses anos. Aos meus irmãos, Leonardo, Lucas e Gabriel.

À Margarida por ser uma pessoa incrível e fascinante que sempre acreditou e incentivou, genuinamente, a perseguir meus objetivos.

À Ana Fávaro, por todo amor, companheirismo, paciência e apoio em todos os momentos dessa minha jornada.

O presente trabalho foi realizado com apoio da Coordenação de Aperfeiçoamento de Pessoal de Nível Superior – Brasil (CAPES) – Código de Financiamento 001

## RESUMO

Estereoquímica é uma importante área da química orgânica, pois a estrutura das moléculas rege propriedades biológicas, físico-químicas e espectroscópicas, além da reatividade dos compostos orgânicos. O isomerismo conformacional, um aspecto da análise conformacional e, consequentemente, da estereoquímica, é regido por fatores clássicos (estéricos e eletrostáticos) e não clássicos (deslocalização eletrônica). Conhecer esses fatores permite o controle conformacional de compostos orgânicos, de modo a otimizar condições reacionais, respostas biológicas e propriedades de materiais. O átomo de flúor possui características estruturais peculiares e também induz efeitos conformacionais já bem estabelecidos, como o efeito *gauche*. A introdução do átomo de flúor em uma molécula é, portanto, uma estratégia única de controle conformacional e os organofluorados são uma classe de compostos orgânicos com aplicações em várias áreas da ciência. Neste trabalho, explorou-se, teórica e experimentalmente, a influência de átomos de flúor sobre as características químicas, físicas e biológicas de alguns sistemas, dado que esse elemento pode ser usado para o aprimoramento de propriedades desejadas em sistemas de interesse. O trabalho foi dividido em duas partes. 1<sup>a)</sup>) Impacto nas características estereoeletrônicas e controle conformacional: estudo do efeito *gauche* em 2-halofluoroetanos e 2-haloetanóis, expandindo para compostos contendo átomo de iodo, dado que efeitos conformacionais para sistemas contendo este elemento não são amplamente explorados. Além disso, o átomo de flúor pode estabelecer efeito *gauche* eletrostático com o átomo de fósforo, à semelhança do que tem sido observado em sais sulfônicos, por isso, um estudo de moléculas  $\beta$ -fluoroetil-fosforadas também foi realizado. 2<sup>a)</sup>) Impacto em propriedades biológicas: foi avaliado o efeito da substituição de átomos de cloro por átomos de flúor em pesticidas organoclorados de uso na agricultura, visto que a ligação C–F gera características desejadas (maior polaridade, ligação geralmente mais estável e menor potencial de bioacumulação). Além disso, foi analisada a influência de efeitos estereoeletrônicos sobre a conformação e coeficiente de partição sangue/gás — um importante parâmetro utilizado para previsão da absorção de fármacos pelo organismo — de anestésicos inalatórios fluorados; sabe-se que características estereoeletrônicas são diretamente relacionadas ao momento dipolar, e este, por sua vez, responsável pela permeação através da membrana celular. Cálculos teóricos foram conduzidos com base nos métodos pós Hartree-Fock (MP2) e teoria do funcional de densidade (DFT). Difração de raio-X também foi empregada. Na segunda parte, a técnica de docking foi empregada para predição de energias e modos de interação de ligantes e proteínas. Foi possível observar que a presença de átomos de flúor permite modular as preferências conformacionais de compostos e, além disso, o flúor promove o efeito *gauche* eletrostático quando está vicinal a átomos de fósforo parcialmente carregados. Ainda na segunda parte, uma importante observação é que a substituição bioisostérica de cloro por flúor aumenta as características desejáveis em compostos com aplicação imediata, como pesticidas, devido à maior polaridade e estabilidade da ligação C–F comparada à ligação C–Cl, bem como à diminuição da lipofilicidade, parâmetro que indica o potencial de bioacumulação nos organismos. Finalmente, foi demonstrada a dependência do coeficiente de partição de anestésicos fluorados com momento dipolar dos confôrmeros mais estáveis das moléculas.

**Palavras-chave:** Química Computacional. Modulação Conformacional. Efeitos Conformatonais. Moléculas de Alta Performance. Sistemas Biológicos.

## ABSTRACT

Stereochemistry is an important area of organic chemistry since the molecular structure rules biological, physicochemical, and spectroscopic properties, besides the reactivity of organic compounds. The conformational isomerism, an aspect of conformational analysis and, therefore, of the stereochemistry field, is ruled by classical (steric and electrostatic) and nonclassical effects (electron delocalization). The knowledge of these factors allows for the conformational control of organic compounds to optimize reaction conditions, biological responses, and material properties. The fluorine atom has unique structural and induces well-known conformational effects, such as the *gauche* effect. Therefore, the fluorine introduction in a molecule is a pivotal strategy for conformational control, and the organofluorine is a chemical class with application in a variety of science fields. In this work, we exploited the impact on chemical, physical and biological characteristics at the molecular level caused by the introduction of fluorine atoms, both theoretically and experimentally, since this element can be used to improve key features in specific systems. This work is divided into two parts. 1<sup>st</sup>) Impact on stereoelectronic features and conformational control: a study of the *gauche* effect in 2-halofluoroethanes and 2-haloethanols, expanding to iodine compounds, since conformational effects involving iodine have not been explored in details. In addition, the fluorine atom can establish an electrostatic *gauche* effect with phosphorus, similar to that found in  $\beta$ -fluoroethyl sulfonium motifs. For this reason, some  $\beta$ -fluoroethyl-phosphorus compounds were also studied. 2<sup>nd</sup>) Impact on biological properties: the replacement of chlorine with fluorine atoms in pesticide molecules with agricultural application was evaluated, since C–F bonds bring desirable features (more polar and, generally, stable bonds, with a lesser propensity to bioaccumulation). Also, inhalational fluorinated anesthetics were further studied to gain insight into the influence of stereoelectronic effects on the conformation and, subsequently, in the gas/blood partition coefficient of these compounds — it is known that the partition coefficient is an important parameter used to predict drug absorption through the body. Stereoelectronic features are directly related to the molecular dipolar moment, which is responsible for the permeation of the drugs throughout the cell membrane. Theoretical calculations based on the post Hartree-Fock method (MP2) and density functional theory (DFT) were performed. X-ray diffraction was also used. In the second part, the docking technique was carried out to predict energies and binding modes of ligand-protein interactions. It was observed that the fluorine atom modulates the conformational preferences of organic compounds. In addition, fluorine provides an electrostatic *gauche* effect when it is in a vicinal position to a partially charged phosphorus atom. Also in the second part, an important finding is that the bioisosteric replacement of chlorine with fluorine improves desirable features in compounds with an application, such as pesticides. This is due to the higher polarity and stability of the C–F bond compared to C–Cl, besides the decrease in lipophilicity, a parameter used as an indication of bioaccumulation in the body. Finally, we demonstrated the dependence of the partition coefficient and dipolar moment of the most stable conformers of volatile fluorinated anesthetics.

**Keywords:** Computational Chemistry. Conformational Modulation. Conformational Effects. High-performance Molecules. Biological Systems.

## LIST OF FIGURES

Figure 1 – Conformational equilibrium of monosubstituted six-membered rings (upper) and preference for equatorial conformation when R = <i>t</i> -Bu group (lower).....	11
Figure 2 – Conformational equilibria dictated by electrostatic interactions.....	11
Figure 3 – The preference for the <i>syn</i> -axial conformer ( <i>Rabbit-ear</i> effect representation on the left bottom). The preference for axial conformer ( <i>Anomeric</i> effect representation on the right upper).....	11
Figure 4 – Conformational equilibrium of a 1,2-disubstituted ethane indicating the <i>gauche</i> effect, even being disfavored by classical parameters (top); stabilizing antiperiplanar $\sigma_{\text{C-H}} \rightarrow \sigma^*_{\text{C-X}}$ interaction (bottom).....	12
Figure 5 – Electrostatic <i>gauche</i> effect between fluorine and a positively charged ammonium group.....	13
Figure 6 – Dihedral angle $\theta$ formed by four atoms and three bonds.....	16
Figure 7 – Potential energy curve of the butane at HF/3-21G level of theory.....	16
Figure 8 – Ring interconversion in cyclohexane showing the axial-equatorial interplay of hydrogens.....	17
Figure 9 – a) $\gamma$ - <i>gauche</i> repulsion in a monosubstituted six-membered ring; b) 1,3-diaxial repulsion in a monosubstituted six-membered ring.....	17
Figure 10 – Orthoester bond formation promoted by a nucleophile capable to establish the reverse anomeric effect.....	19
Figure 11 – Organochlorine pesticides (for X = Cl) and bioisostERICALLY-replaced fluorinated derivatives (for X = F).....	21
Figure 12 – The <i>gauche</i> effect between fluorine and sulfur in a F-C-C-S motif.....	23
Figure 13 – $\beta$ -fluorinated organophosphorus models proposed for conformational studies.....	24
Figure 14 – Competition between two stabilizing stereoelectronic effects in 1-Fluoro-2-iodoethane.....	26
Figure 15 – The precession movement (represented by the blue curve) of a nucleus with a magnetic moment ( $\mu$ ) submitted to an external magnetic field ( $B_0$ ).....	27
Figure 16 – Longitudinal and transverse magnetization (upper) and transverse relaxation (lower).....	28
Figure 17 – The relationship between coupling constant ( ${}^3J_{\text{H,H}}$ ) and the H-C-C-H dihedral angle established by Martin Karplus.....	29
Figure 18 – Interactions considered in a molecule by a Force Field.....	36

## SUMMARY

FIRST PART.....	10
1 INTRODUCTION.....	10
2 THEORETICAL FRAMEWORK.....	15
2.1 Conformational Analysis and Tools.....	15
2.1.1 Basic Concepts.....	15
2.1.2 The Fluorine Chemistry.....	19
2.1.3 The Phosphorus Chemistry.....	21
2.1.4 The Iodine Chemistry.....	24
2.2 Spectroscopic Methods of Conformational and Structural Determination.....	26
2.2.1 Nuclear Magnetic Resonance Spectroscopy.....	26
2.2.2 X-Ray Crystallography.....	30
2.3 Quantum Mechanics Computational Methods.....	31
2.3.1 Methods Based on Wavefunction.....	31
2.3.2 Methods Based on Electron Density.....	33
2.4 Molecular Mechanics Methods.....	35
2.4.1 Docking.....	36
REFERENCES.....	38
SECOND PART .....	47
Stereoelectronic Impact of Fluorine.....	47
Paper 1 – The fluorine <i>gauche</i> effect and a comparison with other halogens in 2-halofluoroethanes and 2-haloethanols.....	48
Paper 2 – Theoretical and X-ray evidence of electrostatic phosphonium <i>anti</i> and <i>gauche</i> effects.....	60
Biological Impact of Fluorine.....	75
Paper 3 – Theoretical study of fluorinated bioisosteres of organochlorine compounds as effective and eco-friendly pesticides.....	76
Paper 4 – Theoretical exploitation of 1,2,3,4,5,6-hexachloro- and 1,2,3,4,5,6-hexafluorocyclohexane isomers as biologically active compounds.....	90
Paper 5 – An examination of the relationship between molecular dipole moment and blood-gas partition for common anaesthetic gases.....	108
APPENDIX A – Supporting Information for: The fluorine <i>gauche</i> effect and a comparison with other halogens in 2-halofluoroethanes and 2-haloethanols....	120

APPENDIX B – Supporting Information for: Theoretical and X-ray evidence of electrostatic phosphonium <i>anti</i> and <i>gauche</i> effects.....	150
APPENDIX C – Supporting Information for: Theoretical study of fluorinated bioisosteres of organochlorine compounds as effective and eco-friendly pesticides....	195
APPENDIX D – Supporting Information for: Theoretical exploitation of 1,2,3,4,5,6-hexachloro- and 1,2,3,4,5,6-hexafluorocyclohexane isomers as biologically active compounds.....	201
APPENDIX E – Supporting Information for: An examination of the relationship between molecular dipole moment and blood-gas partition for common anaesthetic gases.....	226

## FIRST PART

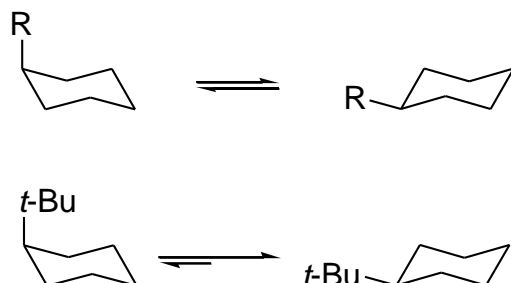
### 1 Introduction

The tridimensional features of a molecule within the stereochemistry field play a central role in organic chemistry since they explain macroscopic properties, reactivity, biological responses, and others (DESLONGCHAMPS, 1975; EVIDENTE; ANDOLFI; CIMMINO, 2011; HIRST *et al.*, 2004). The stereochemistry is divided into some branch fields, and among them is the conformational analysis. In conformational analysis, molecules are studied under the point of view of single bond rotations, in which each step in the rotation around a single bond gives a different shape in space, named conformation. Its stability is attributed to classical – steric and electrostatic – or non-classical effects – electron delocalization. Over the years, the importance of molecular conformation and its impact in miscellaneous areas of science, *e.g.* synthesis, catalysis, materials, and pharmaceuticals have become clear (LAI *et al.*, 2015; MOITESSIER; ENGLEBIENNE; CHAPLEUR, 2005; TANG *et al.*, 2010; ZHANG *et al.*, 2014; ZIMMER; SPARR; GILMOUR, 2011). Therefore, a deep knowledge of conformational stabilities and the factors that rule the conformational preferences are fundamental.

The recent development in conformational analysis and computational chemistry has allowed us to understand the driving effects ruling the molecular shape and provide means to control the molecular conformation and modulate the molecular properties for a given purpose. A classic example relates to the *t*-butyl group. The well-understood conformational isomerism of monosubstituted cyclohexanes is practically represented by two main conformers: the equatorial and axial (Figure 1). Interestingly, when the substituent group is *t*-butyl, the equatorial conformer is highly preferred with a  $\Delta G = 4.9 \text{ kcal mol}^{-1}$  (ANTÚNEZ; JUARISTI, 1996; ELIEL, 1965). The reason for such a preference is explained in classical terms – steric repulsion is smaller when *t*-butyl group adopts the equatorial position. This effect is well known, and the *t*-butyl is used as a lock group in six-membered rings. Conformational modulation can also be done by electrostatic features, in which opposite charges attract each other, and identical charges repel one another (Figure 2). However, after the findings by Pophristic and Goodman (2001), it becomes clear that electron delocalization (a non-classic factor) is also important in some systems. When the preference for certain conformations cannot be fully explained by classical terms, some assumptions for conformational effects arise, such as the *anomeric*, *rabbit-ear*, and *gauche* effects, see Figure 3 (GOODMAN; GU;

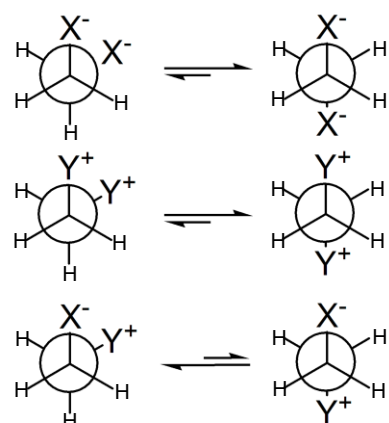
POPHRISTIC, 2005; HUTCHINS; KOPP; ELIEL, 1968; WOLFE; WHANGBO; MITCHELL, 1979). The last one is one of the focuses of this thesis.

Figure 1 — Conformational equilibrium of monosubstituted six-membered rings (upper) and preference for equatorial conformation when R = *t*-Bu group (lower).



Source: from the Author (2022)

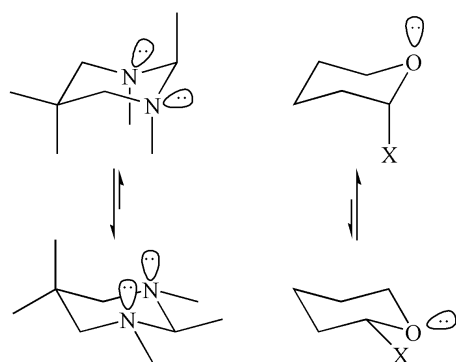
Figure 2 — Conformational equilibria dictated by electrostatic interactions.



Legend: X = negatively charged group and Y = positively charged group.

Source: from the Author (2022)

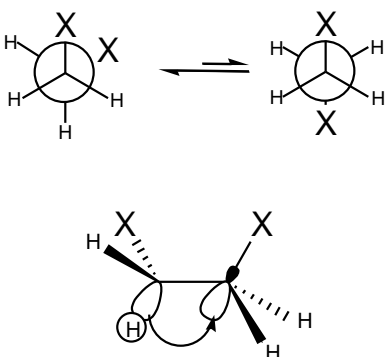
Figure 3 — The preference for the *syn*-axial conformer (*Rabbit-ear* effect representation on the left bottom). The preference for axial conformer (*Anomeric* effect representation on the right upper).



Source: from the Author (2022)

The *gauche* effect is “a tendency to adopt that structure which has the maximum number of *gauche* interactions between the adjacent electron pairs and/or polar bonds” (WOLFE, 1972). This counter-intuitive tendency can be observed in Figure 4, where electronegative X groups should repel each other, but the *gauche* conformation predominates. The *gauche* preference is attributed to antiperiplanar  $\sigma_{\text{C-H}} \rightarrow \sigma^*_{\text{C-X}}$  interactions (Figure 4) (RABLEN *et al.*, 1999; TAVASLI *et al.*, 2002). Fluorine is the benchmark atom leading the *gauche* preference because of the low-lying energy (good electron-accepting ability) of the  $\sigma^*_{\text{C-F}}$  orbital; furthermore, it has interesting features, such as high electronegativity, similar size to the hydrogen atom, highly polarized, and stable bonds with carbon (O’HAGAN, 2008). These features make fluorine an important tool in conformational modulation.

Figure 4 — Conformational equilibrium of a 1,2-disubstituted ethane indicating the *gauche* effect, even being disfavored by classical parameters (top); stabilizing antiperiplanar  $\sigma_{\text{C-H}} \rightarrow \sigma^*_{\text{C-X}}$  interaction (bottom).



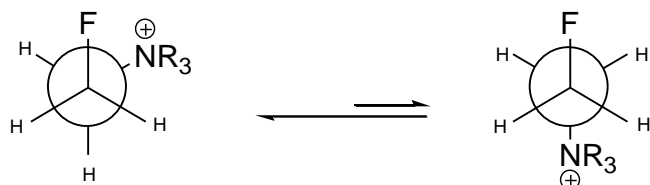
Source: from the Author (2022)

The fluorine *gauche* effect is well known in systems containing the X–C–C–F motif, where X is an electronegative group. Although the conformational behavior for X = F, Cl, Br, and I have been widely explored, the origin of the conformational preferences in these systems is still controversial (RAMASAMI, 2006; SHARGH; BOGGS, 2011; SILVA *et al.*, 2021; YOUNG; BORJEMSCAIA; WLADKOWSKI, 2005). Moreover, from the point of view of stereoelectronic effects, the behavior in systems where X = I is intriguing and may be useful, since organic compounds containing iodine atoms are present in many reactive molecules. Additionally, the  $\sigma^*_{\text{C-I}}$  orbital is lower in energy compared to the other halogens and, consequently, the most prone to act as an electron acceptor, which could lead to a strong  $\sigma_{\text{C-H}} \rightarrow \sigma^*_{\text{C-I}}$  interaction. On the other hand,  $\sigma_{\text{C-I}}$  is the ablest to act as an electron-donating orbital (along with the halogen series), since it lies in the highest energy level (RAUK, 2004). The

competition between  $\sigma_{\text{C-H}} \rightarrow \sigma^*_{\text{C-I}}$  (leading to the *gauche* conformer) and  $\sigma_{\text{C-I}} \rightarrow \sigma^*_{\text{C-F}}$  (leading to the *anti* conformer) in an ethane fragment can be further exploited.

Electrostatics is another perspective of the fluorine *gauche* effect. Since fluorine bears a partial negative charge, it can attract positive sites and repel negative charges in its vicinity. This effect is observed, for example, in some systems where an ammonium or pyridinium group is present (Figure 5) (GOOSEMAN *et al.*, 2007). Attempts to observe the fluorine *gauche* effect involving compounds with an atom (sulfur) beyond the second row have been performed (ALEKSIC; STOJANOVIC; BARANAC-STOJANOVIC, 2015; THIEHOFF *et al.*, 2015; THIEHOFF *et al.*, 2016; THIEHOFF; REY; GILMOUR, 2017), but not all third-row elements are capable of leading fluorine to a preferred *gauche* position (ANDRADE; FREITAS, 2017). The electrostatic fluorine *gauche* effect with sulfur depends on the sulfur oxidation state; higher oxidation states ensure higher positive charges and more effective attraction (ALEKSIC; STOJANOVIC; BARANAC-STOJANOVIC, 2015). In this sense, phosphorus is another interesting atom occupying the third row of the Periodic Table, since it is present in many molecules with agrochemical, ionic liquid, and antimicrobial properties (BLUNDELL; LICENCE, 2014; ETO, 1997; XUE; XIAO; ZHANG, 2015). Similar to sulfur, phosphorus can experience different oxidation states, which allow for the study of the electrostatic fluorine *gauche* effect.

Figure 5 — Electrostatic *gauche* effect between fluorine and a positively charged ammonium group.



Source: from the Author (2022)

All of these demonstrate the potential of the fluorine atom as a conformational tool at the molecular level. The stereoelectronic effects caused by fluorine insertion can be used in conformational modulation to lead to a specific structure. However, the fluorine atom is not limited to structural features in molecules. In biological systems, fluorinated molecules represent 25-30% of therapeutics and agrochemicals licensed worldwide (FUJIWARA; O'HAGAN, 2014; O'HAGAN, 2010), also showing potential to cause biological responses.

In bioactive molecules, fluorine can provide deep changes. It is related to engaging in halogen bonds, which have been a source of stability of active molecules in the enzyme pocket. In addition, this specific interaction has been explored as a tool in drug discovery (MENDEZ *et al.*, 2017; RIEL *et al.*, 2019). Fluorine is the most electronegative atom in the Periodic Table and induces a high C—F bond polarity, then changing the ability of membrane permeation, increasing the molecular stability, and decreasing the bioaccumulation in fatty tissues. It can replace hydrogen atoms without significant steric consequences. Also, it can replace hydroxyl groups since its electronegativity is close to the oxygen and, therefore, it can similarly act as a hydrogen bond acceptor (O'HAGAN, 2008). All these features make fluorine an alternative group for replacement in therapeutics and agrochemistry.

Computational chemistry has long been used to evaluate the conformational equilibrium of small organic molecules, where more sophisticated methods can be applied and, consequently, more accurate results can be obtained. In addition, molecular modeling resources have evolved in such a way that uses in the biological response prediction have been significantly increasing (HILLISCH; HEINRICH; WILD, 2015; MANLY; LOUISE-MAY; HAMMER, 2001). Modern computational chemistry allows an efficient ligand-enzyme interaction prediction for a huge number of biological systems (AZEVEDO; DIAS, 2008). Consequently, preliminary theoretical studies before experimental analysis are a beneficial strategy to optimize the search for promising molecules, besides saving time and money *e.g.* in a drug development process.

For this reason, a theoretical study of the bioisosteric replacement of chlorine by fluorine atoms in organochlorine pesticides was evaluated herein. Organochlorines have been banned in many countries due to the potential to cause adverse effects on human and animal health. Organochlorine compounds can accumulate in fatty tissues and are likely to C—Cl bond cleavage (although this does not ensure toxicity) (EGELEER *et al.*, 1997; LIANG *et al.*, 2017; PUIU *et al.*, 2019). The bioisosteric replacement could be successful because of the desirable features of fluorinated compounds mentioned above. Moreover, a theoretical study can avoid dispendious synthetic and experimental procedures before ensuring the bioisosteric replacement is a safe alternative.

Finally, a recent study found that the stereochemical dependence of molecular polarity determines the lipophilicity ( $\log P$ ) of organofluorine compounds (O'HAGAN; YOUNG, 2016). Consequently, stereoelectronic effects can directly influence the absorption and distribution of fluorinated drugs throughout the body (CONSTANTINESCU; LUNGU; LUNG,

2019). In this sense, the dependence on stereoelectronic effects and lipophilicity can be further exploited by taking some fluorinated compounds as model molecules. Inhalational fluorinated anesthetics are good systems to study the stereoelectronic effects on  $\log P$  due to the stereoelectronic effects caused by fluorine and because of their well-known biological properties. It is well known that vicinal fluorine atoms tend to adopt the *gauche* conformation, and as a consequence, all C—F bonds are pointed out nearly in the same direction, which increases the neat molecular dipole moment ( $\mu$ ). Therefore, the most polar (and probably the most stable) conformer will present a small  $\log P$  value, indicating a high concentration in the (aqueous) blood and poor absorption.

This work aims at improving the understanding of fluorine chemistry, from the point of view of structural, physical, biological and agrochemical perspectives.

## 2 Theoretical Framework

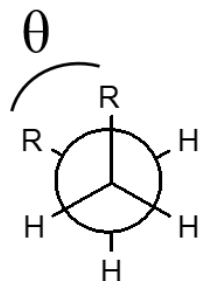
### 2.1 Conformational Analysis and Tools

#### 2.1.1 Basic Concepts

Each step of a rotation around single bonds in a molecule yields different shapes, named conformations. Meanwhile, the conformation corresponding to an energy minimum in a potential energy curve is named conformer. It is known that even the rotation around the single bond for the simplest system ( $\text{H}_3\text{C}-\text{CH}_3$ ) provides an infinite number of conformations. In this system, for example, there are two main conformations, the staggered and eclipsed structures (they represent the extremes – the energy minimum and maximum, respectively – in the potential energy curve). It is worth mentioning that the conformation is characterized by its dihedral angle of rotation ( $\theta$ ), which is the angle formed by four atoms and three bonds (Figure 6). While the system's complexity increases, the number of conformations and conformers can also increase. For instance, disubstituted ethanes  $\text{XH}_2\text{C}-\text{CH}_2\text{X}$  (Figure 7, where  $\text{X} = \text{CH}_3$ ) have four noticeable conformations, and among them are two conformers (the energy minima). However, not only acyclic molecules undergo rotation around single bonds and then present

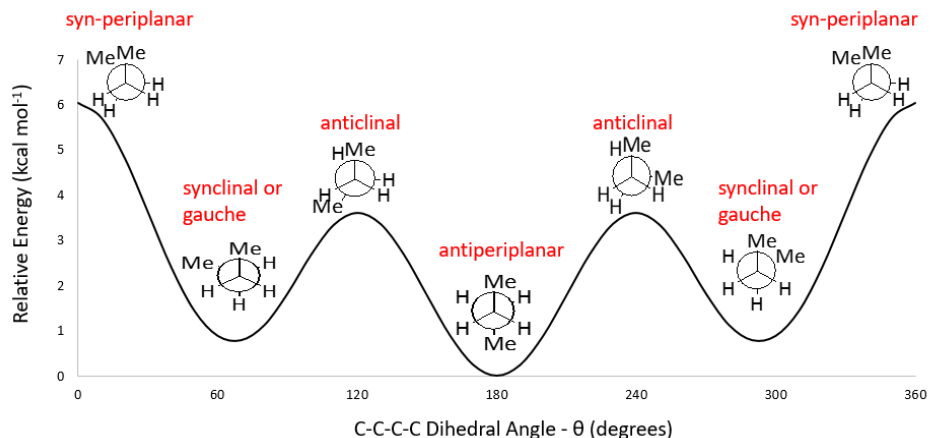
conformations; a remarkable example refers to alicyclic six-membered rings, the most stable ring and widely found in natural systems, which show three main conformations (chair, boat, and twist-boat). The chair conformer is the most stable six-membered ring and, with few exceptions, this ring is exclusively in this form. During the conformational rotation in these systems, the substituents in the ring interconvert from axial to equatorial orientation, see Figure 8 (CLAYDEN; GREEVES; WARREN, 2012).

Figure 6 — Dihedral angle  $\theta$  formed by four atoms and three bonds.



Source: from the Author (2022)

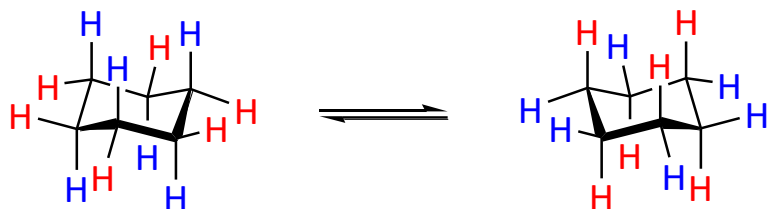
Figure 7 — Potential energy curve for butane at the HF/3-21G level of theory.



Legend: The main conformations – staggered as minimum and eclipsed as maximum – are highlighted in the potential curve.

Source: from the Author (2022)

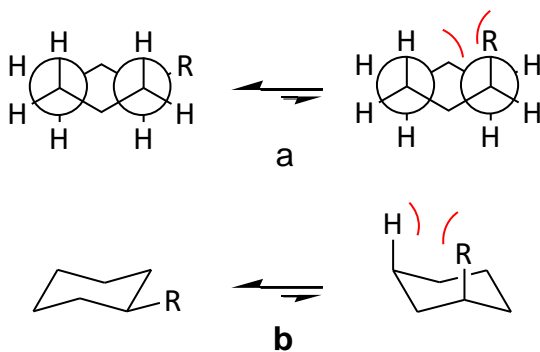
Figure 8 — Ring interconversion of cyclohexane showing the axial-equatorial interplay of hydrogens.



Source: from the Author (2022)

In the early stages of conformational analysis, the conformational equilibrium used to be rationalized in terms of classical interactions – steric and electrostatics. At that time, these concepts were sufficient to explain the conformational behavior of molecules. The preference for the equatorial form in monosubstituted six-membered rings, for example, was based on  $\gamma$ -*gauche* and 1,3-diaxial repulsion (Figure 9) (BARTON, 1953; ELIEL; WILEN, 1994; ORLOFF, 1954; OUELLETTE; RAWN, 2018). In acyclic compounds, the explanation is based on the same argument, *i.e.* the preference for staggered conformers in an *anti*-position to avoid steric and electrostatic (if the substituents have the same charge) repulsion or *gauche* preference if opposite charges are close to each other (TERUI *et al.*, 1974). However, some cases of conformational preferences could not be fully explained by the known classical terms. For example, the unexpected stability of the axial conformer in some  $\alpha$ -substituted pyrans (WOLFE; WHANGBO; MITCHELL, 1979) and the preference for the *gauche* conformer in ethane fragments containing vicinal electronegative atoms or polar bonds (WOLFE, 1972). In these cases, a conformational effect is observed (conformational effect rises when classical terms alone are not sufficient to explain a given conformational behavior).

Figure 9 — a)  $\gamma$ -*gauche* repulsion in a monosubstituted six-membered ring; b) 1,3-diaxial repulsion in a monosubstituted six-membered ring.

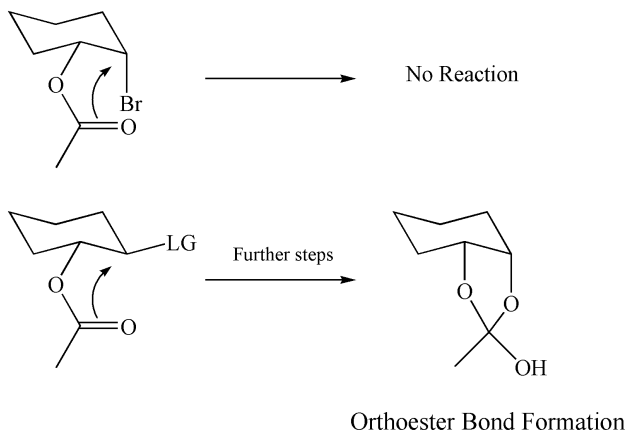


Source: from the Author (2022)

In conformational analysis, some conformational effects are widely known and, therefore, are named in special terms. These effects include the *rabbit-ear effect*, where unshared electron pairs on non-adjacent atoms are preferred in a *syn*-axial position, even being counter-intuitively stable by classical terms (HUTCHINS; KOPP; ELIEL, 1968), see Figure 3; *alpha effect*, which affects the nucleophilicity of atoms due to the presence of an alpha atom with lone pairs of electrons (REN; YAMATAKA, 2007); the *anomeric effect* gives unexpected stability for  $\alpha$ - anomers in pyranoside rings (WOLFE, 1979). Another important conformational effect is the *gauche* effect, which is the tendency of electronegative atoms or polar bonds to adopt a *gauche* position, even being the least stable by classical terms. Such stability has been attributed to electronic delocalization, only possible because of the quantum nature of electrons. The electron delocalization from a filled to a low-lying energy orbital ( $\sigma_{\text{CH}} \rightarrow \sigma^*_{\text{CX}}$ ), only possible in the *gauche* conformer, stabilizes the system (Figure 4).

One of the consequences of the *gauche* effect is the increase in the molecular dipolar moment, since the *gauche* polar bonds are pointed out almost in the same direction. It has an impact on biological responses, such as the absorption throughout the cell membrane, solubility in aqueous solution (*e.g.* the blood), and lower accumulation in fatty tissues (YANG; HINNER, 2015). In organic reactions, it has been proved that conformational effects can be used to optimize processes, for example, exploring the reverse anomeric effect (responsible for increasing the equatorial population in the axial-equatorial equilibrium of monosubstituted pyran-like rings) to increase the yield in the production of orthoester polymers. The formation of orthoester bonds in polymerization requires the  $\alpha$ -substituent to adopt an equatorial position in pyran-like rings. However, these systems are known to experience the *anomeric effect*, which leads to a preference for the  $\alpha$ -substituent in the axial position and, consequently, a low yield for this specific reaction is achieved. Li and co-workers (2015) overcome this limitation by taking advantage of the reverse *anomeric effect*, which favors the equatorial isomer for  $\alpha$ -substituent, Figure 10. Therefore, it was possible to increase reaction rates and yield through conformational effects (Li *et al.*, 2015). Moreover, conformational isomerism has an impact also in organic catalysis. It is known that catalysts based on carbon chains have been developed and are consequently prone to experience conformational isomerism. Conformational modulation can decrease the free rotation to give rigid structures (ZIMMER; SPARR; GILMOUR, 2011). Therefore, a deep knowledge of conformational behavior and its causes is crucial in many areas. A rational way to induce or modulate conformation is valuable to optimize reactions, improve biological responses, and for materials development.

Figure 10 — Orthoester bond formation promoted by a nucleophile capable to establish the reverse anomeric effect.



Source: from the Author (2022)

### 2.1.2 The Fluorine Chemistry

Fluorine is an element with unique properties in the Periodic Table since it is the most electronegative atom and has a small atomic radius (Van der Waals radius of 1.47 angstrom) (ROWLAND; TAYLOR, 1996). In organic chemistry, these features provide organic fluorinated compounds with useful applications and a profound structural impact. The fluorine's high electronegativity makes the C—F bond the most polar in organic chemistry, while the bond polarity is crucial in many aspects. For instance, the bond polarity determines the molecular dipolar moment, which is responsible for intermolecular interactions, thus directly affecting properties such as melting and boiling points and solubility. In biological terms, it is responsible for cell membrane absorption and body distribution.

Because fluorine is small, with dimension compared to the hydrogen atom, the C—F and C—H bonds are similar in steric terms (O'HAGAN 2008). However, this replacement brings high electrostatic consequences to a molecule, which is useful in the conformational analysis, since this helps to elucidate conformational effects without further steric implications (O'HAGAN, 2008, 2010). Another valuable replacement can be done by changing the hydroxyl group by fluorine atom – fluorine and oxygen have similar electronegativity. In addition, it is known that organic fluorine can act as a fairly good hydrogen acceptor but not as a hydrogen donor; this feature makes the fluorine replacement an essential conformational tool to evaluate the role of hydrogen bonds in conformational isomerism. Altogether, these characteristics of

fluorine cause also a deep impact on biological systems, thus allowing for the design of performance molecules.

The increasing number of pharmacological and agrochemical compounds containing fluorine indicates how important are the features attributed to fluorine atoms (FUJIWARA; O'HAGAN, 2014; O'HAGAN, 2010). However, fluorine chemistry is not limited only to biological systems. Fluorine-carbon bonds are also applied in materials science, such as in the development of polymers and liquids crystals (the C—F bond is highly stable and less prone to cleavage) (CAVALLO *et al.*, 2018; FANG *et al.*, 2020; MCKEEN, 2012).

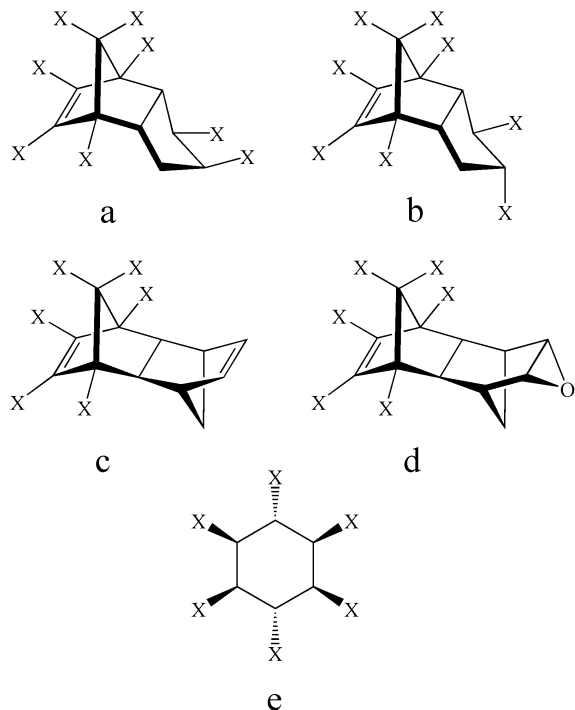
Fluorine plays a central role as a conformational tool. Due to the high C—F bond polarity, the antibonding orbital ( $\sigma^*_{CF}$ ) has relatively low energy, which allows it to act as an electron acceptor. This feature provides a remarkable conformational implication since the low-lying energy of the  $\sigma^*_{CF}$  orbital has been attributed as the main reason for the *gauche* stability in  $FCH_2CH_2F$  fragments (MIYAJIMA; KURITA; HIRANO, 1987; TAVASLI *et al.*, 2002). It is known that  $\sigma_{CH} \rightarrow \sigma^*_{CF}$  interaction, only possible in the *gauche* conformer, is highly stabilizing (Figure 3). As mentioned above, the *gauche* form has a higher dipolar moment than the *anti* conformer, which directly affects the molecular properties.

The conformational effects caused by fluorine can be used for conformational control, leading to a specific conformer or diminishing the number of possible conformations. It allows for designing more effective biological molecules and catalysts based on the carbon chain (EVIDENTE; ANDOLFI; CIMMINO, 2011; ZIMMER; SPARR; GILMOUR, 2011).

In this work, the consequences of a bioisosteric replacement of chlorines by fluorines in some pesticides, namely the aldrin, dieldrin, lindane,  $\alpha$ -chlordane, and  $\beta$ -chlordane pesticides were evaluated (Figure 11). While the need for food around the world increases, organochlorine pesticides have been banned because of their human and animal harm. The main harmful characteristic of organochlorines is the bioaccumulation/biomagnification in the food chain. Organochlorine pesticides act in the GABA<sub>A</sub> receptor, disrupting the chloride flux, which induces an over-excitation of the body and, consequently, respiratory failure (BLOOMQUIST; SODERLUND, 1985; FISHMAN; GIANUTSOS, 1985; POMES; RODRÍGUEZ-FARRÉ; SUÑOL, 1994). The bioaccumulation capacity of organochloride pesticides triggers high doses over the years and throughout the food chain. In this sense, the replacement of chlorine with fluorine atoms can improve the pesticides in some aspects, such as providing lower lipophilicity

(fluorine increases the molecular polarity compared to chlorine) and more stable bonds (C—F is more stable than C—Cl) (THEODORIDIS, 2006).

Figure 11 — Organochlorine pesticides (for X = Cl) and bioisostERICALLY-replaced fluorinated derivatives (for X = F).



Legend: a) alpha chlordane or alpha fluordane; b) beta chlordane or beta fluordane; c) aldrin or F-aldrin; d) dieldrin or F-dieldrin; e) lindane or F-lindane

Source: from the Author (2022)

A theoretical study of fluorinated bioisosteres of organochlorines can open up a new sight in pesticides and agrochemical design. Accordingly, computational insight can be useful to avoid experimental costs before ensuring new molecules as good alternatives.

### 2.1.3 The Phosphorus Chemistry

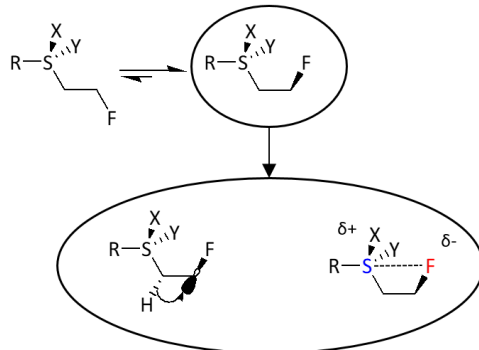
The current number of phosphorus-containing compounds highlights the importance of this atom. The phosphorus atom is a ubiquitous element present in biological systems, such as nucleotide, DNA, enzyme cofactor, and macronutrients. Also, it is important in chemical reactions, like the Wittig and nucleophilic reactions (CLAYDEN; GREEVES; WARREN,

2012), and as a catalyst in some reactions (ASWIN *et al.*, 2014; GIMBERT *et al.*, 2005). Unfortunately, phosphorus compounds are also used as chemical weapons, such as sarin (an organophosphate). These molecules (organophosphates) are capable of inactivating the acetylcholinesterase enzyme, which is an important enzyme responsible for acetylcholine degradation. The accumulation of acetylcholine in the synaptic cleft causes continuous stimulation and respiratory failure (PETER; SUDARSAN; MORAN, 2014). In agrochemistry, phosphorus-containing compounds have a wide range of applications since organophosphates are alternatives to organochlorine pesticides. While organochlorine pesticides act in the GABA receptors, the organophosphate's mode of action is similar to those observed in humans, *i.e.* they act in the acetylcholinesterase enzyme of insects (FUKUTO, 1990). Recently, antimicrobial activity has been assigned to materials containing quaternary phosphonium salts (KANAZAWA; IKEDA; ENDO, 1994; XUE; XIAO; ZHANG, 2015). All these features demonstrate the broad use of phosphorus and its large applicability.

The phosphorus atom plays an important role in fundamental science. It is a third-row element of group 15 (5A) in the Periodic Table and, as a consequence, it shares similarities with the nitrogen atom – an atom extensively studied in conformational analysis, present in conformational effects, such as the *gauche* and *anomeric* effects (BOOTH; DIXON; KHEDHAIR, 1992; ERXLEBEN; KEDZIORA; URBAN, 2014; GOOSEMAN *et al.*, 2007). Stereoelectronic features of P can be further explored in the conformational analysis, since the  $\sigma^*_{CP}$  orbital has lower energy than the  $\sigma^*_{CN}$  orbital, which makes the C—P antibonding orbital a better electron pair receptor (pronounced hyperconjugation). At the same time, the phosphorus electron lone pair is more prone to be donated, since it lies on a higher energy level than the nitrogen lone pair. These characteristics make phosphorus a useful conformational tool to investigate conformational effects.

Recently, an effort has been made to extend the fluorine *gauche* effect to the third row of the Periodic Table. It was observed that vicinal fluorine and sulfur atoms experience the fluorine *gauche* effect, and electrostatics is the main stabilizing factor of the *gauche* conformation, although the observed  $\sigma_{CH} \rightarrow \sigma^*_{CF}$  (see Figure 12) (ALEKSIC; STOJANOVIC; BARANAC-STOJANOVIC, 2015; THIEHOFF *et al.*, 2015). Accordingly, the *gauche* population increases as the sulfur atom becomes more positively charged (THIEHOFF *et al.*, 2016). This is crucial, since one allows to modulate the conformational population by changing the sulfur oxidation state. Santschi *et al.* (2016) have shown the potential of such modulation in organometallic systems.

Figure 12 — The *gauche* effect between fluorine and sulfur in a F–C–C–S motif.



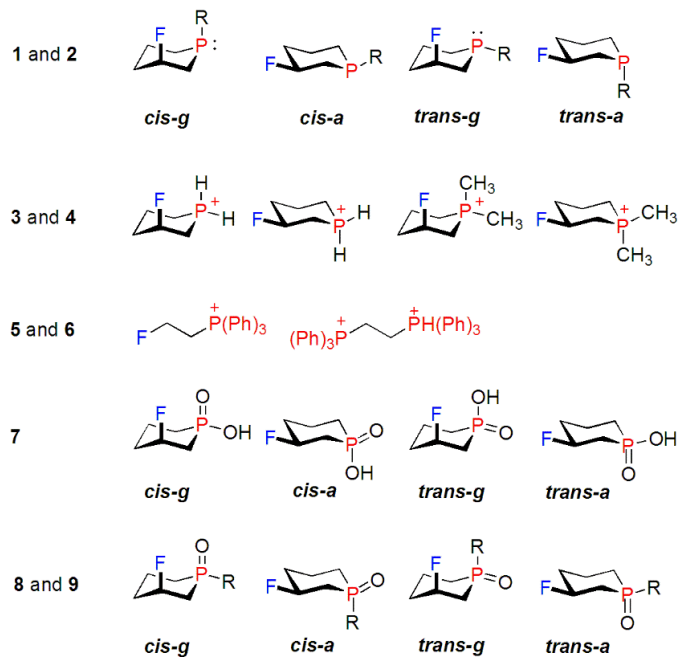
Legend: The hyperconjugation (bottom, at the left) and electrostatic contribution (bottom, at the right).

Source: from the Author (2022)

Phosphorus has been another third-row element to be recently studied in an attempt to induce a *gauche* effect, but  $\beta$ -fluorinated organophosphorus have not been shown to experience any fluorine *gauche* effect (ANDRADE; FREITAS, 2017). Then, not all third-row elements can experience such an effect. However, there is the possibility of inducing the fluorine-phosphorus *gauche* effect by modulating the charge on the phosphorus atom, since it has been demonstrated that the increase in the positive charge of the sulfur atom increases the *gauche* population. It is known that the phosphorus atom in a molecule can present more than one oxidation state, such as phosphine, phosphine oxide, and phosphonium salt.

In this work, the possibility of the appearance of a fluorine-phosphorus *gauche* effect was further explored, considering various phosphorus oxidation levels. Chair-like six-membered rings were the molecular models chosen to evaluate the *gauche* effect (Figure 13). These cyclic systems were proposed to simplify the conformational landscape, since rotation around single bonds in acyclic compounds could originate a variety of conformers rather than only the axial and equatorial conformers in the alicyclic compounds. From the outcomes of this analysis, the fluorine-phosphorus electrostatic *gauche* effect could be further evaluated to an acyclic compound: the (2-fluoroethyl)triphenylphosphonium cation.

Figure 13 —  $\beta$ -fluorinated organophosphorus models proposed for conformational studies.



Legend: From top to bottom: chair conformations and isomers for the studied phosphines **1** ( $R = H$ ) and **2** ( $R = Me$ ), phosphonium cations **3** ( $R = H$ ) and **4** ( $R = Me$ ), (2-fluoroethyl)triphenylphosphonium (**5**) and (ethane-1,2-diy)bis(triphenylphosphonium) (**6**) cations, phosphinic acid **7**, phosphine oxides **8** ( $R = H$ ) and **9** ( $R = Me$ ).

Source: *ChemPhysChem*, 23, (2022), e202100856

## 2.1.4 The Iodine Chemistry

The use of iodine atoms has been increasing over the years, since this halogen presents interesting features from the synthetic and stereoelectronic/structural points of view. Iodine is a large-sized halogen, easily polarizable, low in electronegativity, goes beyond the most common oxidation state of -1 (characteristic of halogens), then presenting hypervalent states, such as +3, +5, and +7 (ZHDANKIN, 2014). Hypervalent iodine compounds are oxidant agents used, for example, to convert alcohols into the corresponding carbonyl compounds and in the  $\alpha$ -oxygenation of carbonyl compounds (MAITI; YADAV, 2001; MORIARTY *et al.*, 1987). In regular courses of organic chemistry, the iodine atom is widely explored as a leaving group in nucleophilic substitution reactions. It is known that C—I bond is the most prone to cleavage in the halogen series; one reason is the small overlap between iodine and a carbon atom, thus yielding a soft bond. Therefore, all these features make organoiodine compounds an important class to study.

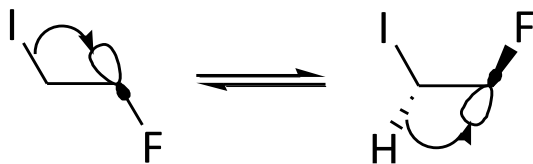
The iodine atom in molecules ensures particular stereoelectronic effects, since the C—I bonding orbital ( $\sigma_{\text{Cl}}$ ) has the highest energy in the halogen series and, consequently, it can act as a good electron donor in delocalization effects. At the same time, the C—I antibonding orbital ( $\sigma^*_{\text{Cl}}$ ) is the lowest in energy along with the halogen series, which leads to a good electron acceptor (RAUK, 2004). It has been earlier mentioned that these interactions are important in conformational isomerism and can be exploited to elucidate conformational effects.

1,2-Dihaloethanes ( $\text{XCH}_2\text{CH}_2\text{Y}$ ) have been extensively studied by experimental and theoretical methods. The 1,2-difluoro-, 1,2-dichloro- and 1,2-dibromoethane, for example, have been studied in all phases by vibrational spectroscopy and theoretical methods (BUTCHER; COHEN; ROUNDS, 1971; KLABOE; NIELSEN, 1960; MIZUSHIMA, 1954). Studies with two different halogens are also known; the conformational equilibria of 1-chloro-2-fluoroethane, 1-bromo-2-fluoroethane, and 1-iodo-2-fluoroethane have been determined by microwave spectroscopy (NIIDE, *et al.*, 1986; NIIDE; OHKOSHI, 1990). It is known that 1,2-difluoroethane is a benchmark molecule exhibiting the *gauche* effect. However, not all 1,2-dihaloethanes can adopt a preferential *gauche* conformation. This fact makes the  $\text{XCH}_2\text{CH}_2\text{Y}$  fragment a good model molecule to explore the conformational effects and their origins. Furthermore, the effects ruling the conformational equilibrium of  $\text{FCH}_2\text{CH}_2\text{I}$  it is not fully understood and, then, are worth to be explored.

In this work, we have studied 1,2-dihaloethanes and 2-haloethanols to gain insight into the role of the competing factors that rule the conformational equilibria in these motifs. Combining two different vicinal halogens, we can explore the steric and electrostatic features, besides the role of intramolecular hydrogen bonds (in the case of 2-haloethanols). Moreover, it has been widely mentioned that the  $\sigma_{\text{CH}} \rightarrow \sigma^*_{\text{CF}}$  interaction is responsible for *gauche* stabilization in 1,2-difluoroethane due to the relatively low energy of the  $\sigma^*_{\text{CF}}$  orbital. Therefore, a  $\sigma_{\text{CH}} \rightarrow \sigma^*_{\text{Cl}}$  interaction is expected to be more stabilizing than that observed in fluorine, since the  $\sigma^*_{\text{Cl}}$  orbital lies in a lower energy level than  $\sigma^*_{\text{CF}}$ . In this case, the *gauche* form of the iodine derivative could be more stable. However, the role of  $\sigma_{\text{Cl}}$  as a good electron donor can lead to a  $\sigma_{\text{Cl}} \rightarrow \sigma^*_{\text{CF}}$  interaction in the *anti* position, which would decrease the *gauche* population (Figure 14). The competitive  $\sigma_{\text{CH}} \rightarrow \sigma^*_{\text{Cl/F}}$  (in *gauche* conformer) and  $\sigma_{\text{Cl}} \rightarrow \sigma^*_{\text{CF}}$  (in *anti* conformer) interactions can be further exploited to give insight into the role of delocalization in the fluorine *gauche* effect. For all these reasons, the study of  $\text{ICH}_2\text{CH}_2\text{F}$  is interesting, *i.e.* the smaller and the bigger halogen are vicinal, and a high number of competitive

interactions can be observed, such as steric effects (caused by the iodine volume), electrostatic and delocalization effects.

Figure 14 — Competition between two stabilizing stereoelectronic effects in 1-fluoro-2-iodoethane.



Legend:  $\sigma_{\text{CI}} \rightarrow \sigma^*_{\text{CF}}$  (favoring the *anti* form) and  $\sigma_{\text{CH}} \rightarrow \sigma^*_{\text{CF}}$  (favoring the *gauche* form) interactions.

Source: from the Author (2022)

## 2.2 Spectroscopic Methods for Conformational and Structural Determination

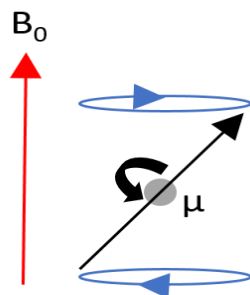
### 2.2.1 Nuclear Magnetic Resonance Spectroscopy

Nuclear magnetic resonance (NMR) is a crucial tool in structural determination since it allows the detection of atomic nuclei, their vicinity, and even the electronic environment of atoms in molecules. NMR spectroscopy is only possible due to an intrinsic nuclear property named *spin* ( $I$ ) that is a form of angular momentum. It can be 0, 1/2, 1, 3/2 ... but only nuclei with  $I \neq 0$  are active in NMR spectroscopy. Furthermore, the nuclear *spin* is associated to the nuclear magnetic moment ( $\mu$ ), if the elementary particle has mass, see Equation 1. In the presence of an external magnetic field ( $B_0$ ), the magnetic vector of nuclei tends to become parallel to  $B_0$ . This tendency, combined with the rotational inertia of the nuclei, creates a precession movement with a given frequency ( $v_0$ ), according to Figure 15 (GEROTHANASSIS *et al.*, 2002).

$$\mu = \gamma I \hbar \quad (1)$$

$\gamma$  is the nucleus gyromagnetic ratio and  $\hbar$  is a constant.

Figure 15 — The precession movement (represented by the blue curve) of a nucleus with magnetic moment ( $\mu$ ) submitted to an external magnetic field ( $B_0$ ).



Source: from the Author (2022)

As a consequence of the quantum nature of nuclei, the nuclear magnetic moment vector can adopt only specific orientations (the stationary states), which are dependent on the *spin* and, consequently, nuclei-dependent (Equation 2).

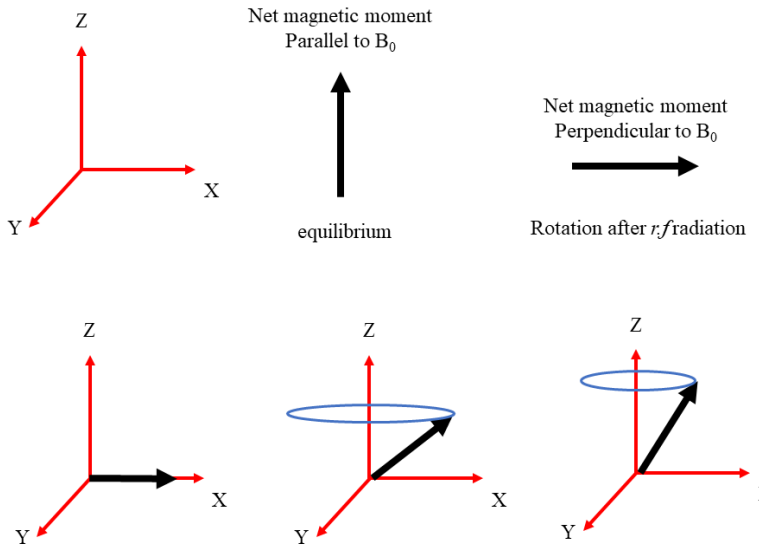
$$\text{Number of stationary states} = 2I + 1 \quad (2)$$

Nuclei with  $I = \frac{1}{2}$  are particularly useful in NMR, since they show only two possible stationary states in the presence of  $B_0$ : aligned to an external magnetic field (lowest energy -  $\alpha$ ) or against it (highest energy -  $\beta$ ). In addition, the energy difference associate to these states is dependent of the external magnetic field and two constants, see Equation 3 (ATKINS, 1998). Common atoms in organic chemistry have  $I = \frac{1}{2}$ , such as  $^1\text{H}$ ,  $^{13}\text{C}$ ,  $^{19}\text{F}$ , and  $^{31}\text{P}$ . Therefore, this fact makes the NMR spectroscopy useful in organic chemistry.

$$\Delta E = -\gamma\hbar B_0 \quad (3)$$

The acquisition of NMR spectra takes advantage of the spin magnetization *perpendicular*, instead of *along*  $B_0$ , since longitudinal magnetization measurement is impractical due to the small magnitude. The magnetic moment vector becomes parallel to  $B_0$  when submitted to an external magnetic field. At this point, a negligible macroscopic magnetization is observed if the equilibrium is achieved. However, by incising electromagnetic radiation (radio frequency, *r.f*), the magnetic moment vector is rotated by  $2/\pi$  radians around the x-axis. Consequently, the spin polarization is transferred from the z-axis to the y-axis. After turning off the *r.f* radiation, the spins of all active nuclei in the sample tend to return to a parallel position to  $B_0$ , Figure 16. Consequently, they decay after a time, and this movement provides an induced current that is measured and used to generate the NMR signal (LEVITT, 2008).

Figure 16 — Longitudinal and transverse magnetization (upper) and transverse relaxation (lower).



Legend: net magnetic moment that represents the summation of all nuclei magnetic moments in dark arrow, cartesian axes in red and the precession movement of net magnetic moment in blue.

Source: from the Author (2022)

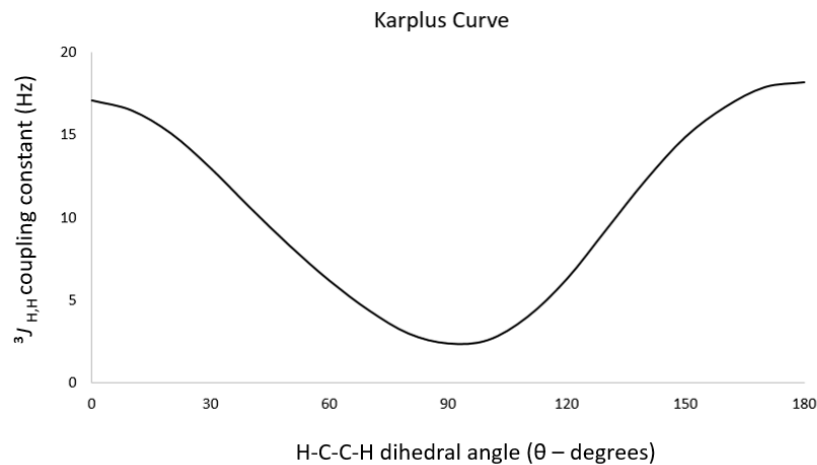
One point rises due to Lenz's law; it is known that electrons are charged particles in movement and, as a consequence, they create their particular magnetic field ( $B_{\text{electron}}$ ), in counterpart to  $B_0$ . This fact ensures a resulting magnetic field ( $B_{\text{effective}}$ ), that represents the real magnetic field over the nuclei ( $B_{\text{effective}} = B_0 - B_{\text{electron}}$ ). The nuclei are shielded, with few exceptions, from the resulting magnetic field created by electron motion, and the magnitude of the shielding is given by  $\sigma B_0$  ( $\sigma$  is the shielding or screening constant). This observation allows for the comprehension of the electronic environment (GEROTHANASSIS *et al.*, 2002; GÜNTHER, 1995; HARRIS, 1983).

In NMR spectroscopy, there are two main parameters. The first one is the chemical shift ( $\delta$ ), a consequence of the electronic shielding. This parameter is used to differentiate nuclei in a distinct magnetic environment, even for the same element. The presence of an electron cloud around the nuclei causes different resonance conditions ( $B_0$  or  $v$ ) and, consequently, different NMR peaks in the spectra. The chemical shift is determined by comparing the shift of the nucleus of interest to a shift of a known nucleus that is attributed to zero, in general, tetramethylsilane (TMS) (HOFFMANN; FORSÉN; GESTBLOM, 1971).

The second NMR parameter is the coupling constant ( $J$ ). The scalar coupling constant is responsible for information about the neighboring of the active atom. The signal multiplicity observed in the NMR spectra is a consequence of the nuclear spin coupling of atoms and indicates the number of active nuclei in its vicinity,  $2nI + 1$  (in which  $n$  is the number of active atoms). In this sense, chemical shift and coupling constant make the NMR a powerful technique for structural elucidation.

In conformational analysis, the coupling constant is most usually explored since Karplus (1963) established a mathematical relationship between a conformational parameter (dihedral angle) and an NMR parameter ( ${}^3J_{H,H}$  – the three-bond coupling between two hydrogens). Therefore, it is possible to gain conformational information using NMR spectroscopy. In the Karplus curve (Figure 17), it is possible to observe a local maximum and global maximum in  $0^\circ$  and  $180^\circ$ , respectively. It is a consequence of a better orbital overlap involving the C–H bonds. A minimum is observed at  $90^\circ$ , in which the overlap is poor. There are different relationships between coupling constant and dihedral angle, for example, for  ${}^3J_{H,H}$ ,  ${}^3J_{C,H}$ ,  ${}^3J_{H,F}$ .

Figure 17 — Relationship between coupling constant ( ${}^3J_{H,H}$ ) and the H–C–C–H dihedral angle established by Martin Karplus.



Legend: The plot was obtained for ethane at the HF/6-31G level of theory.

Source: from the Author (2022)

NMR spectroscopy has been widely employed in conformational studies. This technique allows for understanding the conformational isomerism for a wide variety of molecules, either cyclic or acyclic compounds (ENOMOTO-ROGERS *et al.*, 2016; TORMENA, 2016). Specifically, many studies of ethane-like fragments have been conducted using NMR

techniques (ABRAHAM; GATTI, 1969; HAMMAN, *et al.*, 1983). For flexible molecules in which the conformational interconversion is faster than the NMR time scale, the signals observed in spectra correspond to an average for the conformers, see Equation 4. If the interconversion is slow, the conformers have separate signals for each of them.

$$J_{\text{obs}} = n_A \times J_A + n_B \times J_B \quad (4)$$

in which  $J_{\text{obs}}$  is the coupling constant observed in the NMR spectra,  $J_A$  and  $J_B$  are the coupling constants of conformers A and B, respectively, and  $n_A$  and  $n_B$  are the mole ratio of A and B, respectively.

## 2.2.2 X-Ray Crystallography

X-ray is a well-known electromagnetic radiation, with a wavelength in the order of 1 angstrom ( $10^{-8}$  cm). The energetic X-ray interacts with the inner electrons of an atom beyond the valence interaction present in techniques like infrared and ultraviolet. Due to this property, X-ray spectroscopy is used to determine the elementary composition in complex matrices, since each element has particular lines of X-ray emission (GOLDSTEIN; SLEMMONS; CANAVAN, 1996; KIM; BROWN; RYTUBA, 2000). However, the use of X-rays is far beyond elementary determination and quantification. Currently, chemical structures have been reliably determined by X-ray crystallography, a technique in which X-ray radiation is diffracted by the sample.

Amongst the mentioned spectroscopic methods, X-ray crystallography is the most powerful in structural elucidation – even an arrangement around a chiral center is possible to determine. Its principle is based on the ability of crystalline compounds to diffract X-rays. Diffraction is only possible when the irradiated wavelength is close to the interatomic distances in the sample, typically in crystals (1 to 3 angstroms), and from the resulting diffraction pattern is possible to obtain the spatial arrangement (KRISHNAN; RUPP, 2012; PICKNETT; BRENNER, 2001). The main limitation in X-ray crystallography is the necessity of samples to be crystalline; subsequently, the structural accuracy is dependent on the crystal quality.

Currently, X-ray crystallography is widely employed to determine tridimensional structures in material sciences and biological macromolecules, such as proteins and nucleic acids (HUSSAIN; SARACCO; RUSSO, 2012; ILARI; SAVINO, 2008). Moreover, small

molecules have also been determined by this technique, thus contributing to conformational elucidation. Ceylan *et al.* (2011) obtained the single-crystal X-ray of (2-hydroxyethyl)-triphenylphosphonium chloride salt, a similar compound to the ones envisaged in this work.

## 2.3 Quantum Mechanics Computational Methods

### 2.3.1 Methods Based on Wavefunction

Computational chemistry is a tool within the theoretical chemistry scope, in which mathematical equations, combined with fundamental laws, are solved to understand chemical problems (JENSEN, 2007). Since the advent of electronic computers (1950), computational methods have increased. Its popularity comes mainly from the quantum mechanics theory, which states that all systems have particle and wave behavior. The wave-like features are pronounced in small systems, such as electrons. In this sense, a complete understanding of molecules, bonds, and electron interactions requires an account of this feature. The resolution of such complex equations is possible because of modern computers.

The well-known Schrödinger equation, Equation 5, plays a central role in modern quantum mechanics, since it allows to determine the system's wave function – in quantum mechanics, each system has a wave function, and by the wave function, it is possible to extract much information about the system, such as the energy, momentum, magnetic responses, and others (ALCÁCER, 2007). A problem arising from the Schrödinger equation is that an analytical resolution is only possible for the hydrogen atom, the simplest system.

$$\hat{H}\Psi = E\Psi \quad (5)$$

The Hamiltonian operator ( $\hat{H}$ ) is composed of kinetic (K) and potential (V) energy terms. In addition, the potential term is the contribution of nucleus-electron attraction ( $V_{ne}$ ), nucleus-nucleus repulsion ( $V_{nn}$ ), and electron-electron repulsion ( $V_{ee}$ ), according to Equation 6. The kinetic and potential nucleus-electron attraction terms have a well-known formulation, since they are based on classical equations. Moreover, the potential nucleus-nucleus repulsion component is simplified by the Born-Oppenheimer approximation. In this sense, the most problematic term is the electronic repulsion, which appears for systems with more than one

electron; a complete variable separation is not possible, as required to solve differential equations (JENSEN, 2007).

$$\hat{H} = K + V_{nn} + V_{ne} + V_{ee} \quad (6)$$

In an attempt to overcome this problem, many approximations have been adopted; consequently, many computational methods have emerged. The simplest method created to solve the many-body problems was named the Hartree-Fock method, in which a pseudo-one-particle is admitted. In this model, each electron is considered to be independent, and each one is described by its wave function ( $\varphi_i$ ) and has a given energy ( $\varepsilon_i$ ) (the Hamiltonian operator is  $h_i$ ). Equation 7 describes the Schrödinger equation for each electron (ECHENIQUE; ALONSO, 2007; SLATER, 1951).

$$h_i\varphi_i = \varepsilon_i\varphi_i \quad (7)$$

The system's Hamiltonian is given by the sum of all electrons Hamiltonian ( $H = h_1 + h_2 + \dots + h_n$ ), the system energy is the sum of all electrons energy ( $E = \varepsilon_1 + \varepsilon_2 + \dots + \varepsilon_n$ ), and the total wave function is given by the product of the electronic wave functions ( $\Psi = \varphi_1\varphi_2\dots\varphi_n$ ). In a process called self-consistent field, the equation converges to the lowest energy, and the  $\Psi$  is achieved to the best system's wave function. Although the electron-electron repulsion is taken into account, only an average result is considered. Consequently, a poor description of  $V_{ee}$  is given. Several different methods based on the Hartree-Fock theory have been developed to improve the electron-electron interaction accounting, which is known as post-Hartree-Fock methods (JENSEN, 2007).

There are many post-Hartree-Fock methods in which the electron-electron correlation is considered, but a specific method used in this work is the Moller-Plesset (MP), which will be further discussed.

MP methods are based on the Perturbation theory, where the Hamiltonian operator is the sum of a known unperturbed Hamiltonian ( $\hat{H}_0$  – given by the HF theory) and a small perturbation  $H'$ , Equation 8 (CREMER, 2011).

$$\hat{H} = \hat{H}_0 + \lambda\hat{H}' \quad (8)$$

The  $\lambda$  parameter indicates the strength of perturbation. As the perturbation can vary from zero to a finite number, then the energy and wave function can be written as a Taylor expansion in powers of  $\lambda$ . As follow:

$$E = \lambda^0 E_0 + \lambda^1 E_1 + \lambda^2 E_2 + \dots$$

$$\Psi = \lambda^0 \Psi_0 + \lambda^1 \Psi_1 + \lambda^2 \Psi_2 + \dots$$

The zeroth-order represents the Hartree-Fock theory. The electron correlation starts in the second-order (MP2). The MP2 method is the most economical method, which accounts for 80-90% of the correlation energy. However, it is computationally expensive for large systems (JENSEN, 2007).

The relatively low cost of MP2 method makes this method useful and a diverse number of papers have been published in different science fields (GÓMEZ; PACIOS, 2005; SAGARA, 2005).

### **2.3.2 Methods Based on Electron Density**

Further improvement in quantum mechanics, in particular in minimizing computational effort, was achieved after Hohenberg and Kohn proved E. B. Wilson's arguments. Hohenberg and Kohn showed that the energy ground state is fully determined by the electronic density ( $\rho$ ) (HOHENBERG; KOHN, 1964). In addition, by the integration over the electronic density, it is possible to obtain the number of electrons, the nucleus position, and the nuclear charge (JENSEN, 2007).

In the simplest wave function method (HF) to many-body systems, each electron is solved in three spatial coordinates (x,y,z), and as a consequence, the system with N electrons has  $3N$  variables. In counterpart, the electronic density always has three coordinates, independently of the number of electrons. This fact is an improvement in terms of computational cost (CRAMER, 2004).

The density functional theory is based on the existence of a functional that links the system's energy and its electronic density. Although the clear relationship between energy and electronic density, there is a lack of knowledge of the exact form of the functional. Currently, the functional is based on the wavefunction equation (by analogy), which is also divided into kinetic ( $T[\rho]$ ), potential nucleus-electron ( $E_{ne}[\rho]$ ) and potential electron-electron repulsion ( $E_{ee}[\rho]$ ), and the nucleus-nucleus interaction is approximated by Born-Oppenheimer (Equation 9).

$$E[\rho] = T[\rho] + E_{ne}[\rho] + \hat{E}_{ee}[\rho] \quad (9)$$

The  $\hat{E}_{ee}[\rho]$  is divided into two terms: the first is the coulomb functional ( $J[\rho]$ ), based on classic equations, and the second corresponds to the exchange ( $K[\rho]$ ) functional, which includes the quantum features (Equation 10). The main challenge in functional development lies in the exchange/correlation of functional.

$$E[\rho] = T[\rho] + E_{ne}[\rho] + J[\rho] + K[\rho] \quad (10)$$

Kohn and Sham proposed that the kinetic term could be almost entirely described by HF kinetic energy (99%) and the remaining energy included in the exchange functional. Now, with Kohn-Sham's assumptions, Equation 10 takes the form of Equation 11 (KOHN; SHAM, 1965).

$$E_{DFT}[\rho] = T_{HF}[\rho] + E_{ne}[\rho] + J[\rho] + \text{Exc}[\rho] \quad (11)$$

The  $\text{Exc}[\rho]$  includes the kinetic and potential exchange/correlation energy. All development in DFT lies in  $\text{Exc}[\rho]$  functional design. Modern DFT functional can recover almost 100% of the exchange/correlation energy. However, there is no universal functional capable of describing every system. Deep knowledge about a specific case is crucial to developing a reliable theoretical study.

A particular functional widely used in organic molecules is the B3LYP. This functional has been demonstrated to properly reproduce thermodynamic parameters and geometrical structures (BECKE, 1993). A problem with DFT functional is the absence of long-range interactions, since the energy is dependent on electronic density, and the density decreases rapidly with the distance. However, corrections to include dispersion effects can be found (GRIMME *et al.*, 2010; GRIMME; EHRLICH; GOERIGK, 2011). In B3LYP, corrections to long-range interactions are made by including HF terms in the functional, yielding *e.g.* the B3LYP-D3 and B3LYP-D3BJ methods. Other functionals capable of recovering long-range interactions are also available, such as  $\omega$ B97XD and CAM-B3LYP (CHAI; HEAD-GORDON, 2008; YANAI; TEW; HANDY, 2004).

In this sense, DFT can represent a large number of systems, including dispersion, long-range and relativistic effects. Furthermore, DFT is computationally cheaper than wave function methods and has been applied for different studies, such as materials, biological molecules, thermodynamic properties, and reactions (BAUERFELDT; ARBILLA; SILVA, 2005;

HERRERA; SERRA; D'AMICO, 2017; NEUGEBAUER; HICKEL, 2013; RAUGEI; GERVASIO; CARLONI, 2006).

## 2.4 Molecular Mechanics Methods

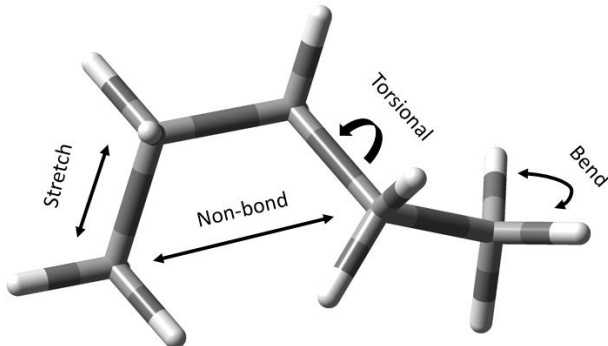
Computational methods based on Newtonian mechanics rather than those based on the Schrödinger equation are known as classical mechanics methods or molecular mechanics methods (MM). In this type of method, the wave nature of the system is not considered, and the particles are rather punctual with positive (nucleus) or negative (electron) charges. For this reason, the Coulomb interactions of these particles are most important for the system. Although the solution to classical equations is known, the computer is required due to the high number of particles involved and, consequently, the high number of equations (JENSEN, 2007).

MM methods are capable of predicting geometric arrangement, relative energies, and many other molecular properties. However, classical concepts are used to describe the system (atoms and bonds are considered balls and springs, respectively). Consequently, the quantum aspects are neglected, and bond information should be explicitly provided. In MM methods, the energy is dependent on many molecular terms, such as bond stretching, bond bending, bond torsion, electrostatic, and Van der Waals interaction (ALLINGER, 1976). All these terms are combined in a Force Field (FF); the difference among the diverse FF available is the type of parameterization used. Equation 12 gives the usual FF energy components.

$$E_{\text{FF}} = E_{\text{str}} + E_{\text{bend}} + E_{\text{tor}} + E_{\text{VDW}} + E_{\text{el}} + E_{\text{cross}} \quad (12)$$

in which  $E_{\text{FF}}$  corresponds to the system's energy, calculated by a given FF.  $E_{\text{str}}$  is the relative energy of bond stretching and shortening.  $E_{\text{bend}}$  is the energy to deform the angle ( $\theta$ ) between three atoms and two bonds.  $E_{\text{tor}}$  is the torsion energy of the angle ( $\omega$ ) between four atoms and three bonds.  $E_{\text{VDW}}$  is the energy relative to the Van der Waals interactions.  $E_{\text{el}}$  refers to the electrostatic interactions, and finally,  $E_{\text{cross}}$  is used to cover the coupling of the five earlier interactions (Figure 18).

Figure 18 — Interactions considered in a molecule by a Force Field.



Source: from the Author (2022)

The solution for a given FF without time evolution gives the system's energy for a given geometry. The process can be done for a set of structures, and the relative energy is found. However, there are solutions for FF with time evolution, since Newtonian mechanics is deterministic, and the equations can be integrated over time. Consequently, it is possible to predict the structure at a given moment or for some time. In this case, the method is known as molecular dynamics. Solutions without time evolution can be useful to predict the enzyme-substrate interaction, such as in docking studies, while dynamics solutions can predict the stability of *e.g.* an enzyme-substrate complex.

#### 2.4.1 Docking

Docking is a computational technique based on the MM method that allows the prediction of possible interaction modes between a small molecule (substrate, which can cause biological response) and a protein, in particular, with the protein's binding pocket (PAGADALA; SYED; TUSZYNSKI, 2017). The method is based on the key-and-lock model, in which a substrate fits in the enzyme's active site. The small molecule can adopt different conformations, which have different binding energies.

The docking study can be conducted basically in three ways: 1) rigid docking, where the substrate is allowed to change, and the active site is forbidden to move, and the energy is computed; 2) semi-flexible, where the small molecule has a free movement and some residues

in the binding site are allowed to move; 3) flexible, where both substrate and active site residues can freely move (MENG *et al.*, 2011).

There are different programs capable of running docking calculations. They generally vary in the FF applied, but the main focus is to find the most-likely bioconformations and the intermolecular interactions governing the induced fit, such as hydrogen bonds, Van der Waals, electrostatic and hydrophobic interactions.

Docking is a useful technique in the development of new compounds with therapeutical activity. Also, this technique allows us to understand the specific ways of coupling between enzyme and substrate and then to rationalize the most affected regions in an enzyme site related to a biological process. These features make the docking procedure a powerful technique in drug/agrochemical discovery and development (DE RUYCK *et al.*, 2016; FAN; FU; ZHANG, 2019).

## REFERENCES

- ABRAHAM, R. J.; GATTI, G. Rotational isomerism. Part VII. Effect of substituents on vicinal coupling constants in  $\text{XCH}_2\text{CH}_2\text{Y}$  fragments. **Journal of the Chemical Society B: Physical Organic**, p. 961-968, 1969.
- ALCÁCER, L. **Introdução à Química Quântica Computacional**. Instituto Superior Técnico, 2007.
- ALEKSIC, J.; STOJANOVIC, M.; BARANAC-STOJANOVIC, M. Origin of fluorine/sulfur *gauche* effect of  $\beta$ -fluorinated thiol, sulfoxide, sulfone, and thionium ion. **The Journal of Organic Chemistry**, v. 80, n. 20, p. 10197-10207, 2015.
- ALLINGER, N. L. Calculation of molecular structure and energy by force-field methods. **Advances in Physical Organic Chemistry**, v. 13, p. 1-82, 1976.
- ANDRADE, L. A. F.; FREITAS, M. P. Not all third-row elements experience the fluorine *gauche* effect:  $\beta$ -fluorinated organophosphorus compounds. **New Journal of Chemistry**, v. 41, n. 20, p. 11672-11678, 2017.
- ANTÚNEZ, S.; JUARISTI, E. Thermodynamics of the axial – equatorial conformational equilibria of *tert*-butylcyclohexane and *tert*-butyl-substituted six-membered heterocycles. Theoretical estimation of non-zero entropy changes. **The Journal of Organic Chemistry**, v. 61, n. 18, p. 6465-6469, 1996.
- ASWIN, K. *et al.* Triphenylphosphine: an efficient catalyst for the synthesis of 4,6-diphenyl-3,4-dihydropyrimidine-2(1*H*)-thione under thermal conditions. **Journal of King Saud University – Science**, v. 26, n. 2, p. 141-148, 2014.
- ATKINS, P. W. **Physical Chemistry**. 6<sup>th</sup> edition, New York: Oxford University Press, 1998.
- AZEVEDO, W. F.; DIAS, R. Computational methods for calculation of ligand-binding affinity. **Current Drug Targets**, v. 9, n. 12, p. 1031-1039, 2008.
- BARTON, D. H. R. The stereochemistry of cyclohexane derivatives. **Journal of the Chemical Society**, p. 1027-1040, 1953.
- BAUERFELDT, G. F.; ARBILLA, G.; SILVA, E. C. Evaluation of reaction thermochemistry using DFT calculated molecular properties: application to *trans*-HONO ( $\text{X}^1\text{A}'$ )  $\rightarrow$  HO( $\text{X}^2\text{P}$ ) + NO( $\text{X}^2\text{P}$ ). **Journal of the Brazilian Chemical Society**, v. 16, n. 2, p. 190-196, 2005.
- BECKE, A. D. Density-functional thermochemistry. III. The role of exact exchange. **The Journal of Chemical Physics**, v. 98, n. 7, p. 5648-5652, 1993.
- BLOOMQUIST, J. R.; SODERLUND, D. M. Neurotoxic insecticides inhibit GABA-dependent chloride uptake by mouse brain vesicles. **Biochemical and Biophysical Research Communications**, v. 133, n. 1, p. 37-43, 1985.
- BLUNDELL, R. K.; LICENCE, P. Quaternary ammonium and phosphonium based ionic liquids: a comparison of common anions. **Physical Chemistry Chemical Physics**, v. 16, n. 29, p. 15278-15288, 2014.

- BOOTH, H.; DIXON, J. M.; KHEDHAIR, A. Experimental studies of the *anomeric* effect. Part VI. Ring inversion equilibria in cyclohexane, tetrahydropyran and piperidine rings substituted by a carbomethoxy or a cyano group. **Tetrahedron**, v. 48, n. 29, p. 6161-6174, 1992.
- BUTCHER, S. S.; COHEN, R. A.; ROUNDS, T. C. Microwave spectrum of 1,2-difluoroethane. **The Journal of Chemical Physics**, v. 54, n. 9, p. 4123-4124, 1971.
- CAVALLO, G. *et al.* From molecules to materials: engineering new ionic liquids crystals through halogen bonding. **JoVE (Journal of Visualized Experiments)**, n. 133, p. e55636, 2018.
- CEYLAN, Ü. *et al.* (2-Hydroxyethyl)triphenylphosphonium chloride. **Acta Crystallographica Section E: Structure Reports Online**, v. 67, n. 3, p. o641-o641, 2011.
- CHAI, J.; HEAD-GORDON, M. Systematic optimization of long-range corrected hybrid density functionals. **The Journal of Chemical Physics**, v. 128, n. 8, p. 084106, 2008.
- CLAYDEN, J; GREEVES, N.; WARREN, S. **Organic Chemistry**. 2nd edition, Oxford: Oxford University Press, 2012.
- CONSTANTINESCU, T.; LUNGU, C. N.; LUNG I. Lipophilicity as a central component of drug-like properties of chalcones and flavonoid derivatives. **Molecules**, v. 24, n. 8, p. 1505, 2019.
- CRAMER, C. J. **Essentials of Computational Chemistry: Theories and Models**. NY, Wiley, 2004.
- CREMER, D. Moller-Plesset perturbation theory: from small molecule methods to methods for thousands of Atoms. **Wiley Interdisciplinary Reviews: Computational Molecular Science**, v. 1, n. 4, p. 509-530, 2011.
- DE RUYCK, J. *et al.* Molecular docking as a popular tool in drug design, an *in silico* travel. **Advances and Applications in Bioinformatics and Chemistry: AABC**. v. 9, p. 1- 11, 2016.
- DESLONGCHAMPS, P. Stereoelectronic control in the cleavage of tetrahedral intermediates in the hydrolysis of esters and amides. **Tetrahedron**, v. 31, n. 20, p. 2463-2490, 1975.
- ECHENIQUE, P.; ALONSO, J. L. A Mathematical and computational review of Hartree-Fock SCF methods in quantum chemistry. **Molecular Physics**, v. 105, n. 23-24, p. 3057-3098, 2007.
- EGELE, P. *et al.* Bioaccumulation of lindane and hexachlorobenzene by tubificid sludgeworms (Oligochaeta) under standardised laboratory conditions. **Chemosphere**, v. 35, n. 4, p. 835-852, 1997.
- ELIEL, E. L. Conformational analysis in mobile cyclohexane systems. **Angewandte Chemie International Edition**, v. 4, n. 9, p. 761- 774, 1965.
- ELIEL, E. L.; WILEN, S. H. **Stereochemistry of Organic Compounds**. 1st, Wiley, 1994.

- ENOMOTO-ROGERS, Y. *et al.* Conformation analysis of D-glucaric acid in deuterium oxide by NMR based on its  $J_{\text{H},\text{H}}$  and  $J_{\text{C},\text{H}}$  coupling constants. **Magnetic Resonance in Chemistry**, v. 54, n. 7, p. 561-567, 2016.
- ERXLEBEN, N. D.; KEDZIORA, G. S.; URBAN, J. J. *Anomeric* effects in fluoro and trifluoromethyl piperidines: a computational study of conformational preferences and hydration. **Theoretical Chemistry Accounts**, v. 133, p. 1491, 2014.
- ETO, M. Functions of phosphorus moiety in agrochemical molecules. **Bioscience, Biotechnology, Biochemistry**, v. 61, n. 1, p. 1-11, 1997.
- EVIDENTE, A.; ANDOLFI, A.; CIMMINO, A. Relationships between the stereochemistry and biological activity of fungal phytotoxins. **Chirality**, v. 23, n. 9, p. 674-693, 2011.
- FAN, J.; FU, A.; ZHANG, L. Progress in molecular docking. **Quantitative Biology**, v. 7, n. 2, p. 83-89, 2019.
- FANG, Z. *et al.* Synthesis of organic liquid crystals containing selectively fluorinated cyclopropanes. **Beilstein Journal of Organic Chemistry**, v. 16, p. 674-680, 2020.
- FISHMAN, B. E.; GIANUTSOS, G. Inhibition of 4-aminobutyric acid (GABA) turnover by chlordane. **Toxicology Letters**, v. 26, n. 2-3, p. 219-223, 1985.
- FUJIWARA, T.; O'HAGAN, D. Successful fluorine-containing herbicide agrochemicals. **Journal of Fluorine Chemistry**, v. 167, p. 16-29, 2014.
- FUKUTO, T. R. Mechanism of action of organophosphorus and carbamate insecticides. **Environmental Health Perspectives**, v. 87, p. 245-254, 1990.
- GEROTHANASSIS, I. P. *et al.* Nuclear magnetic resonance (NMR) spectroscopy: basic principles and phenomena, and their applications to chemistry, biology and medicine. **Chemistry Education Research and Practice**, v. 3, n. 2, p. 229-252, 2002.
- GIMBERT, C. *et al.* Michael additions catalyzed by phosphines. An overlooked synthetic method. **Tetrahedron**, v. 61, n. 36, p. 8598- 8605, 2005.
- GOLDSTEIN, S. J.; SLEMMONS, A. K.; CANAVAN, H. E. Energy-dispersive X-ray fluorescence methods for environmental characterization of soils. **Environmental science & technology**, v. 30, n. 7, p. 2318-2321, 1996.
- GÓMEZ, P. C.; PACIOS, L. F. Environmental effects on proton transfer in a strong hydrogen bond dimer: the 4-methyl-imidazole-aspartate Case. **Physical Chemistry Chemical Physics**, v. 7, n. 7, p. 1374-1381, 2005.
- GOODMAN, L.; GU, H.; POPHRISTIC, V. *Gauche* effect in 1,2-difluoroethane. hyperconjugation, bent bonds, steric Repulsion. **The Journal of Physical Chemistry A**, v. 109, n. 6, p. 1223-1229, 2005.
- GOOSEMAN, N. E. J. *et al.* An electrostatic *gauche* effect in  $\beta$ -fluoro- and  $\beta$ -hydroxy-*N*-ethylpyridinium cations. **Angewandte Chemie International Edition**, v. 46, n. 31, p. 5904-5908, 2007.

GRIMME, S. *et al.* A consistent and accurate *ab initio* parametrization of density functional dispersion correction (DFT-D) for the 94 elements H-Pu. **The Journal of Chemical Physics**, v. 132, n. 15, p. 154104, 2010.

GRIMME, S.; EHRLICH, S.; GOERIGK, L. Effect of the damping function in dispersion corrected density functional theory. **Journal of Computational Chemistry**, v. 32, n. 7, p. 1456-1465, 2011.

GÜNTHER, H. **NMR Spectroscopy - Basic Principles, Concepts, and Applications in Chemistry**. 2<sup>nd</sup> edition, Chichester: Wiley, 1995.

HAMMAN, S. *et al.* Conformational studies on 2-fluoro-1,2-disubstituted ethanes by NMR spectroscopy. Influence of electronegativity on vicinal proton-proton and fluorine-proton coupling constants. **Organic Magnetic Resonance**, v. 21, n. 6, p. 361-366, 1983.

HARRIS, R. K. **Nuclear magnetic resonance spectroscopy. A physicochemical view**. Massachusetts: Pitman Publishing 1983.

HERRERA, M.; SERRA, R. M.; D'AMICO, I. DFT-inspired methods for quantum thermodynamics. **Scientific Reports**, v. 7, n. 1, p. 1-11, 2017.

HILLISCH, A.; HEINRICH, N.; WILD, H. Computational chemistry in the pharmaceutical industry: from childhood to adolescence. **ChemMedChem**, v. 10, n. 12, p. 1958-1962, 2015.

HIRST, A. R. *et al.* Two-component dendritic gel: effects of stereochemistry on the supramolecular chiral assembly. **Chemistry – A European Journal**, v. 10, n. 23, p. 5901-5910, 2004.

HOFFMANN, R. A.; FORSÉN, S.; GESTBLOM, B. **NMR Basic principles and progress**. NY, Springer, 1971.

HOHENBERG, P.; KOHN, W. Inhomogeneous electron gas. **Physical Reviews**, v. 136, n. 3B, p. B864, 1964.

HUSSAIN, M.; SARACCO, G.; RUSSO, N. X-Ray spectroscopy tools for the characterization of nanoparticles, **X-Ray Spectroscopy**, Shatendra K. Sharma, IntechOpen. 2012. Available from: <https://www.intechopen.com/books/x-ray-spectroscopy/x-ray-spectroscopy-tools-for-the-characterization-of-nanoparticles>.

HUTCHINS, R. O.; KOPP, L. D.; ELIEL, E. L. Repulsion of *syn*-axial electron pairs. The “Rabbit-Ear Effect”. **Journal of the American Chemical Society**, v. 90, n. 25, 7174-7175, 1968.

ILARI, A.; SAVINO, C. Protein structure determination by X-ray crystallography. **Bioinformatics**, v. 452, p. 63-87, 2008.

JENSEN, F. **Introduction to Computational Chemistry**. 2nd, NY, Wiley, 2007.

KANAZAWA, A.; IKEDA, T.; ENDO, T. Synthesis and antimicrobial activity of dimethyl- and trimethyl-substituted phosphonium salts with alkyl chains of various lengths. **Antimicrobial Agents and Chemotherapy**, v. 38, n. 5, p. 945-952, 1994.

- KARPLUS, M. Vicinal proton coupling in nuclear magnetic resonance. **Journal of the American Chemical Society**, v. 85, n. 18, p. 2870-2871, 1963.
- KIM, C. S.; BROWN, G. E.; RYTUBA, J. J. Characterization and speciation of mercury-bearing mine wastes using X-ray absorption spectroscopy. **The Science of the Total Environment**, v. 261, n. 1-3, p. 157-168, 2000.
- KLABOE, P.; NIELSEN, R. Infrared and Raman spectra of fluorinated ethanes. XIII. 1,2-Difluoroethane. **The Journal of Chemical Physics**, v. 33, n. 6, p. 1764-1774, 1960.
- KOHN, W.; SHAM, L. J. Self-consistent equations including exchange and correlation effects. **Physical Review**, v. 140, n. 4A, p. A1133-A1138, 1965.
- KRISHNAN, V. V.; RUPP, B. Macromolecular structure determination: comparison of X-ray crystallography and NMR spectroscopy. **eLS**, 2012.
- LAI, C. T. *et al.* Rational modulation of the induced-fit conformational change for slow-onset inhibition in *Mycobacterium Tuberculosis* InhA. **Biochemistry**, v. 54, n. 30, p. 4683-4691, 2015.
- LEVITT, M. H. **Spin dynamics: basics of nuclear magnetic resonance**. John Wiley & Sons, 2nd edition, 2013.
- LIANG, X. *et al.* Highly efficient C—Cl bond cleavage and unprecedented C—C bond cleavage of environmentally toxic DDT through molecular electrochemical catalysis. **Applied Catalysis A: General**, v. 545, p. 44-53, 2017.
- Li, L. *et al.* Syntheses of Sugar Poly(orthoesters) Through reverse *anomeric* effect. **Chemical Communications**, v. 51, n. 32, p. 6972-6975, 2015.
- MAITI, A.; YADAV, J. S. One-pot oxidation and Wittig olefination of alcohols using o-iodoxybenzoic acid and stable Wittig ylide. **Synthetic Communications**, v. 31, n. 10, p. 1499-1506, 2001.
- MANLY, C. J.; LOUISE-MAY, S.; HAMMER, J. D. The impact of informatics and computational chemistry on synthesis and screening. **Drug Discovery Today**, v. 6, n. 21, p. 1101-1110, 2001.
- MCKEEN, L. W. **Film Properties of Plastics and Elastomers**. 3<sup>th</sup> edition, Elsevier, p. 255-313, 2012.
- MENDEZ, L. *et al.* Looking back, looking forward at halogen bonding in drug discovery. **Molecules**, v. 22, n. 9, p. 1397-1412, 2017.
- MENG, X. Y. *et al.* Molecular docking: a powerful approach for structure-based drug discovery. **Current Computer-Aided Drug Design**, v. 7, n. 2, p. 146-157, 2011.
- MISUZISHIMA, S. **Structure of Molecules and Internal Rotation**. 1<sup>st</sup>, Elsevier, 1954.

MIYAJIMA, T.; KURITA, Y.; HIRANO, T. Conformational energies of 1,2-difluoroethane: an *ab initio* molecular orbital study. **Journal of Physical Chemistry**, v. 91, n. 15, p. 3954-3959, 1987.

MOITESSIER, N.; ENGLEBIENNE, P.; CHAPLEUR, Y. Directing-protecting groups for carbohydrates. Design, conformational study, synthesis and application to regioselective functionalization. **Tetrahedron**, v. 61, n. 28, p. 6839-6853, 2005.

MORIARTY, R. M. *et al.* Hypervalent iodine oxidation of silyl enol ethers under Lewis-acid conditions in methanol. A general route to  $\alpha$ -methoxy ketones. **The Journal of Organic Chemistry**, v. 52, n. 1, p. 150-153, 1987.

NEUGEBAUER, J.; HICKEL, T. Density functional theory in materials science. **Wiley Interdisciplinary Reviews: Computational Molecular Science**, v. 3, n. 5, p. 438-448, 2013. NIIDE, Y. *et al.* Microwave spectrum of *gauche* 1-bromo-2-fluoroethane. **Journal of Molecular Spectroscopy**, v. 115, n. 2, p. 305-315, 1986.

NIIDE, Y.; OHKOSHI, I. Microwave spectrum of *gauche* 1-iodo-2-fluoroethane. **Journal of Molecular Spectroscopy**, v. 140, n. 2, p. 301-310, 1990.

O'HAGAN, D. Fluorine in health care: organofluorine containing blockbuster drugs. **Journal of Fluorine Chemistry**, v. 131, n. 11, p. 1071-1081, 2010.

O'HAGAN, D. Understanding organofluorine chemistry. An introduction to the C—F bond. **Chemical Society Reviews**, v. 37, n. 2, p. 308-319, 2008.

O'HAGAN, D.; YOUNG, R. J. Accurate Lipophilicity ( $\log P$ ) Measurements inform on subtle stereoelectronic effects in fluorine chemistry. **Angewandte Chemie International Edition**, v. 55, n. 12, p. 3858-3860, 2016.

ORLOFF, H. D. The stereoisomerism of cyclohexane derivatives. **Chemical Reviews**, v. 54, n. 3, p. 347-447, 1954.

OUELLETTE, R. J.; RAWN, J. D. **Organic chemistry: structure, mechanism and synthesis**. Elsevier. p. 87-126, 2018.

PAGADALA, N. S.; SYED, K.; TUSZYNSKI, J. Software for molecular docking: a review. **Biophysical Reviews**, v. 9, n. 2, p. 91-102, 2017.

PETER, J. V.; SUDARSAN, T. I.; MORAN, J. L. Clinical features of organophosphate poisoning: a review of different classification systems and approaches. **Indian Journal of Critical Care Medicine**, v. 18, n. 11, p. 735-745, 2014.

PICKNETT, T. M.; BRENNER, S. **X-Ray Crystallography**. In Encyclopedia of Genetics; Elsevier: Amsterdam, The Netherlands, v. 219, p. 2154, 2001.

POMES, A.; RODRÍGUEZ-FARRÉ, E.; SUÑOL, C. Disruption of GABA-dependent chloride flux by cyclodienes and hexachlorocyclohexanes in primary cultures of cortical neurons. **Journal of Pharmacology and Experimental Therapeutics**, v. 271, n. 3, p. 1616-1623, 1994.

POPHRISTIC, V.; GOODMAN, L. Hyperconjugation not steric repulsion leads to the staggered structure of ethane. **Nature**, v. 411, n. 6837, p. 565- 568, 2001.

PUIU, D. *et al.* Mobility of some high persistent organochlorine compounds from soil to *Mentha Piperita*. **Revista de Chimie**, v. 70, n. 1, p. 278-282, 2019.

RABLEN, P. R. *et al.* Is hyperconjugation responsible for the “*gauche* effect” in 1-fluoropropane and other 2-substituted-1-fluoroethanes?. **Journal of Chemical Society, Perkin Transaction 2**, n. 8, p 1719-1726, 1999.

RAMASAMI, P. Theoretical gas phase study of *gauche* and *trans* conformers of 1-fluoro-2-haloethanes CH<sub>2</sub>F-CH<sub>2</sub>X (X = Cl, Br, I) by *ab initio* and density functional methods: absence of *gauche* effect. In *International Conference on Computational Science*. Springer, Berlin, Heidelberg, p 153-160, 2006.

RAUGEI, S.; GERVASIO, F. L.; CARLONI, P. DFT Modeling of biological systems. **Physica Status Solidi (B)**, v. 243, n. 11, p. 2500-2515, 2006.

RAUK, A. **Orbital Interaction Theory of Organic Chemistry**. 2<sup>nd</sup> edition, John Wiley & Sons, Inc., 2004.

REN, Y.; YAMATAKA, H. The  $\alpha$ -effect in gas-phase S<sub>N</sub>2 reactions: existence and the origin of the effect. **The Journal of Organic Chemistry**, v. 72, n. 15, p. 5660-5667, 2007.

RIEL, A. M. S. *et al.* Hydrogen bond enhanced halogen bonds: a synergistic interaction in chemistry and biochemistry. **Accounts of Chemical Research**, v. 52, n. 10, p. 2870-2880, 2019.

ROWLAND, R. S.; TAYLOR, R. Intermolecular nonbonded contact distances in organic crystal structures: comparison with distances expected from Van Der Waals radii. **The Journal of Physical Chemistry**, v. 100, n. 18, p. 7384-7391, 1996.

SAGARA, T. *et al.* Binding energies of hydrogen molecules to isoreticular metal-organic framework materials. **The Journal of Chemical Physics**, v. 123, n. 1, p. 014701, 2005.

SANTSCHI, N. *et al.* The sulfur-fluorine *gauche* effect in coinage-metal complexes: augmenting conformational equilibria by complexation. **Organometallics**, v. 35, n. 17, p. 3040-3044, 2016.

SHARGH, D. N.-; BOGGS, J. E. Complete basis set, hybrid-DFT study, and NBO interpretations of the conformational behavior of 1,2-dihaloethanes. **Structural Chemistry**, v. 22, p. 253-262, 2011.

SILVA, D. R. *et al.* The *gauche* effect in XCH<sub>2</sub>CH<sub>2</sub>X revisited. **ChemPhysChem**, v. 22, n. 7, p.641-648, 2021.

SLATER, J. C. A simplification of the Hartree-Fock method. **Physical Review**, v. 81, n. 3, p. 385, 1951.

TANG, H. *et al.* Conformational changes in novel thermotropic liquid crystalline polymer without conventional mesogens: a Raman spectroscopic investigation. **Polymer**, v. 51, n. 23, p. 5482-5489, 2010.

TAVASLI, M. *et al.* The Fluorine *gauche* effect. Langmuir isotherms report the relative conformational stability of ( $\pm$ )-*erythro*- and ( $\pm$ )-*threo*-9,10-difluorostearic acids. **Chemical Communications**, n. 11, p. 1226-1227, 2002.

TERUI, Y. *et al.* Conformational studies of quaternary ammonium ions – I:  $^1\text{H}$  NMR study of  $\beta$ -substituted ethyltrimethylammonium halides: importance of electrostatic interactions in conformational control. **Tetrahedron**, v. 30, n. 11, p. 1465-1471, 1974.

THEODORIDIS, G. Fluorine-containing agrochemicals: an overview of recent developments. **Advances in Fluorine Science**, v. 2, p. 121-175, 2006.

THIEHOFF, C. *et al.* Can acyclic conformational control be achieved *via* a sulfur-fluorine *gauche* effect?. **Chemical Science**, v. 6, n. 6, p. 3565-3571, 2015.

THIEHOFF, C. *et al.* The influence of electronic perturbations on the sulfur-fluorine *gauche* effect. **Journal of Fluorine Chemistry**, v. 182, p. 121-126, 2016.

THIEHOFF, C.; REY, Y. P.; GILMOUR, R. The fluorine *gauche* effect: a brief history. **Israel Journal of Chemistry**, v. 57, p. 92-100, 2017.

TORMENA, C. F. Conformational analysis of small molecules: NMR and quantum mechanics calculations. **Progress in Nuclear Magnetic Resonance Spectroscopy**, v. 96, p. 73-88, 2016.

WOLFE, S. The *gauche* effect. Some stereochemical consequences of adjacent electron pairs and polar bonds. **Accounts of Chemical Research**, v. 5, n. 3, p. 102-111, 1972.

WOLFE, S.; WHANGBO, M.- H; MITCHELL, D. J. On the magnitudes and origins of the “anomeric effects”, “*exo-anomeric* effects”, “*reverse anomeric* effects”, and CX and CY bond-lengths in  $\text{XCH}_2\text{YH}$  molecules. **Carbohydrate Research**, v. 69, n. 1, p. 1-26, 1979.

XUE, Y.; XIAO, H.; ZHANG, Y. Antimicrobial polymeric materials with quaternary ammonium and phosphonium salts. **International Journal of Molecular Sciences**, v. 16, n. 2, p. 3626-3655, 2015.

YANAI, T.; TEW, D. P.; HANDY, N. C. A new hybrid exchange-correlation functional using the Coulomb-attenuating method (CAM-B3LYP). **Chemical Physics Letters**, v. 393, n. 1-3, p. 51-57, 2004.

YANG, N. J.; HINNER, M. J. Getting across the cell membrane: an overview for small molecules, peptides, and proteins. **Methods in Molecular Biology**, v. 1266, p. 29-53, 2015.

YOUNG, M. D.; BORJEMSCAIA. N. C.; WLADKOWSKI, B. D. Quantitative determination of the rotameric energy differences of 1,2-dihaloethanes using Raman spectroscopy. An experimental project for the physical chemistry laboratory. **Journal of Chemical Education**, v. 82, n. 6, p. 912-915, 2005.

ZHANG, A. *et al.* Understanding the conformational impact of chemical modifications on monoclonal antibodies with diverse sequence variation using hydrogen/deuterium exchange mass spectrometry and structural modeling. **Analytical Chemistry**, v. 86, n. 7, p. 3468-3475, 2014.

ZHDANKIN, V. V. **Hypervalent Iodine Chemistry: Preparation, Structure, and Synthetic Applications of Polyvalent Iodine Compounds**. 1<sup>th</sup> edition, John Wiley & Sons. p.1-15, 2014.

ZIMMER, L. E.; SPARR, C.; GILMOUR, R. Fluorine conformational effects in organocatalysis: an emerging strategy for molecular design. **Angewandte Chemie International Edition**, v. 50, n. 50, p. 11860-11871, 2011.

## **SECOND PART**

### **Stereoelectronic Impact of the Fluorine Atom**

## The fluorine *gauche* effect and a comparison with other halogens in 2-halofluoroethanes and 2-haloethanols

Francisco A. Martins, Matheus P. Freitas - *European Journal of Organic Chemistry*, 37 (2019) 6401- 6406. Copyright Wiley-VCH GmbH. Reproduced with permission.

**Abstract:** While the *gauche* effect in 1,2-difluoroethane is widely known as being due to hyperconjugative interactions between  $\sigma_{\text{CH}}$  electron-donating orbitals and  $\sigma^*_{\text{CF}}$  electron-accepting orbitals, the corresponding 1,2-dichloro, 1,2-dibromo and 1,2-diiodo derivatives are preferentially in the *anti* conformation. 2-Halofluoroethanes ( $\text{F}-\text{CH}_2-\text{CH}_2-\text{X}$ ) combine a small halogen (fluorine) and a vicinal low-lying energy antibonding orbital ( $\sigma^*_{\text{CX}}$ ) that activates a stabilizing antiperiplanar  $\sigma_{\text{CH}} \rightarrow \sigma^*_{\text{CX}}$  electron delocalization, which can induce the *gauche* effect. On the other hand,  $\sigma_{\text{CX}}$  orbitals are good electron donors to  $\sigma^*_{\text{CF}}$ , that would favor an “*anti* effect”, in addition to traditional interpretations based on steric and electrostatic repulsion. Therefore, a balance of steric, dipolar and hyperconjugative effects drive the conformational equilibrium of these compounds – hyperconjugation was found to explain the *gauche* effect in some cases, whilst Lewis-type interactions determine the *anti* preference in others. The *gauche* effect takes place in a polar solvent, but not for 1-fluoro-2-iodoethane. According to NMR three-bond spin-spin coupling constants, the *gauche* population increases when fluorine is replaced by a hydroxyl group (except for 2-fluoroethanol relative to 1,2-difluoroethane), but this is not primarily due to intramolecular hydrogen bond.

### Introduction

1,2-Difluoroethane is a benchmark compound exhibiting the *gauche* effect (Figure 1),<sup>[1]</sup> that has *a tendency to adopt that structure which has the maximum number of gauche interactions between the adjacent electron pairs and/or polar bonds*.<sup>[1a]</sup> This behavior is counterintuitive if only traditional steric and electrostatic interactions are taken into consideration, because these repulsive interactions would lead to a preference for the *anti* conformation. In turn, the *gauche* effect in *e.g.* 1,2-difluoroethane can be accounted for stabilizing antiperiplanar hyperconjugative interactions between  $\sigma_{\text{CH}}$  electron-donating orbitals and  $\sigma^*_{\text{CF}}$  electron-accepting orbitals, which are allowed in the *gauche* conformation. However, it is well-known that  $\sigma^*_{\text{CX}}$  antibonding orbitals ( $\text{X} = \text{Cl}, \text{Br}$  and  $\text{I}$ ) lie at a lower energy level than  $\sigma^*_{\text{CF}}$  due to a dominance of the interaction matrix element (overlap dependence, which decreases rapidly across the series  $\text{X} = \text{F}, \text{Cl}, \text{Br}, \text{I}$ ) and, based on the energy splitting of the donor and acceptor orbitals,  $\sigma_{\text{CH}} \rightarrow \sigma^*_{\text{CX}}$  hyperconjugative interactions are anticipated to be more stabilizing than  $\sigma_{\text{CH}} \rightarrow \sigma^*_{\text{CF}}$  electron delocalization.<sup>[2]</sup> On the other hand, earlier studies demonstrated that conformers of 1,2-dihaloethanes (halo = Cl, Br and I) are preferentially in

the *anti* conformation, because steric effect between *gauche* halogens overrides hyperconjugative interactions and also due to stabilizing  $\sigma_{\text{CX}} \rightarrow \sigma^*_{\text{CX}}$  interactions in the *anti* conformer.<sup>[3]</sup>

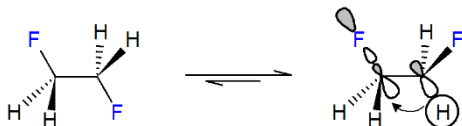


**Figure 1.** *Gauche* effect in 1,2-difluoroethane due to  $\sigma_{\text{CH}} \rightarrow \sigma^*_{\text{CF}}$  hyperconjugation.

This work reports a spectroscopic (NMR) and theoretical conformational study of 2-halofluoroethanes, which have both small and large halogens, as well as bonding and antibonding orbitals with different electron-donating/accepting capabilities, in order to probe the role of steric and hyperconjugative interactions on the conformational equilibrium of these compounds. Although simple, these compounds display structural properties that can be useful to explore: they are 1,2-disubstituted ethanes and organofluorine compounds, whose framework is widely found in pharmaceutical, agrochemical, and material sciences.<sup>[4]</sup> Thus, conformational modulation through stereoelectronic interactions, such as the fluorine *gauche* effect, may be harnessed for the design of performance molecules.

1-Bromo- and 1-chloro-2-fluoroethanes have been found to be preferentially *anti* in the gas phase, and mainly *gauche* in a liquid, solid or solution.<sup>[5]</sup> The reasons for these behaviors are unclear, though. In addition, only the *gauche* form for 1-fluoro-2-iodoethane has been observed through microwave spectroscopy;<sup>[6]</sup> actually, 1-fluoro-2-iodoethane appears to be the most interesting case within this series of compounds, since its conformational equilibrium has not been determined in solution yet and it contains both the largest of these halogens and the best electron-accepting/donating orbital for hyperconjugation. Moreover, replacement of the fluorine substituent by a hydroxyl group provides information about the role of a possible OH···X intramolecular hydrogen bond<sup>[7]</sup> on the conformational equilibrium compared to the fluorine *gauche* effect. Previous work on these systems<sup>[7i]</sup> did not account for Lewis-type analysis to evaluate the contributions from hyperconjugation, H-bond and steric/electrostatic interactions to the conformational equilibrium. The large *gauche* preference in protonated 2-fluoroethylamine and 2-fluoroethanol has been attributed either to an intramolecular F···H bond or to an electrostatic F···O<sup>+</sup>/N<sup>+</sup> interaction.<sup>[8]</sup>

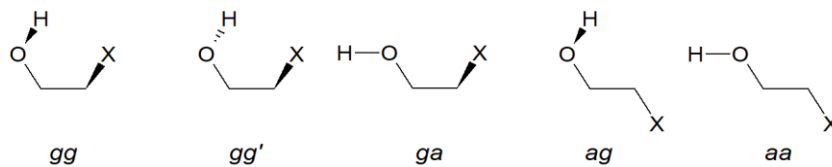
## Results and Discussion

*Ab initio* calculations for the 2-halofluoroethanes in the gas phase indicate that the *gauche* effect takes place only for 1,2-difluoroethane (Table 1), despite the less stabilizing  $\sigma_{\text{CH}} \rightarrow \sigma^*_{\text{CF}}$  interaction compared to  $\sigma_{\text{CH}} \rightarrow \sigma^*_{\text{CX}}$  hyperconjugation (Table 2). Thacker and Popelier explained the fluorine *gauche* effect in 1,2-difluoroethane in terms of a 1,3 F···C electrostatic polarization interaction;<sup>[9]</sup> however, this interpretation is not supported by geometric parameters obtained for the optimized structures of *gauche* ( $\angle_{\text{CCF}} = 110.3^\circ$  and  $d_{\text{F1} \cdots \text{C2}} = 2.375 \text{ \AA}$ ) and *anti* ( $\angle_{\text{CCF}} = 107.9^\circ$  and  $d_{\text{F1} \cdots \text{C2}} = 2.352 \text{ \AA}$ ) 1,2-difluoroethane, nor by the well-known statement that intramolecular interactions with organic fluorine forming five-membered rings or less are not stable.<sup>[10]</sup> The behavior of other 2-halofluoroethanes compared to 1,2-difluoroethane can be explained on the basis of a traditional repulsion model, because the *gauche* conformer becomes sterically disfavored as the halogen at C2 increases in size. Moreover, the second-order perturbation analysis of donor-acceptor interactions in the natural bond orbitals (NBOs) (Table 2) indicates that the  $\sigma_{\text{CX}} \rightarrow \sigma^*_{\text{CF}}$  interaction, which is active in the *anti* conformation, is highly stabilizing and even overcomes the  $\sigma_{\text{CH}} \rightarrow \sigma^*_{\text{CF}}$  interaction in **FI**. These orbital interaction energies are affected by an orbital overlap component [represented by the element of the Fock matrix describing the donor-acceptor interactions –  $F(i,j)$ ] and by the energy splitting of the donor and acceptor orbitals ( $\varepsilon_i - \varepsilon_j$ ). Despite the  $F(\sigma_{\text{CH}}, \sigma^*_{\text{CF/Cl}})$  values for the *gauche* conformation of **FF** and **FI** are similar, the energy gap  $\varepsilon_{\sigma_{\text{CH}}} - \varepsilon_{\sigma^*_{\text{CI}}}$  is smaller than  $\varepsilon_{\sigma_{\text{CH}}} - \varepsilon_{\sigma^*_{\text{CF}}}$ , thus enhancing the orbital interaction energy in **FI** (Supporting Information). On the other hand, both  $F(\sigma_{\text{CX}}, \sigma^*_{\text{CF}})$  and  $\varepsilon_{\sigma_{\text{CX}}} - \varepsilon_{\sigma^*_{\text{CF}}}$  terms indicate a more effective orbital interaction in *anti FI* than in *anti FF*. Overall, the non-Lewis-type interactions owing to electron delocalization favor the *gauche* conformation in all 2-halofluoroethanes, whilst Lewis-type interactions, namely steric plus electrostatic effects, disfavor this conformer by a larger amount, except for **FF** (Table 2). Thus, the conformational equilibrium of 2-halofluoroethanes appears to be similar to that of X–CH<sub>2</sub>–CH<sub>2</sub>–X.<sup>[3]</sup> However, electrostatic components mask the role of steric and stabilizing orbital interactions; the latter intramolecular interactions are not strongly affected by the environment, while the former significantly change with the medium.<sup>[11]</sup>

The relative importance of dipolar interactions on the conformer energies can be evaluated by analyzing the solvent effect on the conformational equilibrium, since the repulsion originated from the interaction between the local dipoles C–X and C–F bonds attenuates as the solvent polarity increases. Indeed, in an environment where steric and hyperconjugative effects

override electrostatic interactions, the *gauche* population increases in comparison to the gas phase and the *gauche* effect appears when hyperconjugation is the dominating factor (see Lewis and non-Lewis energies obtained using solvation models in Supporting Information). The *gauche* effect does not appear for **FI** though, even considering the highly polar solvent DMSO (according to an implicit solvation model – Table 1 and Figure 2); because the *anti* conformation of **FI** remains stabilized by a  $\sigma_{\text{Cl}} \rightarrow \sigma^*_{\text{CF}}$  interaction, the overall non-Lewis contribution that still favors the *gauche* conformation is counterbalanced by the Lewis-type contributions (nearly reduced to steric effects in DMSO) that destabilizes this conformation.

**Table 1.** Relative conformational standard Gibbs free energies (in kcal mol<sup>-1</sup>) and conformer populations (%, in parenthesis) for the studied 2-halofluoroethanes and 2-haloethanols in the gas phase and implicit solvents, obtained at the MP2/6-311++g(d,p) level (def2 TZVP was used for bromine and iodine atoms, and ECP was included to the iodine atom).



Cpd.	Structure	Conf.	$\Delta G^0_{\text{gas}}$	$\Delta G^0_{\text{CHCl}_3}$	$\Delta G^0_{\text{DMSO}}$
<b>FF</b>	F–CH <sub>2</sub> –CH <sub>2</sub> –F	<i>g</i>	0.00 (78)	0.00 (94)	0.00 (97)
		<i>a</i>	0.74 (22)	1.61 (6)	2.09 (3)
<b>FC</b>	F–CH <sub>2</sub> –CH <sub>2</sub> –Cl	<i>g</i>	0.50 (30)	0.00 (63)	0.00 (78)
		<i>a</i>	0.00 (70)	0.31 (37)	0.74 (22)
<b>FB</b>	F–CH <sub>2</sub> –CH <sub>2</sub> –Br	<i>g</i>	0.87 (19)	0.03 (49)	0.00 (66)
		<i>a</i>	0.00 (81)	0.00 (51)	0.40 (34)
<b>FI</b>	F–CH <sub>2</sub> –CH <sub>2</sub> –I	<i>g</i>	1.20 (12)	0.51 (30)	0.12 (45)
		<i>a</i>	0.00 (88)	0.00 (70)	0.00 (55)
<b>OF</b>	HO–CH <sub>2</sub> –CH <sub>2</sub> –F	<i>gg</i>	0.00 (84)	0.00 (62)	0.00 (44)
		<i>gg'</i>	2.33 (2)	1.16 (9)	0.55 (17)
		<i>ga</i>	1.46 (7)	0.58 (23)	0.16 (35)
		<i>ag</i>	2.22 (2)	1.89 (3)	1.77 (2)
		<i>aa</i>	1.70 (5)	1.72 (3)	1.77 (2)
<b>OC</b>	HO–CH <sub>2</sub> –CH <sub>2</sub> –Cl	<i>gg</i>	0.00 (71)	0.00 (51)	0.00 (36)
		<i>gg'</i>	2.26 (2)	1.25 (6)	0.59 (13)
		<i>ga</i>	1.34 (7)	0.49 (22)	0.04 (34)
		<i>ag</i>	1.36 (7)	0.90 (11)	0.78 (10)
		<i>aa</i>	1.03 (13)	0.96 (10)	0.98 (7)
<b>OB</b>	HO–CH <sub>2</sub> –CH <sub>2</sub> –Br	<i>gg</i>	0.00 (75)	0.00 (61)	0.00 (46)
		<i>gg'</i>	2.58 (1)	1.59 (4)	0.85 (11)
		<i>ga</i>	1.59 (5)	0.90 (13)	0.40 (23)
		<i>ag</i>	1.41 (7)	1.02 (11)	0.82 (12)
		<i>aa</i>	1.11 (12)	1.03 (11)	1.03 (8)
<b>OI</b>	HO–CH <sub>2</sub> –CH <sub>2</sub> –I	<i>gg</i>	0.00 (65)	0.00 (48)	0.00 (38)
		<i>gg'</i>	2.29 (1)	1.24 (6)	0.68 (12)
		<i>ga</i>	1.41 (6)	0.75 (14)	0.36 (20)
		<i>ag</i>	1.00 (12)	0.63 (17)	0.43 (18)
		<i>aa</i>	0.81 (16)	0.68 (15)	0.66 (12)

**Table 2.** Lewis (L) and non-Lewis (NL) contributions to the full electronic conformational energies of 2-halofluoroethanes and 2-haloethanols, and important electron delocalization interactions obtained by NBO analysis (data in kcal mol<sup>-1</sup>, for the gas phase molecules).

Cpd	Conf.	$\Delta E_{\text{FULL}}$	$\Delta E_L$	$\Delta E_{\text{NL}}$	$\frac{\sigma_{\text{CH}} \rightarrow}{\sigma^*_{\text{CF/CO}}} \frac{\sigma_{\text{CH}} \rightarrow}{\sigma^*_{\text{CX}}} \frac{\sigma_{\text{CF/CO}} \rightarrow}{\sigma^*_{\text{CH}}} \frac{\sigma_{\text{CX}} \rightarrow}{\sigma^*_{\text{CH}}} \frac{\sigma_{\text{CH}} \rightarrow}{\sigma^*_{\text{CH}}} \frac{\sigma_{\text{CF/CO}} \rightarrow}{\sigma^*_{\text{CX}}} \frac{\sigma_{\text{CX}} \rightarrow}{\sigma^*_{\text{CF/CO}}}$		
<b>FF</b>	<i>g</i>	0.00	7.08	-7.08	4.56 0.67 0.67 4.44	4.56 1.08 -	- 8.16 1.50 1.50
	<i>a</i>	0.80	0.80	0.00	1.08 -	- -	- 4.81 -
<b>FC</b>	<i>g</i>	0.56	3.75	-3.19	4.41 5.32 0.83 1.39	5.32 -	- 9.14 1.81 2.91
	<i>a</i>	0.00	0.00	0.00	1.22 -	- -	- 9.14 1.81 2.91
<b>FB</b>	<i>g</i>	0.88	3.71	-2.83	4.33 6.06 0.87 1.73	6.06 -	- 4.87 -
	<i>a</i>	0.00	0.00	0.00	1.20 -	- -	- 9.34 2.15 3.77
<b>FI</b>	<i>g</i>	1.17	2.85	-1.68	4.34 6.22 0.91 2.19	6.22 -	- 4.94 -
	<i>a</i>	0.00	0.00	0.00	1.24 -	- -	- 9.62 2.23 4.88
<b>OF</b>	<i>gg</i>	0.00	6.26	-6.26	4.02 4.68 0.82 0.84 4.78	4.02 4.68 0.82 0.84 4.78	- -
	<i>gg'</i>	2.56	12.70	-10.10	4.49 4.83 0.71 0.71 4.87	4.49 4.83 0.71 0.71 4.87	- -
	<i>ga</i>	2.10	7.36	-5.26	3.79 4.59 0.87 0.73 4.55	3.79 4.59 0.87 0.73 4.55	- -
	<i>ag</i>	2.40	5.59	-3.19	- 1.07 -	- -	- 8.77 1.68 1.44
	<i>aa</i>	2.17	2.17	0.00	- 1.10 -	- -	- 8.60 1.90 1.35
<b>OC</b>	<i>gg</i>	0.00	5.82	-5.82	4.02 5.52 0.92 1.59 5.04	4.02 5.52 0.92 1.59 5.04	- -
	<i>gg'</i>	2.70	9.51	-6.81	4.36 5.65 0.82 1.40 5.18	4.36 5.65 0.82 1.40 5.18	- -
	<i>ga</i>	2.27	4.51	-2.24	3.59 5.45 1.04 1.44 4.93	3.59 5.45 1.04 1.44 4.93	- -
	<i>ag</i>	1.49	4.47	-2.98	- -	- -	- 9.64 2.04 2.72
	<i>aa</i>	1.51	1.51	0.00	- -	- -	- 9.54 2.35 2.51
<b>OB</b>	<i>gg</i>	0.00	6.35	-6.35	3.92 6.31 0.97 1.87 5.09	3.92 6.31 0.97 1.87 5.09	- -
	<i>gg'</i>	2.71	9.22	-6.51	4.28 6.45 0.87 1.69 5.25	4.28 6.45 0.87 1.69 5.25	- -
	<i>ga</i>	2.38	4.46	-2.08	3.60 6.19 1.12 1.77 5.01	3.60 6.19 1.12 1.77 5.01	- -
	<i>ag</i>	1.31	4.23	-2.92	- -	- -	- 9.80 2.39 3.41
	<i>aa</i>	1.51	1.51	0.00	- -	- -	- 9.70 2.75 3.18
<b>OI</b>	<i>gg</i>	0.00	6.46	-6.46	3.95 6.62 0.98 2.27 5.12	3.95 6.62 0.98 2.27 5.12	- -
	<i>gg'</i>	2.33	7.76	-5.43	4.26 6.63 0.90 2.13 5.29	4.26 6.63 0.90 2.13 5.29	- -
	<i>ga</i>	2.05	3.40	-1.35	3.57 6.40 1.14 2.23 5.09	3.57 6.40 1.14 2.23 5.09	- -
	<i>ag</i>	0.84	3.80	-2.96	- -	- -	- 10.07 2.51 4.31
	<i>aa</i>	1.20	1.20	0.00	- -	- -	- 9.94 2.89 3.97

Replacement of fluorine in 2-halofluoroethanes with a hydroxyl group gives rise to 2-haloethanols, whose X–C–C–OH fragment can experience either an intramolecular hydrogen bond<sup>[18]</sup> or the *gauche* effect, since the C–F and C–O bonds have similar properties regarding polarity and orbital energy levels. However, rotation around the C–O bond originates additional conformers owing to the hydroxyl group orientation either at *gauche* or *anti* positions relative to the C–C bond. In all cases, the potential energy surfaces of Figure 3 indicate that the *gg* conformer, whose O–H bond is directed towards the halogen, is significantly more stable than the others in the gas phase. Despite some spectroscopic evidence that this behavior can be due to an intramolecular hydrogen bond OH…X (stronger when X = F),<sup>[12,13]</sup> others indicate that such interaction may not be an attractive contact<sup>[14]</sup> and that H-bond properties cannot be generally considered to originate from the strong inductive effect of fluorine.<sup>[15]</sup>

From Table 1, the *gauche* preference in 2-haloethanols increases according to **OI** < **OB** ≈ **OC** < **OF**, which is consistent with expectations from both H-bond (stronger H-bond for OH…F) and *gauche* effect perspectives. Regardless whether H-bond determines the conformational equilibrium of *trans*-2-halocyclohexanols or not, their infrared O–H and C–O stretching vibrations show that these bonds are abnormally weaker in the fluorine derivative

than in the other halohydrins (indicating a more effective OH···F engagement).<sup>[12a]</sup> However, the electron delocalization  $n_X \rightarrow \sigma^*_{O-H}$  obtained from NBO analysis, which is a hyperconjugative rather than electrostatic approach for the H-bond, is active in 2-chloro-, 2-bromo- and 2-iodoethanol (ranging from 0.6 to 1.4 kcal mol<sup>-1</sup> stabilizing in this order), but not in 2-fluoroethanol. It is worth mentioning that an electrostatic OH···F H-bond is not necessarily more stabilizing than 0.6–1.4 kcal mol<sup>-1</sup>, since a repulsive through-space  $n_X \rightarrow \sigma_{O-H}$  interaction accompanies the two-electron/two-orbital interaction, and the hyperconjugative H-bond should be therefore dictated by a balance between the attractive and repulsive orbital contributions. Accordingly, if H-bond influences the conformational equilibrium in 2-haloethanols, it is predominantly electrostatic in nature. This is confirmed by the strong solvent dependence of the conformations in 2-haloethanols (Table 1) – a decrease of the gg population from the gas phase to implicit DMSO solvent is observed. Nevertheless, an O···X electrostatic repulsion in the gg' conformation also attenuates as the solvent polarity increases, thus shifting the conformational equilibrium from gg to gg'. It is not obvious if the hydrogen of the hydroxyl group in 2-haloethanols is directed towards the halogen to achieve a stabilizing H-bond or to avoid destabilizing O···X lone pair repulsive interactions. These interactions have been found to be comparable in strength elsewhere,<sup>[16]</sup> while H-bond seems to be absent in a series of aliphatic fluoroalcohols in solution.<sup>[17]</sup>

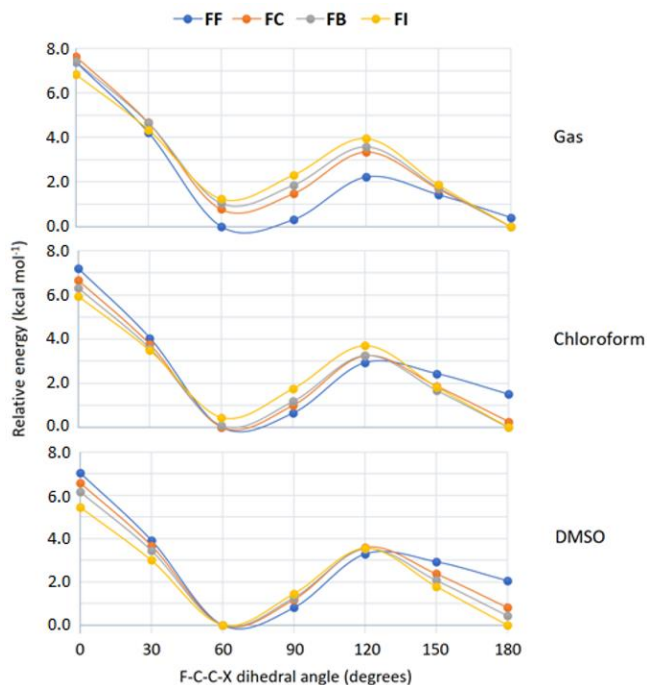


**Figure 2.** Potential energy curves for 2-halofluoroethanes in gas phase and implicit solvents (PCM). **FF** = 1,2-difluoroethane; **FC** = 1-chloro-2-fluoroethane; **FB** = 1-bromo-2-fluoroethane; **FI** = 1-fluoro-2-iodoethane.

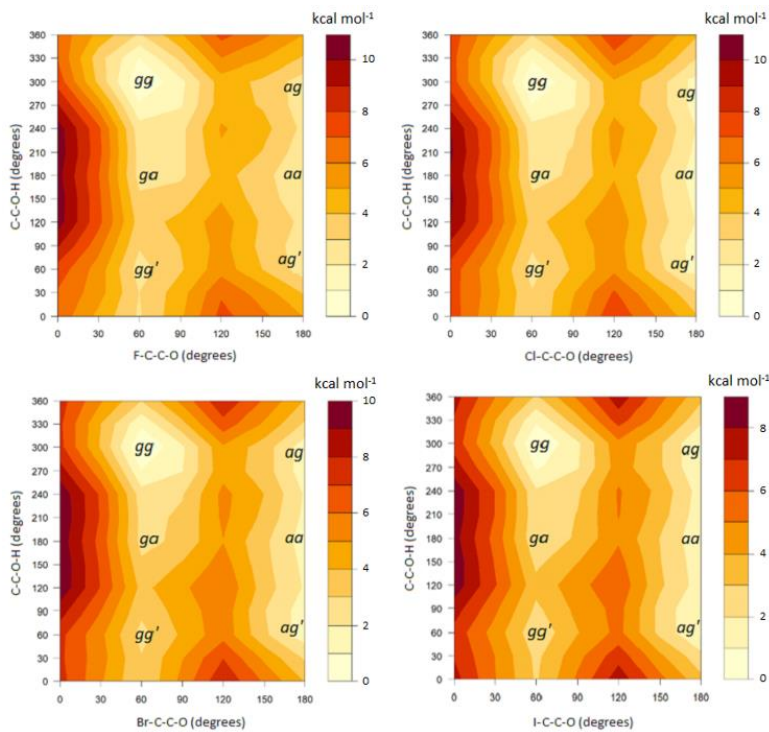


**Figure 3.** Potential energy surfaces for 2-haloethanols in gas phase (rotation around the X–C–C–O and C–C–O–H torsion angles).

It has been claimed that NBO overestimates the role of hyperconjugation on the rotation barrier of ethane;<sup>[18]</sup> therefore, experimental evidence supporting the theoretical outcomes would be useful to better understand the interactions governing the conformational equilibrium of the studied compounds. A comparison between the conformational behavior of 2-haloethanols and the corresponding 2-halofluoroethanes gives insight into the role of H-bond to the conformer stabilization of the halohydrins. While the *gauche* population is larger in 2-haloethanols than in 2-halofluoroethanes when the halogen refers to Cl, Br and I, the opposite behavior is observed comparing the fluorinated derivatives **FF** and **OF** (in solution). This behavior can be experimentally observed using NMR three-bond spin-spin coupling constants (SSCC's) and taking into account the Karplus relationship for the H–C–C–H/F dihedral angle; the two-bond SSCC's appear to be of little diagnostic value (Table 3). Because the experimental *J* values yield an average measure at room temperature, intrinsic SSCC values for each conformer can be calculated theoretically (Supporting Information) to gain insight into approximate conformer populations, according to Eqs. 1 and 2.

$$N_g + N_a = 1 \quad (1)$$

$$^3J_{\text{obs}} = (N_g \times ^3J_g) + (N_a \times ^3J_a) \quad (2)$$

where  $N_g$  and  $N_a$  are the mole ratios of *gauche* and *anti* conformers, respectively,  ${}^3J_{\text{obs}}$  corresponds to the experimental  ${}^3J_{\text{H,H}}$  (obtained from the literature in different solvents), and  ${}^3J_g$  and  ${}^3J_a$  are the intrinsic  ${}^3J_{\text{H,H}}$  values theoretically obtained for the gas phase *gauche* and *anti* conformers (averaged by the calculated populations in the case of 2-haloethanols, where three  $g$  and two  $a$  conformations can exist), respectively (calculated  ${}^3J_{\text{H,H}}$  values did not change significantly with the medium).

**Table 3.** Experimental coupling constants (Hz) for the studied 1,2-disubstituted ethanes.

Name	${}^3J_{\text{HH}}$	${}^3J_{\text{HF}}$	${}^2J_{\text{HF}}$
<b>FF</b>	1.5 and 5.7 (avg. 3.6) <sup>[a]</sup>	30.8 <sup>[a]</sup>	47.9 <sup>[a]</sup>
<b>FC</b>	5.7, <sup>[b]</sup> 6.6 <sup>[c]</sup>	23, <sup>[b]</sup> 20.9 <sup>[c]</sup>	47, <sup>[b]</sup> 47.4 <sup>[c]</sup>
<b>FB</b>	4.9, <sup>[b]</sup> 5.9 <sup>[d]</sup>	18, <sup>[b]</sup> 21.0 <sup>[d]</sup>	46, <sup>[b]</sup> 47.0 <sup>[d]</sup>
<b>FI</b>	6.7 <sup>[b,e]</sup>	18.6 <sup>[b,e]</sup>	46.9 <sup>[b,e]</sup>
<b>OF</b>	4.2 <sup>[f,g]</sup>	30.2, <sup>[f]</sup> 28.2 <sup>[g]</sup>	47.9, <sup>[f]</sup> 48.0 <sup>[g]</sup>
<b>OC</b>	5.0 <sup>[h]</sup>		
<b>OB</b>	5.0 <sup>[i]</sup>		
<b>OI</b>	5.9 <sup>[j]</sup>		

[a] Solvent data not available.<sup>[19]</sup>

[b] Solvent data not available.<sup>[20]</sup>

[c] In  $\text{CDCl}_3$ . [https://www.chemicalbook.com/SpectrumEN\\_762-50-5\\_1HNMR.htm](https://www.chemicalbook.com/SpectrumEN_762-50-5_1HNMR.htm).

[d] In  $\text{CDCl}_3$ . <https://www.sigmaaldrich.com/spectra/fnmr/FNMR008541.PDF>.

[e] In  $\text{C}_6\text{D}_6$ .<sup>[21]</sup>

[f] In  $\text{CDCl}_3$ . <https://www.sigmaaldrich.com/spectra/fnmr/FNMR001832.PDF>.

[g] In  $\text{C}_6\text{Cl}_{12}$ .<sup>[17]</sup>

[h] In  $\text{CDCl}_3$ . <https://www.sigmaaldrich.com/spectra/fnmr/FNMR002360.PDF>.

[i] In  $\text{CDCl}_3$ . <https://www.sigmaaldrich.com/spectra/fnmr/FNMR009498.PDF>.

[j] In  $\text{CDCl}_3$ . <https://www.sigmaaldrich.com/spectra/fnmr/FNMR002123.PDF>.

From the experimental SSCC values available in the literature (Table 3), regardless of measurement uncertainties and the different solvents used to obtain the  ${}^3J_{\text{HH}}$  values, the general trend observed for 2-halofluoroethanes indicates that the *gauche* population increases nearly according to **FI** (33%) < **FC** (36–57%) < **FB** (61–86%) < **FF** (89%). In addition,  ${}^3J_{\text{HH}}$  values are smaller in halohydrins than in 2-halofluoroethanes, except for **OF** relative to **FF**. Accordingly, because  ${}^3J_{\text{HH}}$  and  ${}^3J_{\text{HF}}$  have an opposite trend,  ${}^3J_{\text{HF}}$  in **OF** is smaller than in **FF**. Consequently, the experimentally obtained *gauche* population in **FF** (89%) is larger than that of **OF** (81%); therefore, it is not an OH···F intramolecular hydrogen bond that stabilizes the *gauche* **OF** in solution, but rather the hyperconjugative *gauche* effect caused by  $\sigma_{\text{CH}} \rightarrow \sigma^*_{\text{CO}}$  and  $\sigma_{\text{CH}} \rightarrow \sigma^*_{\text{CF}}$  interactions. According to calculations, the *gg* conformation (in which the O–H bond is directed

towards the halogen) in 2-haloethanols is largely more stable than *gg'* and *ga* (where an oxygen electron lone-pair is directed towards the halogen) in the gas phase, but the corresponding energy difference substantially decreases as the solvent polarity increases. This is consistent with a reduced Lewis-type energy in *gg'* and *ga* in implicit solvents (Supporting Information), while small changes in this term are observed for *gg* going from the gas phase to solution. Thus, H-bond does not seem to dictate the conformational equilibrium of 2-haloethanols.

## Conclusions

2-Halofluoroethanes (except **FF**) do not experience the *gauche* effect in the gas phase, since repulsive interactions in the *gauche* conformer override stabilizing  $\sigma_{\text{CH}} \rightarrow \sigma^*_{\text{CF}}$  (weaker) and  $\sigma_{\text{CH}} \rightarrow \sigma^*_{\text{CX}}$  (stronger) hyperconjugative interactions, rather than because  $\sigma_{\text{CX}} \rightarrow \sigma^*_{\text{CF}}$  interaction in the *anti* conformation would be importantly stabilizing. Such interaction is particularly stabilizing in 1-fluoro-2-iodoethane, which is predominantly *anti* both in the gas phase and solution. However, repulsive Lewis-type interactions in the *gauche* conformation at least cancel out the overall stabilizing non-Lewis interactions of this conformation even in a highly polar medium. Because the *gauche* population increases in solution, since dipolar repulsion in the *gauche* conformer attenuates as the solvent polarity increases, the *gauche* effect just dominates in solution for the chlorine and bromine derivatives, as supported by NMR three-bond spin-spin coupling constants; 1,2-difluoroethane is widely known to exhibit a strong *gauche* effect. Replacement of fluorine in 2-halofluoroethanes by a hydroxyl group leads to an increase of the *gauche* population in the resulting 2-haloethanol, tentatively because the hydroxyl hydrogen directed towards the halogen in a *gauche* conformer yields a smaller Lewis-type energy than a direct O···F contact; therefore, intramolecular hydrogen bond in solution should not be the driving effect of the conformational equilibrium in these cases.

## Computational Section

Potential energy surfaces (PES) for 2-halofluoroethanes (F–C–C–X dihedral rotation) and 2-haloethanols (X–C–C–O and C–C–O–H rotations) were built by scanning the corresponding dihedral angles in steps of 30°, according to calculations at the B3LYP/6-311++(d,p) level of theory.<sup>[22]</sup> The def2 TZVP basis set<sup>[23]</sup> was used for bromine and iodine atoms (for iodine, ECP was used), to account for heavy atom effects and in agreement to earlier studies about systems containing bromine and iodine atoms.<sup>[24]</sup> The energy minima were fully

optimized and the frequencies for the corresponding geometries were computed at the MP2/6-311++(d,p) level of theory<sup>[25]</sup> (def2 TZVP for bromine and iodine atoms). Natural Bonds Orbitals (NBO) analysis was carried out at the B3LYP/6-311++(d,p) level (def2 TZVP for bromine and iodine atoms) to obtain stabilizing orbital interaction energies, as well as the Lewis and non-Lewis contributions to the full electronic energy. Finally, spin-spin coupling constants were calculated at the same level of theory. Calculations were performed in the Gaussian 09 program,<sup>[26]</sup> while the def2 TZVP basis set was obtained from the EMSL Basis Set Exchange (<http://bse.pnl.gov/>).<sup>[27]</sup>

### Acknowledgments

The authors are grateful to Fundação de Amparo à Pesquisa do Estado de Minas Gerais – FAPEMIG for the financial support of this research (grant number CEX-APQ-00383/15), as well as to Coordenação de Aperfeiçoamento de Pessoal de Nível Superior – CAPES (financing code 001) for the studentship (to F.A.M.) and Conselho Nacional de Desenvolvimento Científico e Tecnológico – CNPq for the fellowship (to M.P.F.).

**Keywords:** fluorine *gauche* effect • hyperconjugation • dipolar interactions • steric effects • intramolecular hydrogen bond.

- [1] a) S. Wolfe, *Acc. Chem. Res.* **1972**, *5*, 102-111; b) L. Goodman, H. Gu, V. Popovitsic, *J. Phys. Chem. A* **2005**, *109*, 1223-1229; c) D. Y. Buissonneaud, T. van Mourik, D. O'Hagan, *Tetrahedron* **2010**, *66*, 2196-2202; d) C. Thiehoff, Y. P. Rey, R. Gilmour, *Isr. J. Chem.* **2017**, *57*, 92-100; e) I. V. Alabugin, G. P. Gomes, M. A. Abdo, *Wiley Interdiscip. Rev. Comput. Mol. Sci.* **2019**, *9*, 1-66.
- [2] Rauk, A. *Orbital Interaction Theory of Organic Chemistry*, John Wiley & Sons, New York, 2001.
- [3] a) K. B. Wiberg, M. A. Murcko, *J. Phys. Chem.* **1987**, *91*, 3616-3620; b) D. A. Dixon, N. Matsuzawa, S. C. Walker, *J. Phys. Chem.* **1992**, *96*, 10740-10746; c) M. D. Young, N. C. Borjemscaia, B. D. Wladkowski, *J. Chem. Educ.* **2005**, *82*, 912-915; d) R. K. Sreeruttun, P. Ramasami, *Phys. Chem. Liq.* **2006**, *44*, 315-328; e) F. R. Souza, M. P. Freitas, R. Rittner, *J. Mol. Struct. (Theochem)* **2008**, *863*, 137-140; f) B. M. Wong, M. M. Fadri, S. Raman, *J. Comput. Chem.* **2008**, *29*, 481-487; g) D. Nori-Shargh, J. E. Boggs, *Struct. Chem.* **2011**, *22*, 253-262.
- [4] a) H. J. Böhm, D. Banner, S. Bendels, M. Kansy, B. Kuhn, K. Müller, U. Odst-Sander, M. Stahl, *ChemBioChem* **2004**, *5*, 637-643; b) G. Theodoridis, in *Fluorine and the Environment*, ed. A. Tressaud, Elsevier, Amsterdam, 2006, p. 121; c) D. O'Hagan, *Chem. Soc. Rev.* **2008**, *37*, 308-319; d) T. Fujiwara, D. O'Hagan, *J. Fluor. Chem.* **2014**, *167*, 16-29.
- [5] a) J. R. Durig, J. Liu, T. S. Little, *J. Mol. Struct.* **1991**, *248*, 25-48; b) J. R. Durig, R. R. Hester, J. B. Robb, *J. Mol. Struct. (Theochem)* **2000**, *500*, 293-309; c) J. Durig, J. Liu T. S. Little, *J. Phys. Chem.* **1991**, *95*, 4664-4672; d) K. B. Wiberg, T. A. Keith, M. J. Frisch, M. Murcko, *J. Phys. Chem.* **1995**, *99*, 9072-9079; e) P. R. Rablen, R. W. Hoffmann, D. A. Hrovat, W. T. Borden, *J. Chem. Soc., Perkin Trans. 2* **1999**, 1719-1726; f) C. Cappelli, S. Corni, J.

- Tomasi, *J. Phys. Chem. A* **2001**, *105*, 10807-10815; g) M. Baranac-Stojanović, J. Aleksić, M. Stojanović, *RSC Adv.* **2015**, *5*, 22980-22995.
- [6] Y. Niide, I. Ohkoshi, *J. Mol. Spectrosc.* **1990**, *140*, 301-310.
- [7] a) P. J. Krueger, H. D. Mettee, *Can. J. Chem.* **1964**, *42*, 326-339; b) R. G. Azrak, E. B. Wilson, *J. Chem. Phys.* **1970**, *52*, 5299-5316; c) C. A. Jennings, D. W. Slocum, *Tetrahedron Lett.* **1972**, *34*, 3547-3550; d) Y. Toshiyasu, R. Fujishiro, *Nippon Kagaku Kaishi* **1973**, *3*, 434-438; e) D. Davenport, M. Schwartz, *J. Mol. Struct.* **1978**, *50*, 259-266; f) E. Lombardi, G. Tarantini, *Chem. Phys. Lett.* **1978**, *60*, 85-89; g) A. Gupta, D. Davenport, M. Schwartz, *Spectrochim. Acta A* **1980**, *36*, 601-606; h) K. B. Wiberg, M. A. Murcko, *J. Mol. Struct. (Theochem)* **1988**, *163*, 1-17; i) F. R. Souza, M. P. Freitas, *Comput. Theor. Chem.* **2011**, *964*, 155-159; j) A. I. Vokin, V. K. Turchaninov, *Opt. Spectrosc.* **2015**, *118*, 50-54.
- [8] a) C. R. S. Briggs, M. J. Allen, D. O'Hagan, D. J. Tozer, A. M. Z. Slawin, A. E. Goeta, J. A. K. Howard, *Org. Biomol. Chem.* **2004**, *2*, 732-740; b) N. E. J. Gooseman, D. O'Hagan, M. J. G. Peach, A. M. Z. Slawin, D. J. Tozer, R. J. Young, *Angew. Chem. Int. Ed.* **2007**, *46*, 5904-5908.
- [9] J. C. R. Thacker, P. L. A. Popelier, *J. Phys. Chem. A* **2018**, *122*, 1439-1450.
- [10] a) J. D. Dunitz, R. Taylor, *Chem. -Eur. J.* **1997**, *3*, 89-98; b) R. A. Cormanich, M. P. Freitas, C. F. Tormena, R. Rittner, *RSC Adv.* **2012**, *2*, 4169-4174.
- [11] E. Juaristi, G. P. Gomes, A. O. Terent'Ev, R. Notario, I. V. Alabugin, *J. Am. Chem. Soc.* **2017**, *139*, 10799-10813.
- [12] a) M. P. Freitas, C. F. Tormena, R. Rittner, *J. Mol. Struct.* **2001**, *570*, 175-180; b) M. P. Freitas, C. F. Tormena, R. Rittner, R. J. Abraham, *J. Phys. Org. Chem.* **2003**, *16*, 27-33.
- [13] J. Graton, G. Compain, F. Besseau, E. Bogdan, J. M. Watts, L. Mtashobya, Z. Wang, A. Weymouth-Wilson, N. Galland, J. Y. Le Questel, B. Linclau, *Chem. -Eur. J.* **2017**, *23*, 2811-2819.
- [14] R. A. Cormanich, M. A. Moreira, M. P. Freitas, T. C. Ramalho, C. P. A. Anconi, R. Rittner, R. H. Contreras, C. F. Tormena, *Magn. Reson. Chem.* **2011**, *49*, 763-767.
- [15] J. Graton, Z. Wang, A. -M. Brossard, D. G. Monteiro, J. Y. Le Questel, B. Linclau, *Angew. Chem. Int. Ed.* **2012**, *51*, 6176-6180.
- [16] J. M. Silla, M. P. Freitas, *J. Fluor. Chem.* **2019**, *217*, 8-12.
- [17] R. A. Cormanich, R. Rittner, M. P. Freitas, M. Bühl, *Phys. Chem. Chem. Phys.* **2014**, *16*, 19212-19217.
- [18] a) F. M. Bickelhaupt, E. J. Baerends, *Angew. Chem. Int. Ed.* **2003**, *42*, 4183-4188; b) Y. Mo, J. Gao, *Acc. Chem. Res.* **2007**, *40*, 113-119.
- [19] B. Pedersen, P. Klæboe, T. Torgrimsen, *Acta Chem. Scand.* **1971**, *25*, 2367-2369.
- [20] W. R. Dolbier Jr., *Guide to Fluorine NMR for Organic Chemists*, John Wiley & Sons, Hoboken, 2016.
- [21] P. L. Chesis, D. R. Hwang, M. J. Welch, *J. Med. Chem.* **1990**, *33*, 1482-1490.
- [22] a) A. D. Becke, *J. Chem. Phys.* **1993**, *98*, 5648-5652; b) R. Krishnan, J. S. Binkley, J. A. Pople, *J. Chem. Phys.* **1980**, *72*, 650-654; c) A. D. Mclean, G. S. Chandler, *J. Chem. Phys.* **1980**, *72*, 5639-5648.
- [23] a) F. Weigend, R. Ahlrichs, *Phys. Chem. Chem. Phys.* **2005**, *7*, 3297-3305; b) F. Weigend, *Phys. Chem. Chem. Phys.* **2006**, *8*, 1057-1065.
- [24] a) M. Rauhalahti, S. Taubert, D. Sundholm, V. Liégeois, *Phys. Chem. Chem. Phys.* **2017**, *19*, 7124-7131; b) G. Mazzone, A. D. Quartarolo, N. Russo, *Dyes and Pigm.* **2016**, *130*, 9-15; c) M. M. Naseer, A. Bauzá, H. Alnasr, K. Jurkschat, A. Frontera, *CrystEngComm* **2018**, *20*, 3251-3257; d) D. Y. Ong, C. Tejo, K. Xu, H. Hirao, S. Chiba, *Angew. Chem. Int. Ed.* **2017**, *56*, 1840-1844; e) E. Engelage, N. Schulz, F. Heinen, S. M. Huber, D. G. Truhlar, C. J. Cramer, *Chem. -Eur. J.* **2018**, *24*, 15983-15987.

- [25] a) M. Head-Gordon, J. A. Pople, M. J. Frisch, *Chem. Phys. Lett.* **1988**, *153*, 503-506; b) M. J. Frisch, M. Head-Gordon, J. A. Pople, *Chem. Phys. Lett.* **1990**, *166*, 275-280; c) M. J. Frisch, M. Head-Gordon, J. A. Pople, *Chem. Phys. Lett.* **1990**, *166*, 281-289.
- [26] M. J. Frisch, G. W. Trucks, H. B. Schlegel, G. E. Scuseria, M. A. Robb, J. R. Cheeseman, G. Scalmani, V. Barone, G. A. Petersson, H. Nakatsuji, X. Li, M. Caricato, A. Marenich, J. Bloino, B. G. Janesko, R. Gomperts, B. Mennucci, H. P. Hratchian, J. V. Ortiz, A. F. Izmaylov, J. L. Sonnenberg, D. Williams-Young, F. Ding, F. Lipparini, F. Egidi, J. Goings, B. Peng, A. Petrone, T. Henderson, D. Ranasinghe, V. G. Zakrzewski, J. Gao, N. Rega, G. Zheng, W. Liang, M. Hada, M. Ehara, K. Toyota, R. Fukuda, J. Hasegawa, M. Ishida, T. Nakajima, Y. Honda, O. Kitao, H. Nakai, T. Vreven, K. Throssell, J. A. Montgomery, Jr., J. E. Peralta, F. Ogliaro, M. Bearpark, J. J. Heyd, E. Brothers, K. N. Kudin, V. N. Staroverov, T. Keith, R. Kobayashi, J. Normand, K. Raghavachari, A. Rendell, J. C. Burant, S. S. Iyengar, J. Tomasi, M. Cossi, J. M. Millam, M. Klene, C. Adamo, R. Cammi, J. W. Ochterski, R. L. Martin, K. Morokuma, O. Farkas, J. B. Foresman, D. J. Fox, Gaussian 09, Revision A.02, Gaussian, Inc., Wallingford CT, 2016.
- [27] a) K. L. Schuchardt, B. T. Didier, T. Elsethagen, L. Sun, V. Gurumoorthi, J. Chase, J. Li, T. L. Windus, *J. Chem. Inf. Model.* **2007**, *47*, 1045-1052; b) D. Feller, *J. Comput. Chem.* **1996**, *17*, 1571-1586.

# Theoretical and X-ray evidence of electrostatic phosphonium *anti* and *gauche* effects

Francisco A. Martins, Poliane Chagas, Sérgio S. Thomasi, Luiz C. A. Oliveira, Renata Diniz, and Matheus P. Freitas- *ChemPhysChem*, 23 (2022) e202100856. Copyright Wiley-VCH GmbH. Reproduced with permission.

**Abstract:** Sulfur, not phosphorus, is the only known third-row element capable of experiencing an electrostatic *gauche* effect with fluorine. Some six-membered rings containing an endocyclic phosphorus atom and a  $\beta$ -fluorine substituent that can interconvert to axial (*gauche* relative to phosphorus) and equatorial positions were then analysed. While phosphines do not establish an electrostatic attraction between fluorine and phosphorus, some oxidised forms exhibit surprising stability for the sterically disfavoured axial orientation. Because the nature of this behavior was not obvious, since an intramolecular hydrogen bond can appear, a phosphonium derivative was further studied and its axial conformation was found to be highly stable. A preference for the *gauche* arrangement appears even for the acyclic and sterically hindered (2-fluoroethyl)triphenylphosphonium cation. On the other hand, (ethane-1,2-diyl)bis(phosphonium) cations are exclusively in *anti* conformation due to an (+/+) electrostatic repulsion between the positively charged phosphonium groups.

## Introduction

The conformational control of functionalised organic compounds is of interest to the pharmaceutical, material, agrochemical, and a variety of other application fields. One of the high-appearance approaches to modulate the conformation of organofluorine compounds is the so-called fluorine *gauche* effect.<sup>[1]</sup> 1,2-Difluoroethane is the benchmark compound that exhibits such effect because its *gauche* conformation is surprisingly more stable than the *anti* conformation.<sup>[2]</sup> This effect comes originally from an antiperiplanar stereoelectronic interaction between an electron-rich bonding orbital and the low-lying antibonding orbital of a C–F bond in a 2-substituted fluoroethane motif (substituent = electron-withdrawing group), which corresponds to the  $\sigma_{\text{C-H}} \rightarrow \sigma^*_{\text{C-F}}$  hyperconjugative interaction in 1,2-difluoroethane (Figure 1).<sup>[3]</sup> The negligible steric impact of the small fluorine atom also contributes to the *gauche* effect.<sup>[4]</sup> The fluorine *gauche* effect is responsible for the helical structure of long-chain perfluorinated alkanes<sup>[5]</sup> and it is ubiquitous in biological chemistry, because conformation plays a key role in biological activity, for instance, and organofluorine compounds comprise about 20–30% of the marketed/licensed pharmaceuticals and herbicides worldwide.<sup>[6-9]</sup>

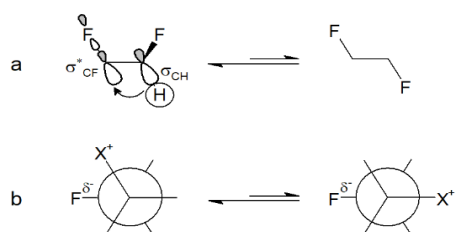


**Figure 1.** a) Hyperconjugative, and b) electrostatic fluorine *gauche* effects.

Despite the well-known role of donor-acceptor orbital interactions in describing the fluorine *gauche* effect,<sup>[10]</sup> an electrostatic rationale appeared later to explain the preferred *gauche* conformation in 2-(+)substituted fluoroethane moieties.<sup>[11]</sup> This is because the C–F bond is the most polar bond in organic chemistry<sup>[12]</sup> and, therefore, the partially negative fluorine atom can interact with positive sites, such as ammonium and pyridinium cations.<sup>[11,13-16]</sup> Such interaction has been found to be highly stabilising, allowing its application in a variety of biological systems, such as in fluorinated derivatives of GABA and NMDA.<sup>[17,18]</sup>

The so-called electrostatic fluorine *gauche* effect has been recently extended to include sulfur as an interacting heteroatom.<sup>[19-22]</sup> The sulfur atom in sulfoxides, sulfones, and thionium salts is partially positive, thus allowing for a Coulombic interaction with *gauche* fluorine.<sup>[19-22]</sup> In addition, the complexation of sulfides with a metal center induces a *gauche* preference along the S–C–C–F motif as a result of the electrostatic interaction mentioned above, thus providing interesting perspectives into the organometallics chemistry.<sup>[23]</sup> On the other hand, it has been shown that not all period 3 elements are capable to attract a fluorine atom through the electrostatic *gauche* effect only by modulating their oxidation state. This is the case of some  $\beta$ -fluorinated organophosphorus compounds, which adopt a preferential *anti* conformation, unless an intramolecular hydrogen bond in the *gauche* conformation takes place, such as in phosphinic and phosphonic acid derivatives.<sup>[24]</sup>

Nevertheless, the conformational equilibrium in  $\beta$ -fluorinated organophosphorus compounds could be better explored, since the conformations of compounds containing a phosphorus element with a formal positive charge have not been thoroughly studied, despite its wide range of applications, such as in Wittig olefination, catalysis, ionic liquids, and drug delivery.<sup>[25]</sup> Also, rotation around unhindered  $\text{C}(\text{sp}^3)\text{--C}(\text{sp}^3)$  bonds in acyclic compounds has been currently evaluated, yielding a pool of conformers that hampers a straightforward analysis.<sup>[24]</sup> In this sense, the ability of an endocyclic phosphorus atom with different oxidation

states in a six-membered ring to induce an axial (*gauche*) fluorine was evaluated herein through high-level *ab initio* and density functional theory calculations. A sterically hindered acyclic  $\beta$ -fluorinated phosphonium compound was also studied to evaluate the limits of the electrostatic *gauche* effect.

On one hand, it is difficult to unambiguously distinguish the concept of dipolar repulsion between two negatively charged groups from Pauli repulsion; on the other hand, the nature of the interaction between two positive sites is most likely electrostatic. However, to the best of our knowledge, the effect of (+/+) electrostatic repulsion on bond rotation, at least involving non-metal elements, has not been explored in conformational studies. Because diphosphonium cations have been employed as bactericidal compounds elsewhere and their conformation may play a critical role in bioactivity mechanisms,<sup>[26]</sup> an analysis of the interactions between two vicinal phosphonium groups bonded in a two-carbon unit aiming at observing an electrostatic *anti* effect was also provided.

## Results and Discussion

An earlier study demonstrated that  $\beta$ -fluorinated phosphines and their respective oxidized forms do not exhibit an electrostatic fluorine *gauche* effect,<sup>[24]</sup> although a similar effect is observed with the third-row element sulfur.<sup>[19-23]</sup> Nevertheless, a detailed evaluation of phosphorus-containing six-membered rings would be valuable, as the chair interconversion yields only a few sets of stable conformers, and the analysis of the stabilizing conformational effects is, therefore, anticipated to be straightforward and accurate. Indeed, phosphine **1** (Figure 2) presents four stable stereoisomers (two pairs of conformers), with a preferential equatorial orientation for the fluorine substituent and an axial position for the P–H bond (Table 1). The second most stable structure also bears an axial P–H bond, indicating that the phosphorus lone pair of electrons is axially disfavoured. Thus, classical steric diaxial repulsion rules the energetics in **1**. The picture changes for **2**, since **2-trans-a** and **2-cis-a** are similarly stable in the gas-phase, indicating that the equatorial fluorine is preferred, while the phosphorus lone pair and the methyl group probably have comparable steric hindrance.

Because a *gauche* preference cannot be observed in the phosphines, we attached a different group at the phosphorus atom to evaluate its ionic form. A fluorine-phosphorus *gauche* preference is clear and conclusive for the phosphonium cations **3** and **4**, as the axial conformer in both compounds corresponds to the single stable form in the gas phase. To ensure that this

axial preference can be asserted as the *gauche* effect, we compared these rings with fluorocyclohexane and 3-fluoro-1,1-dimethyl-cyclohexane. Similar to other monosubstituted cyclohexanes, fluorocyclohexane and 3-fluoro-1,1-dimethyl-cyclohexane are preferred in the equatorial conformation (0.19 and 0.61 kcal mol<sup>-1</sup> more stable than the axial conformer, respectively), which agrees with a previous report.<sup>[27]</sup> Therefore, the behavior found in their phosphorus analogs **3** and **4** can be characterized as a strong *gauche* effect. This is probably due to the positively charged phosphorus (QTAIM atomic charges  $q_P = +1.8$  and  $+1.9$ , respectively) interacting with the negatively charged axial fluorine ( $q_F = -0.5$ ), since the C-counterpart in fluorocyclohexane and 3-fluoro-1,1-dimethyl-cyclohexane is nearly neutral ( $q_C = +0.1$  and  $+0.2$ , respectively). Considering the conformational energies of **3** and **4** relative to fluorocyclohexane and 3-fluoro-1,1-dimethyl-cyclohexane, it follows that the extension of the *gauche* effect in these systems ( $\Delta\Delta E_{eq-ax}$ ) is *ca.* 3.6 kcal mol<sup>-1</sup> in **3** and 3.9 kcal mol<sup>-1</sup> in **4**.

To search for the role of hyperconjugation as the origin of the *gauche* effect in **3** and **4**, our NBO analyses (Supporting Information) demonstrated that the  $\sigma_{C-H} \rightarrow \sigma^*_{C-F}$  interaction in the axial conformer is indeed stabilizing, but of similar magnitude to the corresponding interaction in axial fluoro-cyclohexane and 3-fluoro-1,1-dimethyl-cyclohexane (5.1-5.6 kcal mol<sup>-1</sup>). Therefore, this contribution is not the primary source for the *gauche* preference in the phosphonium cations. In turn, the electrostatic fluorine *gauche* effect is known for systems containing N–C–C–F and S–C–C–F moieties, so the proposal of a P–C–C–F electrostatic *gauche* effect is a logical extension to those earlier found.<sup>[28-30]</sup>

Additional evidence to reinforce the electrostatic nature of the phosphorus-fluorine *gauche* effect for compounds containing a positively charged atom is the strong decrease in the *gauche* preference of **3** and **4** in an implicit polar medium (DMSO). Also, a comparison between the P…F<sub>ax</sub> distances in phosphines and phosphonium cations indicates a significant ring puckering in the latter as a result of the attractive Coulombic interaction; the P…F<sub>ax</sub> distance shortens from 3.258 Å in **1-cis-g** and 3.366 Å in **2-cis-g** to 2.970 Å in axial **3** and 3.096 Å in axial **4**, respectively. This finding appears to extend generally, because the conformational energy for the acyclic and sterically hindered (2-fluoroethyl)triphenylphosphonium cation (**5**) is consistent with those of the cyclic analogs.

A quantum theory of atoms in molecules (QTAIM) analysis was performed to check for a possible hydrogen bond between the axial fluorine and (P)H (**3**) or (P)CH<sub>3</sub> (**4**) hydrogens, but a bond path was found only for the latter (Supporting Information). QTAIM has been applied to conformational analysis<sup>[31]</sup> and, for some organophosphorus compounds, hydrogen bond-

type contributions ( $\text{C}-\text{H}\cdots\text{X}-\text{P}$ ,  $\text{X} = \text{O}$  and  $\text{S}$ ) have shown to activate the anomeric effect.<sup>[32]</sup> According to Koch and Popelier, a few criteria have to be observed to characterize hydrogen bonds using QTAIM.<sup>[33]</sup> The first one states that a bond-critical point (BCP) and a bond path should be present. In this sense, only the molecules with  $\text{R} = \text{CH}_3$  are capable of experiencing such interaction (Supporting Information). Furthermore, local properties over the BCP, such as charge density ( $\rho$ ) and the Laplacian of  $\rho$  ( $\nabla^2\rho$ ), have to be one order of magnitude smaller than those observed for covalent bonds and higher than zero ( $\nabla^2\rho > 0$ ), respectively. Analysis of other parameters based on integrated properties is additionally required. The decrease in the hydrogen volume ( $V(\text{H})$ ), energy( $E(\text{H})$ ), dipolar moment ( $\mu(\text{H})$ ), and charge ( $q(\text{H})$ ) are expected for the hydrogen involved in a hydrogen bond, if compared with hydrogen that not experience such interaction. These data were computed, and the  $\text{CH}_3$  hydrogens were compared. The parameters match the established conditions (see the Supporting Information), and a hydrogen bond is present in a few compounds. Despite such stabilization, hydrogen bond should not be responsible for the *gauche* effect in **4**, since both phosphine (**2**) and their phosphonium cation (**4**) experience this interaction.

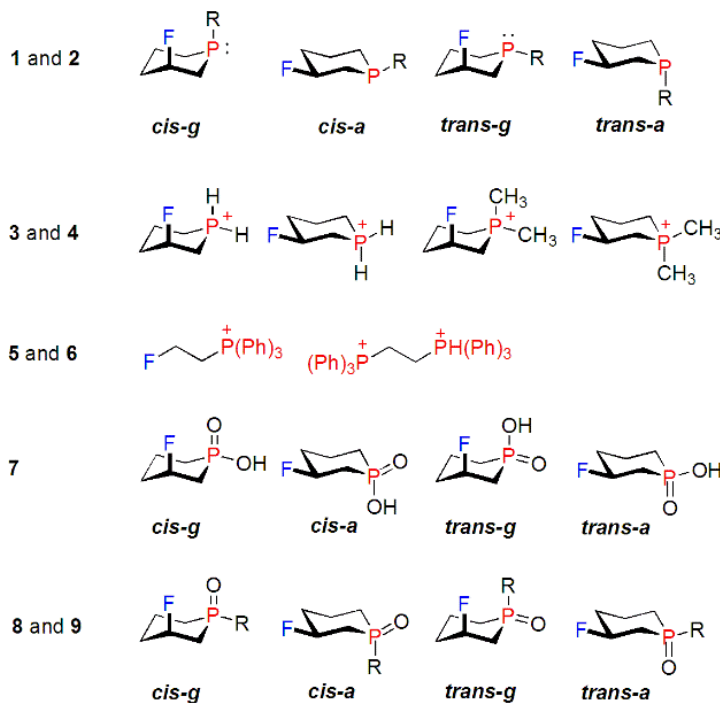


**Figure 2.** From top to bottom: chair conformations and isomers for the studied phosphines **1** ( $\text{R} = \text{H}$ ) and **2** ( $\text{R} = \text{Me}$ ), phosphonium cations **3** ( $\text{R} = \text{H}$ ) and **4** ( $\text{R} = \text{Me}$ ), (2-fluoroethyl)triphenylphosphonium (**5**) and (ethane-1,2-diyl)bis(triphenylphosphonium) (**6**) cations, phosphinic acid **7**, phosphine oxides **8** ( $\text{R} = \text{H}$ ) and **9** ( $\text{R} = \text{Me}$ ).

**Table 1.** Relative Gibbs free energies (in kcal mol<sup>-1</sup>) for the studied compounds in the gas phase and implicit DMSO (IEFPCM), obtained at the B3LYP-D3BJ/6-311++g(d,p) level.

Compound <sup>a</sup>	Gas phase	Implicit DMSO
<b>1-cis-g</b>	1.25	1.37
<b>1-cis-a</b>	2.35	2.48
<b>1-trans-g</b>	3.72	3.46
<b>1-trans-a</b>	0.00	0.00
<b>2-cis-g</b>	0.98	1.48
<b>2-cis-a</b>	0.28	0.49
<b>2-trans-g</b>	1.74	1.52
<b>2-trans-a</b>	0.00	0.00
<b>3<sub>eq-ax</sub></b>	3.41	0.57
<b>4<sub>eq-ax</sub></b>	3.25	0.91
<b>5<sub>anti-gauche</sub></b>	1.90	0.39
<b>7-cis-g_s</b>	2.82	1.12
<b>7-cis-g_a</b>	7.74	2.65
<b>7-cis-g_s'</b>	-	1.03
<b>7-cis-a_s</b>	0.00	-
<b>7-cis-a_g</b>	-	0.00
<b>7-cis-a_g'</b>	-	0.18
<b>7-trans-g_s</b>	1.30	-
<b>7-trans-g_g</b>	-	1.00
<b>7-trans-g_a</b>	2.55	0.47
<b>7-trans-g_g'</b>	-	0.65
<b>7-trans-g_s'</b>	1.94	-
<b>7-trans-a_s</b>	0.66	0.71
<b>7-trans-a_a</b>	4.94	2.03
<b>7-trans-a_s'</b>	-	0.53
<b>8-cis-g</b>	2.72	1.48
<b>8-cis-a</b>	0.10	0.00
<b>8-trans-g</b>	0.00	0.22
<b>8-trans-a</b>	0.08	0.64
<b>9-cis-g</b>	3.35	1.34
<b>9-cis-a</b>	0.64	0.00
<b>9-trans-g</b>	0.42	0.51
<b>9-trans-a</b>	0.00	0.11

<sup>a</sup> **3<sub>eq-ax</sub>** and **4<sub>eq-ax</sub>** correspond to the energy difference between the equatorial and axial conformers. **5<sub>anti-gauche</sub>** is the energy difference between the *anti* and *gauche* conformers of **5**. The last letter in the names of stereoisomers **7** represents the hydroxyl orientation (*syn*, *anti*, or *gauche*). Compound **6** does not appear because there is only a single (*anti*) conformer.

To further understand the role of electrostatic interactions in the conformational equilibrium of the phosphonium cations, the rotational profiles of 2-fluoro-ethylphosphonium ( $\text{H}_3\text{P}^+ - \text{CH}_2 - \text{CH}_2 - \text{F}$ , **PF**) and (ethane-1,2-diyl)bis(phosphonium) ( $\text{H}_3\text{P}^+ - \text{CH}_2 - \text{CH}_2 - \text{PH}_3^+$ , **PP**) cations can be compared to that of butane, whose energy minima are located at staggered conformations due to steric and hyperconjugative considerations.<sup>[34-36]</sup> While butane is widely known to be preferentially in the *anti* conformation, **PF** is clearly more stable in the *gauche* orientation, both in the gas phase and polar solution (Figure 3). This emphasises the pivotal role of the electrostatic *gauche* effect in **PF**. Surprisingly, only a single conformer is observed for

**PP** corresponding to a staggered *anti* geometry in the gas phase, since the *gauche* conformer appears as a high-energy minimum only in solution (Figure 3). Noticeably, the QTAIM atom charges on **P** and **F** in these compounds are positive and negative, respectively, as well for the cyclic compounds (Figure S1, Supporting Information).

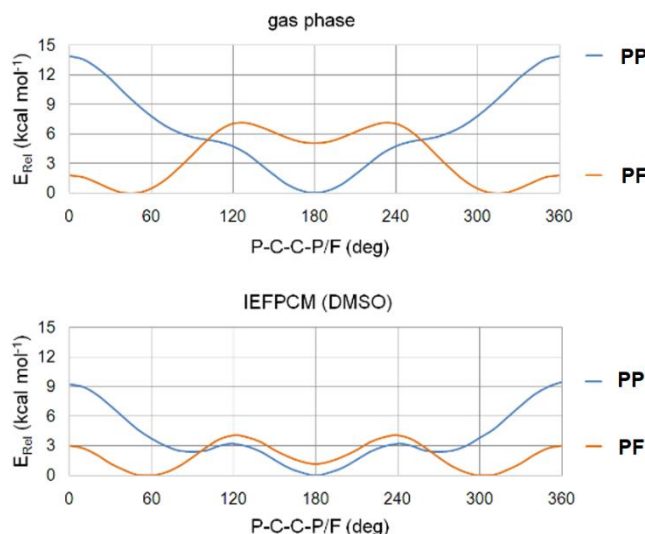


**Figure 3.** Rotational curves for **PF** and **PP** in the gas phase and implicit solvent (DMSO).

Vicinal electron-withdrawing groups – thus bearing negatively charged sites – repel each other due to electrostatic repulsion between the electron densities of the two substituents and to the Pauli repulsion between occupied closed-shell orbitals of both substituents.<sup>[37]</sup> In turn, the contribution to the conformational behavior in **PP** appears to be predominantly due to the repulsion between the nuclei of the substituents, which would give rise to an “(+/-)-electrostatic *anti* effect”. To obtain experimental evidence for the so-called “(+/-)-electrostatic *anti* effect”, the (ethane-1,2-diyl)bis(triphenylphosphonium) salt (**6**) was prepared and its single-crystal X-ray structure was obtained (Figure 4). The P–C–C–P dihedral angle in **6** was found to be *anticlinal* (*ca.* 135°), as expected from repulsive steric and electrostatic considerations, as well as to allow for a  $\pi$ -stacking interaction. Similarly, an *anti* arrangement along the P–P–P–P dihedral angle in 2,3-diphosphino-1,4-diphosphonium cations has also been observed,<sup>[38]</sup> as well as in (C<sub>38</sub>H<sub>34</sub>P<sub>2</sub>)MgBr<sub>4</sub> powders useful for scintillation-based X-ray detection (P–C–C–P dihedral angle = 166.96°).<sup>[39]</sup>



**Figure 4.** Single crystal structure of (ethane-1,2-diyl)bis(triphenylphosphonium) iodide (**6**) with a  $\phi_{\text{P-C-C-P}}$  dihedral angle of  $134.8(3)^\circ$ .

A comprehensive analysis on the nature of the *gauche* and *anti* effects in **PF** and **PP** can be performed using quantum-chemical calculations for natural energy decomposition analysis (NEDA).<sup>[40]</sup> The interaction energy ( $E_{\text{int}}$ ) between two open-shell fragments ( $\bullet\text{CH}_2\text{PH}_3$  and  $\bullet\text{CH}_2\text{X}$ ,  $\text{X} = \text{F}$  for **PF**, and  $\text{PH}_3$  for **PP**) can be decomposed into electrical ( $E_{\text{EL}}$ ), charge transfer ( $E_{\text{CT}}$ ), and core ( $E_{\text{core}}$ ) components. The rotational profile of these energies demonstrates that the  $E_{\text{EL}}$  and  $E_{\text{CT}}$  terms are stabilising, whereas the core repulsion is certainly destabilising (Figure 5). However, the  $E_{\text{CT}}$  term finds two minima with very similar energy for **PF**: a broad one at about  $60^\circ$  (*gauche*) and another minimum at  $180^\circ$  (*anti*). On the other hand, the stabilisation due to  $E_{\text{EL}}$  continuously decreases with  $\phi_{\text{P-C-C-F}}$  going from  $0^\circ$  to  $180^\circ$ . Consequently, the *gauche* effect in **PF** appears to be dominated by the electrical term (comprised of electrostatic –  $E_{\text{ES}}$ , polarization –  $E_{\text{pol}}$ , and energy penalty of polarization –  $E_{\text{SE}}$  contributions), while the core repulsion neither favours nor disfavours the *gauche* conformer relative to the *anti*. In turn,  $E_{\text{int}}$  follows the trend observed for  $E_{\text{EL}}$  in **PP**, *i.e.* its rotational energy profile is dictated by the electrical term, which is more favoured in the *anti* conformer (Figure 5b). Because the electrostatic component rules the  $E_{\text{EL}}$  term (Figure 5c), the *anti* effect observed in **PP** can be unequivocally assigned to an (+/+)–electrostatic *anti* effect.

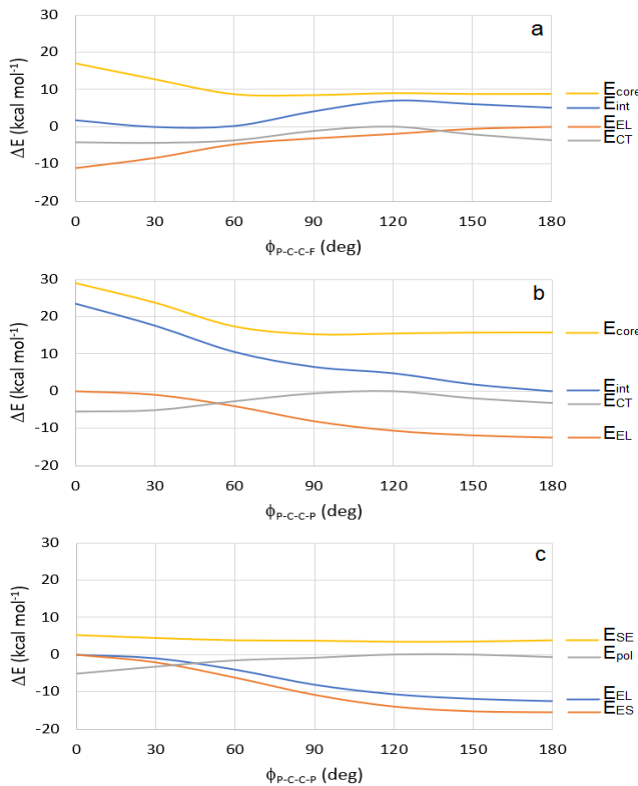


**Figure 5.** Natural energy decomposition analysis for rigid rotation (C–C distance fixed at the equilibrium distances of the *gauche* and *anti* conformers of **PF** and **PP**, respectively) of the  $\phi_{\text{P-C-C-F/P}}$  dihedral angle of **PF** and **PP**. a)  $E_{\text{int}}$  and its components for **PF**; b)  $E_{\text{int}}$  and its components for **PP**; c)  $E_{\text{EL}}$  and its components for **PP**.

To further extend our knowledge about the newly established electrostatic fluorine-phosphorus *gauche* effect, a series of oxidised phosphorus compounds (**7-9**) was investigated. It has been demonstrated that phosphine oxides and derived acids do not show a sufficiently stabilising  $\text{P}^{\delta+}\cdots\text{F}^{\delta-}$  electrostatic attraction in the *gauche* structure; the *gauche* preference appears to be rather due to  $\text{F}\cdots\text{H}-\text{O}$  hydrogen bond.<sup>[24]</sup> However, because the acid is easily dissociated in solution, such an interaction should be absent. Similar behavior is observed in the six-membered ring **7** (Figure 6); conformers with equatorial fluorine are the lowest-energy structures when the  $\text{H}-\text{O}-\text{P}=\text{O}$  dihedral angle is *synperiplanar*, independently of the  $\text{P}=\text{O}$  orientation (either axial or equatorial). A non-*synperiplanar* orientation along the  $\text{H}-\text{O}-\text{P}=\text{O}$  dihedral angle is favoured only for **7-trans-g**, where an  $\text{F}\cdots\text{H}-\text{O}$  hydrogen bond may be present in the gas phase. Yet, this is not the most stable structure for **7**, which is rather the *synperiplanar* structure of **7-cis-a** bearing both the highly polar C–F and P=O bonds in the equatorial position.

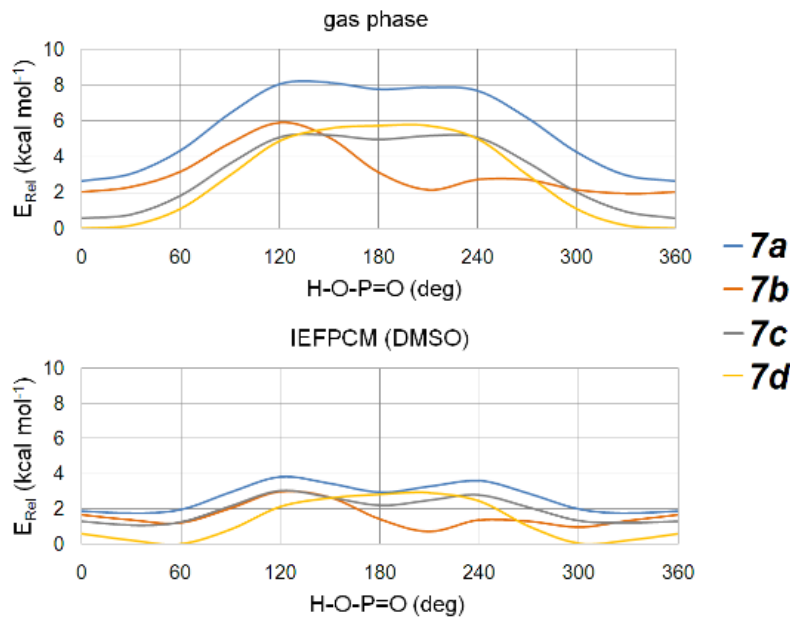


**Figure 6.** Potential energy surfaces accounting for the rotation around the P–OH bond in **3**.

The phosphine oxide **8** adopts a preferential axial orientation for the fluorine substituent (structure **8-trans-g**); however, according to an energy scale earlier reported,<sup>[10]</sup> an energy difference of *ca.* 0.1 kcal mol<sup>-1</sup> does not indicate a "clearly *gauche* preference". It is worth mentioning that **8-cis-g** is anticipated to be destabilised by a dipolar repulsion between the axial C–F and P=O bonds. In addition, because of a possible long-range F···H–P hydrogen bond in **8-trans-g**, the electrostatic phosphorus-fluorine *gauche* effect in **8** cannot be asserted as being the single source of *gauche* stabilisation. Thus, a bulkier group attached to the phosphorus atom was considered with the aim at avoiding dubious interpretation on the ruling interactions of the structural energies, yielding compound **9**; accordingly, the relative stability of **9-trans-g** decreases if compared to **9-trans-g** and an *anti* preference takes place. Nevertheless, an *anti* structure **9-trans-a** is lower in energy than **9-trans-g** by only a small value, which can be due to a weak F···H–C hydrogen bond in the latter. This is confirmed by QTAIM analysis, in which a bond path between the interacting atoms reveals the electrostatic character of such a hydrogen bond (Supporting Information), as discussed earlier. It is worth mentioning that in phosphine oxides **8-trans-g** and **9-trans-g**, whose phosphorus atom bears a partially positive charge, the respective distances are 3.195 Å and 3.278 Å, higher than those found in the phosphonium cations **3** and **4**. Consequently, the preferred fluorine in the axial position cannot be asserted as being due to an electrostatic F···P interaction.

## Conclusion

Although not all  $\beta$ -fluorinated organophosphorus compounds experience the electrostatic phosphorus-fluorine *gauche* effect, phosphonium analogs adopt a *gauche* conformation as the sharply most stable structure both in the gas phase and polar solution. The electrostatic phosphorus-fluorine *gauche* effect is not the dominant effect of the preferential *gauche* structure in six-membered rings containing pentavalent phosphorus; whereas phosphinic acids experience intramolecular hydrogen bond, the short P $\cdots$ F<sub>ax</sub> distance in phosphine oxides compared to that found in the respective phosphines does not clearly explain the *gauche* effect. Whereas dipolar repulsion between negatively charged vicinal groups is known to move these groups away, then usually leading to an *anti* conformation, the electrostatic repulsion between the positively charged phosphonium groups also appeared to be an efficient mechanism for conformational control. In overall terms, the electrostatic fluorine *gauche* effect extends to phosphorus as a period 3 heteroatom, while vicinal phosphonium groups in an ethane moiety provide the newly revealed (+/+) -electrostatic *anti* effect.

## Experimental

**Computational.** The geometries for the stable structures of **1-7** were fully optimised at the *ab initio* MP2/6-311++g(d,p) level,<sup>[41,42]</sup> since this is a robust method for structure prediction of organic molecules, both in the gas phase and considering a polar implicit solvent (DMSO) through the polarisable continuum model.<sup>[43]</sup> For the acids (**3**), the H–O–P=O dihedral angle was scanned in steps of 30° at the same level of theory to identify the hydroxyl orientation, whereas the scans for **PF** and **PP** were carried out in steps of 10°. Frequency calculations were performed at the B3LYP-D3BJ/6-311++g(d,p)<sup>[44-46]</sup> level of theory for all stable conformers to ensure the absence of imaginary frequencies and to obtain the Gibbs free energies. This level of theory requires less computational cost than traditional *ab initio* MP2, but usually presents similar or even better thermochemical results.<sup>[47,48]</sup> The energy decomposition analysis based on natural bond orbitals (NEDA) was performed considering a rigid rotation around the C–C bond of **PF** and **PP**; the C–C distance between the •CH<sub>2</sub>PH<sub>3</sub> and •CH<sub>2</sub>X (X = F for **PF** and PH<sub>3</sub> for **PP**) open-shell fragments was fixed at the corresponding equilibrium distance of the *gauche* (for **PF**) and *anti* (for **PP**) conformers. The same procedure was done considering minus and plus 0.5 Å to the C–C distance to confirm that the rotational profiles were independent of the C–C distance. These calculations were performed using the Gaussian program and the software

NBO 7.0.<sup>[49,50]</sup> The quantum theory of atoms in molecules (QTAIM) analysis<sup>[51]</sup> was performed using the wavefunctions obtained from the optimised geometries using the AIMAII software package.<sup>[52]</sup>

**(Ethane-1,2-diyI)bis(triphenylphosphonium) iodide (9).** A mixture of 1.474 g (8.0 mmol) of 1-fluoro-2-iodoethane and 0.528 g (2.0 mmol) of triphenylphosphine in acetonitrile (3 mL) was stirred under reflux for one hour. The mixture was cooled, and the solvent was distilled off on a rotatory evaporator. The solid was washed with diethyl ether and air-dried to give compound **9** (0.430 g). The solid was solubilised in hot acetonitrile for further purification. The solution was cooled, no solid was observed. The crystals precipitated after three days (0.215 g, 30.0 %). Compound **9** was subsequently analysed through X-ray crystallography.

**Supporting Information.** Standard coordinates of the optimised geometries, DFT and NBO results, and X-ray diffraction data. The X-ray crystallographic data for this paper has been deposited at the Cambridge Crystallographic Data Centre (CCDC), under deposition number 1971685.

## Acknowledgements

The authors are thankful to Fundação de Amparo à Pesquisa do Estado de Minas Gerais (FAPEMIG, grant number CEX-APQ-00383/15), Coordenação de Aperfeiçoamento de Pessoal de Nível Superior (CAPES, funding code 001) and Conselho Nacional de Desenvolvimento Científico e Tecnológico (CNPq) for the financial support of this research, as well as by a scholarship (to F.A.M.) and fellowships (to L.C.A.O., R.D. and M.P.F.).

**Keywords:** conformational analysis • *gauche* effect • *anti* effect • organophosphorus compounds • electrostatic interactions

- [1] S. Wolfe, *Acc. Chem. Res.* **1972**, *5*, 102-111.
- [2] L. Goodman, H. Gu, V. Pophristic, *J. Phys. Chem. A* **2005**, *109*, 1223-1229.
- [3] I. V. Alabugin, G. P. Gomes, M. A. Abdo, *WIREs Comput. Mol. Sci.* **2019**, *9*, e1389.
- [4] D. R. Silva, L. A. Santos, T. A. Hamlin, C. F. Guerra, M. P. Freitas, M. F. Bickelhaupt, *ChemPhysChem* **2021**, *22*, 641-648.
- [5] R. A. Cormanich, D. O'Hagan, M. Bühl, *Angew. Chem. Int. Ed.* **2017**, *56*, 7867-7870.

- [6] H. -J. Böhm, D. Banner, S. Bendels, M. Kansy, B. Kuhn, K. Müller, U. Obst-Sander, M. Stahl, *ChemBioChem.* **2004**, *5*, 637-643.
- [7] G. Theodoridis in *Fluorine and the Environment: Agrochemicals, Archaeology, Green Chemistry and Water* (Ed.: A. Tressaud), Elsevier, Amsterdam, **2006**, pp. 121-175.
- [8] D. O'Hagan, *J. Fluor. Chem.* **2010**, *131*, 1071-1081.
- [9] T. Fujiwara, D. O'Hagan, *J. Fluor. Chem.* **2014**, *167*, 16-29.
- [10] D. Y. Buissonneaud, T. van Mourik, D. O'Hagan, *Tetrahedron* **2010**, *66*, 2196-2202.
- [11] N. E. J. Gooseman, D. O'Hagan, M. J. G. Peach, A. M. Z. Slawin, D. J. Tozer, R. J. Young, *Angew. Chem. Int. Ed.* **2007**, *46*, 5904-5908.
- [12] D. O'Hagan, *J. Org. Chem.* **2012**, *77*, 3689-3699.
- [13] A. Sun, D. C. Larkin, K. Hardcastle, J. P. Snyder, *Chem. Eur. J.* **2005**, *11*, 1579-1591.
- [14] C. R. S. Briggs, M. J. Allen, D. O'Hagan, D. J. Tozer, A. M. Z. Slawin, A. E. Goeta, J. A. K. Howard, *Org. Biomol. Chem.* **2004**, *2*, 732-740.
- [15] J. M. Silla, W. G. D. P. Silva, R. A. Cormanich, R. Rittner, C. F. Tormena, M. P. Freitas, *J. Phys. Chem. A* **2014**, *118*, 503-507.
- [16] J. M. Silla, C. J. Duarte, R. A. Cormanich, R. Rittner, M. P. Freitas, *Beilstein J. Org. Chem.* **2014**, *10*, 877-882.
- [17] J. Cao, R. Bjornsson, M. Bühl, W. Thiel, T. van Mourik, *Chem. Eur. J.* **2012**, *18*, 184-195.
- [18] P. W. Chia, M. R. Livesey, A. M. Z. Slawin, T. van Mourik, D. J. A. Wyllie, D. O'Hagan, *Chem. Eur. J.* **2012**, *18*, 8813-8819.
- [19] J. Aleksić, M. Stojanovic, M. Baranac-Stojanovic, *J. Org. Chem.* **2015**, *80*, 10197-10207.
- [20] C. Thiehoff, M. C. Holland, C. G. Daniliuc, K. N. Houk, R. Gilmour, *Chem. Sci.* **2015**, *6*, 3565-3571.
- [21] C. Thiehoff, L. Schifferer, C. G. Daniliuc, N. Santschi, R. Gilmour, *J. Fluor. Chem.* **2016**, *182*, 121-126.
- [22] C. Thiehoff, Y. P. Rey, R. Gilmour, *Isr. J. Chem.* **2017**, *57*, 92-100.
- [23] N. Santschi, C. Thiehoff, M. C. Holland, C. G. Daniliuc, K. N. Houk, R. Gilmour, *Organometallics* **2016**, *35*, 3040-3044.
- [24] L. A. F. Andrade, M. P. Freitas, *New J. Chem.* **2017**, *41*, 11672-11678.
- [25] A. C. Vetter, K. Nikitin, D. G. Gilheany, *Chem. Commun.* **2018**, *54*, 5843-5846.
- [26] B. Yuan, W. Hu, S. Lv, J. Huang, K. Huang, *Chem. J. Mold.* **2017**, *12*, 81-86.
- [27] A. V. Belyakov, A. A. Baskakov, A. D. Ivanov, A. V. Garabadzhiu, I. Arnason, *Struct. Chem.* **2013**, *24*, 763-768.
- [28] Y. P. Rey, L. E. Zimmer, C. Sparr, E.-M. Tanzer, W. B. Schweizer, H. M. Senn, S. Lakhdar, R. Gilmour, *Eur. J. Org. Chem.* **2014**, 1202-1211
- [29] S. Paul, W. B. Schweizer, G. Rugg, H. M. Senn, R. Gilmour, *Tetrahedron* **2013**, *69*, 5647-5659.

- [30] C. Sparr, W. B. Schweizer, H. M. Senn, R. Gilmour, *Angew. Chem.* **2009**, *121*, 3111; *Angew. Chem. Int. Ed.* **2009**, *48*, 3065.
- [31] J. Hernández-Trujillo, F. Cortés-Guzmán, G. Cuevas in *The Quantum Theory of Atoms and Molecules: From Solid State to DNA and Drug Design* (Eds.: C. F. Matta, R. J. Boyd), Wiley-VCH Verlag GmbH & Co. KGaA, Weinheim, **2007**, pp. 375-397.
- [32] G. Cuevas, *J. Am. Chem. Soc.* **2000**, *122*, 692-698.
- [33] U. Koch, P. L. A. Popelier, *J. Phys. Chem.* **1995**, *99*, 9747- 9754.
- [34] S. Liu, N. Govind, *J. Phys. Chem. A* **2008**, *112*, 6690-6699.
- [35] R. A. Cormanich, M. P. Freitas, *J. Org. Chem.* **2009**, *74*, 8384-8387.
- [36] Y. Mo, *J. Org. Chem.* **2010**, *75*, 2733-2736.
- [37] D. R. Silva, L. A. Santos, T. A. Hamlin, F. M. Bickelhaupt, M. P. Freitas, C. F. Guerra, *Phys. Chem. Chem. Phys.* **2021**, in press. DOI: 10.1039/D1CP02502C.
- [38] Y. -Y. Carpenter, C. A. Dyker, N. Burford, M. D. Lumsden, A. Decken, *J. Am. Chem. Soc.* **2008**, *130*, 15732-15741.
- [39] L. -J. Xu, X. Lin, Q. He, M. Worku, B. Ma, *Nat. Commun.* **2020**, *11*, 4329.
- [40] E. D. Glendening, *J. Phys. Chem. A* **2005**, *109*, 11936-11940.
- [41] M. J. Frisch, M. Head-Gordon, J. A. Pople, *Chem. Phys. Lett.* **1990**, *166*, 275-280.
- [42] M. J. Frisch, J. A. Pople, J. S. Binkley, *J. Chem. Phys.* **1984**, *80*, 3265-3269.
- [43] J. Tomasi, B. Mennucci, R. Cammi, *Chem. Rev.* **2005**, *105*, 2999-3094.
- [44] A. D. Becke, *J. Chem. Phys.* **1993**, *98*, 5648-5652.
- [45] S. Grimme, J. Antony, S. Ehrlich, H. Krieg, *J. Chem. Phys.* **2010**, *132*, 154104-154123.
- [46] S. Grimme, S. Ehrlich, L. Goerigk, *J. Comp. Chem.* **2011**, *32*, 1456-1465.
- [47] M. W. Wong, *Chem. Phys. Lett.* **1996**, *256*, 391-399.
- [48] M. J. Frisch, G. W. Trucks, J. R. Cheeseman, *Comput. Theor. Chem.* **1996**, *4*, 679-707.
- [49] M. J. Frisch, G. W. Trucks, H. B. Schlegel, G. E. Scuseria, M. A. Robb, J. R. Cheeseman, G. Scalmani, V. Barone, G. A. Petersson, H. Nakatsuji, X. Li, M. Caricato, A. Marenich, J. Bloino, B. G. Janesko, R. Gomperts, B. Mennucci, H. P. Hratchian, J. V. Ortiz, A. F. Izmaylov, J. L. Sonnenberg, D. Williams-Young, F. Ding, F. Lipparini, F. Egidi, J. Goings, B. Peng, A. Petrone, T. Henderson, D. Ranasinghe, V. G. Zakrzewski, J. Gao, N. Rega, G. Zheng, W. Liang, M. Hada, M. Ehara, K. Toyota, R. Fukuda, J. Hasegawa, M. Ishida, T. Nakajima, Y. Honda, O. Kitao, H. Nakai, T. Vreven, K. Throssell, J. A. Montgomery, Jr., J. E. Peralta, F. Ogliaro, M. Bearpark, J. J. Heyd, E. Brothers, K. N. Kudin, V. N. Staroverov, T. Keith, R. Kobayashi, J. Normand, K. Raghavachari, A. Rendell, J. C. Burant, S. S. Iyengar, J. Tomasi, M. Cossi, J. M. Millam, M. Klene, C. Adamo, R. Cammi, J. W. Ochterski, R. L. Martin, K. Morokuma, O. Farkas, J. B. Foresman, D. J. Fox, Gaussian 09, Revision A.02, Gaussian, Inc., Wallingford CT, 2016.
- [50] E. D. Glendening, J. K. Badenhoop, A. E. Reed, J. E. Carpenter, J. A. Bohmann, C. M. Morales, P. Karafiloglou, C. R. Landis, and F. Weinhold, Theoretical Chemistry Institute, University of Wisconsin, Madison, 2018.

- [51] R. F. W. Bader in *Encyclopedia of Computational Chemistry* (Ed.: P.v.R. Schleyer), John Wiley and Sons, Chichester, **1998**, pp. 64-86.
- [52] AIMAll (Version 19.02.13), T. A. Keith, TK Gristmill Software, Overland Park KS, USA, 2019 ([aim.tkgristmill.com](http://aim.tkgristmill.com)).

## **SECOND PART**

### **Biological and Environmental Impact of Fluorine Atom**

# Theoretical study of fluorinated bioisosteres of organochlorine compounds as effective and eco-friendly pesticides

(Published - *Ecotoxicology and Environmental Safety*, 199 (2020) 110679)

Francisco A. Martins, Joyce K. Daré and Matheus P. Freitas

## ABSTRACT

Chlordane is a worldwide banned organochlorine insecticide because of its hazard to animal and human health. It is also a persistent organic pollutant, which can affect either the soil or the aquatic life. The same applies to other chlorinated cyclodienes, such as dieldrin and aldrin. In turn, organofluorine compounds have a widespread use in agriculture. Therefore, density functional calculations and docking studies showed that the bioisosteric replacement of chlorines in the above-mentioned compounds by fluorines improves some physicochemical parameters used to estimate the toxicity and environmental risk of these compounds, as well as the ligand-enzyme ( $\text{GABA}_A$  receptor-chloride channel complex) interactions related to their insecticidal activity. This work is an effort to provide an improved new class of organofluorine pesticides.

**Keywords:** Organofluorines; Chlorinated Cyclodienes; Insecticides; Environment; Molecular Modeling

## INTRODUCTION

Chlordane is a chemical that can be prepared through a Diels-Alder reaction followed by a double bond chlorination, which yields a mixture of *cis* and *trans* isomers, also named  $\alpha$ - and  $\beta$ -chlordane, respectively (Figure 1). Both isomers are organochlorine compounds effective against insects that threaten the agriculture. Their mode of action involves the opening of ion channels in the nerve cells of the insects, whilst the  $\text{GABA}_A$  receptor works as a major ligand-activated ionic channel responsible for mediating the effects of the  $\gamma$ -aminobutyric acid (GABA) neurotransmitter (Fishman and Gianutsus, 1985; Anand et al., 1998). However, all uses of chlordane were banned by the United States Environmental Protection Agency (EPA) because of its harm to human health and environment, although it is still used in many developing countries (ATSDR, 2018). Just as chlordane, aldrin and dieldrin are also classified as cyclodienes and interact by the same mechanism of action with  $\text{GABA}_A$  (Bloomquist and Soderlund, 1985; Pomes et al., 1994). It is worth mentioning that these compounds are structurally similar to the picrotoxin, a known noncompetitive antagonist at  $\text{GABA}_A$  receptors that has been used as potency indicator (Abalis et al., 1986). This class of compounds has been

reported as one of the causes of diseases, such as Parkinson's disease and some types of cancer (Mathur et al., 2002; Uversky et al., 2001; Sharma et al., 2010; Davis and Fitzhugh, 1962).

The presence of chlorine in organic compounds does not ensure toxicity, but this halogen has a lipophilic character, which enhances the persistence of the organochloride both in soil and aquatic living systems. Accordingly, organochlorines can move from soil to plants and then be transferred to the food chain, while in water they can accumulate in the fatty tissue of aquatic living systems (Piu et al., 2019; Egeler et al., 1997). Risks to animal and human health have also been reported, which can be related to the relative ease for C–Cl bond cleavage (Liang et al., 2017). In turn, organofluorine agrochemicals have been widely used as pesticides (herbicides, fungicides and insecticides) (Fujiwara and O'Hagan, 2014; Theodoridis, 2006), with several advantages over organochlorine compounds. These include lower lipophilicity, reduced steric effects, enhanced electronic effects (which result in modified physical properties and chemical reactivity), and higher stability of the C–F bond (Theodoridis, 2006). Nevertheless, a more detailed comprehension of organofluorine pesticides is necessary, once the high stability of the C–F bond hampers their degradation; therefore, it has been found that they can persist in the environment (Murphy et al., 2011). However, these compounds are usually inert agents and more polar (less hydrophobic) than organochlorine compounds, thus suggesting a lower toxicity.

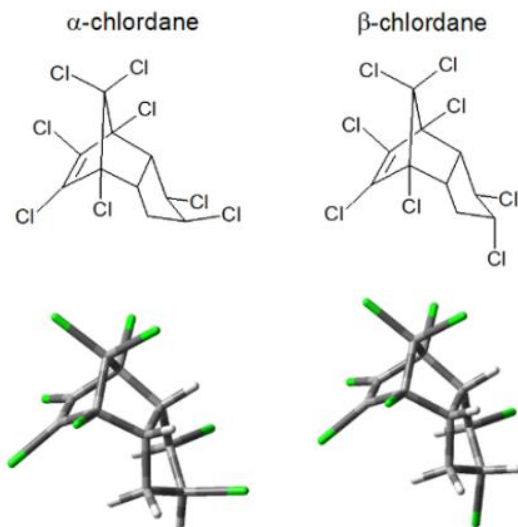


**Figure 1.** Isomers *cis* ( $\alpha$ ) and *trans* ( $\beta$ ) of chlordane. Computationally optimized structures are also shown.

Since the C–F bond brings desirable properties to an agrochemical, the bioisosteric replacement of the chlorines by fluorines in chlordane may lead to a novel, improved class of

pesticides for use in agriculture – exemplified as “fluordane” herein. The same approach can be applied to other chlorinated cyclodiene insecticides, such as aldrin and dieldrin. In this sense, a computational exploitation can be performed before time and cost-demanding experimental procedures by calculating physicochemical data for health and environment risk assessment. Inhibition of the cytochrome P450 enzymes is also worth to predict, since they also function to metabolize toxic compounds, principally in the liver. In addition, the insecticide-likeness of the proposed compounds may be searched taking into consideration their interaction with the GABA<sub>A</sub> receptor-chloride channel through docking studies. Accordingly, this computer simulation study may be helpful to generate baseline data for experimental work, thus alerting the community to a possible strategy for next-generation agrochemicals.

## MATERIALS AND METHODS

The geometry optimization of both isomers of chlordane, as well as of their fluorinated bioisosteres, was carried out at the density functional theory (DFT) B3LYP/6-311++g(d,p) level (Becke, 1988; Lee et al., 1988; Krishnan et al., 1980), in order to obtain the molecular dipole moments of the compounds. The same procedure was carried out for aldrin, dieldrin and pentachlorophenol, as well as for their fluorinated derivatives, which do not have stereoisomers. These calculations were performed using the Gaussian 09 program (Frisch et al., 2016). Physicochemical properties and toxicity endpoints were predicted using the Percepta platform of the ACD/Labs program, which provides all required data (ACD/Labs Percepta, 2012); these estimations are obtained either by additive atomic contributions (*e.g.* for the calculation of lipophilicity – log *P*) or by interpolation of the chemical structure descriptors in an empirical or calculated model.

The ligand-enzyme fitting was obtained by docking studies, using Glide module with standard precision (Friesner et al., 2004; Halgren et al., 2004). The crystal structure of  $\alpha 1\beta 3\gamma 2$ -GABA<sub>A</sub> in complex with picrotoxin, GABA and megobody Mb38 was obtained from the Protein Data Bank (PDB code: 6HUG) with resolution of 3.1 Å (Masiulis et al., 2019). The receptor crystal structure was prepared using the Protein Preparation Wizard (from Schrödinger Suite 2011) with OPLS2005 force field; the co-crystallized ligand and megobody Mb38 were excluded, and missing atoms/connections were added.

The ligands were prepared apart from the receptor. The structures of chlordane, aldrin and dieldrin, as well as of their corresponding fluorinated analogs, were optimized at the density functional theory (DFT) B3LYP/6-311++g(d,p) level (Becke, 1988; Lee et al., 1988; Krishnan et al., 1980). The charges were calculated according to the electrostatic potential scheme of

CHELPG (Breneman and Wiberg, 1990) at the B3LYP/6-311++g(d,p) level using the Gaussian 09 program (Frisch et al., 2016).

Finally, the prepared ligands were docked at the picrotoxin binding site of the Cys-loop receptor, since earlier studies demonstrated that cyclodienes act by the same mechanism of picrotoxin (Abalis et al., 1986). A rigid docking was performed, in which the ligands are allowed to move, but the residues remain rigid in the active site. Forty poses were generated for each cyclodiene. The best poses were chosen by superposition similarity with picrotoxin and energy criteria, *i.e.* the lowest energy pose which shows an acceptable superposition with picrotoxin was used for each ligand. Moreover, the superposition of the chlorinated compounds with the corresponding fluorinated bioisosteres was taken as reference. Docking results were also analyzed according to the docking scores of intermolecular interaction energies

## RESULTS AND DISCUSSION

Lipophilicity is ubiquitous in the estimation of bioactivity and toxicity of drug-like and agrochemical-like molecules (Waring, 2010). It is usually described in terms of the octanol-water partition coefficient ( $\log P$ ), which can be calculated from additive contributions of atoms and/or group fragments. Such approach does not account for stereochemistry though, despite a recent study describing that accurate lipophilicity measurements inform on subtle stereoelectronic effects (O'Hagan and Young, 2016); consequently, the stereochemistry that controls the molecular polarity can also modulate the  $\log P$  of a substance. Accordingly, the molecular geometries of chlordane (Figure 1) and of the corresponding fluorinated derivatives were optimized in gas phase, and the molecular dipole moments were then obtained. Because of the orientation and high polarity of the C–F bonds, both fluordane isomers are more polar than the respective chlordane isomers (2.99 against 2.57 Db for the  $\alpha$  isomers, and 2.48 against 1.81 Db for the  $\beta$  isomers – Figure 2). This suggests that fluordane is more water soluble than chlordane and also less absorbed either by soil particles or fatty tissues of living organisms. Indeed, this finding is confirmed by direct  $\log P$  calculations using the Percepta program: 5.96 for chlordane (in good agreement with the experimental  $\log P = 6.16$ ) (Simpson et al., 1995) and 2.96 for fluordane. The calculated solubility is also consistent with the lipophilicity data, since chlordane is calculated to be rather insoluble (experimental aqueous solubility at 25°C =  $1.37 \times 10^{-7}$  mol L<sup>-1</sup>) (Sanborn et al., 1976), while fluordane is calculated to be about a thousand-fold more soluble than chlordane ( $1.44 \times 10^{-4}$  mol L<sup>-1</sup>). Because soil can be rich in organic matter, the soil sorption of an agrochemical is usually dependent on its lipophilicity (Sabljić et

al., 1995). Therefore, fluorinated derivatives of organochlorides should have limited persistence in soil. In turn, these organofluorines should be more soluble in water, thus affecting the aquatic life through bioconcentration or bioaccumulation – also directly related to  $\log P$  (Devillers et al., 1996) – in a smaller extent.

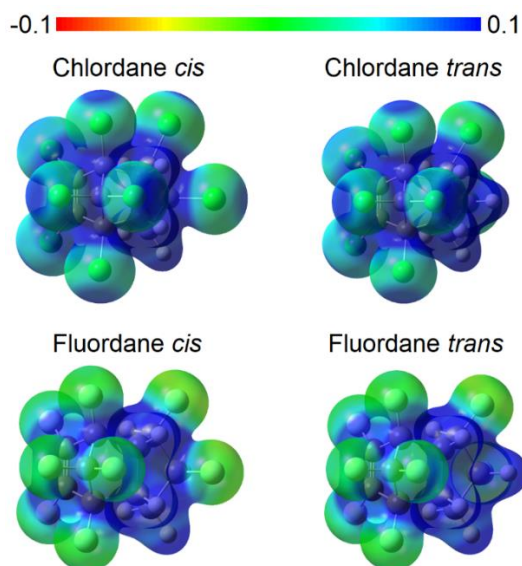


**Figure 2.** Electrostatic potential surfaces (at 0.02 a.u.) from -0.1 (red) to 0.1 (blue) a.u. for chlordane and fluordane obtained at the B3LYP/6-311++g(d,p) level; colors are more contrasting in the latter, indicating more polar bonds.

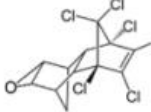
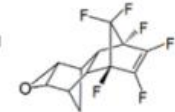
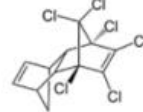
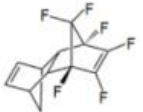
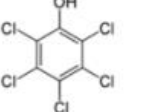
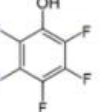
Despite both fluordane and chlordane not being prone to cause mutagenicity according to the calculations for simulation of the Ames test through the ACD/Labs Percepta program, the latter compound was calculated to be a probable CYP3A4 enzyme inhibitor. The cytochrome P450 3A4 (CYP3A4) is a key oxidizing enzyme involved in molecule metabolism, *e.g.* by the hydroxylation of  $C(sp^3)$ -H bonds (Meunier et al., 2004). While inhibition of the CYP3A4 enzyme is undesirable, the insecticidal activity of chlordane is related to targets at the central nervous system, particularly by blocking specific GABA receptors, contributing to its neurotoxic effects (Narahashi et al., 1998). Since fluordane appears to be advantageous in many aspects compared to chlordane, the binding affinity of both ligands towards the known picrotoxin binding site at the  $GABA_A$  receptor of the Cys-loop ligand-gated ion channel superfamily can be searched and compared to each other with the aim at estimating the pesticide-likeness of fluordane.

Docking studies were performed in order to gain insight into the insecticidal potency of fluordane compared to chlordane. Because of the lack of a suitable  $GABA_A$  receptor from an insect, the human  $\alpha 1\beta 3\gamma 2$ - $GABA_A$  in complex with picrotoxin, GABA and megobody Mb38 was considered (Masiulis et al., 2019). Since the effect caused by a small amount of active

fluordane/chlordanes bound to the human receptor is possibly negligible compared to the effect in the insect, its human toxicity should be proportionally lower than in the insect. In addition, the bioaccumulation problem is attenuated in the case of fluorinated compounds, since they have lower lipophilicity. It is worth mentioning that although the GABA receptors exhibit considerable pharmacological variety between invertebrates and vertebrates, they have remarkable structural similarities – the GABA receptor subunits of invertebrates are between 30% and 47% of identity to vertebrates (Hosie et al., 1997). Moreover, alanine (which interacts with most of compounds studied herein, see the Supplementary Material) is an important residue involved in pesticide activity; in many cases, insecticide resistance is observed when alanine is replaced (Ffrench-Constant et al., 2016). The receptor selection step also took into account the structural similarity among the crystallized ligand (picrotoxin) and the chlordanes derivatives. In addition, the picrotoxin is similar to the biological ligand TBPS (*t*-butyl bicyclic phosphorothionate), which is employed for indication of activity potency in sample preparations from mammalian brains (Coats, 1990; Casida and Lawrence, 1985).

The fluorinated analogs of chlordanes showed lower protein-ligand energies, suggesting higher complex ligand-protein stabilities (Table 1). While the complex protein/ $\alpha$ -chlordanes showed a docking score (the free energy of protein-ligand binding) of  $-5.61\text{ kcal mol}^{-1}$ , the corresponding value for the complex with  $\alpha$ -fluordane is  $-6.56\text{ kcal mol}^{-1}$ . The same pattern was observed for  $\beta$ -compounds:  $-5.73$  against  $-6.61\text{ kcal mol}^{-1}$ . It is worth mentioning that  $\beta$ -chlordanes are known to be more active than  $\alpha$ -chlordanes (Metcalf, 2000), which is in agreement with the docking scores. Moreover, the satisfactory superposition of the cyclodienes with picrotoxin also validates our approach.

**Table 1.** Calculated physicochemical data (molecular dipole moments in  $\text{D}_\mu - \mu$ , octanol-water partition coefficient –  $\log P$ , and water solubility –  $S_{\text{water}}$  – in  $\text{mol L}^{-1}$ ), cytochrome P450 target (CYP), and docking score ( $E_{\text{docking score}}$ ) data for the studied compounds (in  $\text{kcal mol}^{-1}$ ). Available experimental data are given in parenthesis (second entries).

						
Compound	$\mu$	$\log P$	$S_{\text{water}}$	CYP	$E_{\text{docking score}}$	
$\alpha$ -Chlordane	2.57	5.96 (6.16) <sup>a</sup>	Insoluble $(1.37 \times 10^{-7})^b$	CYP3A4	-5.61	
$\beta$ -Chlordane	1.81	5.96 (6.16) <sup>a</sup>	Insoluble $(1.37 \times 10^{-7})^b$	CYP3A4	-5.73	
$\alpha$ -Fluordane	2.99	2.96	$1.44 \times 10^{-4}$	-	-6.56	
$\beta$ - Fluordane	2.48	2.96	$1.44 \times 10^{-4}$	-	-6.61	
Aldrin	3.03	6.07 (6.50) <sup>c</sup>	Insoluble $(4.66 \times 10^{-8})^d$	CYP3A4	-6.19	
F-aldrin	3.71	3.54	Insoluble	-	-6.83	
Dieldrin	1.47	4.81 (5.40) <sup>c</sup>	Insoluble $(5.80 \times 10^{-7})^e$	-	-4.99	
F-dieldrin	2.31	2.22	Insoluble	-	-6.21	
Pentachloropheno (PCP)	1.76	5.12 (5.12) <sup>f</sup>	$4.8 \times 10^{-3}$ $(5.26 \times 10^{-5})^g$	CYP1A2 CYP2C9	-	
Pentafluorophenol (PFP)	2.15	2.91	0.39		-	

<sup>a</sup> Simpson et al. (1995); <sup>b</sup> Sanborn et al. (1976); <sup>c</sup> De Bruijn et al. (1989); <sup>d</sup> Dannenfelser and Yalkowsky (1991); <sup>e</sup> Biggar and Riggs (1974); <sup>f</sup> Hansch et al. (1995); <sup>g</sup> Yalkowsky and He (2003).

It is also possible to observe specific interactions, such as hydrogen bond and hydrophobic interactions, between picrotoxin and some amino acid residues in GABA<sub>A</sub> (Supplementary Material). Since the action mechanisms of picrotoxin and cyclodienes are similar, it is worth paying attention to these interactions in the picrotoxin-protein complex.

THR256 and SER267 residues are involved in hydrogen bonds with picrotoxin; at least one of these residues also interacts with all fluorinated bioisosteres (and also with dieldrin). These interactions determine the higher affinity of fluorinated compounds with the protein. Furthermore, the fluorinated derivatives presented a reasonable superposition with their chlorinated analogs, thus allowing for a direct comparison of the fluorinated bioisosteres with the corresponding chlorinated compounds. As an example, it is possible to observe more effective interactions (hydrogen bonds) in the protein/fluordane complex than in the protein/chlordan complex (Figure 3).

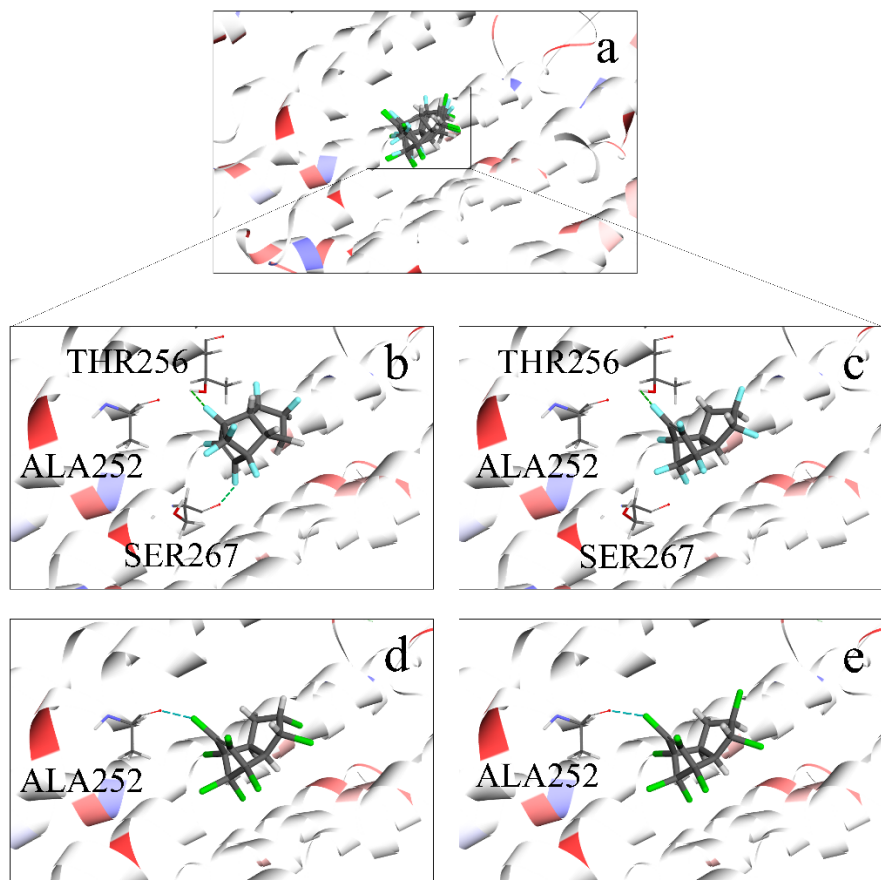


**Figure 3.** a) Superposition of chlordan and fluordane inside the binding site of GABA<sub>A</sub>; b) and c) specific interactions of  $\alpha$ - and  $\beta$ -fluordane, respectively, in the binding site of GABA<sub>A</sub>; d) and e) specific interactions of  $\alpha$ - and  $\beta$ -chlordan, respectively, in the binding site of GABA<sub>A</sub>. ALA = alanine, SER = serine, and THR = threonine.

These outcomes are supported by other aromatic and alicyclic organochlorines, whose fluorinated analogs resemble the same advantages of fluordane over chlordan. Accordingly, dieldrin and its synthetic precursor, aldrin, as well as their respective fluorinated derivatives (F-dieldrin and F-aldrin), were further analyzed on the basis of their potential toxicity, environmental risk and insecticidal potency (Table 1). Pentachlorophenol (PCP) and its fluorinated analog pentafluorophenol (PFP) were also evaluated, except for their insecticidal

potential, because the mode of action of phenol insecticides is rather dictated by an oxidation mechanism (Michałowicz and Duda, 2007). The hydrophobicity of the fluorinated analogs is lower than that of the corresponding chlorinated compounds, while the water solubility is higher. Cytochrome inhibition appeared only for the chlorinated compounds; similar to cytochrome P450 3A4, the CYP1A2 and CYP2C9 enzymes (efficiently inhibited by PCP, according to Percepta predictions) are monooxygenases involved in the metabolism of compounds.

Persistence and toxicity are major topics to be accounted for when designing performance pesticides. Some studies have established a critical role for lipophilicity on the bioconcentration (BCF), bioaccumulation (BAF) and biomagnification (BMF) factors of organochlorines in fish species (Thomann, 1989; Moses et al., 2015; Arnot and Gobas, 2003), whilst others included additional descriptors to encode persistence-related parameters, such as molecular weight and topological polar surface area (Fatemi and Baher, 2009; Miller et al., 2019). According to Thomann (1989), food chain effects are not significant up to  $\log P$  of *ca.* 5, while for  $\log P$  of 5-7, calculated and observed BCF's in top predators indicate significant elevations above calculated field BCF values; above  $\log P$  of 7, food chain effects are sensitive to the chemical assimilation efficiency and phytoplankton BCF. Therefore, according to the experimental and calculated  $\log P$  values in Table 1, the fluorinated pesticides would be advantageous over their chlorinated analogs, as the organofluorines exhibit  $\log P$  values below 5, while the corresponding organochlorines all have  $\log P$  between 5 and 7.

Pierre et al. (2019) developed a predictive QSAR model for the estimation of toxicity data ( $\log LC_{50}$ ,  $LC_{50}$  = lethal concentration required to kill 50% of a population of *Poecilia reticulata*, the rainbow fish) of a series of organochlorine compounds using quite a few molecular descriptors. This model applies  $\log P$ , index of refraction (IR), surface tension (ST), density ( $d$ ), and polarizability (pol) as molecular descriptors in the following multilinear regression equation (1):

$$\log LC_{50} = 9.95 - 0.11 \times \log P - 3.31 \times IR + 0.03 \times ST - 0.73 \times d - 0.22 \times pol \quad (1)$$

$$N = 50; R^2 = 0.90; MSE = 0.12; R^2_{adj} = 0.89; R^2_{cv} = 0.89$$

The calculated molecular descriptors obtained through the ACD/Labs program for the studied compounds were used in the equation above, thus yielding the predicted  $\log LC_{50}$  values of Table 2. According to this model, the most toxic compound is assumed to display the smallest  $\log LC_{50}$  value, that is chlordane. Actually, the chlorinated compounds were all calculated to be

more toxic than the fluorinated analogs, therefore confirming organofluorines as promising alternatives for chlordane, Aldrin and Dieldrin.

**Table 2.** Molecular descriptors and predicted toxicity ( $\log LC_{50}$ ) for the organochlorine pesticides and their respective fluorinated analogs.

Compound	$\log P$	IR	ST (dyne cm <sup>-1</sup> )	$d$ (g cm <sup>-3</sup> )	Pol ( $\times 10^{-24}$ cm <sup>3</sup> )	$\log LC_{50}$
Chlordane	5.96	1.63	54.0	1.80	31.82	-2.8
Fluordane	2.96	1.40	20.9	1.58	16.87	0.8
Aldrin	6.07	1.66	55.3	1.73	30.81	-2.6
F-aldrin	3.54	1.48	27.6	1.54	19.60	0.1
Dieldrin	4.81	1.68	60.2	1.84	30.71	-2.4
F-dieldrin	2.22	1.50	30.6	1.68	19.50	0.1
PCP	5.12	1.63	54.7	1.80	20.85	-0.3
PFP	2.91	1.43	31.4	1.69	11.14	2.2

Overall, prospective next-generation organofluorine agrochemicals have been explored and they are expected to display a better performance than their chlorinated analogs. Future challenges include the synthesis of fluorinated derivatives of known chlorinated pesticides and further comparison of their potency and physicochemical parameters related to toxicity and environmental persistence with the chlorinated compounds. This seems to be feasible, since *e.g.* a route to obtain the all-*cis*-hexafluorocyclohexane, a fluorinated stereoisomer of the insecticide lindane ( $\gamma$ -hexachlorocyclohexane), has already been developed (Keddie et al., 2015) and its preparation is currently quite straightforward (Wiesenfeldt et al., 2017). Indeed, preparation of perfluorocyclopentadiene has long been known (Banks et al., 1965; 1967).

## CONCLUSIONS

Although the proposal of fluordane as a new pesticide was not the pivotal goal in this study, the bioisosteric switch of chlorine with fluorine atoms may be beneficial in all cases, either by accounting for the predicted bioactivity (once the stability of the compounds inside the biding site of GABA<sub>A</sub> is enhanced) or environmental impact (a lower bioaccumulative capability is expected). Facing these results, fluordane can indeed be considered an example of

compound that opens the possibility of studying other organofluorines as a novel benchmark class of pesticides.

## ACKNOWLEDGEMENTS

Authors are thankful to Fundação de Amparo à Pesquisa do Estado de Minas Gerais – FAPEMIG for the financial support of this research (grant number: CEX-APQ-00383/15), as well as to Coordenação de Aperfeiçoamento de Pessoal de Nível Superior – CAPES (funding code 001) and Conselho Nacional de Desenvolvimento Científico e Tecnológico – CNPq (grant number: 301371/2017-2) for the studentships (to F.A.M. and J.K.D.) and a fellowship (to M.P.F.).

## REFERENCES

- Abalis, I. M.; Eldefrawi, M. E.; Eldefrawi, A. T. Effects of insecticides on GABA-induced chloride influx into rat brain microsacs. *J. Toxicol. Environ. Health Part A* **1986**, *18*, 13-23.
- ACD/Labs Percepta, Advanced Chemistry Development, Inc., Toronto, ON, Canada, [www.acdlabs.com](http://www.acdlabs.com), 2012.
- Agency for Toxic Substances and Disease Registry (ATSDR). *Toxicological profile for chlordane*. Atlanta, Department of Health and Human Services, Public Health Service, 2018.
- Anand, M.; Agrawal, A. K.; Rehmani, B. N. H.; Gupta, G. S. D.; Rana, M. D.; Seth, P. K. Role of GABA receptor complex in low dose lindane (HCH) induced neurotoxicity: neurobehavioural, neurochemical and electrophysiological studies. *Drug Chem. Toxicol.* **1998**, *21*, 35-46.
- Arnot, J. A.; Gobas, F. A. P. C. A generic QSAR for assessing the bioaccumulation potential of organic chemicals in aquatic food webs. *QSAR Comb. Sci.* **2003**, *22*, 337-345.
- Banks, R. E.; Harrison, A. C.; Haszeldine, R. N.; Orrell, K. G. Diels-Alder reactions involving perfluorocyclopentadiene. *Chem. Commun.* **1965**, 41-42.
- Banks, R. E.; Harrison, A. C.; Haszeldine, R. N.; Orrell, K. G. Polyfluorocyclopentadienes. Part II: Diels-Alder reactions of perfluorocyclopentadiene. *J. Chem. Soc. C* **1967**, 1608-1621.
- Becke, A. D. Density-functional exchange-energy approximation with correct asymptotic behavior. *Phys. Rev. A* **1988**, *38*, 3098-3100.
- Biggar, J. W.; Riggs, R. I. Apparent solubility of organochlorine insecticides *Hilgardia* **1974**, *42*, 383-391.
- Bloomquist, J. R.; Soderlund, D. M. Neurotoxic insecticides inhibit GABA-dependent chloride uptake by mouse brain vesicles. *Biochem. Biophys. Res. Commun.* **1985**, *133*, 37-43.
- Breneman, C. M.; Wiberg, K. B. Determining atom-centered monopoles from molecular electrostatic potentials. The need for high sampling density in formamide conformational analysis. *J. Comp. Chem.* **1990**, *11*, 361-373.
- Casida, J. E.; Lawrence, L. J. Structure-activity correlations for interactions of bicycophosphorus esters and some polychlorocycloalkane and pyrethroid insecticides with the brain-specific t-butylbicycophosphorothionate receptor. *Environ. Health Perspect.* **1985**, *61*, 123-132.
- Coats, J. R. Mechanisms of toxic action and structure-activity relationships for organochlorine and synthetic pyrethroid insecticides. *Environ. Health Perspect.* **1990**, *87*, 255-262.

- Dannenfelser, R. M.; Yalkowsky, S. H. Data base of aqueous solubility for organic non-electrolytes. *Sci. Total Environ.* **1991**, *109*, 625-628.
- Davis, K. J.; Fitzhugh, O. G. Tumorigenic potential of aldrin and dieldrin for mice. *Toxicol. Appl. Pharmacol.* **1962**, *4*, 187-189.
- De Bruijn, J.; Busser, F.; Seinen, W.; Hermens, J. Determination of octanol/water partition coefficients for hydrophobic organic chemicals with the “slow-stirring” method. *Environ. Toxicol. Chem.* **1989**, *8*, 499-512.
- Devillers, J.; Bintein, S.; Domine, D. Comparison of BCF models based on log P. *Chemosphere* **1996**, *33*, 1047-1065.
- Egeler, P.; Römbke, J.; Meller, M.; Knacker, T.; Franke, C.; Studinger, G.; Nagel, R. Bioaccumulation of lindane and hexachlorobenzene by tubificid sludge worms (Oligochaeta) under standardised laboratory conditions. *Chemosphere* **1997**, *35*, 835-852.
- Fatemi, M. H.; Baher, E. A novel quantitative structure-activity relationship model for prediction of biomagnification factor of some organochlorine pollutants. *Mol. Divers.* **2009**, *13*, 343-352.
- Ffrench-Constant, R. H.; Williamson, M. S.; Davies, T. G. E; Bass, C. Ion channels as insecticide targets. *J. Neurogenet.* **2016**, *30*, 163-177.
- Fishman, B. E.; Gianutsus, G. Inhibition of 4-aminobutyric acid (GABA) turnover by chlordane. *Toxicol. Lett.* **1985**, *26*, 219-223.
- Friesner, R. A.; Banks, J. L.; Murphy, R. B.; Halgren, T. A.; Klicic, J. J.; Mainz, D. T.; Shaw, D. E. Glide: a new approach for rapid, accurate docking and scoring. 1. Method and assessment of docking accuracy. *J. Med. Chem.* **2004**, *47*, 1739-1749.
- Frisch, M. J.; Trucks, G. W.; Schlegel, H. B.; Scuseria, G. E.; Robb, M. A.; Cheeseman, J. R.; Scalmani, G.; Barone, V.; Petersson, G. A.; Nakatsuji, H.; Li, X.; Caricato, M.; Marenich, A. V.; Bloino, J.; Janesko, B. G.; Gomperts, R.; Mennucci, B.; Hratchian, H. P.; Ortiz, J. V.; Izmaylov, A. F.; Sonnenberg, J. L.; Williams-Young, D.; Ding, F.; Lipparini, F.; Egidi, F.; Goings, J.; Peng, B.; Petrone, A.; Henderson, T.; Ranasinghe, D.; Zakrzewski, V. G.; Gao, J.; Rega, N.; Zheng, G.; Liang, W.; Hada, M.; Ehara, M.; Toyota, K.; Fukuda, R.; Hasegawa, J.; Ishida, M.; Nakajima, T.; Honda, Y.; Kitao, O.; Nakai, H.; Vreven, T.; Throssell, K.; Montgomery, J. A., Jr.; Peralta, J. E.; Ogliaro, F.; Bearpark, M. J.; Heyd, J. J.; Brothers, E. N.; Kudin, K. N.; Staroverov, V. N.; Keith, T. A.; Kobayashi, R.; Normand, J.; Raghavachari, K.; Rendell, A. P.; Burant, J. C.; Iyengar, S. S.; Tomasi, J.; Cossi, M.; Millam, J. M.; Klene, M.; Adamo, C.; Cammi, R.; Ochterski, J. W.; Martin, R. L.; Morokuma, K.; Farkas, O.; Foresman, J. B.; Fox, D. J. Gaussian 09, Revision A.02, Gaussian, Inc., Wallingford CT, 2016.
- Fujiwara, T.; O'Hagan, D. Successful fluorine-containing herbicide agrochemicals. *J. Fluor. Chem.* **2014**, *167*, 16-29.
- Halgren, T. A.; Murphy, R. B.; Friesner, R. A.; Beard, H. S.; Frye, L. L.; Pollard, W. T.; Banks, J. L. Glide: a new approach for rapid, accurate docking and scoring. 2. Enrichment factors in database screening. *J. Med. Chem.* **2004**, *47*, 1750-1759.
- Hansch, C.; Leo, A.; Hoekman, D. *Exploring QSAR – Hydrophobic, Electronic, and Steric Constants*; American Chemical Society, Washington, 1995.
- Hosie, A. M.; Aronstein, K.; Sattelle, D. B.; Ffrench-Constant, R. H. Molecular biology of insect neuronal GABA receptors. *Trends Neurosci.* **1997**, *20*, 578-583.
- Keddie, N. S.; Slawin, A. M.; Lebl, T.; Philp, D.; O'Hagan, D. All-cis 1,2,3,4,5,6-hexafluorocyclohexane is a facially polarized cyclohexane. *Nat. Chem.* **2015**, *7*, 483-488.
- Krishnan, R.; Binkley, J. S.; Seeger, R.; Pople, J. A. Self-consistent molecular orbital methods. XX. A basis set for correlated wave functions. *J. Chem. Phys.* **1980**, *72*, 650-654.
- Lee, C.; Yang, W.; Parr, R. G. Development of the Colle-Salvetti correlation-energy formula into a functional of the electron density. *Phys. Rev. B* **1988**, *37*, 785-789.

- Liang, X.; Huang, T.; Li, M.; Mack, J.; Wildervanck, M.; Nyokong, T.; Zhu, W. Highly efficient C-Cl bond cleavage and unprecedented C-C bond cleavage of environmentally toxic DDT through molecular electrochemical catalysis. *Appl. Catal.* **2017**, *545*, 44-53.
- Masiulis, S.; Desai, R.; Uchański, T.; Martin, I. S.; Laverty, D.; Karia, D.; Steyaert, J. GABA A receptor signalling mechanisms revealed by structural pharmacology. *Nature* **2019**, *565*, 454-459.
- Mathur, V.; Bhatnagar, P.; Sharma, R. G., Acharya, V.; Sexana, R. Breast cancer incidence and exposure to pesticides among women originating from Jaipur. *Environ. Int.* **2002**, *28*, 331-336.
- Metcalf, R. L. Insect Control. In *Ullmann's Encyclopedia of Industrial Chemistry*; Wiley-VCH, Weinheim, 2000.
- Meunier, B.; de Visser, S. P.; Shaik, S. Mechanism of oxidation reactions catalyzed by cytochrome P450 enzymes. *Chem. Rev.* **2004**, *104*, 3947-3980.
- Michałowicz, J.; Duda, W. Phenols-sources and toxicity. *Pol. J. Environ. Stud.* **2007**, *16*, 347-362.
- Miller, T. H.; Gallidabino, M. D.; MacRae, J. I.; Owen, S. F.; Bury, N. R.; Barron, L. P. Prediction of bioconcentration factors in fish and invertebrates using machine learning. *Sci. Tot. Environ.* **2019**, *648*, 80-89.
- Moses, S. K.; Harley, J. R.; Lieske, C. L.; Muir, D. C. G.; Whiting, A. V.; O'Hara, T. M. Variation in bioaccumulation of persistent organic pollutants based on octanol-air partitioning: Influence of respiratory elimination in marine species. *Mar. Pollut. Bull.* **2015**, *100*, 122-127.
- Murphy M. B.; Loi E. I. H.; Kwok K. Y.; Lam P. K. S. Ecotoxicology of Organofluorous Compounds. In *Top. Curr. Chem.: Fluorous Chemistry*; Horváth, I. T., Ed.; Springer, Heidelberg, 2011; 308, 339-363.
- Narahashi, T.; Ginsburg, K. S.; Nagata, K.; Song, J. H.; Tatebayashi, H. Ion channels as targets for insecticides. *Neurotoxicol.* **1998**, *19*, 581-590.
- O'Hagan, D.; Young, R. J. Accurate lipophilicity ( $\log P$ ) measurements inform on subtle stereoelectronic effects in fluorine chemistry. *Angew. Chem. Int. Ed.* **2016**, *55*, 3858-3860.
- Pierre, M. O.; Kafoumba, B.; Kouakou, N. N.; Nahossé, Z. Determination of descriptors which influence the toxicity of organochlorine compounds using QSAR method. *Chem. Sci. Int. J.* **2019**, *27*, 1-13.
- Piu, D.; Popescu, M.; Niculescu, M.; Pascu, L. F.; Galaon, T.; Postolache, C. Mobility of some high persistent organochlorine compounds from soil to mentha piperita. *Rev. Chim.* **2019**, *70*, 278-282.
- Pomes, A.; Rodríguez-Farré, E.; Suñol, C. Disruption of GABA-dependent chloride flux by cyclodienes and hexachlorocyclohexanes in primary cultures of cortical neurons. *J. Pharmacol. Exp. Ther.* **1994**, *271*, 1616-1623.
- Sabljić, A.; Güsten, H.; Verhaar, H.; Hermens, J. QSAR modelling of soil sorption. Improvements and systematics of  $\log K_{OC}$  vs.  $\log K_{OW}$  correlations. *Chemosphere* **1995**, *31*, 4489-4514.
- Sanborn, J. R.; Metcalf, R. L.; Bruce, W. N.; Lu, P. Y. The fate of chlordane and toxaphene in a terrestrial-aquatic model ecosystem. *Environ. Entomol.* **1976**, *5*, 533-538.
- Sharma, H.; Zhang, P.; Barber, D. S.; Liu, B. Organochlorine pesticides dieldrin and lindane induce cooperative toxicity in dopaminergic neurons: Role of oxidative stress. *Neurotoxicol.* **2010**, *31*, 215-222.
- Simpson, C. D.; Wilcock, R. J.; Smith, T. J.; Wilkins, A. L.; Langdon, A. G. Determination of octanol-water partition coefficients for the major components of technical chlordane. *Bull. Environ. Contam. Toxicol.* **1995**, *55*, 149-153.

- Theodoridis, G. Fluorine-containing Agrochemicals: An Overview of Recent Developments. In *Fluorine and the Environment: Agrochemicals, Archaeology, Green Chemistry and Water*; Tressaud, A., Ed.; Elsevier, Amsterdam, 2006.
- Thomann, R. V. Bioaccumulation model of organic chemical distribution in aquatic food chains. *Environ. Sci. Technol.* **1989**, *23*, 699-707.
- Uversky, V. N.; Li, J.; Fink, A. L. Pesticides directly accelerate the rate of  $\alpha$ -synuclein fibril formation: a possible factor in Parkinson's disease. *FEBS Lett.* **2001**, *500*, 105-108.
- Waring, M. J. Lipophilicity in drug discovery. *Exp. Opin. Drug Discov.* **2010**, *5*, 235-248.
- Wiesenfeldt, M. P.; Nairoukh, Z.; Li, W.; Glorius, F. Hydrogenation of fluoroarenes: Direct access to all-cis-(multi) fluorinated cycloalkanes. *Science* **2017**, *357*, 908-912.
- Yalkowsky, S. H.; He, H. *Handbook of Aqueous Solubility Data*; CRC Press, Boca Raton, 2003.

# Theoretical exploitation of 1,2,3,4,5,6-hexachloro- and 1,2,3,4,5,6-hexafluorocyclohexane isomers as biologically active compounds

(Submitted)

Francisco A. Martins and Matheus P. Freitas

**Abstract:** Hexachlorocyclohexanes (HCHs) have been widely explored as biological compounds during the last century. However, most of them were banned due to their potential toxicity in humans, animals, and the environment. Revisiting HCHs to explore their biological activity while improving key features is valuable and may lead to a new class of pesticides that utilizes the biological response of HCHs without their toxic characteristics. In this sense, the fluorine atom can be a possible alternative since a large number of therapeutics and agrochemicals have been developed with this halogen in their structure. We have evaluated herein the conformational behavior of HCHs and their bioisosteric fluorinated compounds, namely, hexafluorocyclohexanes (HFHs), through quantum-chemical calculations. We also explored the potential of the HCH and HFH isomers as biological compounds by docking them inside three possible targets. It was demonstrated that HCH and HFH have similar ligand–protein interactions with three pockets: the picrotoxin and barbiturate sites of the GABA<sub>A</sub> receptor and the ryanodine receptor. The results support HFHs as possible alternatives for HCHs since the replacement of Cl with F does not forfeit the main ligand–protein interactions. Finally, we demonstrated that HFHs have a lower log *P* than HCHs by almost two logarithmic units. This result highlights the role of fluorine in distribution and bioaccumulation.

## Introduction

Over the past decades, the increasing number of agrochemicals in use indicates the critical role of these compounds in the development of society. While new molecules have been proposed or improved, the use of a variety of chemicals *such as* organochlorines has been restricted due to health and environmental issues.<sup>1</sup> Organochlorines used to be widely employed in pest control during the mid-20th century.<sup>2</sup> However, the indiscriminate use of these compounds leads to severe ecological problems. Organochlorines have shown high mobility since trace amounts are present in places where they have never been used before around the globe.<sup>3</sup> Likewise, the toxicity of organochlorines extends to mammals, and the effects can be pronounced in humans due to bioaccumulation and biomagnification through the food chain.<sup>4</sup> In addition, risks are related to the relative ease of C–Cl bond cleavage, which leads to distinct metabolites that can be even more toxic than the original molecule.<sup>5</sup> Despite the serious issues related to organochlorine compounds, they have performed well against crop plagues.<sup>6</sup> In this sense, taking advantage of the biological activity of these compounds while mitigating the

toxicity can lead to new molecules with high potential in agrochemistry. Therefore, revisiting molecules and optimizing parameters to improve biological properties is necessary since pest control is challenging and food demand is high.

Organochlorine pesticides are classified into three main classes, namely, dichlorodiphenylethylenes, cyclodienes, and hexachlorocyclohexanes (HCHs);<sup>7</sup> the latter is the focus of this work. The HCH class is represented by eight diastereomers (Figure 1). These molecules are six-membered rings in which each carbon has one chlorine attached, that is, the isomers differentiate from each other only by their spatial orientation, not by their positions.<sup>8</sup> This fact makes the study of these compounds through ligand-based approaches challenging since only subtle structural changes explain the variance in the biological response in different targets.<sup>9</sup> However, structure-based modeling studies are valuable for gaining insight into the binding modes of these compounds. As mentioned, the stereochemistry of these compounds plays a pivotal role in bioactivity. For example, delta- and beta-isomers have a depressant response, while the gamma-isomer (lindane) is a widely known pesticide with stimulant properties.<sup>10</sup> Additionally, some HCH isomers have unknown biological properties and have never been synthesized (*e.g.*,  $\zeta$ -HCH), so they can be further explored.

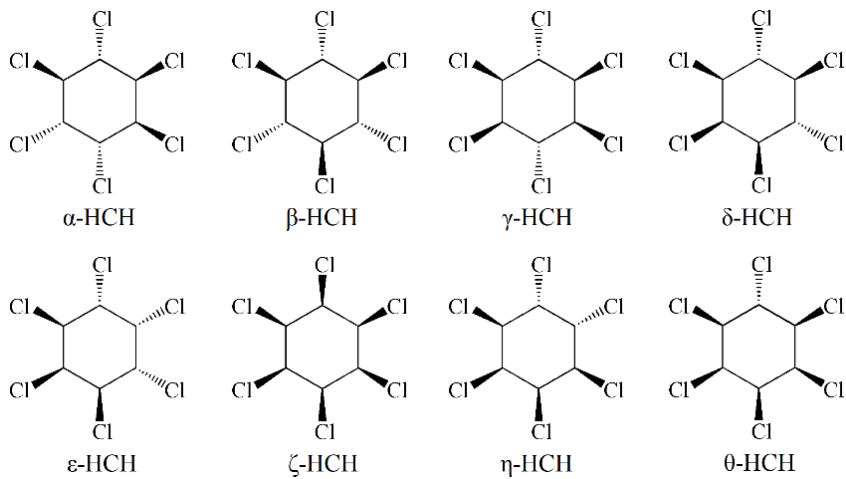


**Figure 1.** Diastereomers of 1,2,3,4,5,6-hexachlorocyclohexanes (HCHs).

HCH molecules may act on many targets and produce different biological responses, but their mechanisms of action remain poorly understood. For instance, lindane ( $\gamma$ -HCH) has been used as an agricultural insecticide and pharmaceutical treatment for lice and scabies, and it has stimulant properties.<sup>11</sup> Unlike cyclodienes, lindane is a poor inhibitor *via* GABA receptors, and its biological properties are related to releasing calcium rather than avoiding chloride influx by targeting the picrotoxin site.<sup>12</sup>  $\delta$ -HCH is a non-insecticide isomer with depressant effects, but it can act as a stimulant at higher doses. In addition, the effects of both

lindane and  $\delta$ -HCH are dose-dependent in GABA receptors.<sup>10</sup> On the other hand,  $\alpha$ - and  $\beta$ -HCH are more toxic than lindane and lack insecticidal activity.<sup>13</sup>

Studies suggest that some HCHs act in the picrotoxin site as organochlorine cyclodienes and are responsible for the excitatory response due to disruption in chlorine influx to the cell; on the other hand, depressant effects are due to the interaction of HCHs with the barbiturate site of the GABA receptor.<sup>14</sup> Although the interaction with GABA receptors is well known, alternative targets and mechanisms of action are expected to produce the same HCH response since lindane is one of the least active pesticides inhibiting GABA-dependent chlorine uptake.<sup>15</sup> HCHs have a lipophilic character; consequently, they interact with intracellular components. In this sense, intracellular calcium storage is an important component responsible for muscle contraction. Signaling occurs by releasing  $\text{Ca}^{2+}$  from the intracellular storage.<sup>16</sup> Several studies report HCH molecules acting in intracellular calcium channels and producing an excitatory response, making intracellular calcium storage signaling one of the possible alternative mechanisms of action of HCH compounds.<sup>17</sup>

There are two major intracellular calcium channels: the ryanodine receptor (RyR) and the inositol (1,4,5)-triphosphate receptor (InsP<sub>3</sub>R). These receptors are responsible for intracellular calcium modulation.<sup>18</sup> Some observations support the HCH action over the  $\text{Ca}^{2+}$  channel. For example, dantrolene is a RyR inhibitor that inhibits intracellular calcium release in the cell. When dantrolene is applied with lindane, no convulsant effect is observed, indicating that the action of the lindane is related to this specific receptor.<sup>19</sup> Furthermore, InsP<sub>3</sub>R has an endogenous ligand [inositol (1,4,5)-triphosphate], and its ring shares a similar stereochemistry as  $\delta$ -HCH, which makes InsP<sub>3</sub>R a natural receptor for HCH. In addition, it has been shown that  $\delta$ -HCH is capable of releasing  $\text{Ca}^{2+}$  cations from both receptors.<sup>12b,20</sup>

While chlorine may be hazardous for biological and environmental systems,<sup>21</sup> organofluorine compounds have been widely employed as bioactive chemicals.<sup>22</sup> It has been estimated that almost 30% of agrochemicals and therapeutics in use worldwide contain at least one fluorine atom.<sup>23</sup> This element provides interesting features for biological compounds in terms of pharmacokinetics and pharmacodynamics.<sup>24</sup> It is worth mentioning that the C–F bond is highly polarized; consequently, it has a minor potential for bioaccumulation and biomagnification compared to the C–Cl bond since having fewer lipophilic molecules makes the compound less prone to interactions with the cell's phospholipid bilayer.<sup>25</sup> For these reasons, replacing chlorine atoms with fluorine is an intuitive way to explore organochlorine optimization.

Therefore, the arguments presented give us intriguing topics to observe for future applications of HCHs and their fluorinated bioisosteres—hexafluorocyclohexanes (HFHs). In this sense, we report herein the evaluation of HCHs and their fluorinated bioisosteres to gain insight into the protein–ligand interactions and the possible effects of chlorine replacement. Furthermore, HCHs have different stereochemistries that can be employed to explore the role of the chemical space in biological activity. The last topic we investigated was the characteristics of all HCH diastereomers since not all HCHs have well-understood biological properties.

## Results and Discussion

### Conformational Analysis

The replacement of one hydrogen in each carbon of cyclohexane produces 1,2,3,4,5,6-hexasubstituted rings. The highly substituted pattern creates a significant number of isomers with distinct configurational and conformational isomerism, where the conformers can interconvert through ring flip inversion (Figure 2). In this study, we evaluate the conformational preferences of eight diastereomers of 1,2,3,4,5,6-hexachloro- (HCH) and 1,2,3,4,5,6-hexafluorocyclohexane (HFH), namely,  $\alpha$ -,  $\beta$ -,  $\gamma$ -,  $\delta$ -,  $\varepsilon$ -,  $\zeta$ -,  $\eta$ -, and  $\theta$ -isomers, through *ab initio* calculations. It is known that substituents in cyclohexane rings adopt axial or equatorial positions, and their preference is ruled by steric, dipolar, and hyperconjugative interactions. Additionally, it is generally accepted that substituents in equatorial positions attenuate the 1,3-dipolar and steric repulsion, while hyperconjugative interactions can favor axial or equatorial groups.<sup>26</sup> Therefore, the conformational behavior is dictated by these competing factors.

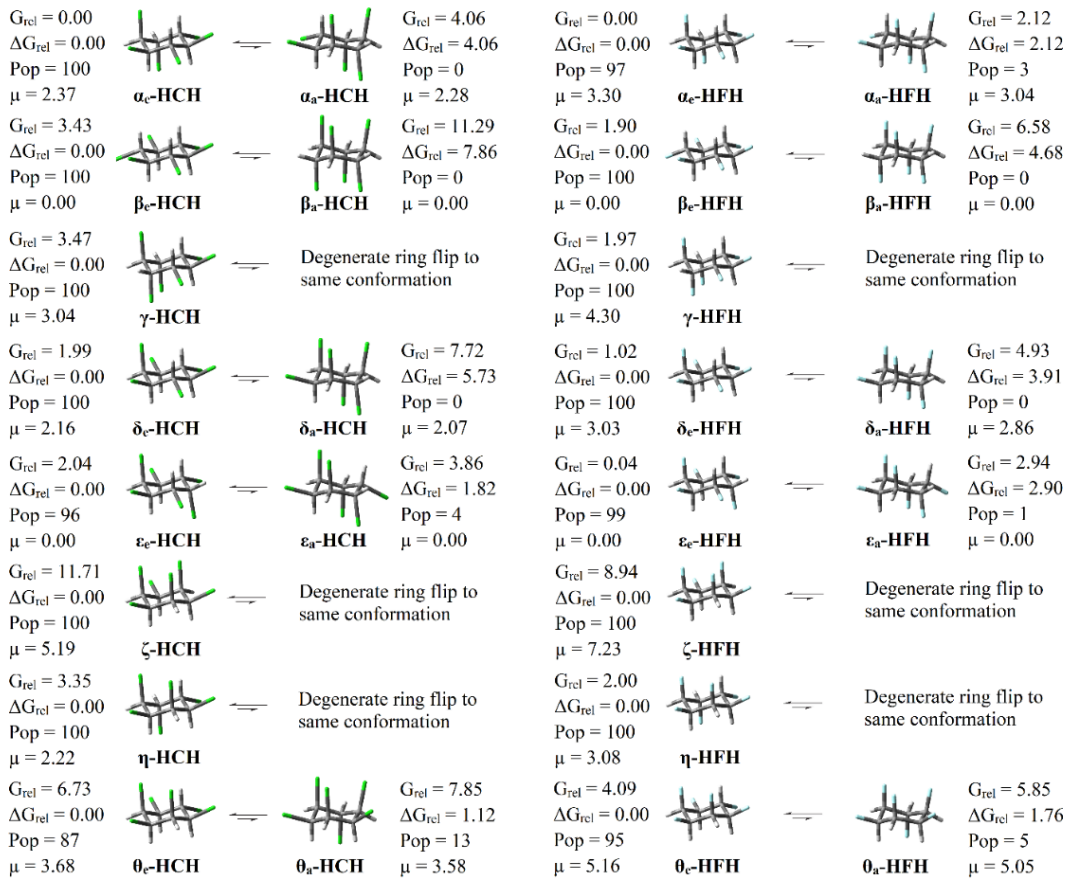


**Figure 2.** All eight isomers,  $\alpha$ ,  $\beta$ ,  $\gamma$ ,  $\delta$ ,  $\epsilon$ ,  $\zeta$ ,  $\eta$ , and  $\theta$ , of HCH and HFH in the chair form and their conformational flip. The relative conformational Gibbs free energies ( $\Delta G_{\text{rel}}$ ), and relative configurational Gibbs free energies ( $G_{\text{rel}}$ ) are given in kcal mol<sup>-1</sup>, conformational population in %, and dipole moment in debye (Db). Data obtained through calculations at the MP2/6-311++g(d,p) level. Labels: H = white, C = gray, F = cyan, Cl = green.

The results are straightforward about the chair flip isomerism of HCH and HFH diastereomers since the equilibrium is shifted to conformers with more substituents in equatorial positions. For example, the  $\alpha$ -diastereomer is found to be in equilibrium between two chairs, named  $\alpha_e$  and  $\alpha_a$ . The subscripts e and a denote a chair with predominant equatorial and axial substituents, respectively. The equilibrium is completely shifted toward conformer  $\alpha_e$ , which has two axial and four equatorial halogens (Figure 2). This observation extends to all compounds in the gas phase, since the least stable equatorial conformer shows a population of 87% ( $\theta_e\text{-HCH}$ ). These findings suggest a high cost to conformers bearing more axial groups in the ring flip inversion.

Despite the clear conformational behavior of HCHs and HFHs, by inspecting the whole set of isomers, it is possible to observe that  $\beta_e$ , the most equatorially substituted ring, is not the lowest energy isomer. This observation demonstrates that all groups in equatorial regions do

not ensure a higher stability to the molecule; however, a balance between axial and equatorial groups seems to dictate the molecular stability. The conformer  **$\delta_e$ -HCH** ( $G_{\text{rel}} = 2.0 \text{ kcal mol}^{-1}$ ) has one axial halogen; and is less stable than  **$\alpha_e$ -HCH** ( $G_{\text{rel}} = 0.0 \text{ kcal mol}^{-1}$ ) and more stable than  **$\beta_e$ -HCH** ( $G_{\text{rel}} = 3.4 \text{ kcal mol}^{-1}$ ), which have two and zero halogens in the axial position, respectively. This fact indicates that two axial halogens are the ideal number to produce stability in the chairs in 1,2,3,4,5,6-hexachloro- and 1,2,3,4,5,6-hexafluorocyclohexanes.

A closer inspection of  **$\alpha_e$** ,  **$\epsilon_e$** , and  **$\theta_e$**  is insightful since they differ in relative configurational energy but share the feature of two axial and four equatorial halogens. The conformers  **$\alpha_e$**  and  **$\epsilon_e$**  have their axial substituents in an antiparallel orientation, while in  **$\theta_e$** , these groups are parallel. This fact explains why  **$\theta_e$**  lies in a higher energy level, since both C–X bonds are on the same side of the ring, and it provides more steric/electrostatic repulsion than conformers with both bonds on opposite sides. According to natural bond orbital (NBO) analysis, steric/electrostatic effects are the primary factor governing the energy differences among diastereomers since the total energy ( $E_{\text{Full}}$ ) is dictated by the Lewis energy component ( $E_{\text{Lewis}}$ ); see Supporting Information. The  $E_{\text{Full}}$  is divided into two terms: one relative to classical factors,  $E_{\text{Lewis}}$ , and a second relative to delocalization effects,  $E_{\text{non-Lewis}}$ . By inspecting the energy components, it is possible to observe that the most stabilizing  $E_{\text{non-Lewis}}$  term is unable to generate a minimum  $E_{\text{Full}}$  due to the higher  $E_{\text{Lewis}}$  value. However, hyperconjugative effects may play a critical role in determining the preference of  **$\alpha_e$**  over  **$\epsilon_e$** . For example, both  **$\alpha_e$ -HCH** and  **$\epsilon_e$ -HCH** have the same substitution pattern, but the vicinal axial groups are preferred since  **$\alpha_e$**  is  $2.0 \text{ kcal mol}^{-1}$  more stable than  **$\epsilon_e$** . This preference can be attributed to the interactions of the  $\sigma_{\text{CCl}}$  and  $\sigma^*_{\text{CCl}}$  orbitals of axial chlorine with vicinal bonds. In the  **$\alpha_e$**  isomer, each axial chlorine experiences one  $\sigma_{\text{CH}} \rightarrow \sigma^*_{\text{CCl}}$  ( $6.35 \text{ kcal mol}^{-1}$ ), one  $\sigma_{\text{CCl}} \rightarrow \sigma^*_{\text{CH}}$  ( $1.74 \text{ kcal mol}^{-1}$ ), and two  $\sigma_{\text{CCl}} \rightarrow \sigma^*_{\text{CCl}}$  ( $3.79 \text{ kcal mol}^{-1}$ ) interactions, while the  **$\epsilon_e$**  isomer exhibits two  $\sigma_{\text{CH}} \rightarrow \sigma^*_{\text{CCl}}$  ( $1.78 \text{ kcal mol}^{-1}$ ) and two  $\sigma_{\text{CCl}} \rightarrow \sigma^*_{\text{CH}}$  ( $5.78 \text{ kcal mol}^{-1}$ ) interactions. In this sense,  **$\alpha_e$**  comprises  $15.47 \text{ kcal mol}^{-1}$  of stabilization, while  **$\epsilon_e$**  comprises  $15.12 \text{ kcal mol}^{-1}$  of stabilization.

The results are in good agreement with previous reports on the conformational analysis of HCH and HFH.<sup>27</sup> In addition, several studies indicate that steric and dipolar factors rule the conformational isomerism of dihalocyclohexanes, while hyperconjugative interactions play a secondary role.<sup>28</sup> In this sense, a comparison between HCH and HFH can be useful to decide whether steric or electrostatic effects are the primary source for the energetic profile of the 1,2,3,4,5,6-hexa-halogenocyclohexane isomers. Fluorine is smaller than chlorine and provides more polar bonds since it is a more electronegative atom. Therefore, the replacement of chlorine

with fluorine works as a tool to evaluate the competing steric/electrostatic factors responsible for the 1,2,3,4,5,6-hexa-halogenocyclohexane isomers. If steric factors are the primary contributor to the molecular stability, the replacement will increase the ring stability; on the other hand, if dipolar repulsion is the source of the energetic behavior, the fluorine atoms will cause a decrease in stability.

Accordingly, all fluorinated compounds have lower  $G_{\text{rel}}$  values than their HCH analogs and show higher dipole moments, except for those with zero dipole moments (Figure 2). For example,  $G_{\text{rel}}$  ranges from 0.00 to 11.71 kcal mol<sup>-1</sup> in the HCH series, while the corresponding range in HFH decreases by almost 3 kcal mol<sup>-1</sup> (0.00 to 8.94 kcal mol<sup>-1</sup>). Therefore, steric repulsion among halogens dictates the molecular preferences. Previous reports evaluating 1,2-difluoro-, 1,2-dichloro-, and 1,2-bromocyclohexane demonstrated the role of steric repulsion in the axial–axial (aa) preference. It was shown that the 1,2-dihalocyclohexane preference for the aa conformer increases from fluorine to bromine substituents; therefore, by increasing the halogen size, the aa population increases due to steric hindrance in the ee conformer.<sup>28a</sup> In our case, the high substitution pattern provides a more complex conformational behavior, in which all axial or all equatorial substituents are not the most stable forms.

Finally, an analysis was carried out considering the HCH and HFH isomers in an implicit water environment through the polarizable continuum model (PCM). This analysis aids the evaluation of the compounds in polar media and gives more insight into the steric/electrostatic effects. Because steric repulsion has been found to be the main source of molecular stability, polar solvents are expected to favor conformers with higher dipole moments without drastically changing the stability profile, since steric effects, not electrostatic effects, contribute the most to the molecular preferences. The observation is still the same for HCH in water compared to HCH in the gas phase, with small changes (e.g.,  $\eta$  and  $\beta_e$  have almost the same  $G_{\text{rel}}$ ; however,  $\eta$  is more stable in the gas phase, while  $\beta_e$  is more stable in water). It is possible to observe an increase in  $\Delta G_{\text{rel}}$  for HCH and HFH molecules in water. This increase is a consequence of the polar medium acting in favor of the conformer with a higher dipole moment (Supporting Information). For the fluorinated compounds, the solvent effect is more pronounced since fluorine ensures more polar bonds and produces a higher dipole moment and, in general, the conformational energy range decreases in conformers with more equatorial substituents. In other words, electrostatic effects from the solvent affect fluorinated compounds more than chlorinated compounds. However, molecular stability is governed by steric factors, so the configurational energy profile does not change significantly in water.

## Docking Study

The biological activity of HCHs varies with the diastereoisomers and doses; for example,  $\delta$ -HCH exhibits depressant effects at lower doses, but it is a stimulant at higher doses. Furthermore,  $\gamma$ -HCH (lindane) is related to GABA receptor inhibition, while  $\alpha$ -HCH and  $\beta$ -HCH seem to act poorly in this regard. The picrotoxin and barbiturate sites are mentioned in the literature as possible targets for HCH in chloride flux modulation in the GABA receptor.<sup>14</sup> On the other hand, some studies suggest intracellular calcium storage as the source of the HCH biological response.<sup>17</sup> Since our goal is to evaluate the impact of chlorine replacement, and due to the unclear target for HCHs, we explore the interaction of HCHs and their fluorinated bioisosteres (HFHs) with a few different proteins to determine their potential to cause a biological response. The proteins studied in this work are the human GABA<sub>A</sub> receptor, human-type 3 1,4,5-inositol triphosphate (InsP<sub>3</sub>R), and human ryanodine receptor 3 (RyR). PDB ID codes of 6X40 and 6X3W for GABA<sub>A</sub>, 6DQN for InsP<sub>3</sub>R, and 4ERV for RyR were used for docking purposes. We chose human proteins because the three targets are available simultaneously, which allows us to compare the ligand interactions in the same species.

All HCH and HFH isomers were docked into the picrotoxin and barbiturate sites of GABA<sub>A</sub>, InsP<sub>3</sub>, and ryanodine receptors. The results show that InsP<sub>3</sub>R provides a poor ligand–protein interaction with hexahalocyclohexanes, and among all receptors, it has the lowest docking score values (best D<sub>score</sub> = -1.30 kcal mol<sup>-1</sup>) (Supporting Information). Moreover, the superposition of HCH and HFH with the cocrystallized ligand is not efficient, even with the same ring core. This finding indicates that other targets may be responsible for the HCH mechanism of action. The interactions of halogenated cyclohexanes with RyR and GABA<sub>A</sub> yield almost the same level of energy. The docking scores in the picrotoxin site range from -3.0 to -4.2 kcal mol<sup>-1</sup>, -3.4 to -4.7 kcal mol<sup>-1</sup> in the barbiturate site, and -2.6 to -3.7 kcal mol<sup>-1</sup> in the RyR site (Figure 3). The docking results do not allow us to properly conclude which target is responsible for the HCH activity, since the interactions in all of them are close in energy, and other factors beyond ligand–protein interaction may be critical to bioactivity. However, these findings indicate that the three binding sites are prone to bind in almost the same manner. Since our primary goal is to explore the bioisosteric replacement of chlorine by fluorine atoms, we will further discuss the differences between HCH and HFH in each target.

In the picrotoxin site of the GABA<sub>A</sub> receptor, HCH and HFH isomers do not differ significantly in interaction energy, since no clear preference has been observed for fluorinated or chlorinated molecules in the pocket. In addition, the maximum energy difference is 0.5 kcal

$\text{mol}^{-1}$ ; for example,  **$\alpha_e\text{-HCH}$**  interacts with an energy of -3.72 kcal  $\text{mol}^{-1}$ , while the corresponding value for  **$\alpha_e\text{-HFH}$**  is -3.80 kcal  $\text{mol}^{-1}$ . The only exception is the  $\zeta$ -isomer, in which the fluorinated molecule binds more effectively than the chlorinated molecule by 1.0 kcal  $\text{mol}^{-1}$  (Figure 3). The observation does not change appreciably in the barbiturate site of the GABA<sub>A</sub> receptor and RyR. However, there is a slight preference for HFH isomers in these two pockets (Figure 3). The docking results are insightful about chlorine replacement with fluorine in 1,2,3,4,5,6-hexahalocyclohexanes. Since the interaction energies do not change drastically, the bioisosteric replacement of chlorine with fluorine does not forfeit the ligand–protein interaction and can be further explored.

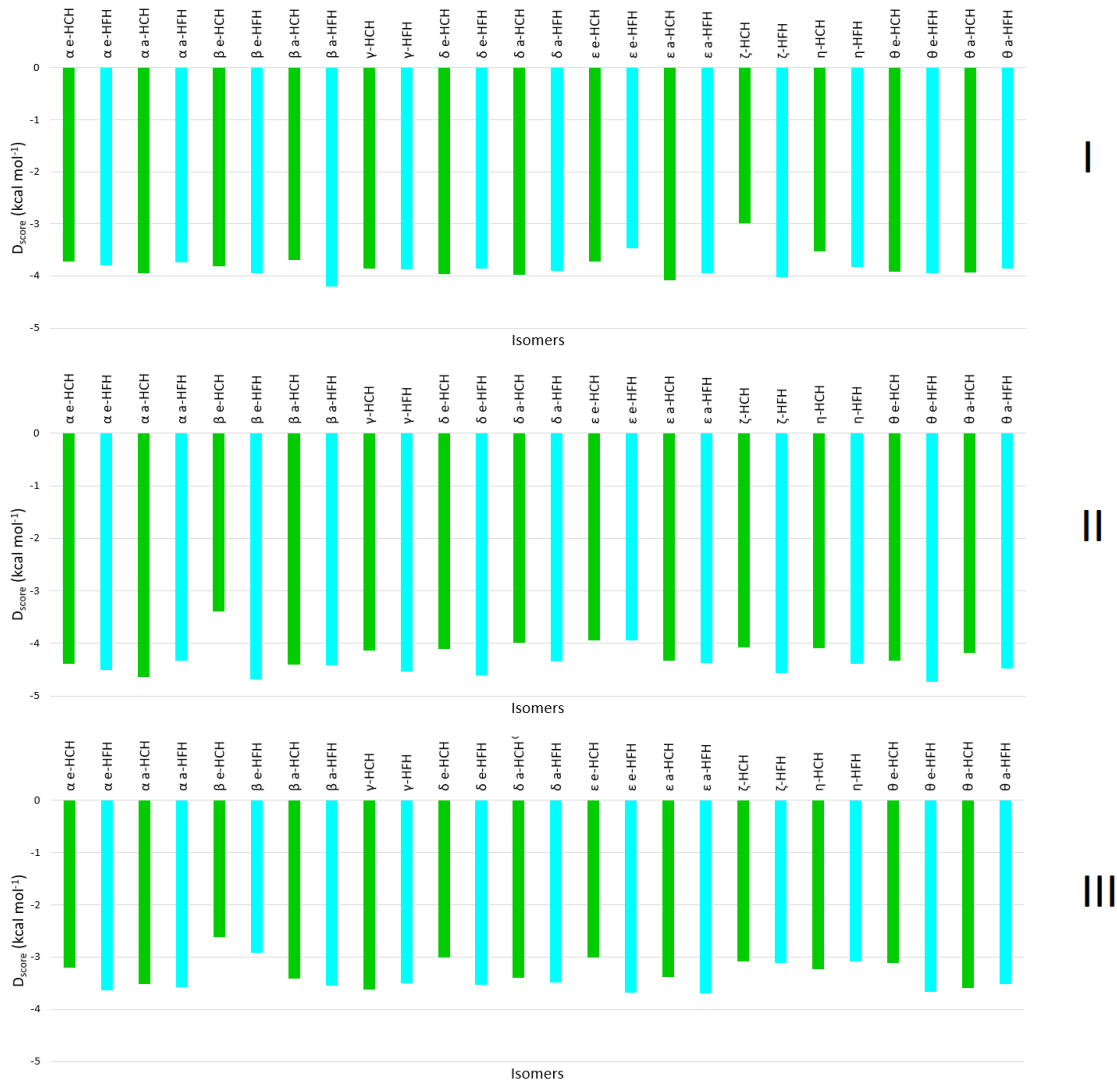


**Figure 3.** HCH (green) and HFH (cyan) docking scores computed for all isomers in the picrotoxin binding site of GABA<sub>A</sub> receptor (I), barbiturate binding site of GABA<sub>A</sub> receptor (II), and RyR (III).

The evaluation of specific ligand–protein interactions supports the idea that HFHs are suitable alternatives for HCH since these molecules share similar types of interactions in the

protein pockets. In the picrotoxin site, not all chlorinated and fluorinated molecules display interactions with residues, but if present, most of the interactions are halogen interactions with carbonyl or CH groups. However, in the barbiturate and RyR pockets, all molecules show at least one ligand–protein interaction. In this case, beyond halogen–carbonyl and halogen–HC interactions, it is possible to observe classical hydrogen bonds ( $X\cdots HO/N$ ) and  $R\cdots R$  interactions (Figure 4).

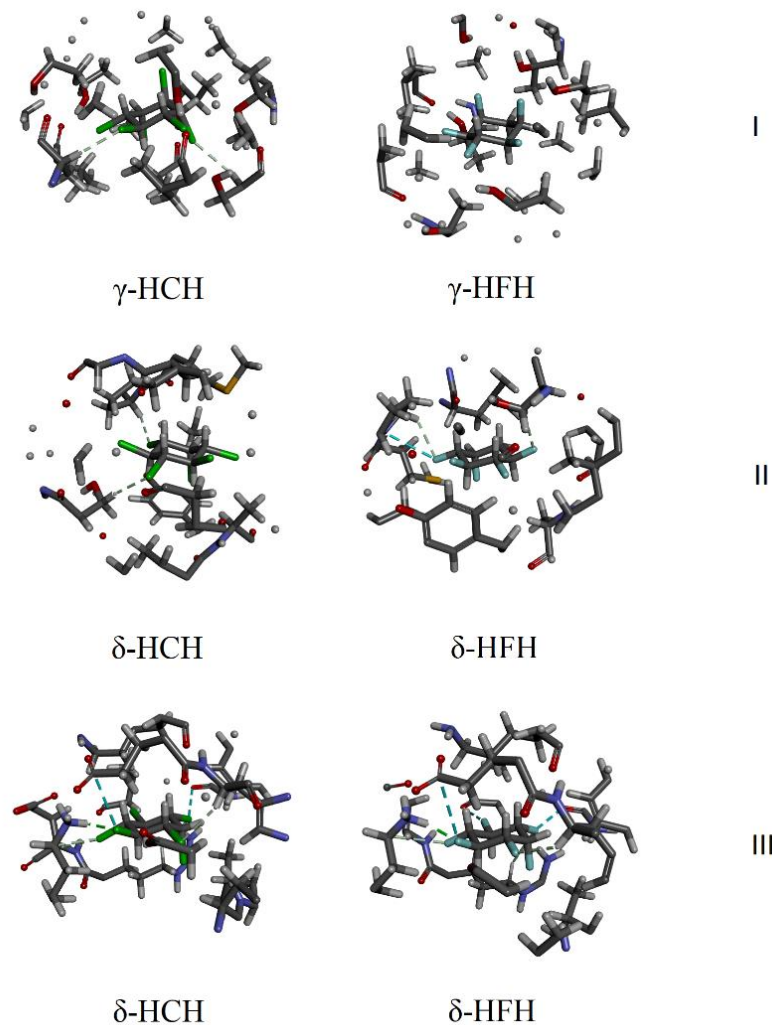


**Figure 4.** Receptor pockets of GABA<sub>A</sub> receptor and RyR. Specific ligand–protein interactions for  $\gamma$ -HCH and  $\gamma$ -HFH in the picrotoxin pocket of GABA<sub>A</sub> receptor (I). Specific ligand–protein interactions for  $\delta$ -HCH and  $\delta$ -HFH in the barbiturates pocket of GABA<sub>A</sub> receptor (II). Specific ligand–protein interactions for  $\delta$ -HCH and  $\delta$ -HFH in the pocket of RyR (III). H = white, C = gray, N = blue, F = cyan, Cl = green, O = red, S = yellow,  $X\cdots HO/N$  interaction = green dashed line,  $X-HC$  interaction = gray dashed line,  $X-\pi_{C=O}$  interaction = cyan dashed line. Note that the  $\gamma$  isomer interacts in the picrotoxin site to cause an excitatory response, while its  $\delta$  isomer acts in the barbiturate site to cause depressant effects. On the other hand, it is known that  $\delta$  binds to the RyR site. This explains the choice for the exemplification in this Figure.

Since all isomers show similar affinity to the protein amino acid residues, parameters other than the ligand–protein interaction may be responsible for the difference in the biological activity of the HCH compounds. Pharmacokinetics plays an essential role in drug response because it is related to the movement of a drug through the organism. Therefore, evaluation of pharmacokinetic features for these compounds may be valuable. It has been found that the solubility of HCHs in phospholipids and the degree of inhibition of phosphatidylinositol synthase and other membrane-associated enzymes follow the same order ( $\delta > \gamma > \alpha > \beta$ ).<sup>29</sup> This fact reinforces the crucial role of pharmacodynamics over HCH biological activity. The octanol-water partition coefficient described in terms of  $\log P$  is an important parameter that gives information about the drug distribution through the body. Despite its experimental nature, it is possible to estimate  $\log P$  using computational tools. However, most of the computational methods are based on additive contributions from molecular fragments; therefore, it is difficult to predict the  $\log P$  values for isomers. For this reason, we indirectly evaluate the  $\log P$  values of the HCH and HFH isomers through quantum-chemical calculations.

The octanol-water partition coefficient ( $K_{\text{ow}}$  or  $P$ ) provides a way to measure the molecular affinity for the organic phase since it is defined as the substance's concentration ratio in two phases (octanol and water) when the system achieves equilibrium.<sup>30</sup> It is a ubiquitous parameter in medicinal chemistry and agrochemistry since it is related to drug distribution and chemical fate. Moreover,  $\log P$  provides a way to estimate the potential of bioaccumulation of chemical compounds, e.g., molecules with  $\log P > 5$  are known to have a high potential for bioaccumulation, while this feature is less pronounced in compounds with  $\log P < 2$ .<sup>31</sup> The  $\log P$  for the HCH isomers in the literature is slightly divergent, and generally, this value falls within the range of 3.50 and 4.50, depending on the measurement procedure. For example, the  $\log P$  for lindane has been reported to be 3.30–3.61 experimentally and 3.83–4.26 theoretically. The same is observed for other isomers, such as  $\alpha$ -,  $\beta$ -, and  $\delta$ -HCH,<sup>32</sup> which is in agreement with our findings (Table 1).

Although the predicted  $\log P$  values show a small range for the chlorinated isomers, it is valuable for comparison with the HFHs. The fluorinated compounds show a clear decrease in the lipophilicity, since the  $\log P$  lies in the range of 1.0–2.3, while the corresponding values for the HCHs are higher than 3. This feature provides HFHs with a lower bioaccumulation potential than HCHs. It is worth noting that the all-*cis* isomer ( $\zeta$ ) possesses the smallest  $\log P$ , but to the best of our knowledge, the corresponding HCH is the only 1,2,3,4,5,6-hexachlorocyclohexane not yet prepared, perhaps due to its low stability (it is the least stable

HCH isomer, Figure 1). However,  **$\zeta$ -HCH** has been formerly synthesized through a multistep reaction,<sup>33</sup> and can be obtained by a straightforward procedure.<sup>34</sup> In addition to its potential application as a cation and anion carrier,<sup>35</sup>  **$\zeta$ -HCH** has been found to be one of the most promising barbiturate and RyR inhibitors among HFHs (Figure 3). Therefore,  **$\zeta$ -HCH** is both synthetically challenging and biologically interesting to study.

**Table 1.** Theoretical prediction of log *P* for each diastereomer (weighted by the conformational populations) performed at the  $\omega$ B97XD/6-311++g(2d,p) level of theory for the hexachloro- and hexafluorocyclohexanes.

Diastereomer	HCH log <i>P</i>	HFH log <i>P</i>
$\alpha$	4.54 (3.94) <sup>a</sup>	2.26
$\beta$	3.89 (3.92) <sup>a</sup>	1.74
$\gamma$	4.43 (3.83) <sup>a</sup>	2.20
$\delta$	3.93 (3.19) <sup>a</sup>	1.93
$\epsilon$	4.26	2.04
$\zeta$	3.25	1.03
$\eta$	4.31	2.08
$\theta$	3.74	1.58

<sup>a</sup> Computationally predicted log *P* by Hale *et al.*<sup>32a</sup>

## Methodology

The HCH and HFH diastereomers and their possible chair-flip conformers were fully optimized with vibrational frequencies accounted for using the *ab initio* MP2/6-311++g(d,p) level of theory,<sup>36</sup> both in the gas phase and when considering an implicit polar solvent (water) through the polarizable continuum model (PCM).<sup>37</sup> This step was carried out to gain insight into the ring stabilities and the conformational flip on molecules capable of establishing conformational isomerism. In this step, we also computed the molecular dipole moments. We performed a second set of calculations in the  $\omega$ B97XD/6-311++g(2d,p) level of theory<sup>38</sup> to determine the octanol-water partition coefficient. In this step, we also considered the implicit solvent model. However, we employed the solvation model based on density (SMD) using the SMD keyword. SMD has been attributed to performing better in the prediction of solvation free energy ( $\Delta G_w$  and  $\Delta G_o$ ),<sup>39</sup> which was used to estimate the log *P* according to Equation 1.<sup>40</sup> Since each conformer had one  $\Delta G_w$  and  $\Delta G_o$  and, consequently, a given log *P*, the log *P* for each diastereoisomer could be calculated by conformationally weighing the log *P*. These values are presented in Table 1. It is worth mentioning that the choice for the DFT method was based

on a reduced computational cost compared to the MP2 method. All described calculations were carried out using the Gaussian 09 package.<sup>41</sup>

$$\log P = \frac{\Delta G_w - \Delta G_o}{2.303RT} \quad (1)$$

The docking studies were performed using the Schrödinger suite 2011 with the OPLS2005 force field.<sup>42</sup> The first step was ligand preparation, in which MP2-optimized HCH and HFH structures were employed. We determined the molecular charges through the B3LYP/6-311++g(d,p) level of theory<sup>43</sup> using the electrostatic potential scheme of CHELPG with the Gaussian 09 program.<sup>41,44</sup> The second step was protein preparation; in this step, we obtained crystal structures of the human GABA<sub>A</sub> receptor in a complex with picrotoxin, the GABA<sub>A</sub> receptor in a complex with GABA and phenobarbital, the type-3 1,4,5-inositol triphosphate receptor (InsP3) in a complex with D-myo-inositol-1,4,5-triphosphate, and ryanodine receptor 3.<sup>45</sup> The PDB IDs (and protein resolution) are 6X40 (2.86 Å), 6X3W (3.30 Å), 6DQN (3.33 Å), and 4ERV (1.75 Å), respectively. After the protein acquisition and using the protein preparation wizard,<sup>46</sup> all missing hydrogens, side chains, and loops were included, and bond orders were assigned. All water molecules and hetero groups were deleted.

With all proteins properly prepared, we used the Receptor Grid Generation module of the Schrödinger suite to build the receptor grid. Here, two slightly different procedures were employed for grid generation. Since GABA<sub>A</sub> and InsP3 receptors include cocrystallized ligands, the receptor grid was generated based on cocrystallized ligands. Picrotoxin, phenobarbital, and D-myo-inositol-1,4,5-triphosphate were used for this purpose. In addition, due to the presence of the cocrystallized ligand, it was possible to redock the model to validate the methodology. The redocking results show a respective RMSD and docking score of 0.62 Å and -5.81 kcal mol<sup>-1</sup> for picrotoxin, 0.12 Å and -7.38 kcal mol<sup>-1</sup> for phenobarbital, and 0.71 Å and -6.43 kcal mol<sup>-1</sup> for D-myo-inositol-1,4,5-triphosphate. However, RyR did not include a cocrystallized ligand. For this reason, we employed the SiteMap tool<sup>47</sup> to determine the protein cavities that most likely act as receptors. For RyR, three pockets were generated with SiteScores of 1.01, 0.89, and 0.85. Because drug insertion sites should have a SiteScore higher than 1.00, we chose the first pocket for the docking studies. The results show that the first pocket is the largest at 213 Å<sup>2</sup> and has the highest volume of 394 Å<sup>3</sup>.

Finally, all HCH and HFH isomers were docked in each receptor pocket using the Glide module with extra precision.<sup>48</sup> Here, we accounted for no ring inversion, since we manually built the possible conformers to evaluate each ring conformation.

## Conclusion

The quantum-chemical calculations have shown a clear conformational behavior for HCH and HFH isomers. As expected from steric considerations, isomers that establish a conformational ring flip are preferred in rings with more halogens in the equatorial position. However, when comparing the diastereomers, neither  $\beta_e$ -HCH nor  $\beta_e$ -HFH are the most stable structures, which indicates that an overall energy minimum cannot be achieved if all substituents adopt the equatorial position. Therefore, a balance between the equatorial and axial substituents is needed, with the former in majority. According to experiments,  $\zeta$ -HFH is by far the least stable isomer of HFH, while the unknown  $\zeta$ -HCH is still higher in energy than its diastereoisomers, which makes it a challenging synthetic target.

The docking results showed that, except in the InsP<sub>3</sub> receptor, all isomers of HCH and HFH have a close docking score range in three pockets: the picrotoxin and barbiturate sites of the GABA<sub>A</sub> receptor and RyR. Although the literature is unclear about the primary target of HCH, our results demonstrated that the bioisosteric replacement of chlorine with fluorine atoms does not attenuate the ligand–protein interactions in these three possible targets. Moreover, such replacement can be beneficial to parameters related to bioaccumulation and distribution, such as log P, since HFHs have lower log P values than HCHs by almost two logarithmic units.

## References

- [1] G. Karlaganis, R. Marioni, I. Sieber, A. Weber, *Environ. Sci. Pollut. Res. Int.* **2001**, *8*, 216-221.
- [2] a) D. B. Barr, B. Buckley, In *Reproductive and developmental Toxicology*, Elsevier Enhanced Reader, **2011**, Ch. 20; b) R. W. Russell, S. J. Hecnar, G. D. Haffner, *Environ. Toxicol. Chem.* **1995**, *14*, 815-817.
- [3] a) K. Kalbitz, P. Popp, *Environ. Pollut.* **1999**, *106*, 139-141; b) Y. -F. Li, R. W. Macdonald, L. M. M. Jantunen, T. Harner, T. F. Bidleman, W. M. J. Strachan, *Sci. Total Environ.* **2002**, *291*, 229-246; c) D. C. G. Muir, N. P. Grift, W. L. Lockhart, P. Wilkinson, B. N. Billeck, G. J. Brunskill, *Sci. Total Environ.* **1995**, *160*, 447-457; d) F. Wania, D. Mackay, *Environ. Sci. Technol.* **1996**, *30*, 390A-396A; e) Y. -F. Li, R. W. Macdonald, *Sci. Total Environ.* **2005**, *342*, 87-106.
- [4] a) N. Wang, L. Yi, L. Shi, D. Kong, D. Cai, D. Wang, Z. Shan, *J. Environ. Sci.* **2012**, *24*, 1854-1860; b) Y. K. Das, D. Guven, D. Guvenc, O. Tokur, A. Aksoy, *Toxicol. Res.* **2017**, *6*, 664-670; c) Y. Yu, X. Wang, D. Yang, B. Lei, X. Zhang, X. Zhang, *Food Chem. Toxicol.* **2014**, *69*, 86-93; d) B. C. Kelly, M. G. Ikonomou, J. D. Blair, A. E. Morin, F. A. P. C. Gobas, *Science* **2007**, *317*, 236-239.

- [5] a) X. Liang, T. Huang, M. Li, J. Mack, M. Wildervanck, T. Nyokong, W. Zhu, *Appl. Catal.* **2017**, 545, 44-53; b) Z. Mehmood, M. P. Williamson, D. E. Kelly, S. L. Kelly, *Chemosphere* **1996**, 33, 759-769; c) D. Lu, D. Wang, R. Ni, Y. Lin, C. Feng, Q. Xu, X. Jia, G. Wang, Z. Zhou, *Environ. Sci. Pollut. Res. Int.* **2015**, 22, 9293-9306.
- [6] a) J. Park, S. Y. Park, J. Han, S. Y. Lee, G. E. Kim, Y. S. Jeong, J. H. Kim, E. J. Lee, E. Lee, T. H. Kim, *Am. J. Infect. Control* **2019**, 47, 588-590; b) L. K. Kagaruki, *Trop. Pest Manage.* **1991**, 37, 33-36; c) J. H. M. Lourens, R. J. Tatchell, *Bull. Ent. Res.* **1979**, 69, 235-242.
- [7] W. -T. Tsai, In *Encyclopedia of Toxicology*, Elsevier, third edition, **2014**, 711-713.
- [8] G. Chen, In *Encyclopedia of Toxicology*, Elsevier, third edition, **2014**, 874-876.
- [9] a) A. Pomés, E. R.-. Farré, C. Suñol, *J. Pharmacol. Exp. Ther.* **1994**, 271, 1616-1623; b) M. Christou, T. W. K. Fraser, V. Berg, E. Ropstad, J. H. Kamstra, *Environ. Res.* **2020**, 187, 109702-109713.
- [10] a) F. Matsumura, In *Toxicology of Insecticides*, Plenum Press, New York, **1985**, 111-202; b) K. Nagata, T. Narahashi, *Brain Res.* **1995**, 704, 85-91.
- [11] D. Mackey, W. Y. Shiu, K. C. Ma, In *Illustrated handbook of physical-chemical properties and environmental fate for organic chemicals*. Lewis Publishers, Boca Raton, **1997**.
- [12] a) J. M. Tusell, M. Vendrell, J. Serratosa, R. Trullas, *Brain Res.* **1992**, 593, 209-214; b) I. N. Pessah, F. C. Mohr, M. Schiedt, R. M. Joy, *J. Pharmacol. Exp. Ther.* **1992**, 262, 661-669; c) B. E. Fishman, G. Gianutsos, *Toxicol. Appl. Pharmacol.* **1988**, 93, 146-153.
- [13] Agency for toxic substances and disease registry, U.S. Department of Health and Human Services. Toxicologic profile for alpha-, beta-, gama- and deltahexachlorocyclohexane. August 2005. <http://www.atsdr.cdc.gov/toxprofiles/tp43.pdf>.
- [14] a) L. S. Aspinwall, I. Bermudez, L. A. King, K. A. Wafford, *J. Pharmacol. Exp. Ther.* **1997**, 282, 1557-1564; b) D. Belelli, D. Pau, G. Cabras, J. A. Peters, J. J. Lambert, *Br. J. Pharmacol.* **1999**, 127, 601-604.
- [15] a) J. R. Bloomquist, P. M. Adams, D. M. Soderlund, *Neurotoxicology* **1986**, 7, 11-20; b) M. Vendrell, J. M. Tusell, J. Serratosa, *J. Neurochem.* **1992**, 58, 862-869.
- [16] C. -R. Jan, J. -L. Wang, M. -C. Lin, K. C. Lee, K. -J. Chou, H. -T. Chiang, *Drug Dev. Res.* **2000**, 50, 186-192.
- [17] a) J. O-. Verbel, A. G-. Castilla, N. R. Ramos, *Rev. Environ. Contam. Toxicol.* **2011**, 212, 1-28; b) C. Solà, S. Barrón, J. M. Tusell, J. Serratosa, *Int. J. Biochem. Cell Biol.* **2001**, 33, 439-455; c) H. J. Heusinkveld, R. H. S. Westerink, *Environ. Sci. Technol.* **2012**, 46, 1842-1848; d) A. Srivastava, T. Shivanandappa, *Chem. Biol. Interact.* **2010**, 183, 34-39; e) H. J. Heusinkveld, G. O. Thomas, I. Lamot, M. Berg, A. B. A. Kroese, R. H. S. Westerink, *Toxicol. Appl. Pharmacol.* **2010**, 248, 12-19.
- [18] a) M. J. Berridge, *Nature* **1993**, 361, 315-325; b) S. L. Hamilton, *Cell Calcium* **2005**, 38, 253-260; c) G. Meissner, *Annu. Rev. Physiol.* **1994**, 56, 485-508.

- [19] R. Rosa, C. Sanfeliu, C. Suñol, A. Pomés, E. R.-. Farré, A. Schousboe, A. Frandsen, *Toxicol. Appl. Pharmacol.* **1997**, *142*, 31-39.
- [20] F. C. Mohr, S. V. Alojipan, S. K. Dunston, I. N. Pessah, *Mol. Pharmacol.* **1995**, *48*, 512-522.
- [21] a) K. Nolan, J. Kamrath, J. Levitt, *Pediatr. Dermatol.* **2012**, *29*, 141-146; b) R. Jayaraj, P. Megha, P. Sreedev, *Interdiscip. Toxicol.* **2016**, *9*, 90-100.
- [22] a) K. F. Murray, W. F. Balistreri, S. Bansal, S. Whitworth, H. M. Evans, R. P. G-. Peralta, J. Wen, B. Massetto, K. Kersey, J. Shao, K. L. Garrison, B. Parhy, D. M. Brainard, R. Arnon, L. A. Gillis, M. M. Jonas, C. -H. Lin, M. R. Narkwicz, K. Schwarz, P. Rosenthal, *Hepatol.* **2018**, *68*, 2158-2166; b) T. M. Kadia, F. Ravandi, G. Borthakur, M. Konopleva, C. D. DiNardo, N. Daver, N. Pemmaraju, R. K-. Shamanna, X. Wang, X. Huang, S. Pierce, C. Rausch, J. Burger, A. Ferrajoli, N. Jain, U. Popat, Z. Estrov, S. Verstovsek, E. Jabbour, G. G-. Manero, H. Kantarjian, *Am. J. Hematol.* **2021**, *96*, 914-924.
- [23] a) T. Fujiwara, D. O'Hagan, *J. Fluor. Chem.* **2014**, *167*, 16-29; b) D. O'Hagan, *J. Fluor. Chem.* **2010**, *131*, 1071-1081.
- [24] F. M. D. Ismail, *J. Fluor. Chem.* **2002**, *118*, 27-33.
- [25] S. S. Mansy, *Cold Spring Harb. Perspect. Biol.* **2010**, *2*, a002188.
- [26] a) V. Dragojlovic, *ChemTexts* **2015**, *1*, 1-30; b) T. D. Phien, S. A. Shlykov, *Comput. Theor. Chem.* **2016**, *1087*, 26-35.
- [27] a) Z. Zdravkovski, *Bull. Chem. Technol. Maced.* **2004**, *23*, 131-137; b) Q. Luo, K. R. Randall, H. F. Schaefer, *RSC Adv.* **2013**, *3*, 6572-6585; c) S. Gong, Y. Chen, Q. Luo, H. F. Schaefer, *New J. Chem.* **2019**, *43*, 18546-18558.
- [28] a) M. P. Freitas, C. F. Tormena, P. R. Oliveira, R. Rittner, *J. Mol. Struct.* **2002**, *589*, 147-151; b) M. P. Freitas, R. Rittner, C. F. Tormena, R. J. Abraham, *Spectrochim. Acta A: Mol. Biomol.* **2005**, *61*, 1771-1776; c) R. J. Abraham, Z. L. Rossetti, *J. Chem. Soc., Perkin Trans. 2* **1973**, 582-587.
- [29] a) G. M. Omann, J. R. Lakowicz, *Biochim. Biophys. Acta* **1982**, *684*, 83-95; b) G. S. Parries, M. H-. Neaverson, *J. Biol. Chem.* **1985**, *260*, 2687-2603.
- [30] H. Cumming, C. Rücker, *ACS Omega* **2017**, *2*, 6244-6249.
- [31] National Research Council, In *A Framework to Guide Selection of Chemical Alternatives.*, National Academies Press (US), **2014**.
- [32] a) S. E. Hale, T. J. Martin, K. -U. Goss, H. P. H. Arp, D. Werner, *Environ. Pollut.* **2010**, *158*, 2511-2517; b) I. Lessigiarska, A. P. Worth, T. I. Netzeva, J. C. Dearden, M. T. D. Cronin, *Chemosphere* **2006**, *65*, 1878-1887; c) J. Falandysz, B. Brudnowska, M. Kawano, T. Wakimoto, *Arch. Environ. Contam. Toxicol.* **2001**, *40*, 173-178; d) ATSDR, 2005. Toxicological Profile for HCHs., U.S. Dep. Health & Human Services. Public Health Service. Agency for Toxic Substances and Disease Registry, (ATSDR, **2005**).

- [33] N. S. Keddie, A. M. Z. Slawin, T. Lebl, D. Philp, D. O'Hagan. *Nat. Chem.* 2015, **7**, 483-488.
- [34] M. P. Wiesenfeldt, Z. Nairoukh, W. Li, F. Glorius, *Science* 2017, **357**, 908-912.
- [35] B. E. Ziegler, M. Lecours, R. A. Marta, J. Featherstone, E. Fillion, W. S. Hopkins, V. Steinmetz, N. S. Keddie, D. O'Hagan, T. B. McMahon. *J. Am. Chem. Soc.* **2016**, *138*, 7460-7463.
- [36] a) M. J. Frisch, M. H.-Gordon, J. A. Pople, *Chem. Phys. Lett.* **1990**, *166*, 275-280; b) M. J. Frisch, J. A. Pople, J. S. Binkley, *J. Chem. Phys.* **1984**, *80*, 3265-3269.
- [37] J. Tomasi, B. Mennucci, R. Cammi, *Chem. Rev.* **2005**, *105*, 2999-3094.
- [38] Y. S. Lin, G. D. Li, S. P. Mao, J. D. Chai, *J. Chem. Theory Comput.* **2013**, *9*, 263-272.
- [39] a) A. V. Marenich, C. J. Cramer, D. G. Truhlar, *J. Phys. Chem. B* **2009**, *113*, 6378-6396; b) J. Ho, M. Z. Ertem, *J. Phys. Chem. B* **2016**, *120*, 1319-1329.
- [40] S. Hossain, A. Kabedev, A. Parrow, C. A. S. Bergström, *Eur. J. Pharm. Biopharm.* **2019**, *137*, 46-55.
- [41] Gaussian 09, Revision A.02, M. J. Frisch, G. W. Trucks, H. B. Schlegel, G. E. Scuseria, M. A. Robb, J. R. Cheeseman, G. Scalmani, V. Barone, G. A. Petersson, H. Nakatsuji, X. Li, M. Caricato, A. Marenich, J. Bloino, B. G. Janesko, R. Gomperts, B. Mennucci, H. P. Hratchian, J. V. Ortiz, A. F. Izmaylov, J. L. Sonnenberg, D. Williams-Young, F. Ding, F. Lipparini, F. Egidi, J. Goings, B. Peng, A. Petrone, T. Henderson, D. Ranasinghe, V. G. Zakrzewski, J. Gao, N. Rega, G. Zheng, W. Liang, M. Hada, M. Ehara, K. Toyota, R. Fukuda, J. Hasegawa, M. Ishida, T. Nakajima, Y. Honda, O. Kitao, H. Nakai, T. Vreven, K. Throssell, J. A. Montgomery, Jr., J. E. Peralta, F. Ogliaro, M. Bearpark, J. J. Heyd, E. Brothers, K. N. Kudin, V. N. Staroverov, T. Keith, R. Kobayashi, J. Normand, K. Raghavachari, A. Rendell, J. C. Burant, S. S. Iyengar, J. Tomasi, M. Cossi, J. M. Millam, M. Klene, C. Adamo, R. Cammi, J. W. Ochterski, R. L. Martin, K. Morokuma, O. Farkas, J. B. Foresman, and D. J. Fox, Gaussian, Inc., Wallingford CT, 2016.
- [42] Schrödinger Release 2011: Maestro, Schrödinger, LLC, New York, NY, 2011.
- [43] a) A. D. Becke, *Phys. Rev. A* **1988**, *38*, 3098-3100; b) C. Lee, W. Yang, R. G. Parr, *Phys. Rev. B Condens. Matter* **1988**, *37*, 785-789; c) R. Krishnan, J. S. Binkley, R. Seeger, J. A. Pople, *J. Chem. Phys.* **1980**, *72*, 650-654.
- [44] C. M. Breneman, K. B. Wiberg, *J. Comput. Chem.* **1990**, *11*, 361-373.
- [45] a) J. J. Kim, A. Gharpure, J. Teng, Y. Zhuang, R. J. Howard, S. Zhu, C. M. Noviello, R. M. Walsh, E. Lindahl, R. E. Hibbs, *Nature* **2020**, *585*, 303-308; b) N. Paknejad, R. K. Hite, *Nat. Struct. Mol. Biol.* **2018**, *25*, 660-668; c) Z. Yuchi, K. Lau, F. Petegem, *Structure* **2012**, *20*, 1201-1211.
- [46] Schrödinger Release 2011: Protein Preparation Wizard; Epik, Schrödinger, LLC, New York, NY, 2011; Impact, Schrödinger, LLC, New York, NY; Prime, Schrödinger, LLC, New York, NY, 2011.

- [47] a) T. A. Halgren, *Chem. Biol. Drug Des.* **2007**, *69*, 146-148; b) T. A. Halgren, *J. Chem. Inf. Model.* **2009**, *49*, 377-389.
- [48] R. A. Friesner, R. B. Murphy, M. P. Repasky, L. L. Frye, J. R. Greenwood, T. A. Halgren, P. C. Sanschagrin, D. T. Mainz, *J. Med. Chem.* **2006**, *49*, 6177-6196.

# An examination of the relationship between molecular dipole moment and blood-gas partition for common anaesthetic gases

Reproduced from *Organic & Biomolecular Chemistry*, 19 (2021) 6665-6670 with permission from the Royal Society of Chemistry

Francisco A. Martins and Matheus P. Freitas

**Abstract:** The solubility of inhalational anaesthetics in the bloodstream is related to the minimum alveolar concentration (MAC), which is an indicator of anaesthetic gas potency. The blood-gas partition coefficient ( $K_{bg}$ ) is a measure of how much anaesthetics bind to plasma proteins in the blood compared to air. Just like the octanol-water partition coefficient, the  $K_{bg}$  may be related to the molecular dipole moment ( $\mu$ ), which can be modulated by the molecular conformation. Our quantum-chemical calculations demonstrated that subtle stereoelectronic interactions, namely those responsible for the anomeric and *gauche* effects, control the conformational equilibrium of some widely used volatile fluorinated anaesthetics and, consequently, of their molecular dipole moments. Since a remarkable correlation between empirical  $K_{bg}$  and calculated  $\mu$  was found for these anaesthetics, the average molecular dipole moments may be used to predict the anaesthetic gas potency and other properties, such as lipid solubility, of inhalational anaesthetic analogs.

## Introduction

The anaesthetic potency of inhalational anaesthetics appears to be dictated by the affinity of these compounds to plasma proteins in the blood, although their mechanism of action is not completely known and it may be a physical rather than a chemical bonding process.<sup>1</sup> To access these plasma proteins, the volatile anaesthetics should be reasonably soluble in the bloodstream and, therefore, the Ostwald coefficient for blood-gas, or simply the blood-gas partition coefficient ( $K_{bg}$ ), can be a valuable descriptor for the prediction of the anaesthetic potency. The anaesthetic gas potency may be described by the minimum alveolar concentration (MAC), which is correlated to  $K_{bg}$  according to Figure 1 for six last-generation fluorinated inhalational drugs.<sup>2,3</sup> However, the experimental measurement of  $K_{bg}$  may not be an easy task and, therefore, a straightforward method to obtain a parameter related to  $K_{bg}$  would be valuable for drug-likeness prediction purposes.

Linclau et al.<sup>4</sup> and then O'Hagan & Young<sup>5</sup> have recently found an interesting relationship between stereoelectronic effects and the lipophilicity of various fluorine-containing molecules, described as the octanol-water partition coefficient ( $\log P$ ). These studies

demonstrated that the lipophilicity of a molecule is related to its polarity, which is in turn governed by the molecular dipole moment ( $\mu$ ) balanced by the molecule's conformational populations. Since the conformational preferences of polar fluorocarbons are consistently driven by stereoelectronic effects, such as the fluorine *gauche* effect,<sup>6</sup> the authors concluded that lipophilicity informs on subtle stereoelectronic effects in fluorine chemistry. Indeed, the calculated average molecular dipole moments of a series of organofluorine herbicides have been properly correlated with the corresponding experimental log  $P$ ; such correlation was even better than that obtained from calculated log  $P$  values instead of  $\mu$ .<sup>7</sup> Therefore, a similar approach may be used to analyze the relationship between polarity and the  $K_{bg}$  of key fluorinated inhalational anaesthetics.

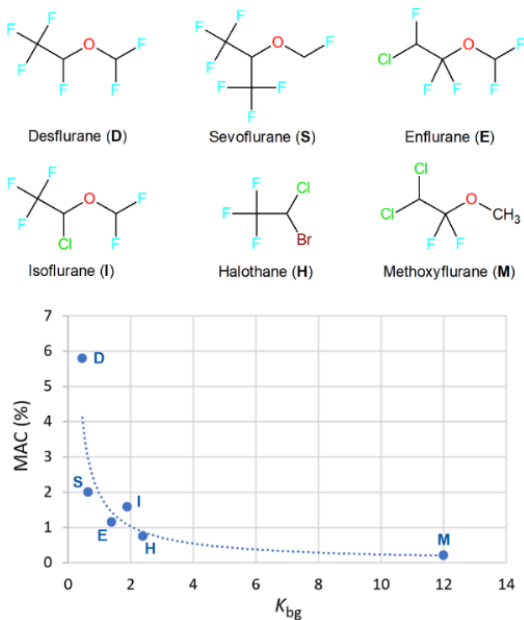


**Fig. 1** Correlation between MAC (%) and blood-gas partition coefficients ( $K_{bg}$ ) for six fluorinated inhalational anaesthetics ( $MAC = 1.958 \times K_{bg}^{-0.931}$ ,  $R^2 = 0.923$ ).

The conformational behavior and experimental  $K_{bg}$  values for the six last-generation volatile anaesthetics of Figure 1 are well-known.<sup>2,3,8-12</sup> Since most of them possesses oxygen electron lone pairs ( $n_O$ ), electron-donating bonds (for example, C–H and C–C), and low-lying energy antibonding orbitals (for C–X, X = O, F, and Cl), some stereoelectronic interactions may appear to stabilize the conformations with geometric requirements for orbital overlapping, such as the *gauche* effect (*e.g.* due to  $\sigma_{C-H/C-C} \rightarrow \sigma^*_{C-F}$  hyperconjugation) and the anomeric effect (*e.g.* due to  $n_O \rightarrow \sigma^*_{C-F/C-Cl}$  electron delocalization).<sup>13</sup> Organofluorine compounds are remarkable in stereochemistry for exhibiting the fluorine *gauche* effect, whose benchmark is the 1,2-difluoroethane

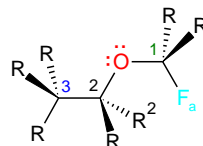
moiety. The surprising stability of its *gauche* conformer over the *anti* conformer is due especially to the antiperiplanar interactions between good electron-donating orbitals ( $\sigma_{C-H}$ ) and low-lying energy electron-accepting orbitals ( $\sigma^*_{C-F}$ ).<sup>14</sup> In turn, the generalized anomeric effect that takes place in the O–C–X fragment-containing molecules (X = electronegative atom or group) is also importantly stabilizing if a  $n_O \rightarrow \sigma^*_{C-X}$  electron delocalization is allowed.<sup>15</sup> These non-Lewis-type interactions counterbalance the Lewis-type contributions stemming from steric and electrostatic interactions, thus yielding the conformational energy differences.<sup>16</sup>

Therefore, the average molecular dipole moments for each fluorinated inhalational anaesthetic of Figure 1 were obtained using *ab initio* calculations, rationalized in terms of the stereoelectronic interactions governing the conformational equilibria, and then correlated with  $K_{bg}$ . The outcomes may be useful for the modeling and prediction of new organofluorine compounds with anaesthetic properties.

## Results and discussion

Whereas halothane (**H**) does not exhibit conformational isomerism, the remaining five fluorinated anaesthetics of Figure 1 (**D**, **S**, **E**, **I**, and **M**) undergo rotation around the dihedral angles  $\phi_1$  (H—C<sub>1</sub>—O—C<sub>2</sub>),  $\phi_2$  (C<sub>1</sub>—O—C<sub>2</sub>—C<sub>3</sub>), and  $\phi_3$  (O—C<sub>2</sub>—C<sub>3</sub>—H, for **E** and **M**). The conformational Gibbs free energies for the main conformers of each compound are given in Table 1, and the optimized geometries for the whole series of compounds and respective conformers are shown in the ESI. The overall molecular dipole moment of a molecule is the summation of the individual dipole moment vectors originated from the polar bonds. If this molecule experiences conformational isomerism, the resulting molecular dipole moment corresponds to an average value of the conformations. Considering that stereoelectronic effects rule the conformational preferences of compounds in the gas phase, thus the observed molecular dipole moments are also influenced by the stereoelectronic interactions operating in the system. It is worth mentioning that solvent effects on the conformational preferences are in general small for at least most of the studied compounds,<sup>8-10</sup> and, considering that implicit solvation calculations do not account properly for specific solute-solvent interactions (*e.g.* hydrogen bonding), only the molecular dipole moments obtained for the gas phase conformers will be considered.

**Table 1** Conformational Gibbs free energies (in kcal mol<sup>-1</sup>) and population (%), in parenthesis), molecular dipole moments ( $\mu$ , in Db), bond lengths (in Å), and dihedral angles (degrees) obtained for the main conformers of the studied fluorinated anaesthetic compounds (**C**).<sup>a</sup>



<b>C</b> <sub><math>\phi_1\phi_2\phi_3</math></sub>	G <sup>0</sup> <sub>rel</sub> (%)	$\mu$	O—C <sub>1</sub>	C <sub>2</sub> —O	C <sub>1</sub> —F <sub>a</sub>	C <sub>2</sub> —R <sup>2</sup>	$\Phi_1$	$\Phi_2$	$\Phi_3$
<b>H</b>	- (100)	1.49	-	-	-	-	-	-	58.29
<b>Esag</b>	0.0 (21)	1.26	1.39	1.36	1.34	1.36	17.26	176.77	56.14
<b>Es'a'g</b>	0.1 (19)	0.45	1.39	1.37	1.34	1.35	340.46	185.33	57.62
<b>Esag'</b>	0.2 (14)	1.06	1.39	1.37	1.34	1.35	20.12	176.57	300.55
<b>Es'a'g'</b>	0.2 (14)	1.81	1.39	1.37	1.34	1.35	342.37	184.84	301.67
<b>Es'a'a'</b>	0.3 (13)	2.37	1.39	1.36	1.34	1.36	340.40	182.66	180.03
<b>Esaa</b>	0.3 (13)	2.51	1.39	1.36	1.34	1.36	19.33	174.25	178.90
<b>Es'g'g'</b>	1.6 (2)	1.48	1.39	1.38	1.34	1.35	353.25	282.10	302.91
<b>Eg'gg</b>	1.6 (1)	1.78	1.39	1.38	1.35	1.35	327.29	107.34	55.14
<b>Esga</b>	1.8 (1)	2.52	1.39	1.37	1.34	1.36	17.39	69.43	175.99
<b>Eg'g'g</b>	2.0 (1)	2.06	1.38	1.38	1.36	1.36	306.15	276.46	62.44
<b>Egg'a</b>	2.0 (1)	2.97	1.39	1.37	1.35	1.35	31.72	255.70	180.00
<b>Iag</b>	0.0 (61)	1.72	1.37	1.40	1.35	1.77	177.22	136.85	58.40
<b>Iga</b>	0.4 (31)	2.11	1.38	1.39	1.36	1.78	60.05	169.45	59.41
<b>Ig'a</b>	1.3 (7)	2.91	1.38	1.39	1.35	1.77	322.35	154.39	59.46
<b>Is'g'</b>	2.5 (1)	1.84	1.39	1.39	1.35	1.78	335.79	295.71	68.55
<b>Dag</b>	0.0 (76)	1.89	1.37	1.39	1.35	1.36	174.93	143.71	56.48
<b>Dga</b>	0.9 (18)	2.02	1.38	1.38	1.36	1.37	57.98	170.26	57.35
<b>Dg'a</b>	1.5 (5)	3.13	1.38	1.38	1.35	1.36	318.43	157.60	57.24
<b>Ds'g'</b>	2.9 (1)	1.59	1.39	1.38	1.35	1.37	336.92	296.68	67.23
<b>Sgg</b>	0.0 (100)	2.56	1.39	1.41	1.38	1.53	51.09	133.73	54.89
<b>Mgaa</b>	0.0 (58)	1.62	1.44	1.34	-	1.37	61.22	180.00	180.00
<b>Mgag</b>	0.2 (42)	2.62	1.44	1.35	-	1.36	59.25	179.07	57.60

<sup>a</sup> Conformers for compounds **C** are named according to the dihedral angles  $\phi_1$ ,  $\phi_2$ , and  $\phi_3$ , which can be either *anti* (*a* and *a'*, from 150° to 210°), *syn* (*s* and *s'*, from 330° to 30°), or *gauche* (*g* and *g'*). The C<sub>1</sub>—F<sub>a</sub> stands for the bond length involving the fluorine at anomeric orientation. The C—F, C—Cl, and C—Br bond lengths for halothane are 1.34, 1.76, and 1.91 Å, respectively.

**Table 2** Lewis (L) and non-Lewis (NL) contributions to the full conformational electronic energies, and anomeric interactions for the rotationally flexible fluorinated anaesthetic compounds (**C**) studied herein (kcal mol<sup>-1</sup>).<sup>a</sup>

C <sub>Φ1Φ2Φ3</sub>	E <sub>full</sub>	E <sub>NL</sub>	E <sub>L</sub>	n <sub>O</sub> →σ* <sub>C1-Fa</sub>	n <sub>O</sub> →σ* <sub>C2-CF3</sub>	n <sub>O</sub> →σ* <sub>C2-Fa</sub>	n <sub>O</sub> →σ* <sub>C2-Cl</sub>
<b>Esag</b>	0.03	-2.27	2.30	13.31	-	32.44	-
<b>Es'a'g</b>	0.00	-1.96	1.96	13.67	-	32.38	-
<b>Esag'</b>	0.17	-2.05	2.22	13.73	-	31.78	-
<b>Es'a'g'</b>	0.22	-2.48	2.70	13.52	-	31.83	-
<b>Es'a'a'</b>	0.18	-3.58	3.76	13.62	-	33.56	-
<b>Esaa</b>	0.19	-3.79	3.98	13.73	-	33.52	-
<b>Es'g'g'</b>	1.18	-0.86	2.04	11.83	-	20.36	-
<b>Eg'gg</b>	1.33	-2.05	3.38	15.92	-	20.12	-
<b>Esga</b>	1.24	-2.78	4.02	13.86	-	22.03	-
<b>Eg'g'g</b>	1.65	0.00	1.65	15.48	-	18.92	-
<b>Egg'a</b>	1.67	-3.44	5.11	15.94	-	20.71	-
<b>Iag</b>	0.00	0.00	0.00	13.07	-	-	13.09
<b>Iga</b>	0.21	-0.75	0.96	12.55	-	-	16.28
<b>Ig'a</b>	1.93	-6.10	8.03	16.17	-	-	16.15
<b>Is'g'</b>	1.92	-6.04	7.96	15.38	-	-	15.66
<b>Dag</b>	0.00	-1.79	1.79	13.70	-	16.20	-
<b>Dga</b>	0.90	0.00	0.90	13.48	-	17.21	-
<b>Dg'a</b>	1.90	-8.97	10.8	16.57	-	18.41	-
<b>Ds'g'</b>	2.34	-6.75	9.09	15.34	-	15.67	-
<b>Sgg</b>	0.00	0.00	0.00	15.78	8.84	-	-
<b>Mgaa</b>	0.00	-1.91	1.91	-	-	39.18	-
<b>Mgag</b>	0.29	0.00	0.29	-	-	37.15	-

<sup>a</sup> The n<sub>O</sub>→σ\*<sub>C1-Fa</sub> interaction corresponds to the contribution involving the fluorine at anomeric orientation; n<sub>O</sub>→σ\*<sub>C2-CF3</sub> corresponds only to the antiperiplanar interaction; n<sub>O</sub>→σ\*<sub>C2-CF</sub> corresponds to the sum of these interaction energies for the two C–F bonds when possible (for **E** and **M**).

Whereas compounds **E** and **M** have the requirements to experience the fluorine *gauche* effect, the compounds **D**, **S**, **I**, **E**, and **M** may present the anomeric effect. To gain insight into how these non-Lewis-type interactions contribute to the conformational electronic energies (E<sub>full</sub>) of the studied compounds, the wavefunctions were localized with all natural bond orbitals (NBO) doubly occupied, and the resulting energy (E<sub>L</sub>) was subtracted from E<sub>full</sub> to give the electron delocalization energy E<sub>NL</sub>, according to Equation 1 (Table 2).

$$E_{NL} = E_{full} - E_L \quad (1)$$

**E** and **M** are capable of turning on the fluorine *gauche* effect through the  $\sigma_{C-H} \rightarrow \sigma^*_{C-F}$  hyperconjugation along the  $\phi_3$  dihedral angle. However, since  $\sigma_{C-Cl}$  is a good electron-donating orbital but worse than  $\sigma_{C-H}$ , and  $\sigma^*_{C-O}$  is a good electron-accepting orbital but worse than  $\sigma^*_{C-F}$ , some competing interactions contribute to the rotation around the O—C<sub>2</sub>—C<sub>3</sub>—H dihedral angle in **E** and **M**. Considering that electron delocalizations from  $\sigma_{C-H}$  and to  $\sigma^*_{C-F}$  are only slightly more favoring than that from  $\sigma_{C-Cl}$  and to  $\sigma^*_{C-O}$  (see ESI), the small differences in the rotational preferences for  $\phi_3$  are well explained by these stereoelectronic interactions. On the other hand, the anomeric effect appears in most of the studied systems (Table 2). The  $no \rightarrow \sigma^*_{C-X}$  anomeric interactions are expected to shorten the C—O distance and lengthen the C—X bond. For instance, more stabilizing  $no \rightarrow \sigma^*_{C-F}$  interactions in some conformers of **E** cause an increase in the respective C—F bonds of *ca.* 0.01 to 0.02 Å in a comparison with the conformers that experience weaker interactions. The effect of these interactions on the dihedral angles is also remarkable, once the bonds rotate to maximize the overlap between the orbitals involved in the anomeric interactions. Therefore, the stereoelectronic effects operating in these systems strongly affect the molecular geometries, conformer stabilities, and, consequently, the overall molecular dipole moment.

Compound **M** experiences both *gauche* and anomeric effects, but the overall contribution from the latter is weaker than in **E** because C-1 is not attached to any fluorine. On the other hand, the two fluorine atoms at C-2 allow for an effective *gauche* effect. These two factors lead **M** to a preferential conformational behaviour in which all bonds are staggered. For the remaining molecules **D**, **S**, and **I**, there is a competition between the  $no \rightarrow \sigma^*_{C1-R1}$  (leading to a *syn*  $\phi_1$ ) and  $no \rightarrow \sigma^*_{C2-R2}$  interactions (leading to a *gauche*  $\phi_2$ ). Compound **S** bears a worse R<sup>2</sup>-containing electron-accepting orbital ( $\sigma^*_{C-CF_3}$ ) compared to **D** and **I**, leading to less stabilizing  $no \rightarrow \sigma^*_{C2-R2}$  interactions in **S** than in **D** and **I**. Even though, compound **S** presents a single stable conformer in the gas phase, whereas the conformers with a *gauche*  $\phi_2$  dominate the conformational equilibrium in **D** (**Dag**) and **I** (**Iag**). According to the energy decomposition analysis of Table 2, this behaviour is due to a balance of Lewis and non-Lewis-type interactions; whereas the single stable conformer of **S** is substantially more favoured than its metastable conformers due to a large  $E_{NL} - E_L$  energy difference, both **Dag** and **Iag** are little destabilized by steric effects but also only slightly stabilized by electron delocalization, leading to a non-monotonic conformational equilibrium. The six geometries corresponding to the most stable

conformer in the gas phase for each compound, which are consistent with the literature,<sup>8-12</sup> are shown in Figure 2.

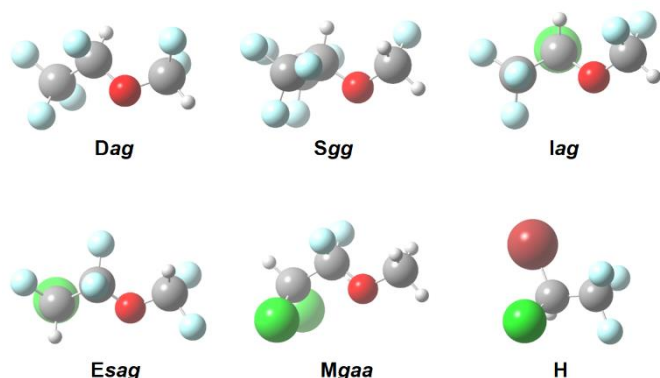


**Fig. 2** Most stable conformer for each halogenated anaesthetic.

Considering that the molecular polarity of organofluorine compounds is related to their octanol-water partition coefficient,<sup>4,5,7,17</sup> as well as that blood is mostly constituted by water,<sup>18</sup> the solubility of fluorinated anaesthetics in the bloodstream, described in terms of the blood-gas partition coefficient, may be correlated to the average molecular dipole moment. At first glance, compound **M** demonstrates an outlier behaviour due to its exceedingly high  $K_{bg}$  of 12 for an average  $\mu$  of 2.04 Db (see discussion on vapour pressure further in this discussion). Nevertheless, it is worth mentioning that other factors than binding to plasma proteins may appear to set anaesthetic molecules in the blood, such as the affinity to red blood cells.<sup>19</sup> Accordingly, the average dipole moments for the remaining five fluorinated anaesthetics were plotted against the respective  $K_{bg}$  values (Figure 3), yielding a determination coefficient  $R^2$  of 0.65, which is acceptable for quantitative structure-activity relationship purposes.<sup>20</sup> Yet, considering that **D** appears to abnormally influence the regression line, the resulting plot obtained after exclusion of this compound gives an impressive correlation with  $R^2 = 0.93$ . Although the origin of this outlier behaviour is not clear, it is worth considering an effect of the vapour pressure, which is considerably higher for **D** (667.6 mmHg)<sup>21</sup> in a comparison with **S** (157.5 mmHg),<sup>22</sup> **I** (240.0 mmHg),<sup>23</sup> **E** (174.5 mmHg),<sup>24</sup> **M** (22.5 mmHg),<sup>25</sup> and **H** (243.0 mmHg)<sup>26</sup> at 20°C.

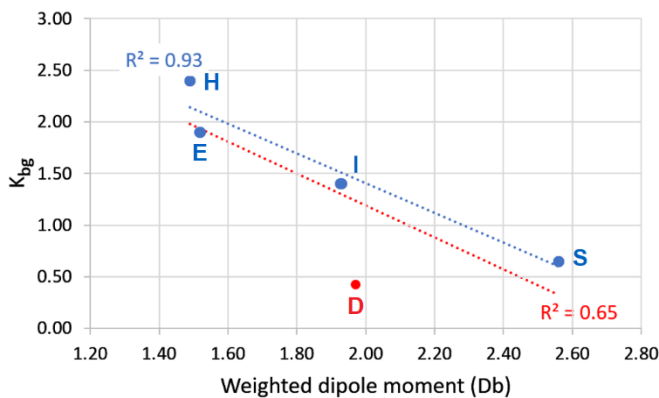


**Fig. 3** Linear correlation plots of average dipole moments ( $\mu$ ) *versus* blood-gas partition coefficients ( $K_{bg}$ ) for **H**, **E**, **S**, and **I** (blue line) and also including **D** (red line).  $K_{bg} = -1.4417\mu + 4.2907$  (blue line);  $K_{bg} = -1.5463\mu + 4.2811$  (red line).

### Computational methods

The geometries corresponding to all possible staggered conformations depicted in Figure 4 were fully optimized and the absence of imaginary frequencies was checked to guarantee that the located conformers were real energy minima. These procedures were performed at the *ab initio* MP2/aug-cc-pVTZ level of theory<sup>27-30</sup> using the Gaussian 09 program.<sup>31</sup> The calculations were carried out using the default integration grid of G09: FineGrid, with 75 radial shells and 302 angular points per shell. The geometries for the main conformers (*i.e.* those with Gibbs population of at least 1% in the gas phase) were consistent with the structures available in the literature<sup>8-12</sup> and, therefore, the molecular dipole moments considered to build a correlation with the experimental blood-gas partition coefficients<sup>2,3</sup> were weighted by these populations. The MP2-derived dipole moments have been demonstrated to be reliable and accurate.<sup>32</sup> The electron delocalization and Lewis-type contributions to the conformational energies were obtained through second-order perturbation analysis of donor-acceptor interactions in the natural bond orbitals (NBO).<sup>16</sup> The Lewis-type energy ( $E_L$ ) results from the perfectly localized NBO's and nearly represents the steric energy between doubly occupied orbitals, which is higher than the original energy ( $E_{full}$ ). The non-Lewis type energy ( $E_{NL}$ ) corresponds to the stabilizing effect of delocalizing contributions. The NBO calculations were performed using density functional theory at the B3LYP/aug-cc-pVTZ level of theory,<sup>33,34</sup> including the empirical dispersion corrections proposed by Grimme and co-workers.<sup>35,36</sup>

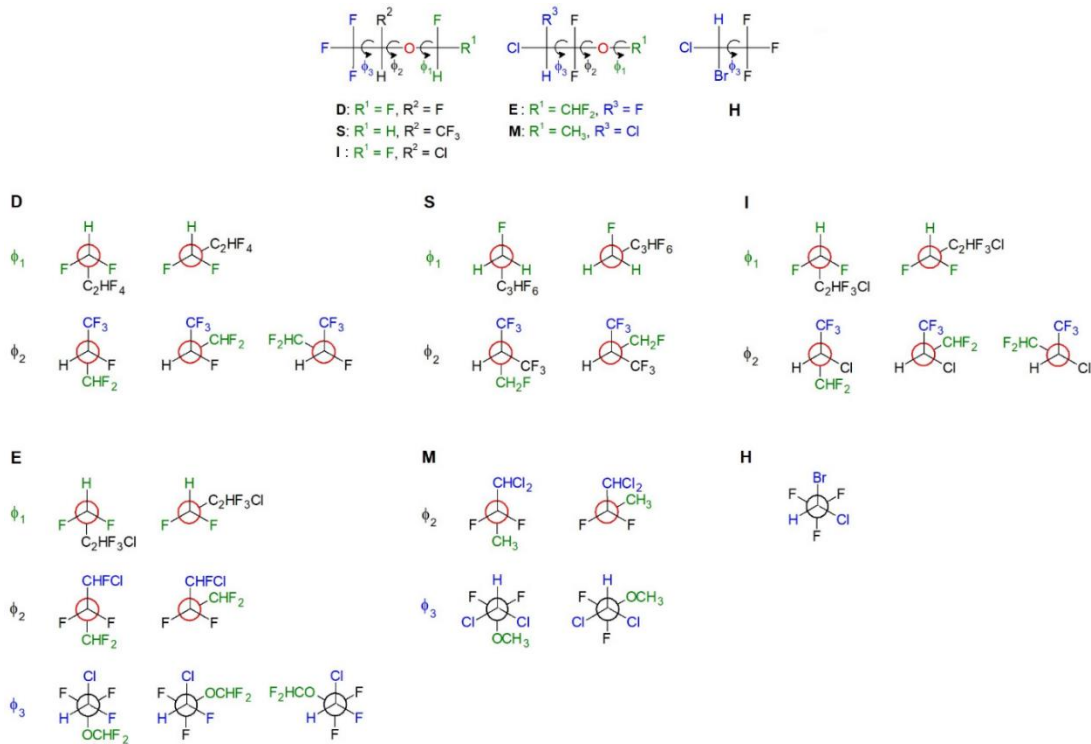


**Fig. 4** Staggered conformations for each dihedral angle of the six fluorinated anaesthetics studied herein.

## Conclusions

The conformational equilibrium of five fluorinated anaesthetics was discussed in terms of electron delocalization and Lewis-type interactions. Although the classical steric and electrostatic interactions contribute to the conformational balance, the stereoelectronic interactions that rule the anomeric and *gauche* effects appeared to stabilize some conformers with specific geometries more than others. Because each conformer has a given dipole moment, the overall molecular dipole moment  $\mu$  is a combination of the individual dipole moments balanced by the respective conformer populations. We found a linear dependence of  $K_{bg}$  with these average dipole moments for **H**, **E**, **I**, **S**, and **D**, which greatly improves if **D** is removed from the regression. This demonstrates the importance of this parameter for rational drug design. Although the  $K_{bg}$  of **M** and **D** may be affected by other physical or chemical mechanisms than the solubility of the anaesthetic in the bloodstream and their interaction with the blood plasma proteins, our findings open the possibility to describe crucial pharmacokinetic data by an easily accessible quantum-chemical parameter.

## Acknowledgements

The authors are thankful to Coordenação de Aperfeiçoamento de Pessoal de Nível Superior (CAPES, funding code 001), Conselho Nacional de Desenvolvimento Científico e Tecnológico (CNPq, grant number 301371/2017-2), and Fundação de Amparo à Pesquisa do Estado de Minas Gerais (FAPEMIG) for financial support of this research.

## Notes and references

- 1 J. Travis, *Sci. News*, 2004, **166**, 8.
- 2 J. J. Nagelhout and S. Elisha. *Nurse Anesthesia*, 6th ed., Elsevier, Amsterdam, 2017.
- 3 J. F. Butterworth, J. D. Wasnick and D. C. Mackey, *Morgan & Mikhail's Clinical Anesthesiology*, 6th ed., McGraw-Hill Education, New York, 2018.
- 4 B. Linclau, Z. Wang, G. Compain, V. Paumelle, C. Fontenelle, N. Wells and A. Weymouth-Wilson, *Angew. Chem. Int. Ed.*, 2016, **55**, 674.
- 5 D. O'Hagan and R. J. Young, *Angew. Chem. Int. Ed.*, 2016, **55**, 3858.
- 6 D. Y. Buissonneaud, T. van Mourik and D. O'Hagan, *Tetrahedron*, 2010, **66**, 2196.
- 7 D. R. Silva, J. K. Daré and M. P. Freitas, *Beilstein J. Org. Chem.*, 2020, **16**, 2469.
- 8 M. P. Freitas, M. Bühl, D. O'Hagan, R. A. Cormannich and C. F. Tormena, *J. Phys. Chem. A*, 2012, **116**, 1677.
- 9 L. A. F. Andrade, J. M. Silla, S. L. Stephens, K. Marat, E. F. F. da Cunha, T. C. Ramalho, J. van Wijngaarden and M. P. Freitas, *J. Phys. Chem. A*, 2015, **119**, 10735.
- 10 M. C. Guimarães, M. H. Duarte, J. M. Silla and M. P. Freitas, *Beilstein J. Org. Chem.*, 2016, **12**, 760.
- 11 S. M. Milikova, K. S. Rutkowski, B. Czarnik-Matusewicz and M. Rospenk, *Chem. Phys. Lett.*, 2015, **637**, 77.
- 12 Y. S. Li and J. R. Durig, *J. Mol. Struct.*, 1982, **81**, 181.
- 13 I. V. Alabugin, *Stereoelectronic Effects*, Wiley, Chichester, 2016.
- 14 D. R. Silva, L. A. Santos, T. A. Hamlin, C. F. Guerra, M. P. Freitas and F. M. Bickelhaupt, *ChemPhysChem*, 2021, **22**, 641.
- 15 M. P. Freitas, *Org. Biomol. Chem.*, 2013, **11**, 2885.
- 16 F. Weinhold and C. R. Landis, *Discovering Chemistry with Natural Bond Orbitals*, Wiley, Hoboken, 2012.
- 17 B. F. J. Jeffries, Z. Wang, H. R. Felstead, J.-Y. Le Questel, J. Scott, E. Chiarpolini, J. Graton and B. Linclau, *J. Med. Chem.*, 2020, **63**, 1002.
- 18 H. P. Wright, *Br. Med. J.*, 1953, **2**, 1312.
- 19 K. S. Khan, I. Hayes and D. J. Buggy, *Cont. Edu. Anaest. Crit. Care Pain*, 2013, **14**, 106.
- 20 R. Todeschini, V. Consonni, D. Ballabio and F. Grisoni, in *Comprehensive Chemometrics*, ed. S. D. Brown, R. Tauler and B. Walczak, Elsevier, Amsterdam, 2020, pp. 599-634.
- 21 a) M. J. O'Neil, *The Merck Index – An Encyclopedia of Chemicals, Drugs, and Biologicals*, Whitehouse Station, Merck and Co., Inc., 2006.
- 22 International Labour Organization, [https://www.ilo.org/dyn/icsc/showcard.display?p\\_version=2&p\\_card\\_id=1436](https://www.ilo.org/dyn/icsc/showcard.display?p_version=2&p_card_id=1436).
- 23 International Labour Organization, [https://www.ilo.org/dyn/icsc/showcard.display?p\\_version=2&p\\_card\\_id=1435](https://www.ilo.org/dyn/icsc/showcard.display?p_version=2&p_card_id=1435).

- 24 R. J. Lewis Sr, *Hawley's Condensed Chemical Dictionary*, John Wiley & Sons, Inc., New York, 2007.
- 25 International Labour Organization,  
[https://www.ilo.org/dyn/icsc/showcard.display?p\\_version=2&p\\_card\\_id=1636](https://www.ilo.org/dyn/icsc/showcard.display?p_version=2&p_card_id=1636).
- 26 International Labour Organization,  
[https://www.ilo.org/dyn/icsc/showcard.display?p\\_version=2&p\\_card\\_id=0277](https://www.ilo.org/dyn/icsc/showcard.display?p_version=2&p_card_id=0277).
- 27 M. J. Frisch, M. Head-Gordon and J. A. Pople, *Chem. Phys. Lett.*, 1990, **166**, 275.
- 28 M. Head-Gordon, J. A. Pople and M. J. Frisch, *Chem. Phys. Lett.*, 1988, **153**, 503.
- 29 R. A. Kendall, T. H. Dunning and R. J. Harrison, *J. Chem. Phys.*, 1992, **96**, 6796.
- 30 P. A. Fantin, P. L. Barbieri, A. C. Neto and F. E. Jorge, *J. Mol. Struct. Theochem*, 2007, **810**, 103.
- 31 Gaussian 09, Revision D.01, M. J. Frisch, G. W. Trucks, H. B. Schlegel, G. E. Scuseria, M. A. Robb, J. R. Cheeseman, G. Scalmani, V. Barone, G. A. Petersson, H. Nakatsuji, X. Li, M. Caricato, A. Marenich, J. Bloino, B. G. Janesko, R. Gomperts, B. Mennucci, H. P. Hratchian, J. V. Ortiz, A. F. Izmaylov, J. L. Sonnenberg, D. Williams-Young, F. Ding, F. Lipparini, F. Egidi, J. Goings, B. Peng, A. Petrone, T. Henderson, D. Ranasinghe, V. G. Zakrzewski, J. Gao, N. Rega, G. Zheng, W. Liang, M. Hada, M. Ehara, K. Toyota, R. Fukuda, J. Hasegawa, M. Ishida, T. Nakajima, Y. Honda, O. Kitao, H. Nakai, T. Vreven, K. Throssell, J. A. Montgomery, Jr., J. E. Peralta, F. Ogliaro, M. Bearpark, J. J. Heyd, E. Brothers, K. N. Kudin, V. N. Staroverov, T. Keith, R. Kobayashi, J. Normand, K. Raghavachari, A. Rendell, J. C. Burant, S. S. Iyengar, J. Tomasi, M. Cossi, J. M. Millam, M. Klene, C. Adamo, R. Cammi, J. W. Ochterski, R. L. Martin, K. Morokuma, O. Farkas, J. B. Foresman and D. J. Fox, Gaussian, Inc., Wallingford, 2016.
- 32 E. D. Simandiras, R. D. Amos and N. C. Handy, *Chem. Phys.*, 1987, **114**, 9.
- 33 A. D. Becke, *J. Chem. Phys.*, 1993, **98**, 5648.
- 34 R. A. Kendall, T. H. Dunning and R. J. Harrison, *J. Chem. Phys.*, 1992, **96**, 6796.
- 35 S. Grimme, S. Ehrlich and L. Goerigk, *J. Comput. Chem.*, 2011, **32**, 1456.
- 36 E. R. Johnson and A. D. Becke, *J. Chem. Phys.*, 2005, **123**, 024101.

## APPENDICES

## APPENDIX A

Supporting Information for:

### The fluorine *gauche* effect and a comparison with other halogens in 2-halofluoroethanes and 2-haloethanols

## INDEX

Standard Coordinates in gas phase	121
Standard Coordinates in chloroform implicit solvent	128
Standard Coordinates in DMSO implicit solvent	135
<b>Figure S1.</b> Potential energy surface for 2-Haloethanols in chloroform	142
<b>Figure S2.</b> Potential energy surface for 2-Haloethanols in DMSO	143
<b>Table S1.</b> Natural Bonds Orbital (NBO) energies in chloroform	144
<b>Table S2.</b> Natural Bonds Orbital (NBO) energies in DMSO	145
<b>Table S3.</b> Orbital overlap component and energy splitting in gas phase	146
<b>Table S4.</b> Orbital overlap component and energy splitting in chloroform	146
<b>Table S5.</b> Orbital overlap component and energy splitting	146
<b>Table S6.</b> Spin-spin coupling constants in gas phase	147
<b>Table S7.</b> Spin-spin coupling constants in chloroform	148
<b>Table S8.</b> Spin-spin coupling constants in DMSO	149

## STANDARD COORDINATES IN THE GAS PHASE

**FFg:** MP2 energy=-277.7203574 (Hartrees), Zero Point Energy =0.0621737 (Hartrees), imaginary frequency = 0

Standard orientation:

Center Number	Atomic Number	Atomic Type	Coordinates (Angstroms)		
			X	Y	Z
1	6	0	0.264808	0.704165	0.516253
2	1	0	1.352922	0.706354	0.418774
3	1	0	-0.030113	1.206800	1.442707
4	6	0	-0.264808	-0.704165	0.516253
5	1	0	0.030113	-1.206800	1.442707
6	1	0	-1.352922	-0.706354	0.418774
7	9	0	-0.264808	1.417097	-0.551000
8	9	0	0.264808	-1.417097	-0.551000

**FFa:** MP2 energy=-277.7191662 (Hartrees), Zero Point Energy=0.0623141 (Hartrees), imaginary frequency = 0

Standard orientation:

Center Number	Atomic Number	Atomic Type	Coordinates (Angstroms)		
			X	Y	Z
1	6	0	0.426862	0.626197	0.000012
2	1	0	1.051248	0.672343	-0.894026
3	1	0	1.051272	0.672385	0.894035
4	6	0	-0.426862	-0.626197	0.000012
5	1	0	-1.051272	-0.672385	0.894035
6	1	0	-1.051248	-0.672343	-0.894026
7	9	0	-0.426862	1.726003	-0.000009
8	9	0	0.426862	-1.726003	-0.000009

**FCg:** MP2 energy=-637.7014765 (Hartrees), Zero Point Energy=0.0608512 (Hartrees), imaginary frequency = 0

Standard orientation:

Center Number	Atomic Number	Atomic Type	Coordinates (Angstroms)		
			X	Y	Z
1	6	0	1.192953	0.418316	0.362832
2	1	0	1.053238	0.246826	1.432390
3	1	0	1.956327	1.186404	0.202309
4	6	0	-0.095631	0.844974	-0.296544
5	1	0	-0.381247	1.831583	0.073684
6	1	0	0.032140	0.881802	-1.378793
7	9	0	1.652205	-0.761828	-0.203751
8	17	0	-1.418484	-0.286465	0.065085

**FCa:** MP2 energy=-637.7023653 (Hartrees), Zero Point Energy=0.0609604 (Hartrees), imaginary frequency = 0

Standard orientation:

Center Number	Atomic Number	Atomic Type	Coordinates (Angstroms)		
			X	Y	Z
1	6	0	0.998726	-0.489121	-0.000080
2	1	0	0.907253	-1.109951	-0.893503
3	1	0	0.907382	-1.110102	0.893252
4	6	0	-0.032714	0.620763	0.000067
5	1	0	0.067681	1.238696	0.891692
6	1	0	0.067623	1.238849	-0.891460
7	9	0	2.265499	0.089731	-0.000118
8	17	0	-1.655030	-0.109113	0.000068

**FBg:** MP2 energy ==-2750.745897(Hartrees), Zero Point Energy=0.0599783(Hartrees), imaginary frequency = 0

Standard orientation:

Center Number	Atomic Number	Atomic Type	Coordinates (Angstroms)		
			X	Y	Z
1	6	0	1.734435	0.366581	0.375429
2	1	0	1.560878	0.193306	1.439977
3	1	0	2.577501	1.053017	0.240227
4	6	0	0.511309	0.947348	-0.293260
5	1	0	0.302635	1.942321	0.104375
6	1	0	0.644976	0.997429	-1.374268
7	9	0	2.074498	-0.842907	-0.211733
8	35	0	-1.063741	-0.128100	0.028636

**FBa:** MP2 energy==-2750.7473668(Hartrees), Zero Point Energy=0.0600582(Hartrees), imaginary frequency = 0

Standard orientation:

Center Number	Atomic Number	Atomic Type	Coordinates (Angstroms)		
			X	Y	Z
1	6	0	1.561362	-0.483894	-0.000248
2	1	0	1.447894	-1.099308	-0.895049
3	1	0	1.448043	-1.099467	0.894465
4	6	0	0.574454	0.666129	-0.000081
5	1	0	0.678317	1.280046	0.894115
6	1	0	0.678071	1.280096	-0.894274
7	9	0	2.848957	0.052142	-0.000297
8	35	0	-1.220224	-0.054973	0.000154

**Fig:** MP2 energy=-475.2094337 (Hartrees), Zero Point Energy=0.0593936(Hartrees), imaginary frequency = 0

Standard orientation:

Center Number	Atomic Number	Atomic Type	Coordinates (Angstroms)		
			X	Y	Z
1	6	0	2.118707	0.328515	0.377341
2	1	0	1.944201	0.164883	1.443402
3	1	0	3.009976	0.950731	0.237348
4	6	0	0.936791	0.999025	-0.283406
5	1	0	0.779048	1.992306	0.140818
6	1	0	1.078285	1.071082	-1.362182
7	9	0	2.369149	-0.901243	-0.214369
8	53	0	-0.876733	-0.076095	0.017100

**Fla:** MP2 energy=-475.2114557 (Hartrees), Zero Point Energy=0.0594677 (Hartrees), imaginary frequency = 0

Standard orientation:

Center Number	Atomic Number	Atomic Type	Coordinates (Angstroms)		
			X	Y	Z
1	6	0	1.958346	-0.480294	-0.000054
2	1	0	1.834430	-1.094324	-0.894693
3	1	0	1.834330	-1.094478	0.894468
4	6	0	1.000213	0.692591	-0.000037
5	1	0	1.114038	1.303684	0.894919
6	1	0	1.114005	1.303700	-0.894995
7	9	0	3.260832	0.023607	0.000059
8	53	0	-0.999918	-0.035940	0.000006

**OFgg:** MP2 energy=-253.7223362 (Hartrees), Zero Point Energy=0.0747795 (Hartrees), imaginary frequency = 0

Standard orientation:

Center Number	Atomic Number	Atomic Type	Coordinates (Angstroms)		
			X	Y	Z
1	6	0	-0.714535	0.559477	-0.285462
2	1	0	-0.688856	0.518774	-1.376506
3	1	0	-1.296463	1.420242	0.054707
4	6	0	0.682196	0.575331	0.287169
5	1	0	1.190445	1.488691	-0.032769
6	1	0	0.624329	0.573641	1.383215
7	9	0	-1.363169	-0.600131	0.158504
8	8	0	1.457041	-0.512047	-0.188734
9	1	0	0.976776	-1.312641	0.044452

**OFgg':** MP2 energy=-253.7181412 (Hartrees), Zero Point Energy=0.0744489 (Hartrees), imaginary frequency = 0

Standard orientation:

Center Number	Atomic Number	Atomic Type	Coordinates (Angstroms)		
			X	Y	Z
1	6	0	0.714686	0.506578	0.314523
2	1	0	0.662253	0.402488	1.403990
3	1	0	1.268514	1.417498	0.065506
4	6	0	-0.667568	0.556420	-0.295891
5	1	0	-1.134772	1.505929	0.004899
6	1	0	-0.584159	0.543532	-1.384233
7	9	0	1.428480	-0.579419	-0.175316
8	8	0	-1.476277	-0.555801	0.046352
9	1	0	-1.540649	-0.586253	1.005075

**OFga:** MP2 energy=-253.7189569 (Hartrees), Zero Point Energy=0.0741382 (Hartrees), imaginary frequency = 0

Standard orientation:

Center Number	Atomic Number	Atomic Type	Coordinates (Angstroms)		
			X	Y	Z
1	6	0	0.717982	0.504462	0.309457
2	1	0	0.642115	0.397067	1.394268
3	1	0	1.273750	1.412438	0.057629
4	6	0	-0.656318	0.544089	-0.307577
5	1	0	-1.107353	1.520822	-0.082281
6	1	0	-0.557146	0.444205	-1.394723
7	9	0	1.435242	-0.582918	-0.179435
8	8	0	-1.424917	-0.513356	0.248645
9	1	0	-2.139191	-0.712730	-0.360419

**OFag:** MP2 energy=-253.7183493 (Hartrees), Zero Point Energy=0.0745651 (Hartrees), imaginary frequency = 0

Standard orientation:

Center Number	Atomic Number	Atomic Type	Coordinates (Angstroms)		
			X	Y	Z
1	6	0	-0.575173	0.499015	0.047278
2	1	0	-0.520631	1.200094	-0.791729
3	1	0	-0.539304	1.052561	0.987938
4	6	0	0.550445	-0.519702	-0.016874
5	1	0	0.479421	-1.200691	0.832257
6	1	0	0.466396	-1.106737	-0.938751
7	9	0	-1.798108	-0.163536	-0.029700
8	8	0	1.812694	0.126261	0.088499
9	1	0	1.943906	0.640626	-0.712835

**OFaa:** MP2 energy=-253.7187593 (Hartrees), Zero Point Energy=0.0738524(Hartrees), imaginary frequency = -71.15

Standard orientation:

Center Number	Atomic Number	Atomic Type	Coordinates (Angstroms)		
			X	Y	Z
1	6	0	-0.582291	-0.503656	-0.000004
2	1	0	-0.544104	-1.129036	0.894114
3	1	0	-0.544151	-1.129078	-0.894095
4	6	0	0.548838	0.504773	-0.000041
5	1	0	0.469554	1.137636	-0.891596
6	1	0	0.469485	1.137760	0.891420
7	9	0	-1.793509	0.186255	0.000003
8	8	0	1.750558	-0.257334	0.000049
9	1	0	2.487055	0.358398	0.000002

**OCgg:** MP2 energy=-613.7039954 (Hartrees), Zero Point Energy=0.0734768(Hartrees), imaginary frequency = 0

Standard orientation:

Center Number	Atomic Number	Atomic Type	Coordinates (Angstroms)		
			X	Y	Z
1	6	0	-0.104596	0.891803	-0.291183
2	1	0	-0.000047	0.942591	-1.375147
3	1	0	-0.424577	1.856558	0.105381
4	6	0	1.200156	0.451800	0.344789
5	1	0	1.959032	1.212231	0.140264
6	1	0	1.070245	0.370326	1.431316
7	8	0	1.692030	-0.753789	-0.207957
8	1	0	1.012879	-1.421499	-0.066726
9	17	0	-1.395714	-0.293618	0.065114

**OCgg':** MP2 energy=-613.6998155(Hartrees), Zero Point Energy=0.0730991(Hartrees), imaginary frequency = 0

Standard orientation:

Center Number	Atomic Number	Atomic Type	Coordinates (Angstroms)		
			X	Y	Z
1	6	0	0.123262	0.853990	0.301041
2	1	0	0.014630	0.895853	1.387818
3	1	0	0.435749	1.835950	-0.060366
4	6	0	-1.187092	0.458865	-0.355446
5	1	0	-1.909481	1.267507	-0.169535
6	1	0	-1.048168	0.361237	-1.433510
7	8	0	-1.687506	-0.789573	0.084045
8	1	0	-1.793648	-0.742009	1.038466
9	17	0	1.422585	-0.304652	-0.065223

**OCga:** MP2 energy=-613.7005207(Hartrees), Zero Point Energy=0.0727521(Hartrees), imaginary frequency = 0

Standard orientation:

Center Number	Atomic Number	Atomic Type	Coordinates (Angstroms)		
			X	Y	Z
1	6	0	-0.127794	0.850903	-0.295840
2	1	0	0.005412	0.874946	-1.378171
3	1	0	-0.449424	1.830974	0.059914
4	6	0	1.172689	0.456318	0.365844
5	1	0	1.879851	1.290323	0.251518
6	1	0	1.003816	0.282235	1.434565
7	8	0	1.659626	-0.708378	-0.282369
8	1	0	2.264119	-1.151983	0.316502
9	17	0	-1.426479	-0.311929	0.067918

**OCag:** MP2 energy=-613.7013974 (Hartrees), Zero Point Energy=0.0732448(Hartrees), imaginary frequency = 0

Standard orientation:

Center Number	Atomic Number	Atomic Type	Coordinates (Angstroms)		
			X	Y	Z
1	6	0	-0.045076	0.604723	0.043587
2	1	0	0.052461	1.283082	-0.806539
3	1	0	0.055435	1.169050	0.970540
4	6	0	1.000527	-0.498737	-0.015631
5	1	0	0.879667	-1.168047	0.837358
6	1	0	0.872298	-1.085461	-0.932829
7	8	0	2.310432	0.041747	0.086175
8	1	0	2.482576	0.544178	-0.715107
9	17	0	-1.679917	-0.100747	-0.012386

**OCaa:** MP2 energy=-613.7013742(Hartrees), Zero Point Energy=0.0724203(Hartrees), imaginary frequency = -27.40

Standard orientation:

Center Number	Atomic Number	Atomic Type	Coordinates (Angstroms)		
			X	Y	Z
1	6	0	0.050255	0.612125	-0.000005
2	1	0	-0.047362	1.230991	0.891469
3	1	0	-0.047364	1.230986	-0.891482
4	6	0	-0.996346	-0.484242	0.000001
5	1	0	-0.870508	-1.111180	-0.890509
6	1	0	-0.870486	-1.111192	0.890500
7	8	0	-2.257810	0.175355	0.000022
8	1	0	-2.940258	-0.500682	-0.000027
9	17	0	1.677353	-0.112298	-0.000006

**OBgg:** MP2 energy=-2726.7490106(Hartrees), Zero Point Energy=0.0725105(Hartrees), imaginary frequency = 0

Standard orientation:

Center Number	Atomic Number	Atomic Type	Coordinates (Angstroms)		
			X	Y	Z
1	6	0	0.507492	0.997147	-0.289326
2	1	0	0.617480	1.057615	-1.372395
3	1	0	0.270901	1.976395	0.130057
4	6	0	1.740417	0.390687	0.356625
5	1	0	2.585180	1.062056	0.173466
6	1	0	1.586481	0.310895	1.440423
7	8	0	2.095511	-0.853360	-0.212947
8	1	0	1.336737	-1.435840	-0.093436
9	35	0	-1.047095	-0.127750	0.029190

**OBgg':** MP2 energy=-2726.7444269(Hartrees), Zero Point Energy=0.0722478(Hartrees), imaginary frequency = 0

Standard orientation:

Center Number	Atomic Number	Atomic Type	Coordinates (Angstroms)		
			X	Y	Z
1	6	0	-0.490543	0.960257	0.299031
2	1	0	-0.608802	1.009126	1.384300
3	1	0	-0.259145	1.956541	-0.083109
4	6	0	-1.735066	0.405146	-0.372386
5	1	0	-2.542921	1.137149	-0.219395
6	1	0	-1.564859	0.299110	-1.445352
7	8	0	-2.109807	-0.876789	0.093924
8	1	0	-2.254198	-0.811797	1.042456
9	35	0	1.070344	-0.136235	-0.028290

**OBga:** MP2 energy=-2726.7450559(Hartrees), Zero Point Energy=0.0718177(Hartrees), imaginary frequency = 0

Standard orientation:

Center Number	Atomic Number	Atomic Type	Coordinates (Angstroms)		
			X	Y	Z
1	6	0	0.486080	0.966259	-0.290516
2	1	0	0.621796	1.008298	-1.372045
3	1	0	0.247717	1.957399	0.098159
4	6	0	1.720845	0.404945	0.378873
5	1	0	2.518656	1.157652	0.294093
6	1	0	1.514600	0.228787	1.440788
7	8	0	2.088030	-0.790394	-0.291909
8	1	0	2.608133	-1.322789	0.314240
9	35	0	-1.070191	-0.140955	0.029426

**OBag:** MP2 energy=-2726.7463862(Hartrees), Zero Point Energy=0.0723293(Hartrees), imaginary frequency = 0

Standard orientation:

Center Number	Atomic Number	Atomic Type	Coordinates (Angstroms)		
			X	Y	Z
1	6	0	0.567747	0.647451	0.048251
2	1	0	0.667229	1.317135	-0.808453
3	1	0	0.669238	1.213380	0.974308
4	6	0	1.573727	-0.493733	-0.008283
5	1	0	1.437051	-1.150574	0.852120
6	1	0	1.420242	-1.081212	-0.921152
7	8	0	2.901204	0.008936	0.079099
8	1	0	3.080315	0.497176	-0.729698
9	35	0	-1.238073	-0.051134	-0.006849

**OBaa:** MP2 energy=-2726.7463588(Hartrees), Zero Point Energy=0.0715683(Hartrees), imaginary frequency = -50.03

Standard orientation:

Center Number	Atomic Number	Atomic Type	Coordinates (Angstroms)		
			X	Y	Z
1	6	0	0.562857	0.659614	0.000027
2	1	0	0.661599	1.274576	-0.894089
3	1	0	0.661587	1.274522	0.894182
4	6	0	1.566086	-0.477433	-0.000004
5	1	0	1.417405	-1.097574	0.891870
6	1	0	1.417380	-1.097544	-0.891895
7	8	0	2.850831	0.139400	-0.000008
8	1	0	3.508840	-0.561028	0.000008
9	35	0	-1.235632	-0.05178	-0.000004

**OIgg:** MP2 energy=-451.2122769(Hartrees), Zero Point Energy=0.0718522(Hartrees), imaginary frequency = 0

Standard orientation:

Center Number	Atomic Number	Atomic Type	Coordinates (Angstroms)		
			X	Y	Z
1	6	0	0.933040	1.039051	-0.284596
2	1	0	1.056158	1.108319	-1.365883
3	1	0	0.749803	2.024413	0.147397
4	6	0	2.120735	0.348782	0.365627
5	1	0	3.005202	0.972163	0.197221
6	1	0	1.956310	0.265072	1.447643
7	8	0	2.415186	-0.905264	-0.216327
8	1	0	1.629520	-1.453462	-0.104643
9	53	0	-0.868701	-0.075498	0.017409

**OIgg':** MP2 energy=-451.2082845(Hartrees), Zero Point Energy=0.0716881(Hartrees), imaginary frequency = 0

Standard orientation:

Center Number	Atomic Number	Atomic Type	Coordinates (Angstroms)		
			X	Y	Z
1	6	0	-0.919519	1.015721	0.289820
2	1	0	-1.046205	1.085018	1.372967
3	1	0	-0.741962	2.013327	-0.116822
4	6	0	-2.121300	0.364873	-0.376166
5	1	0	-2.982509	1.033921	-0.223717
6	1	0	-1.950475	0.265228	-1.449767
7	8	0	-2.399671	-0.938736	0.097887
8	1	0	-2.550402	-0.878384	1.045846
9	53	0	0.881393	-0.080996	-0.016859

**OIga:** MP2 energy ==-451.208745(Hartrees), Zero Point Energy=0.07124 (Hartrees), imaginary frequency = 0

Standard orientation:

Center Number	Atomic Number	Atomic Type	Coordinates (Angstroms)		
			X	Y	Z
1	6	0	0.915765	1.021906	-0.283259
2	1	0	1.058003	1.083693	-1.363066
3	1	0	0.732098	2.014359	0.130589
4	6	0	2.108101	0.367167	0.379420
5	1	0	2.962817	1.053503	0.279774
6	1	0	1.904218	0.213067	1.445736
7	8	0	2.369388	-0.857832	-0.287270
8	1	0	2.945607	-1.382343	0.274200
9	53	0	-0.881152	-0.084039	0.017999

**OIag:** MP2 energy==-451.2104291 (Hartrees), Zero Point Energy=0.0717605 (Hartrees), imaginary frequency = 0

Standard orientation:

Center Number	Atomic Number	Atomic Type	Coordinates (Angstroms)		
			X	Y	Z
1	6	0	0.996713	0.673248	0.045851
2	1	0	1.103092	1.337963	-0.813943
3	1	0	1.110804	1.239504	0.970402
4	6	0	1.976138	-0.490954	-0.010982
5	1	0	1.827164	-1.147542	0.847774
6	1	0	1.814214	-1.074639	-0.925175
7	8	0	3.315547	-0.019043	0.079734
8	1	0	3.499897	0.482882	-0.719669
9	53	0	-1.013522	-0.033577	-0.003896

**OIaa:** MP2 energy==-451.2101458 (Hartrees), Zero Point Energy=0.0709462 (Hartrees), imaginary frequency = -61.82

Standard orientation:

Center Number	Atomic Number	Atomic Type	Coordinates (Angstroms)		
			X	Y	Z
1	6	0	0.991132	0.687087	0.000076
2	1	0	1.099683	1.299619	-0.894673
3	1	0	1.099634	1.299500	0.894912
4	6	0	1.967123	-0.473386	0.000018
5	1	0	1.807356	-1.091693	0.891551
6	1	0	1.807353	-1.091601	-0.891578
7	8	0	3.267559	0.112360	0.000049
8	1	0	3.907989	-0.604714	0.000057
9	53	0	-1.011548	-0.037589	-0.000023

## STANDARD COORDINATES IN CHLOROFORM

**FFg:** MP2 energy=-277.7254635 (Hartrees), Zero Point Energy=0.0621742 (Hartrees), imaginary frequency = 0

Standard orientation:

Center Number	Atomic Number	Atomic Type	Coordinates (Angstroms)		
			X	Y	Z
1	6	0	0.261954	0.704079	0.527243
2	1	0	1.349746	0.717451	0.439301
3	1	0	-0.050244	1.213235	1.442406
4	6	0	-0.261954	-0.704079	0.527243
5	1	0	0.050244	-1.213235	1.442406
6	1	0	-1.349746	-0.717451	0.439301
7	9	0	-0.261954	1.406867	-0.560574
8	9	0	0.261954	-1.406867	-0.560574

**FFa:** MP2 energy=-277.7227706 (Hartrees), Zero Point Energy=0.0622585 (Hartrees), imaginary frequency = 0

Standard orientation:

Center Number	Atomic Number	Atomic Type	Coordinates (Angstroms)		
			X	Y	Z
1	6	0	0.429061	0.624479	0.000058
2	1	0	1.050345	0.674796	-0.894904
3	1	0	1.050301	0.674926	0.895051
4	6	0	-0.429061	-0.624479	0.000058
5	1	0	-1.050301	-0.674926	0.895051
6	1	0	-1.050345	-0.674796	-0.894904
7	9	0	-0.429061	1.728121	-0.000055
8	9	0	0.429061	-1.728121	-0.000055

**FCg:** MP2 energy=-637.7059534 (Hartrees), Zero Point Energy=0.0608612 (Hartrees), imaginary frequency = 0

Standard orientation:

Center Number	Atomic Number	Atomic Type	Coordinates (Angstroms)		
			X	Y	Z
1	6	0	1.195346	0.424972	0.358939
2	1	0	1.067835	0.262188	1.430334
3	1	0	1.965457	1.179788	0.179761
4	6	0	-0.092799	0.855082	-0.294578
5	1	0	-0.381108	1.835450	0.087177
6	1	0	0.024820	0.899760	-1.377013
7	9	0	1.637413	-0.774045	-0.202132
8	17	0	-1.413470	-0.287712	0.065457

**FCa:** MP2 energy=-637.7054666 (Hartrees), Zero Point Energy=0.0609149 (Hartrees), imaginary frequency = 0

Standard orientation:

Center Number	Atomic Number	Atomic Type	Coordinates (Angstroms)		
			X	Y	Z
1	6	0	0.995617	-0.491335	-0.000074
2	1	0	0.909235	-1.110092	-0.894450
3	1	0	0.909437	-1.110217	0.894235
4	6	0	-0.031119	0.622275	0.000082
5	1	0	0.065345	1.238470	0.892801
6	1	0	0.065295	1.238613	-0.892548
7	9	0	2.268143	0.090112	-0.000172
8	17	0	-1.655858	-0.109025	0.000086

**FBg:** MP2 energy=-2750.7504574 (Hartrees), Zero Point Energy=0.0599534 (Hartrees), imaginary frequency = 0

Standard orientation:

Center Number	Atomic Number	Atomic Type	Coordinates (Angstroms)		
			X	Y	Z
1	6	0	1.736528	0.371301	0.371992
2	1	0	1.575576	0.205608	1.438666
3	1	0	2.584919	1.044730	0.218597
4	6	0	0.515077	0.955790	-0.291838
5	1	0	0.304378	1.945692	0.115139
6	1	0	0.640079	1.012172	-1.372974
7	9	0	2.058693	-0.854829	-0.209985
8	35	0	-1.061223	-0.127923	0.028843

**FBa:** MP2 energy=-2750.750534 (Hartrees), Zero Point Energy=0.0600055 (Hartrees), imaginary frequency = 0

Standard orientation:

Center Number	Atomic Number	Atomic Type	Coordinates (Angstroms)		
			X	Y	Z
1	6	0	1.558209	-0.485754	-0.000226
2	1	0	1.449898	-1.099373	-0.895959
3	1	0	1.450053	-1.099491	0.895446
4	6	0	0.576176	0.667768	-0.000084
5	1	0	0.675823	1.280071	0.895269
6	1	0	0.675593	1.280088	-0.895455
7	9	0	2.851752	0.052309	-0.000284
8	35	0	-1.220670	-0.054976	0.000146

**Fig:** MP2 energy =-475.21379 (Hartrees), Zero Point Energy=0.0594145 (Hartrees), imaginary frequency = 0

Standard orientation:

Center Number	Atomic Number	Atomic Type	Coordinates (Angstroms)		
			X	Y	Z
1	6	0	2.119760	0.332627	0.374347
2	1	0	1.955812	0.174435	1.441816
3	1	0	3.014294	0.943620	0.218678
4	6	0	0.939397	1.005572	-0.282469
5	1	0	0.779905	1.994020	0.150997
6	1	0	1.073287	1.084504	-1.361186
7	9	0	2.355883	-0.911377	-0.212574
8	53	0	-0.875117	-0.075913	0.017200

**Fla:** MP2 energy =-475.2145918(Hartrees), Zero Point Energy=0.0594124 (Hartrees), imaginary frequency = 0

Standard orientation:

Center Number	Atomic Number	Atomic Type	Coordinates (Angstroms)		
			X	Y	Z
1	6	0	1.954543	-0.481926	-0.000057
2	1	0	1.836275	-1.094244	-0.895650
3	1	0	1.836181	-1.094405	0.895417
4	6	0	1.001169	0.693807	-0.000039
5	1	0	1.110880	1.303385	0.896162
6	1	0	1.110858	1.303389	-0.896249
7	9	0	3.263676	0.023912	0.000062
8	53	0	-1.000029	-0.035936	0.000006

**OFgg:** MP2 energy=-253.7273907 (Hartrees), Zero Point Energy=0.0745773 (Hartrees), imaginary frequency = 0

Standard orientation:

Center Number	Atomic Number	Atomic Type	Coordinates (Angstroms)		
			X	Y	Z
1	6	0	-0.714041	0.560303	-0.286476
2	1	0	-0.689674	0.518665	-1.376828
3	1	0	-1.293335	1.420990	0.054819
4	6	0	0.679497	0.574410	0.290563
5	1	0	1.181761	1.493005	-0.021727
6	1	0	0.622064	0.561247	1.385432
7	9	0	-1.371135	-0.601861	0.156781
8	8	0	1.464956	-0.508590	-0.192285
9	1	0	1.007016	-1.316722	0.061028

**OFgg':** MP2 energy=-253.7252632 (Hartrees), Zero Point Energy=0.0743852 (Hartrees), imaginary frequency = 0

Standard orientation:

Center Number	Atomic Number	Atomic Type	Coordinates (Angstroms)		
			X	Y	Z
1	6	0	0.712597	0.515163	0.315608
2	1	0	0.660561	0.414075	1.403325
3	1	0	1.271249	1.418348	0.056165
4	6	0	-0.664554	0.556025	-0.302963
5	1	0	-1.140009	1.501856	-0.011168
6	1	0	-0.576126	0.534359	-1.390635
7	9	0	1.427651	-0.584486	-0.170116
8	8	0	-1.469146	-0.562284	0.049368
9	1	0	-1.599620	-0.537118	1.002547

**OFga:** MP2 energy=-253.7256002 (Hartrees), Zero Point Energy=0.0740572 (Hartrees), imaginary frequency = 0

Standard orientation:

Center Number	Atomic Number	Atomic Type	Coordinates (Angstroms)		
			X	Y	Z
1	6	0	0.718739	0.514545	0.306251
2	1	0	0.662471	0.416119	1.392321
3	1	0	1.276311	1.414035	0.035531
4	6	0	-0.658965	0.550225	-0.298406
5	1	0	-1.117199	1.513916	-0.040207
6	1	0	-0.575743	0.479599	-1.388507
7	9	0	1.431085	-0.588696	-0.180460
8	8	0	-1.409773	-0.536051	0.234325
9	1	0	-2.206061	-0.625627	-0.296664

**OFag:** MP2 energy=-253.7240898 (Hartrees), Zero Point Energy=0.0744781 (Hartrees), imaginary frequency = 0

Standard orientation:

Center Number	Atomic Number	Atomic Type	Coordinates (Angstroms)		
			X	Y	Z
1	6	0	-0.571946	0.503286	0.043950
2	1	0	-0.524367	1.198584	-0.798145
3	1	0	-0.539874	1.056720	0.984043
4	6	0	0.549063	-0.519924	-0.019604
5	1	0	0.472295	-1.203416	0.827110
6	1	0	0.471470	-1.100176	-0.945279
7	9	0	-1.800497	-0.165086	-0.026681
8	8	0	1.813976	0.124514	0.092092
9	1	0	1.950442	0.637779	-0.710401

**OFaa:** MP2 energy=-253.7239885 (Hartrees), Zero Point Energy=0.0737812 (Hartrees), imaginary frequency = -82.84

Standard orientation:

Center Number	Atomic Number	Atomic Type	Coordinates (Angstroms)		
			X	Y	Z
1	6	0	-0.580895	0.506140	0.000007
2	1	0	-0.550027	1.129981	-0.894799
3	1	0	-0.550091	1.129981	0.894817
4	6	0	0.548760	-0.503488	0.000034
5	1	0	0.473515	-1.135380	0.891640
6	1	0	0.473470	-1.135462	-0.891510
7	9	0	-1.796862	-0.188277	-0.000027
8	8	0	1.753887	0.256855	-0.000022
9	1	0	2.486609	-0.365371	0.000023

**OCgg:** MP2 energy=-613.7084301 (Hartrees), Zero Point Energy=0.0733459 (Hartrees), imaginary frequency = 0

Standard orientation:

Center Number	Atomic Number	Atomic Type	Coordinates (Angstroms)		
			X	Y	Z
1	6	0	-0.104507	0.893132	-0.290612
2	1	0	-0.004103	0.946899	-1.374441
3	1	0	-0.423934	1.855679	0.109873
4	6	0	1.199290	0.454507	0.345206
5	1	0	1.954181	1.218040	0.140910
6	1	0	1.072411	0.367224	1.430521
7	8	0	1.696254	-0.753907	-0.209929
8	1	0	1.028479	-1.430005	-0.051566
9	17	0	-1.397986	-0.294848	0.064504

**OCgg':** MP2 energy=-613.7062584 (Hartrees), Zero Point Energy=0.0732248 (Hartrees), imaginary frequency = 0

Standard orientation:

Center Number	Atomic Number	Atomic Type	Coordinates (Angstroms)		
			X	Y	Z
1	6	0	0.120131	0.859318	0.301849
2	1	0	0.013390	0.899261	1.387567
3	1	0	0.436839	1.836931	-0.064947
4	6	0	-1.184630	0.459068	-0.359408
5	1	0	-1.911009	1.261869	-0.174507
6	1	0	-1.042990	0.360471	-1.436837
7	8	0	-1.681164	-0.793928	0.085622
8	1	0	-1.846307	-0.721194	1.031037
9	17	0	1.422728	-0.305661	-0.063643

**OCga:** MP2 energy=-613.7064767 (Hartrees), Zero Point Energy=0.0727296 (Hartrees), imaginary frequency = 0

Standard orientation:

Center Number	Atomic Number	Atomic Type	Coordinates (Angstroms)		
			X	Y	Z
1	6	0	-0.127059	0.857033	-0.297001
2	1	0	-0.009796	0.889696	-1.380428
3	1	0	-0.449672	1.831179	0.071119
4	6	0	1.175435	0.460977	0.355791
5	1	0	1.887706	1.282748	0.203197
6	1	0	1.026476	0.317819	1.431661
7	8	0	1.637403	-0.733474	-0.262368
8	1	0	2.402558	-1.039192	0.233154
9	17	0	-1.426279	-0.313089	0.069853

**OCag:** MP2 energy ==-613.7065699 (Hartrees), Zero Point Energy=0.0731315 (Hartrees), imaginary frequency = 0

Standard orientation:

Center Number	Atomic Number	Atomic Type	Coordinates (Angstroms)		
			X	Y	Z
1	6	0	-0.042602	0.607896	0.043057
2	1	0	0.052038	1.283988	-0.807950
3	1	0	0.051626	1.170629	0.971245
4	6	0	0.998766	-0.499340	-0.015655
5	1	0	0.875683	-1.169283	0.836589
6	1	0	0.875413	-1.081558	-0.935342
7	8	0	2.311142	0.040987	0.087291
8	1	0	2.485323	0.539047	-0.717565
9	17	0	-1.680365	-0.101298	-0.012336

**OCaa:** MP2 energy==-613.706056 (Hartrees), Zero Point Energy =0.0723877 (Hartrees), imaginary frequency = -56.54

Standard orientation:

Center Number	Atomic Number	Atomic Type	Coordinates (Angstroms)		
			X	Y	Z
1	6	0	0.049679	0.614760	-0.000023
2	1	0	-0.040924	1.233052	0.892338
3	1	0	-0.040930	1.232991	-0.892426
4	6	0	-0.996104	-0.482613	0.000019
5	1	0	-0.874535	-1.108862	-0.890579
6	1	0	-0.874516	-1.108814	0.890648
7	8	0	-2.261189	0.174602	0.000015
8	1	0	-2.939037	-0.507855	-0.000007
9	17	0	1.678706	-0.113542	-0.000004

**OBgg:** MP2 energy=-2726.7534363 (Hartrees), Zero Point Energy=0.0723701 (Hartrees), imaginary frequency = 0

Standard orientation:

Center Number	Atomic Number	Atomic Type	Coordinates (Angstroms)		
			X	Y	Z
1	6	0	0.508514	0.999076	-0.288142
2	1	0	0.613949	1.064003	-1.371049
3	1	0	0.272347	1.975522	0.136377
4	6	0	1.741029	0.393711	0.356199
5	1	0	2.582503	1.067657	0.171088
6	1	0	1.591342	0.309043	1.439041
7	8	0	2.098730	-0.854793	-0.215000
8	1	0	1.350780	-1.447096	-0.074003
9	35	0	-1.048515	-0.128214	0.028863

**OBgg':** MP2 energy ==-2726.7509554 (Hartrees), Zero Point Energy=0.0724859 (Hartrees), imaginary frequency = 0

Standard orientation:

Center Number	Atomic Number	Atomic Type	Coordinates (Angstroms)		
			X	Y	Z
1	6	0	-0.494989	0.963135	0.300572
2	1	0	-0.612587	1.006097	1.384965
3	1	0	-0.259433	1.957084	-0.082872
4	6	0	-1.732790	0.404946	-0.377287
5	1	0	-2.542234	1.133073	-0.226536
6	1	0	-1.558861	0.297528	-1.449332
7	8	0	-2.107202	-0.879130	0.095876
8	1	0	-2.309766	-0.794672	1.033243
9	35	0	1.071633	-0.136416	-0.027605

**OBga:** MP2 energy=-2726.7511133 (Hartrees), Zero Point Energy=0.0718975 (Hartrees), imaginary frequency = 0

Standard orientation:

Center Number	Atomic Number	Atomic Type	Coordinates (Angstroms)		
			X	Y	Z
1	6	0	0.488807	0.973459	-0.291598
2	1	0	0.608838	1.026850	-1.374039
3	1	0	0.248504	1.957742	0.110788
4	6	0	1.725491	0.409599	0.367821
5	1	0	2.529377	1.147928	0.240005
6	1	0	1.545059	0.265324	1.438887
7	8	0	2.057028	-0.815683	-0.272669
8	1	0	2.760809	-1.226419	0.238220
9	35	0	-1.069560	-0.141266	0.030576

**OBag:** MP2 energy=-2726.751653 (Hartrees), Zero Point Energy=0.0723398 (Hartrees), imaginary frequency = 0

Standard orientation:

Center Number	Atomic Number	Atomic Type	Coordinates (Angstroms)		
			X	Y	Z
1	6	0	0.570742	0.650448	0.047444
2	1	0	0.667467	1.318185	-0.810069
3	1	0	0.665539	1.214481	0.975034
4	6	0	1.571857	-0.494590	-0.008986
5	1	0	1.432576	-1.152688	0.850101
6	1	0	1.423696	-1.076997	-0.924994
7	8	0	2.901592	0.007840	0.080550
8	1	0	3.081369	0.495606	-0.729658
9	35	0	-1.238256	-0.051327	-0.006730

**OBaa:** MP2 energy=-2726.7511176 (Hartrees), Zero Point Energy =0.0715509 (Hartrees), imaginary frequency = -66.19

Standard orientation:

Center Number	Atomic Number	Atomic Type	Coordinates (Angstroms)		
			X	Y	Z
1	6	0	0.564126	0.661986	0.000040
2	1	0	0.656031	1.276460	-0.894984
3	1	0	0.656013	1.276375	0.895124
4	6	0	1.566389	-0.476251	-0.000005
5	1	0	1.422162	-1.095898	0.891985
6	1	0	1.422151	-1.095835	-0.892037
7	8	0	2.854198	0.138835	0.000010
8	1	0	3.508130	-0.567078	0.000028
9	35	0	-1.236605	-0.057689	-0.000012

**OIgg:** MP2 energy=-451.2165692 (Hartrees), Zero Point Energy =0.0717348 (Hartrees), imaginary frequency = 0

Standard orientation:

Center Number	Atomic Number	Atomic Type	Coordinates (Angstroms)		
			X	Y	Z
1	6	0	0.933637	1.039735	-0.283947
2	1	0	1.052776	1.113219	-1.365127
3	1	0	0.750531	2.022703	0.152272
4	6	0	2.121732	0.352368	0.365293
5	1	0	3.002624	0.979300	0.195362
6	1	0	1.960826	0.263522	1.446243
7	8	0	2.420544	-0.906024	-0.217947
8	1	0	1.644706	-1.464624	-0.087329
9	53	0	-0.869963	-0.075822	0.017247

**OIgg':** MP2 energy=-451.2145102 (Hartrees), Zero Point Energy=0.0717494 (Hartrees), imaginary frequency = 0

Standard orientation:

Center Number	Atomic Number	Atomic Type	Coordinates (Angstroms)		
			X	Y	Z
1	6	0	-0.922717	1.015997	0.292341
2	1	0	-1.049037	1.076164	1.375073
3	1	0	-0.741281	2.013011	-0.112574
4	6	0	-2.117922	0.365301	-0.382361
5	1	0	-2.978110	1.034328	-0.236132
6	1	0	-1.940220	0.261837	-1.454260
7	8	0	-2.403116	-0.938002	0.100280
8	1	0	-2.615767	-0.859528	1.036000
9	53	0	0.882890	-0.081313	-0.016419

**OIga:** MP2 energy=-451.2145721 (Hartrees), Zero Point Energy=0.0713437 (Hartrees), imaginary frequency = 0

Standard orientation:

Center Number	Atomic Number	Atomic Type	Coordinates (Angstroms)		
			X	Y	Z
1	6	0	0.917796	1.028053	-0.283934
2	1	0	1.046367	1.101735	-1.364325
3	1	0	0.731441	2.013812	0.143051
4	6	0	2.111740	0.370909	0.369919
5	1	0	2.970263	1.043249	0.230397
6	1	0	1.934237	0.245056	1.444131
7	8	0	2.343194	-0.879354	-0.266526
8	1	0	3.079310	-1.300826	0.187489
9	53	0	-0.880837	-0.084188	0.018407

**OIag:** MP2 energy=-451.2155641 (Hartrees), Zero Point Energy=0.0718114 (Hartrees), imaginary frequency = 0

Standard orientation:

Center Number	Atomic Number	Atomic Type	Coordinates (Angstroms)		
			X	Y	Z
1	6	0	0.998789	0.675453	0.045737
2	1	0	1.103396	1.338415	-0.814771
3	1	0	1.106000	1.239890	0.972006
4	6	0	1.973652	-0.492003	-0.010973
5	1	0	1.823219	-1.149522	0.846851
6	1	0	1.816758	-1.071246	-0.927863
7	8	0	3.315484	-0.019631	0.080419
8	1	0	3.499182	0.481881	-0.720669
9	53	0	-1.013341	-0.033643	-0.003915

**OIaa:** MP2 energy=-451.2148032 (Hartrees), Zero Point Energy=0.070905 (Hartrees), imaginary frequency = -73.30

Standard orientation:

Center Number	Atomic Number	Atomic Type	Coordinates (Angstroms)		
			X	Y	Z
1	6	0	0.991669	0.689131	0.000077
2	1	0	1.093662	1.301386	-0.895595
3	1	0	1.093625	1.301252	0.895845
4	6	0	1.967058	-0.472144	0.000007
5	1	0	1.812019	-1.090072	0.891642
6	1	0	1.812021	-1.089957	-0.891708
7	8	0	3.270794	0.111901	0.000048
8	1	0	3.906961	-0.610556	0.000054
9	53	0	-1.012019	-0.037909	-0.000021

## STANDARD COORDINATES IN DMSO

**FF g:** MP2 energy=-277.7275486 (Hartrees), Zero Point Energy=0.0621587 (Hartrees), imaginary frequency = 0

Standard orientation:

Center Number	Atomic Number	Atomic Type	Coordinates (Angstroms)		
			X	Y	Z
1	6	0	0.260723	0.704026	0.532219
2	1	0	1.348372	0.721888	0.448252
3	1	0	-0.058499	1.216130	1.442466
4	6	0	-0.260723	-0.704026	0.532219
5	1	0	0.058499	-1.216130	1.442466
6	1	0	-1.348372	-0.721888	0.448252
7	9	0	-0.260723	1.401463	-0.564893
8	9	0	0.260723	-1.401463	-0.564893

**FFa:** MP2 energy=-277.7240649 (Hartrees), Zero Point Energy=0.0622302 (Hartrees), imaginary frequency = 0

Standard orientation:

Center Number	Atomic Number	Atomic Type	Coordinates (Angstroms)		
			X	Y	Z
1	6	0	0.429822	0.623872	-0.000021
2	1	0	1.049847	0.675746	-0.895402
3	1	0	1.049934	0.675731	0.895309
4	6	0	-0.429822	-0.623872	-0.000021
5	1	0	-1.049934	-0.675731	0.895309
6	1	0	-1.049847	-0.675746	-0.895402
7	9	0	-0.429822	1.728935	0.000024
8	9	0	0.429822	-1.728935	0.000024

**FCg:** MP2 energy=-637.70782 (Hartrees), Zero Point Energy=0.0608672 (Hartrees), imaginary frequency = 0

Standard orientation:

Center Number	Atomic Number	Atomic Type	Coordinates (Angstroms)		
			X	Y	Z
1	6	0	-1.196162	-0.427617	0.357700
2	1	0	-1.073045	-0.267749	1.429632
3	1	0	-1.968517	-1.177566	0.171695
4	6	0	0.091455	-0.858840	-0.294002
5	1	0	0.380881	-1.836987	0.091482
6	1	0	-0.022732	-0.905745	-1.376452
7	9	0	-1.632309	0.778718	-0.201501
8	17	0	1.411908	0.288137	0.065586

**FCa:** MP2 energy=-637.7065981 (Hartrees), Zero Point Energy=0.0608918 (Hartrees), imaginary frequency = 0

Standard orientation:

Center Number	Atomic Number	Atomic Type	Coordinates (Angstroms)		
			X	Y	Z
1	6	0	0.994480	-0.492229	-0.000067
2	1	0	0.909931	-1.110208	-0.894788
3	1	0	0.910229	-1.110124	0.894743
4	6	0	-0.030507	0.622701	0.000019
5	1	0	0.064684	1.238206	0.893153
6	1	0	0.064538	1.238170	-0.893158
7	9	0	2.269053	0.090333	-0.000310
8	17	0	-1.656159	-0.108934	0.000184

**FBg:** MP2 energy=-2750.7523741 (Hartrees), Zero Point Energy=0.0599722 (Hartrees), imaginary frequency = 0

Standard orientation:

Center Number	Atomic Number	Atomic Type	Coordinates (Angstroms)		
			X	Y	Z
1	6	0	1.737412	0.373271	0.369865
2	1	0	1.581612	0.211831	1.437560
3	1	0	2.588471	1.040198	0.208097
4	6	0	0.516370	0.960363	-0.290852
5	1	0	0.304803	1.947264	0.122124
6	1	0	0.637353	1.021364	-1.371889
7	9	0	2.050356	-0.860670	-0.209058
8	35	0	-1.059661	-0.127898	0.028901

**FBa:** MP2 energy=-2750.7516958 (Hartrees), Zero Point Energy=0.0599763 (Hartrees), imaginary frequency = 0

Standard orientation:

Center Number	Atomic Number	Atomic Type	Coordinates (Angstroms)		
			X	Y	Z
1	6	0	1.556998	-0.486497	-0.000205
2	1	0	1.450550	-1.099327	-0.896356
3	1	0	1.450690	-1.099436	0.895889
4	6	0	0.576816	0.668264	-0.000078
5	1	0	0.674961	1.279846	0.895770
6	1	0	0.674753	1.279854	-0.895948
7	9	0	2.852681	0.052430	-0.000252
8	35	0	-1.220799	-0.054955	0.000132

**Fig:** MP2 energy=-475.2156155 (Hartrees), Zero Point Energy=0.0594152 (Hartrees), imaginary frequency = 0

Standard orientation:

Center Number	Atomic Number	Atomic Type	Coordinates (Angstroms)		
			X	Y	Z
1	6	0	2.120092	0.334362	0.373552
2	1	0	1.959994	0.177856	1.441427
3	1	0	3.015718	0.941074	0.211980
4	6	0	0.940539	1.007885	-0.282321
5	1	0	0.780050	1.994667	0.153790
6	1	0	1.071939	1.088680	-1.361015
7	9	0	2.350617	-0.915319	-0.211982
8	53	0	-0.874473	-0.075809	0.017250

**Fla:** MP2 energy=-475.2157538 (Hartrees), Zero Point Energy=0.0593826 (Hartrees), imaginary frequency = 0

Standard orientation:

Center Number	Atomic Number	Atomic Type	Coordinates (Angstroms)		
			X	Y	Z
1	6	0	1.953024	-0.482598	-0.000059
2	1	0	1.836790	-1.094176	-0.896067
3	1	0	1.836699	-1.094338	0.895829
4	6	0	1.001462	0.694149	-0.000040
5	1	0	1.109640	1.303036	0.896704
6	1	0	1.109624	1.303035	-0.896798
7	9	0	3.264587	0.024106	0.000064
8	53	0	-1.000018	-0.035921	0.000007

**OFgg:** MP2 energy=-253.7293577 (Hartrees), Zero Point Energy=0.0744799 (Hartrees), imaginary frequency = 0

Standard orientation:

Center Number	Atomic Number	Atomic Type	Coordinates (Angstroms)		
			X	Y	Z
1	6	0	-0.714201	0.560839	-0.285961
2	1	0	-0.690875	0.520568	-1.376211
3	1	0	-1.292479	1.421066	0.056906
4	6	0	0.678551	0.574456	0.291582
5	1	0	1.178087	1.494882	-0.018846
6	1	0	0.622609	0.557208	1.386004
7	9	0	-1.373640	-0.603065	0.155596
8	8	0	1.467299	-0.507496	-0.194327
9	1	0	1.020929	-1.317934	0.072662

**OFgg':** MP2 energy=-253.7283569 (Hartrees), Zero Point Energy=0.0743786 (Hartrees), imaginary frequency = 0

Standard orientation:

Center Number	Atomic Number	Atomic Type	Coordinates (Angstroms)		
			X	Y	Z
1	6	0	0.711667	0.519626	0.315758
2	1	0	0.659777	0.420473	1.402879
3	1	0	1.272927	1.418859	0.050965
4	6	0	-0.663379	0.556212	-0.305920
5	1	0	-1.142916	1.499778	-0.017071
6	1	0	-0.573106	0.531509	-1.393430
7	9	0	1.426179	-0.587133	-0.167730
8	8	0	-1.464585	-0.565760	0.051025
9	1	0	-1.625346	-0.515372	0.998998

**OFga:** MP2 energy=-253.7284632 (Hartrees), Zero Point Energy=0.0740977 (Hartrees), imaginary frequency = 0

Standard orientation:

Center Number	Atomic Number	Atomic Type	Coordinates (Angstroms)		
			X	Y	Z
1	6	0	0.719295	0.520300	0.304717
2	1	0	0.672251	0.427648	1.391496
3	1	0	1.278164	1.415131	0.024002
4	6	0	-0.659990	0.553671	-0.293954
5	1	0	-1.124097	1.508172	-0.016241
6	1	0	-0.584603	0.501708	-1.385557
7	9	0	1.426943	-0.591744	-0.180235
8	8	0	-1.399642	-0.549969	0.222919
9	1	0	-2.242892	-0.571037	-0.239519

**OFag:** MP2 energy=-253.7263834 (Hartrees), Zero Point Energy=0.0744715 (Hartrees), imaginary frequency = 0

Standard orientation:

Center Number	Atomic Number	Atomic Type	Coordinates (Angstroms)		
			X	Y	Z
1	6	0	-0.570420	0.504641	0.043685
2	1	0	-0.523596	1.198687	-0.798642
3	1	0	-0.540370	1.056938	0.984275
4	6	0	0.548526	-0.520495	-0.020221
5	1	0	0.470580	-1.204861	0.825786
6	1	0	0.472457	-1.097793	-0.947483
7	9	0	-1.801241	-0.165358	-0.026275
8	8	0	1.814411	0.123635	0.092499
9	1	0	1.948175	0.641291	-0.708241

**OFaa:** MP2 energy=-253.7259839 (Hartrees), Zero Point Energy =0.0737559 (Hartrees), imaginary frequency = -80.87

Standard orientation:

Center Number	Atomic Number	Atomic Type	Coordinates (Angstroms)		
			X	Y	Z
1	6	0	-0.580508	0.507021	0.000034
2	1	0	-0.552326	1.130360	-0.895029
3	1	0	-0.552411	1.130232	0.895189
4	6	0	0.548646	-0.502991	0.000006
5	1	0	0.475139	-1.134550	0.891576
6	1	0	0.475117	-1.134510	-0.891590
7	9	0	-1.797998	-0.189043	-0.000063
8	8	0	1.755175	0.256738	0.000014
9	1	0	2.486237	-0.368234	0.000062

**OCgg:** MP2 energy=-613.7101824 (Hartrees), Zero Point Energy=0.0732725 (Hartrees), imaginary frequency = 0

Standard orientation:

Center Number	Atomic Number	Atomic Type	Coordinates (Angstroms)		
			X	Y	Z
1	6	0	-0.104739	0.894048	-0.289619
2	1	0	-0.006163	0.949893	-1.373374
3	1	0	-0.423753	1.855420	0.113298
4	6	0	1.198959	0.455580	0.345247
5	1	0	1.952110	1.220498	0.140735
6	1	0	1.073900	0.365645	1.430067
7	8	0	1.697400	-0.753731	-0.211830
8	1	0	1.038969	-1.435291	-0.037384
9	17	0	-1.398799	-0.295534	0.063972

**OCgg':** MP2 energy=-613.7091052 (Hartrees), Zero Point Energy=0.0731918 (Hartrees), imaginary frequency = 0

Standard orientation:

Center Number	Atomic Number	Atomic Type	Coordinates (Angstroms)		
			X	Y	Z
1	6	0	0.118602	0.860382	0.302773
2	1	0	0.010427	0.897166	1.387857
3	1	0	0.437004	1.837056	-0.063935
4	6	0	-1.182827	0.458463	-0.362539
5	1	0	-1.910136	1.260050	-0.181272
6	1	0	-1.037813	0.356962	-1.439261
7	8	0	-1.680803	-0.794702	0.087029
8	1	0	-1.878723	-0.706312	1.025223
9	17	0	1.424177	-0.305904	-0.062720

**OCga:** MP2 energy=-613.7091025 (Hartrees), Zero Point Energy=0.0727356 (Hartrees), imaginary frequency = 0

Standard orientation:

Center Number	Atomic Number	Atomic Type	Coordinates (Angstroms)		
			X	Y	Z
1	6	0	-0.126476	0.860390	-0.297594
2	1	0	-0.016035	0.897302	-1.381394
3	1	0	-0.449074	1.831957	0.076333
4	6	0	1.176605	0.462889	0.351626
5	1	0	1.892842	1.275981	0.178674
6	1	0	1.037258	0.338071	1.430895
7	8	0	1.627467	-0.747261	-0.248243
8	1	0	2.463923	-0.978865	0.166984
9	17	0	-1.426437	-0.313296	0.070015

**OCag:** MP2 energy=-613.7086763 (Hartrees), Zero Point Energy=0.0731693 (Hartrees), imaginary frequency = 0

Standard orientation:

Center Number	Atomic Number	Atomic Type	Coordinates (Angstroms)		
			X	Y	Z
1	6	0	-0.041266	0.608563	0.043898
2	1	0	0.053905	1.283789	-0.807155
3	1	0	0.050218	1.170082	0.972976
4	6	0	0.998027	-0.500237	-0.015202
5	1	0	0.875171	-1.170495	0.836915
6	1	0	0.875700	-1.080178	-0.936075
7	8	0	2.311302	0.040507	0.086603
8	1	0	2.481190	0.543371	-0.716812
9	17	0	-1.680421	-0.101211	-0.012638

**OCaa:** MP2 energy=-613.7078781 (Hartrees), Zero Point Energy=0.0723751 (Hartrees), imaginary frequency = -54.48

Standard orientation:

Center Number	Atomic Number	Atomic Type	Coordinates (Angstroms)		
			X	Y	Z
1	6	0	-0.049465	0.615339	-0.000005
2	1	0	0.038773	1.233346	-0.892755
3	1	0	0.038793	1.233366	0.892730
4	6	0	0.996008	-0.482362	-0.000005
5	1	0	0.876480	-1.108340	0.890625
6	1	0	0.876453	-1.108365	-0.890614
7	8	0	2.262270	0.174660	-0.000034
8	1	0	2.938757	-0.509860	-0.000013
9	17	0	-1.679216	-0.113841	0.000021

**OBgg:** MP2 energy=-2726.7551933 (Hartrees), Zero Point Energy=0.0723052 (Hartrees), imaginary frequency = 0

Standard orientation:

Center Number	Atomic Number	Atomic Type	Coordinates (Angstroms)		
			X	Y	Z
1	6	0	0.508868	1.000407	-0.286864
2	1	0	0.611886	1.068535	-1.369669
3	1	0	0.272908	1.975126	0.141017
4	6	0	1.741507	0.394870	0.355629
5	1	0	2.581741	1.069485	0.168758
6	1	0	1.594517	0.308456	1.438200
7	8	0	2.099065	-0.855542	-0.216676
8	1	0	1.358840	-1.453566	-0.059072
9	35	0	-1.048990	-0.128439	0.028617

**OBgg':** MP2 energy =-2726.7538437 (Hartrees), Zero Point Energy=0.0723743 (Hartrees), imaginary frequency = 0

Standard orientation:

Center Number	Atomic Number	Atomic Type	Coordinates (Angstroms)		
			X	Y	Z
1	6	0	-0.496585	0.965383	0.300853
2	1	0	-0.613164	1.007200	1.384845
3	1	0	-0.259089	1.957637	-0.084864
4	6	0	-1.731137	0.404760	-0.379329
5	1	0	-2.541915	1.130482	-0.230532
6	1	0	-1.554627	0.296474	-1.450880
7	8	0	-2.104516	-0.880533	0.097177
8	1	0	-2.346070	-0.785237	1.024639
9	35	0	1.071924	-0.136662	-0.027136

**OBga:** MP2 energy=-2726.753784 (Hartrees), Zero Point Energy=0.0719051 (Hartrees), imaginary frequency = 0

Standard orientation:

Center Number	Atomic Number	Atomic Type	Coordinates (Angstroms)		
			X	Y	Z
1	6	0	0.490120	0.976992	-0.291706
2	1	0	0.603374	1.036016	-1.374377
3	1	0	0.248766	1.957789	0.117632
4	6	0	1.727516	0.411494	0.363070
5	1	0	2.534307	1.141791	0.215387
6	1	0	1.559257	0.283069	1.437920
7	8	0	2.044839	-0.827640	-0.261384
8	1	0	2.817022	-1.183556	0.189554
9	35	0	-1.069350	-0.141283	0.030765

**OBag:** MP2 energy=-2726.7537992 (Hartrees), Zero Point Energy=0.0723333 (Hartrees), imaginary frequency = 0

Standard orientation:

Center Number	Atomic Number	Atomic Type	Coordinates (Angstroms)		
			X	Y	Z
1	6	0	0.571918	0.651320	0.048127
2	1	0	0.668768	1.317999	-0.809655
3	1	0	0.663729	1.214464	0.976463
4	6	0	1.571060	-0.495171	-0.008366
5	1	0	1.431856	-1.153351	0.850763
6	1	0	1.424010	-1.075636	-0.925409
7	8	0	2.901747	0.007441	0.080011
8	1	0	3.079086	0.497046	-0.730264
9	35	0	-1.238265	-0.051341	-0.006873

**OBaa:** MP2 energy=-2726.7529681 (Hartrees), Zero Point Energy=0.0715329 (Hartrees), imaginary frequency = -63.12

Standard orientation:

Center Number	Atomic Number	Atomic Type	Coordinates (Angstroms)		
			X	Y	Z
1	6	0	0.564472	0.662759	0.000026
2	1	0	0.653867	1.277013	-0.895390
3	1	0	0.653859	1.276956	0.895481
4	6	0	1.566388	-0.475874	-0.000007
5	1	0	1.424173	-1.095371	0.891999
6	1	0	1.424157	-1.095332	-0.892039
7	8	0	2.855418	0.138754	-0.000003
8	1	0	3.507744	-0.569311	0.000012
9	35	0	-1.236923	-0.057866	-0.000004

**OIgg:** MP2 energy=-451.2182729 (Hartrees), Zero Point Energy=0.0716559 (Hartrees), imaginary frequency = 0

Standard orientation:

Center Number	Atomic Number	Atomic Type	Coordinates (Angstroms)		
			X	Y	Z
1	6	0	0.933754	1.040310	-0.283170
2	1	0	1.051300	1.116219	-1.364273
3	1	0	0.750676	2.022074	0.155163
4	6	0	2.122243	0.353759	0.364992
5	1	0	3.001694	0.981939	0.193722
6	1	0	1.963432	0.262854	1.445577
7	8	0	2.421879	-0.906400	-0.219261
8	1	0	1.652397	-1.470719	-0.075304
9	53	0	-0.870387	-0.075954	0.017137

**OIgg'**: MP2 energy=-451.2172645 (Hartrees), Zero Point Energy=0.0717754 (Hartrees), imaginary frequency = 0

Standard orientation:

Center Number	Atomic Number	Atomic Type	Coordinates (Angstroms)		
			X	Y	Z
1	6	0	-0.924007	1.017215	0.292955
2	1	0	-1.049908	1.075261	1.375407
3	1	0	-0.740613	2.013168	-0.112913
4	6	0	-2.116440	0.365544	-0.384164
5	1	0	-2.977115	1.032789	-0.238354
6	1	0	-1.937135	0.261963	-1.455763
7	8	0	-2.401589	-0.938867	0.101121
8	1	0	-2.640594	-0.854102	1.030363
9	53	0	0.883033	-0.081409	-0.016235

**OIga:** MP2 energy=-451.217135 (Hartrees), Zero Point Energy=0.0713789 (Hartrees), imaginary frequency = 0

Standard orientation:

Center Number	Atomic Number	Atomic Type	Coordinates (Angstroms)		
			X	Y	Z
1	6	0	0.918919	1.029902	-0.284622
2	1	0	1.042444	1.106879	-1.365189
3	1	0	0.730477	2.013223	0.146385
4	6	0	2.113243	0.372661	0.366980
5	1	0	2.972993	1.038681	0.211963
6	1	0	1.945940	0.258728	1.443861
7	8	0	2.335823	-0.888289	-0.255651
8	1	0	3.130754	-1.262853	0.137450
9	53	0	-0.881173	-0.084221	0.018426

**OIag:** MP2energy=-451.2176633 (Hartrees), Zero Point Energy=0.0717922 (Hartrees), imaginary frequency = 0

Standard orientation:

Center Number	Atomic Number	Atomic Type	Coordinates (Angstroms)		
			X	Y	Z
1	6	0	0.999406	0.676451	0.046322
2	1	0	1.103938	1.338277	-0.814588
3	1	0	1.103588	1.240308	0.973235
4	6	0	1.972472	-0.492283	-0.010033
5	1	0	1.822081	-1.149501	0.848121
6	1	0	1.816772	-1.070076	-0.927637
7	8	0	3.315446	-0.019776	0.079947
8	1	0	3.498415	0.479577	-0.723282
9	53	0	-1.013201	-0.033687	-0.004022

**OIaa:** MP2 energy=-451.2166347 (Hartrees), Zero Point Energy=0.0708837 (Hartrees), imaginary frequency = -74.70

Standard orientation:

Center Number	Atomic Number	Atomic Type	Coordinates (Angstroms)		
			X	Y	Z
1	6	0	0.991657	0.690000	0.000074
2	1	0	1.091117	1.302111	-0.896018
3	1	0	1.091080	1.301985	0.896255
4	6	0	1.966804	-0.471581	0.000010
5	1	0	1.813820	-1.089404	0.891640
6	1	0	1.813824	-1.089300	-0.891694
7	8	0	3.272037	0.111704	0.000048
8	1	0	3.906264	-0.613089	0.000062
9	53	0	-1.012135	-0.038046	-0.000021

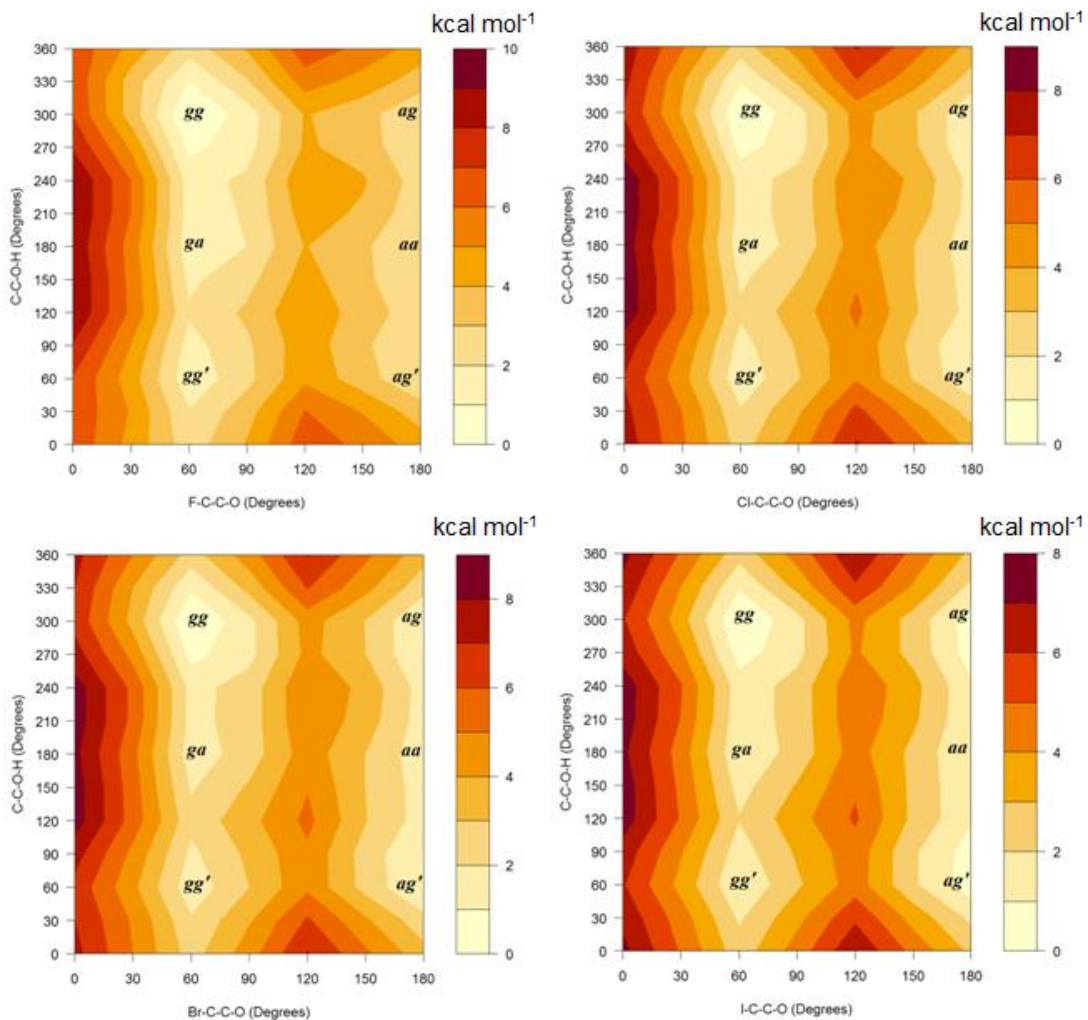


**Figure S1.** Potential energy surfaces for 2-haloethanols(X–C–C–O and C–C–O–H torsion in the *gauche* and *anti* conformers) in chloroform implicit solvent obtained at the B3LYP/6-311++(d,p) level of theory (def2 TZVP was used for bromine and iodine atoms, and ECP was included for the iodine atom).

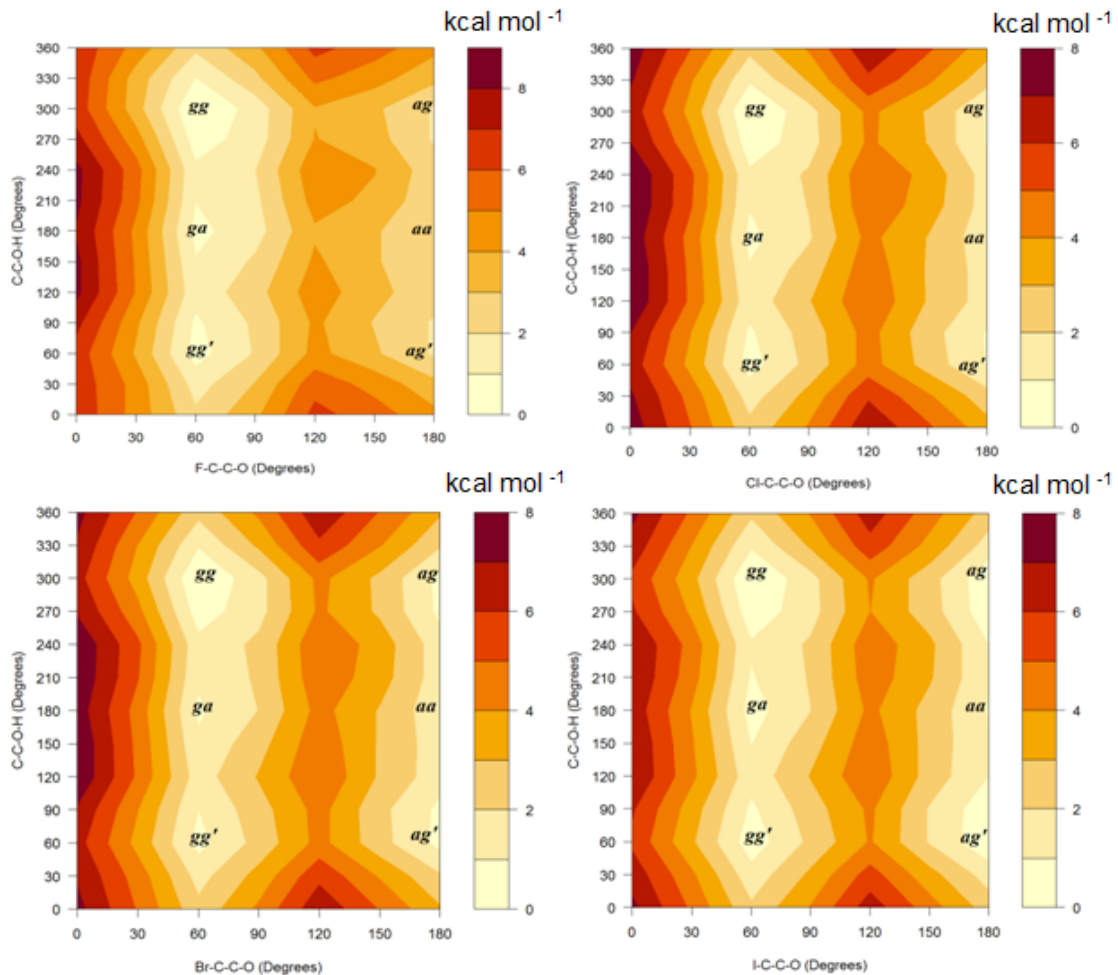


**Figure S2.** Potential energy surfaces for 2-haloethanols(X–C–C–O and C–C–O–H torsion in the *gauche* and *anti* conformers) in DMSO implicit solvent obtained at the B3LYP/6-311++(d,p) level of theory (def2 TZVP was used for bromine and iodine atoms, and ECP was included for the iodine atom).

**Table S1.** Lewis (L) and non-Lewis (NL) contributions to the full electronic conformational energies of 2-halofluoroethanes and 2-haloethanols, and important electron delocalization interactions obtained by NBO analysis (data in kcal mol<sup>-1</sup>) in chloroform implicit solvent obtained at the B3LYP/6-311++(d,p) level of theory (def2-TZVP was used for bromine and iodine atoms, and ECP was included for the iodine atom).

Name	Conf.	$\Delta E_{\text{FULL}}$	$\Delta E_L$	$\Delta E_{\text{NL}}$	$\sigma_{\text{CH} \rightarrow \sigma}^*$ ${}^*\text{CF(OH)}$	$\sigma_{\text{CX} \rightarrow \sigma}^*$ ${}^*\text{CX}$	$\sigma_{\text{CF(OH)} \rightarrow \sigma}^*$ ${}^*\text{CH}$	$\sigma_{\text{CX} \rightarrow \sigma}^*$ ${}^*\text{CH}$	$\sigma_{\text{CH} \rightarrow \sigma}^*$ ${}^*\text{CH}$	$\sigma_{\text{CF(OH)} \rightarrow \sigma}^*$ ${}^*\text{CX}$	$\sigma_{\text{CX} \rightarrow \sigma}^*$ ${}^*\text{CF(OH)}$
<b>FF</b>	<i>g</i>	0.00	6.41	-6.41	4.71	4.71	0.68	0.68	4.46	-	-
	<i>a</i>	1.77	1.77	0.00	1.10	1.10	-	-	8.04	1.52	1.52
<b>FC</b>	<i>g</i>	0.00	3.00	-3.00	4.59	5.50	0.82	1.38	4.81	-	-
	<i>a</i>	0.39	0.39	0.00	1.24	-	-	-	9.02	1.83	2.96
<b>FB</b>	<i>g</i>	0.00	2.73	-2.73	4.50	6.27	0.87	1.71	4.87	-	-
	<i>a</i>	0.01	0.01	0.00	1.22	-	-	-	9.26	2.16	3.84
<b>FI</b>	<i>g</i>	0.40	1.97	-1.57	4.53	6.42	0.90	2.16	4.94	-	-
	<i>a</i>	0.00	0.00	0.00	1.22	-	-	-	9.58	2.27	4.99
<b>OF</b>	<i>gg</i>	0.00	6.28	-6.28	4.19	4.84	0.78	0.82	4.76	-	-
	<i>gg'</i>	1.27	9.48	-8.21	4.55	4.89	0.71	0.72	4.80	-	-
	<i>ga</i>	1.10	5.92	-4.82	3.86	4.91	0.84	0.72	4.65	-	-
	<i>ag</i>	2.00	4.65	-2.65	-	1.10	-	-	8.66	1.70	1.47
	<i>aa</i>	2.09	2.09	0.00	-	1.14	-	-	8.56	1.96	1.36
<b>OC</b>	<i>gg</i>	0.00	5.71	-5.71	4.17	5.66	0.89	1.56	5.02	-	-
	<i>gg'</i>	1.39	7.10	-5.71	4.43	5.79	0.81	1.38	5.11	-	-
	<i>ga</i>	1.24	3.76	-2.52	3.73	5.81	1.02	1.41	5.00	-	-
	<i>ag</i>	1.05	3.75	-2.70	-	-	-	-	9.52	2.06	2.74
	<i>aa</i>	1.39	1.39	0.00	-	-	-	-	9.48	2.40	2.51
<b>OB</b>	<i>gg</i>	0.00	6.14	-6.14	4.08	6.45	0.93	1.83	5.07	-	-
	<i>gg'</i>	1.40	7.05	-5.65	4.33	6.62	0.86	1.67	5.17	-	-
	<i>ga</i>	1.34	3.75	-2.41	3.68	6.59	1.08	1.73	5.07	-	-
	<i>ag</i>	0.81	3.55	-2.74	-	-	-	-	9.69	2.42	3.43
	<i>aa</i>	1.33	1.33	0.00	-	-	-	-	9.66	2.80	3.16
<b>OI</b>	<i>gg</i>	0.00	6.24	-6.24	4.13	6.75	0.94	2.23	5.10	-	-
	<i>gg'</i>	1.16	6.07	-4.91	4.32	6.82	0.89	2.09	5.22	-	-
	<i>ga</i>	1.14	3.04	-1.90	3.70	6.81	1.12	2.16	5.15	-	-
	<i>ag</i>	0.37	3.23	-2.86	-	-	-	-	9.95	2.54	4.33
	<i>aa</i>	1.02	1.02	0.00	-	-	-	-	9.92	2.93	3.97

**Table S2.** Lewis (L) and non-Lewis (NL) contributions to the full electronic conformational energies of 2-halofluoroethanes and 2-haloethanols, and important electron delocalization interactions obtained by NBO analysis (data in kcal mol<sup>-1</sup>) in DMSO implicit solvent obtained at the B3LYP/6-311++(d,p) level of theory (def2-TZVP was used for bromine and iodine atoms, and ECP was included for the iodine atom).

Name	Conf.	$\Delta E_{\text{FULL}}$	$\Delta E_L$	$\Delta E_{\text{NL}}$	$\sigma_{\text{CH} \rightarrow \sigma}^{\ast_{\text{CF(OH)}}}$	$\sigma_{\text{CH} \rightarrow \sigma}^{\ast_{\text{CX}}}$	$\sigma_{\text{CF(OH)} \rightarrow \sigma}^{\ast_{\text{CH}}}$	$\sigma_{\text{CX} \rightarrow \sigma}^{\ast_{\text{CH}}}$	$\sigma_{\text{CH} \rightarrow \sigma}^{\ast_{\text{CH}}}$	$\sigma_{\text{CF(OH)} \rightarrow \sigma}^{\ast_{\text{CX}}}$	$\sigma_{\text{CX} \rightarrow \sigma}^{\ast_{\text{CF(OH)}}}$
<b>FF</b>	<i>g</i>	0.00	6.06	-6.06	4.76	4.76	0.68	0.68	4.46	-	-
	<i>a</i>	2.28	2.28	0.00	1.10	1.10	-	-	8.00	1.53	1.53
<b>FC</b>	<i>g</i>	0.00	3.20	-3.20	4.67	5.55	0.82	1.42	4.82	-	-
	<i>a</i>	0.90	0.90	0.00	1.24	-	-	-	8.98	1.84	2.98
<b>FB</b>	<i>g</i>	0.00	2.64	-2.64	4.58	6.34	0.86	1.70	4.87	-	-
	<i>a</i>	0.50	0.50	0.00	1.22	-	-	-	9.22	2.17	3.86
<b>FI</b>	<i>g</i>	0.00	1.56	-1.56	4.60	6.51	0.89	2.14	4.92	-	-
	<i>a</i>	0.02	0.02	0.00	1.22	-	-	-	9.56	2.28	5.03
<b>OF</b>	<i>gg</i>	0.00	6.29	-6.29	4.26	4.91	0.77	0.81	4.75	-	-
	<i>gg'</i>	0.56	7.87	-7.31	4.56	4.91	0.71	0.73	4.77	-	-
	<i>ga</i>	0.54	5.03	-4.49	3.91	5.04	0.84	0.72	2.70	-	-
	<i>ag</i>	1.81	4.26	-2.45	-	1.11	-	-	8.60	1.71	1.47
	<i>aa</i>	2.08	2.08	0.00	-	1.14	-	-	8.56	1.97	1.36
<b>OC</b>	<i>gg</i>	0.00	5.67	-5.67	4.24	5.71	0.87	1.54	5.01	-	-
	<i>gg'</i>	0.66	5.84	-5.18	4.45	5.86	0.81	1.37	5.08	-	-
	<i>ga</i>	0.67	3.04	-2.37	3.82	5.97	1.01	1.39	5.03	-	-
	<i>ag</i>	0.85	3.46	-2.61	-	-	-	-	9.47	2.07	2.74
	<i>aa</i>	1.37	1.37	0.00	-	-	-	-	9.48	2.42	2.51
<b>OB</b>	<i>gg</i>	0.00	6.08	-6.08	4.15	6.51	0.91	1.82	5.07	-	-
	<i>gg'</i>	0.71	5.94	-5.23	4.36	6.68	0.85	1.66	5.14	-	-
	<i>ga</i>	0.79	3.24	-2.45	3.76	6.77	1.06	1.71	5.11	-	-
	<i>ag</i>	0.61	3.30	-2.69	-	-	-	-	9.65	2.43	3.43
	<i>aa</i>	1.31	1.31	0.00	-	-	-	-	9.66	2.82	3.16
<b>OI</b>	<i>gg</i>	0.00	6.19	-6.19	4.19	6.79	0.92	2.21	5.09	-	-
	<i>gg'</i>	0.52	5.21	-4.69	4.35	6.91	0.88	2.08	5.18	-	-
	<i>ga</i>	0.63	2.58	-1.95	3.76	6.99	1.11	2.13	5.16	-	-
	<i>ag</i>	0.15	3.00	-2.85	-	-	-	-	9.91	2.54	4.35
	<i>aa</i>	0.96	0.96	0.00	-	-	-	-	9.9	2.94	3.97

**Table S3.**  $\varepsilon_i - \varepsilon_j$  and  $F(i,j)$  contributions to electron delocalization energies (kcal mol<sup>-1</sup>) for 2-halofluoroethanes in gas phase.

Name	Structure	Conformer	$\sigma_{\text{CH}} \rightarrow \sigma^*_{\text{CX}}$		$\sigma_{\text{CX}} \rightarrow \sigma^*_{\text{CF}}$	
			$\varepsilon_i - \varepsilon_j$	$F(i,j)$	$\varepsilon_i - \varepsilon_j$	$F(i,j)$
<b>FF</b>	F-CH <sub>2</sub> -CH <sub>2</sub> -F	<i>g</i>	0.76	0.053	-	-
		<i>a</i>	-	-	1.15	0.037
<b>FC</b>	F-CH <sub>2</sub> -CH <sub>2</sub> -Cl	<i>g</i>	0.66	0.053	-	-
		<i>a</i>	-	-	0.90	0.046
<b>FB</b>	F-CH <sub>2</sub> -CH <sub>2</sub> -Br	<i>g</i>	0.61	0.054	-	-
		<i>a</i>	-	-	0.83	0.050
<b>FI</b>	F-CH <sub>2</sub> -CH <sub>2</sub> -I	<i>g</i>	0.58	0.053	-	-
		<i>a</i>	-	-	0.74	0.054

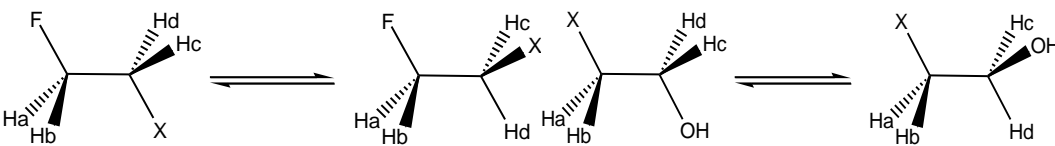
**Table S4.**  $\varepsilon_i - \varepsilon_j$  and  $F(i,j)$  contributions to electron delocalization energies (kcal mol<sup>-1</sup>) for 2-halofluoroethanes in chloroform implicit solvent.

Name	Structure	Conformer	$\sigma_{\text{CH}} \rightarrow \sigma^*_{\text{CX}}$		$\sigma_{\text{CX}} \rightarrow \sigma^*_{\text{CF}}$	
			$\varepsilon_i - \varepsilon_j$	$F(i,j)$	$\varepsilon_i - \varepsilon_j$	$F(i,j)$
<b>FF</b>	F-CH <sub>2</sub> -CH <sub>2</sub> -F	<i>g</i>	0.75	0.053	-	-
		<i>a</i>	-	-	1.14	0.037
<b>FC</b>	F-CH <sub>2</sub> -CH <sub>2</sub> -Cl	<i>g</i>	0.65	0.054	-	-
		<i>a</i>	-	-	0.89	0.046
<b>FB</b>	F-CH <sub>2</sub> -CH <sub>2</sub> -Br	<i>g</i>	0.60	0.055	-	-
		<i>a</i>	-	-	0.82	0.050
<b>FI</b>	F-CH <sub>2</sub> -CH <sub>2</sub> -I	<i>g</i>	0.57	0.054	-	-
		<i>a</i>	-	-	0.73	0.054

**Table S5.**  $\varepsilon_i - \varepsilon_j$  and  $F(i,j)$  contributions to electron delocalization energies (kcal mol<sup>-1</sup>) for 2-halofluoroethanes in DMSO implicit solvent.

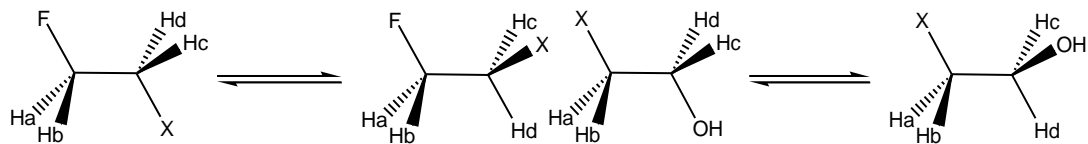
Name	Structure	Conformer	$\sigma_{\text{CH}} \rightarrow \sigma^*_{\text{CX}}$		$\sigma_{\text{CX}} \rightarrow \sigma^*_{\text{CF}}$	
			$\varepsilon_i - \varepsilon_j$	$F(i,j)$	$\varepsilon_i - \varepsilon_j$	$F(i,j)$
<b>FF</b>	F-CH <sub>2</sub> -CH <sub>2</sub> -F	<i>g</i>	0.74	0.053	-	-
		<i>a</i>	-	-	1.14	0.037
<b>FC</b>	F-CH <sub>2</sub> -CH <sub>2</sub> -Cl	<i>g</i>	0.65	0.053	-	-
		<i>a</i>	-	-	0.89	0.046
<b>FB</b>	F-CH <sub>2</sub> -CH <sub>2</sub> -Br	<i>g</i>	0.60	0.055	-	-
		<i>a</i>	-	-	0.81	0.050
<b>FI</b>	F-CH <sub>2</sub> -CH <sub>2</sub> -I	<i>g</i>	0.57	0.054	-	-
		<i>a</i>	-	-	0.72	0.054

**Table S6.** Calculated spin-spin coupling constants (Hz) for the studied 2-halofluoroethanes and 2-haloethanols in gas phase obtained at the B3LYP/6-311++(d,p) level of theory (def2-TZVP was used for bromine and iodine atoms, and ECP was included for the iodine atom).



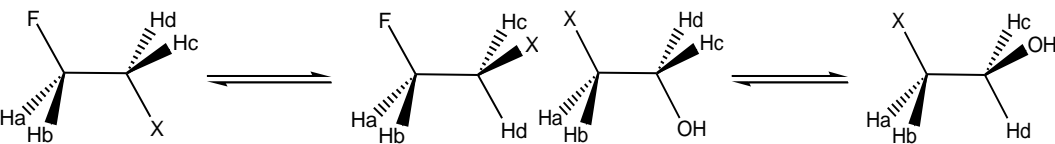
Gas								
Name	Conf.	$^3J_{\text{HaHc}}$	$^3J_{\text{HaHd}}$	$^3J_{\text{HbHc}}$	$^3J_{\text{HbHd}}$	$^3J_{\text{FHc}}$	$^3J_{\text{FHD}}$	$^2J_{\text{FHa}}$
<b>FF</b>	<i>g</i>	1.11	1.48	8.61	1.11	17.27	33.75	46.58
	<i>a</i>	10.01	5.42	5.42	10.01	1.27	1.26	47.13
<b>FC</b>	<i>g</i>	2.40	1.97	9.91	1.45	13.14	31.92	47.37
	<i>a</i>	10.68	5.47	5.47	10.68	3.68	3.68	47.89
<b>FB</b>	<i>g</i>	2.88	2.28	10.55	1.69	11.46	32.72	48.33
	<i>a</i>	11.06	5.49	5.50	11.06	4.86	4.86	48.42
<b>FI</b>	<i>g</i>	3.00	1.85	10.73	1.23	8.64	34.06	49.04
	<i>a</i>	11.07	4.79	4.79	11.07	5.98	5.98	48.63
<b>OF</b>	<i>gg</i>	2.01	1.04	9.22	1.81	15.98	34.40	47.32
	<i>gg'</i>	2.15	1.25	9.67	1.31	14.85	33.24	46.78
	<i>ga</i>	1.14	1.93	8.43	0.92	14.43	34.06	47.51
	<i>ag</i>	9.68	5.48	4.93	10.32	1.83	1.54	47.73
	<i>aa</i>	9.56	5.34	5.33	9.56	2.85	2.85	47.51
<b>OC</b>	<i>gg</i>	1.92	1.99	9.92	2.63	-	-	-
	<i>gg'</i>	2.44	1.76	10.73	2.54	-	-	-
	<i>ga</i>	1.69	2.41	9.71	2.07	-	-	-
	<i>ag</i>	10.26	5.29	5.06	10.92	-	-	-
	<i>aa</i>	10.30	5.35	5.35	10.30	-	-	-
<b>OB</b>	<i>gg</i>	2.11	2.27	10.49	3.07	-	-	-
	<i>gg'</i>	2.55	2.11	11.25	2.92	-	-	-
	<i>ga</i>	1.97	2.69	10.35	2.51	-	-	-
	<i>ag</i>	10.65	5.35	5.06	11.31	-	-	-
	<i>aa</i>	10.69	5.41	5.41	10.69	-	-	-
<b>OI</b>	<i>gg</i>	1.44	2.07	10.44	2.90	-	-	-
	<i>gg'</i>	2.07	1.69	11.30	2.98	-	-	-
	<i>ga</i>	1.55	2.23	10.48	2.63	-	-	-
	<i>ag</i>	10.60	4.55	4.40	11.25	-	-	-
	<i>aa</i>	10.65	4.70	4.70	10.65	-	-	-

**Table S7.** Calculated spin-spin coupling constants (Hz) for the studied 2-halofluoroethanes and 2-haloethanols in chloroform implicit solvent obtained at the B3LYP/6-311++(d,p) level of theory (def2-TZVP was used for bromine and iodine atoms, and ECP was included for the iodine atom).



Chloroform								
Name	Conf.	$^3J_{\text{HaHc}}$	$^3J_{\text{HaHd}}$	$^3J_{\text{HbHc}}$	$^3J_{\text{HbHd}}$	$^3J_{\text{FHc}}$	$^3J_{\text{FHD}}$	$^2J_{\text{FHa}}$
<b>FF</b>	<i>g</i>	1.27	1.23	8.68	1.27	17.89	36.73	46.10
	<i>a</i>	10.03	5.43	5.43	10.03	1.34	1.33	46.88
<b>FC</b>	<i>g</i>	2.54	1.75	9.94	1.59	13.40	35.03	47.23
	<i>a</i>	10.71	5.47	5.47	10.71	3.88	3.87	47.78
<b>FB</b>	<i>g</i>	3.00	2.07	10.56	1.80	11.65	35.91	48.29
	<i>a</i>	11.09	5.50	5.50	11.09	5.10	5.10	48.38
<b>FI</b>	<i>g</i>	3.10	1.68	10.71	1.34	8.71	37.44	49.19
	<i>a</i>	11.10	4.79	4.79	11.10	6.33	6.34	48.71
<b>OF</b>	<i>gg</i>	1.98	1.09	9.10	1.73	16.86	37.43	47.02
	<i>gg'</i>	2.16	1.17	9.52	1.29	16.47	36.58	46.87
	<i>ga</i>	1.66	1.74	8.73	1.11	18.87	38.26	47.14
	<i>ag</i>	9.71	5.41	5.03	10.30	1.75	2.03	47.70
	<i>aa</i>	9.72	5.34	5.34	9.72	3.09	3.09	47.43
<b>OC</b>	<i>gg</i>	1.95	1.97	9.89	2.60	-	-	-
	<i>gg'</i>	2.44	1.70	10.58	2.49	-	-	-
	<i>ga</i>	1.90	2.28	9.88	2.26	-	-	-
	<i>ag</i>	10.29	5.26	5.09	10.90	-	-	-
	<i>aa</i>	10.45	5.35	5.35	10.45	-	-	-
<b>OB</b>	<i>gg</i>	2.15	2.23	10.47	3.06	-	-	-
	<i>gg'</i>	2.50	2.07	11.06	2.82	-	-	-
	<i>ga</i>	2.21	2.51	10.54	2.73	-	-	-
	<i>ag</i>	10.69	5.31	5.09	11.29	-	-	-
	<i>aa</i>	10.83	5.40	5.40	10.83	-	-	-
<b>OI</b>	<i>gg</i>	1.47	2.04	10.43	2.88	-	-	-
	<i>gg'</i>	1.97	1.71	11.10	2.82	-	-	-
	<i>ga</i>	1.76	2.06	10.61	2.85	-	-	-
	<i>ag</i>	10.64	4.52	4.42	11.22	-	-	-
	<i>aa</i>	10.79	4.69	4.69	10.79	-	-	-

**Table S8.** Calculated spin-spin coupling constants (Hz) for the studied 2-halofluoroethanes and 2-haloethanols in DMSO implicit solvent obtained at the B3LYP/6-311++(d,p) level of theory (def2-TZVP was used for bromine and iodine atoms, and ECP was included for the iodine atom).



DMSO								
Name	Conf.	$^3J_{\text{HaHc}}$	$^3J_{\text{HaHd}}$	$^3J_{\text{HbHc}}$	$^3J_{\text{HbHd}}$	$^3J_{\text{FHc}}$	$^3J_{\text{FHD}}$	$^2J_{\text{FHa}}$
<b>FF</b>	<i>g</i>	1.34	1.12	8.68	1.34	18.16	37.93	45.93
	<i>a</i>	10.03	5.43	5.44	10.03	1.36	1.36	46.78
<b>FC</b>	<i>g</i>	2.58	1.67	9.92	1.63	13.56	36.35	47.24
	<i>a</i>	10.71	5.47	5.47	10.71	3.95	3.95	47.74
<b>FB</b>	<i>g</i>	3.06	1.97	10.54	1.87	11.58	37.15	48.38
	<i>a</i>	11.09	5.50	5.50	11.09	5.19	5.19	48.36
<b>FI</b>	<i>g</i>	3.12	1.61	10.68	1.37	8.80	38.89	49.31
	<i>a</i>	11.10	4.79	4.80	11.10	6.48	6.49	48.75
<b>OF</b>	<i>gg</i>	1.98	1.09	9.06	1.71	17.10	38.51	46.93
	<i>gg'</i>	2.17	1.13	9.42	1.29	17.19	38.00	46.97
	<i>ga</i>	1.79	1.62	8.85	1.24	18.85	40.25	46.92
	<i>ag</i>	9.71	5.39	5.06	10.26	1.76	2.17	47.75
	<i>aa</i>	9.78	5.34	5.34	9.78	3.18	3.18	47.39
<b>OC</b>	<i>gg</i>	1.96	1.95	9.86	2.60	-	-	-
	<i>gg'</i>	2.39	1.70	10.46	2.43	-	-	-
	<i>ga</i>	1.99	2.21	9.92	2.37	-	-	-
	<i>ag</i>	10.30	5.25	5.10	10.85	-	-	-
	<i>aa</i>	10.50	5.35	5.35	10.50	-	-	-
<b>OB</b>	<i>gg</i>	2.18	2.20	10.46	3.07	-	-	-
	<i>gg'</i>	2.48	2.05	10.96	2.78	-	-	-
	<i>ga</i>	2.31	2.42	10.59	2.85	-	-	-
	<i>ag</i>	10.69	5.31	5.10	11.25	-	-	-
	<i>aa</i>	10.89	5.39	5.39	10.89	-	-	-
<b>OI</b>	<i>gg</i>	1.49	2.01	10.41	2.89	-	-	-
	<i>gg'</i>	1.94	1.69	11.00	2.78	-	-	-
	<i>ga</i>	1.82	1.99	10.62	2.93	-	-	-
	<i>ag</i>	10.64	4.51	4.42	11.19	-	-	-
	<i>aa</i>	10.84	4.68	4.68	10.84	-	-	-

## APPENDIX B

Supporting Information for:

### **Theoretical and X-ray evidence of electrostatic phosphonium *anti* and *gauche* effects**

#### INDEX

Standard coordinates of the compounds in the gas phase	151
Standard coordinates of the compounds in implicit DMSO	167
<b>Table S1.</b> Relative Gibbs free energies (kcal mol <sup>-1</sup> ) and conformational populations (%) obtained in the gas phase and implicit DMSO (IEFPCM) at the B3LYP-D3BJ/6-311++g(d,p) theory level.	185
<b>Table S2.</b> Relative full energies ( $E_{\text{FULL}}$ ), non-Lewis ( $E_{\text{NL}}$ ) and Lewis-type ( $E_{\text{L}}$ ) contributions, and the main electron delocalization energies obtained for the gas phase compounds at the B3LYP-D3BJ/6-311++g(d,p) theory level (in kcal mol <sup>-1</sup> ).	186
<b>Table S3.</b> Relative full energies ( $E_{\text{FULL}}$ ), non-Lewis ( $E_{\text{NL}}$ ) and Lewis-type ( $E_{\text{L}}$ ) contributions, and the main electron delocalization energies obtained for compounds in implicit DMSO at the B3LYP-D3BJ/6-311++g(d,p) theory level (in kcal mol <sup>-1</sup> ).	187
<b>Table S4.</b> Electron density and the Laplacian of electron density at the BCP, bond ellipticity, average number of electrons, net charge, intratomic dipole moment contribution, volume obtained at 0.001 isodensity surface, and interacting quantum atoms (IQA) intratomic energy component in the hydrogen atom (in au).	188
<b>Table S5.</b> NEDA energies in kcal mol <sup>-1</sup> for <b>PF</b> : energy of interaction ( $E_{\text{int}}$ ), electrical interaction ( $E_{\text{EL}}$ ), charge transfer ( $E_{\text{CT}}$ ), Core repulsion ( $E_{\text{CORE}}$ ), classical electrostatic interaction ( $E_{\text{ES}}$ ), polarization contribution ( $E_{\text{POL}}$ ), the penalty of polarization ( $E_{\text{SE}}$ ), deformation cost ( $E_{\text{DEF}}$ ), and exchange interaction ( $E_{\text{XC}}$ ). The energies for <b>PF</b> in the gas phase are presented for the C–C equilibrium distance in the <i>gauche</i> conformer (1.53 Å), as well as with -0.5 Å and +0.5 Å.	188
<b>Table S6.</b> NEDA energies in kcal mol <sup>-1</sup> for <b>PP</b> : energy of interaction ( $E_{\text{int}}$ ), electrical interaction ( $E_{\text{EL}}$ ), charge transfer ( $E_{\text{CT}}$ ), Core repulsion ( $E_{\text{CORE}}$ ), classical electrostatic interaction ( $E_{\text{ES}}$ ), polarization contribution ( $E_{\text{POL}}$ ), the penalty of polarization ( $E_{\text{SE}}$ ), deformation cost ( $E_{\text{DEF}}$ ), and exchange interaction ( $E_{\text{XC}}$ ). The energies for <b>PP</b> in the gas phase are presented for the C–C equilibrium distance in the <i>gauche</i> conformer (1.53 Å), as well as with -0.5 Å and +0.5 Å.	189
<b>Figure S1.</b> QTAIM plots for <b>PF</b> and <b>PP</b> in the gas phase (the P and F atomic charges, in a.u., are shown).	189
<b>Figure S2.</b> QTAIM plots indicating bond paths between interacting atoms for <b>1-cis-g</b> , <b>2-cis-g</b> , <b>3ax</b> , <b>4ax</b> , <b>8-trans-g</b> and <b>9-trans-g</b> . The atomic charges (q, in a.u.), electron densities at the bond critical point ( $\rho$ ), and the distances between interacting atoms ( $r$ , in angstroms) are also depicted	190
X-ray diffraction	190

## Standard coordinates of the compounds in the gas phase

***1-cis-g***

Standard orientation:

Center Number	Atomic Number	Atomic Type	Coordinates (Angstroms)		
			X	Y	Z
1	6	0	0.003408	1.657035	-0.302449
2	6	0	-1.364957	1.072191	0.057141
3	6	0	0.074942	-1.246947	0.714242
4	6	0	1.308605	-0.427532	0.365679
5	6	0	1.135341	1.071880	0.545989
6	1	0	-1.612093	1.306073	1.101423
7	1	0	-2.149462	1.530705	-0.555767
8	1	0	0.216927	1.467805	-1.360513
9	1	0	-0.011822	2.745488	-0.167270
10	1	0	-0.099753	-1.165632	1.794463
11	1	0	0.276463	-2.303155	0.505568
12	1	0	0.945074	1.265226	1.610645
13	1	0	2.083311	1.558262	0.292273
14	15	0	-1.504089	-0.768884	-0.146332
15	9	0	1.644031	-0.670489	-0.978060
16	1	0	2.163919	-0.779168	0.954662
17	1	0	-0.991549	-0.817705	-1.461571

***1-trans-g***

Standard orientation:

Center Number	Atomic Number	Atomic Type	Coordinates (Angstroms)		
			X	Y	Z
1	6	0	-0.001238	1.654011	-0.317193
2	6	0	-1.358778	1.072350	0.101108
3	6	0	0.051685	-1.214574	0.752331
4	6	0	1.302528	-0.431160	0.375325
5	6	0	1.154431	1.077311	0.507290
6	1	0	-1.515559	1.236572	1.174358
7	1	0	-2.166571	1.578458	-0.437911
8	1	0	0.178994	1.453161	-1.379922
9	1	0	-0.012405	2.742919	-0.195518
10	1	0	-0.160845	-1.017427	1.809636
11	1	0	0.255572	-2.283992	0.639000
12	1	0	1.005042	1.309517	1.570370
13	1	0	2.099929	1.539071	0.203376
14	15	0	-1.401132	-0.739716	-0.322138
15	1	0	-2.402953	-1.131095	0.595657
16	9	0	1.632584	-0.722577	-0.959712
17	1	0	2.150755	-0.775880	0.977274

***1-trans-a***

Standard orientation:

Center Number	Atomic Number	Atomic Type	Coordinates (Angstroms)		
			X	Y	Z
1	6	0	0.569103	1.669980	0.253997
2	6	0	1.645991	0.753173	-0.332630
3	6	0	-0.350054	-1.224237	-0.281621
4	6	0	-1.211641	-0.128108	0.309297
5	6	0	-0.844334	1.262490	-0.174066
6	1	0	1.646373	0.829430	-1.427774
7	1	0	2.641255	1.070066	-0.000054
8	1	0	0.634370	1.652966	1.349922
9	1	0	0.752420	2.705322	-0.058071
10	1	0	-0.474304	-1.230953	-1.371255
11	1	0	-0.685291	-2.199211	0.087547
12	1	0	-0.929036	1.284085	-1.268425
13	1	0	-1.578627	1.970082	0.225040
14	15	0	1.464286	-1.045861	0.089109
15	1	0	1.315081	-0.858864	1.485512
16	1	0	-1.174129	-0.167455	1.405078
17	9	0	-2.551865	-0.374150	-0.046001

**1-cis-a**

Standard orientation:

Center Number	Atomic Number	Atomic Type	Coordinates (Angstroms)		
			X	Y	Z
1	6	0	-0.564177	1.665178	-0.246640
2	6	0	-1.623767	0.752578	0.386973
3	6	0	0.324075	-1.208533	0.315615
4	6	0	1.212214	-0.147996	-0.307612
5	6	0	0.864415	1.261346	0.141053
6	1	0	-1.516079	0.765782	1.477886
7	1	0	-2.627001	1.116487	0.141368
8	1	0	-0.665581	1.644488	-1.340245
9	1	0	-0.736173	2.701087	0.065158
10	1	0	0.389846	-1.130806	1.406348
11	1	0	0.680054	-2.198662	0.013934
12	1	0	0.985746	1.313437	1.230600
13	1	0	1.586225	1.954739	-0.302967
14	15	0	-1.425391	-0.968765	-0.287610
15	9	0	2.543871	-0.408512	0.059453
16	1	0	1.177241	-0.215875	-1.402284
17	1	0	-2.064811	-1.678024	0.752954

**2-cis-g**

Standard orientation:

Center Number	Atomic Number	Atomic Type	Coordinates (Angstroms)		
			X	Y	Z
1	6	0	-0.640997	1.517095	0.662809
2	6	0	0.681570	1.594121	-0.105813
3	6	0	-0.096394	-0.898286	-1.160426
4	6	0	-1.390857	-0.679411	-0.389463
5	6	0	-1.726573	0.778718	-0.123658
6	1	0	0.531240	2.161961	-1.033989
7	1	0	1.432540	2.146654	0.472259
8	1	0	-0.496986	1.021211	1.628331
9	1	0	-0.993655	2.531952	0.883021
10	1	0	-0.270077	-0.568143	-2.193465
11	1	0	0.111838	-1.973388	-1.212357
12	1	0	-1.884835	1.271007	-1.093182
13	1	0	-2.677883	0.816275	0.418132
14	15	0	1.444860	-0.031282	-0.579479
15	6	0	1.704042	-0.786853	1.087388
16	1	0	1.980008	-1.837698	0.956019
17	1	0	2.552813	-0.283139	1.560952
18	1	0	0.836938	-0.739959	1.746832
19	9	0	-1.306710	-1.341131	0.850961
20	1	0	-2.219200	-1.159631	-0.924031

**2-trans-g**

Standard orientation:

Center Number	Atomic Number	Atomic Type	Coordinates (Angstroms)		
			X	Y	Z
1	6	0	0.935838	1.617926	-0.226962
2	6	0	-0.580572	1.484712	-0.026452
3	6	0	-0.077307	-1.148073	0.582203
4	6	0	1.400049	-0.804472	0.439377
5	6	0	1.720812	0.663295	0.678211
6	1	0	-0.828154	1.630557	1.035400
7	1	0	-1.107607	2.254656	-0.601290
8	1	0	1.192286	1.416370	-1.273509
9	1	0	1.249979	2.645734	-0.012747
10	1	0	-0.374187	-0.931011	1.618210
11	1	0	-0.211446	-2.221377	0.409181
12	1	0	1.504778	0.887931	1.731487
13	1	0	2.797089	0.803556	0.530422
14	15	0	-1.149938	-0.185769	-0.597251
15	9	0	1.818243	-1.139388	-0.860040
16	1	0	1.993935	-1.428631	1.116778
17	6	0	-2.745383	-0.311702	0.326378
18	1	0	-3.487986	0.345727	-0.135971
19	1	0	-3.127853	-1.335096	0.262935
20	1	0	-2.636572	-0.037504	1.381695

**2-trans-a**

Standard orientation:

Center Number	Atomic Number	Atomic Type	Coordinates (Angstroms)		
			X	Y	Z
1	6	0	0.033850	1.789868	0.404734
2	6	0	1.135768	1.288932	-0.534939
3	6	0	-0.385895	-1.070905	-0.658261
4	6	0	-1.315411	-0.345795	0.293104
5	6	0	-1.327543	1.158124	0.094090
6	1	0	0.907810	1.606120	-1.561204
7	1	0	2.098854	1.748413	-0.279943
8	1	0	0.300141	1.586349	1.449105
9	1	0	-0.050468	2.879698	0.317103
10	1	0	-0.741477	-0.903428	-1.682703
11	1	0	-0.434786	-2.150816	-0.477464
12	1	0	-1.612563	1.369538	-0.945046
13	1	0	-2.101010	1.586551	0.740307
14	15	0	1.398131	-0.548199	-0.594609
15	9	0	-2.623240	-0.827272	0.082254
16	1	0	-1.076344	-0.585502	1.334979
17	6	0	1.796520	-0.900879	1.178833
18	1	0	1.766720	-1.984053	1.333644
19	1	0	2.821590	-0.572646	1.376608
20	1	0	1.134992	-0.427852	1.908107

**2-cis-a**

Standard orientation:

Center Number	Atomic Number	Atomic Type	Coordinates (Angstroms)		
			X	Y	Z
1	6	0	0.511300	1.882355	-0.124161
2	6	0	-0.892689	1.401467	0.270481
3	6	0	0.137304	-1.139736	0.085720
4	6	0	1.445448	-0.471420	-0.293702
5	6	0	1.608569	0.907494	0.322571
6	1	0	-0.938717	1.250321	1.358326
7	1	0	-1.638679	2.158839	0.004370
8	1	0	0.562477	2.017847	-1.212719
9	1	0	0.705500	2.862757	0.324485
10	1	0	0.070372	-1.194502	1.180584
11	1	0	0.123297	-2.159169	-0.314769
12	1	0	1.590712	0.798303	1.414527
13	1	0	2.594520	1.296972	0.048086
14	15	0	-1.294095	-0.178443	-0.612144
15	6	0	-2.640798	-0.833007	0.466894
16	1	0	-3.551712	-0.247739	0.309927
17	1	0	-2.861705	-1.868382	0.190947
18	1	0	-2.371545	-0.796493	1.527837
19	9	0	2.507681	-1.279093	0.152045
20	1	0	1.542983	-0.413199	-1.384659

**3axial**

Standard orientation:

Center Number	Atomic Number	Atomic Type	Coordinates (Angstroms)		
			X	Y	Z
1	6	0	-0.098909	1.681077	0.269485
2	6	0	1.316041	1.153646	-0.049490
3	6	0	-0.084115	-1.287605	-0.746504
4	6	0	-1.321734	-0.478791	-0.333454
5	6	0	-1.200980	1.020527	-0.568768
6	1	0	1.586673	1.363089	-1.091188
7	1	0	2.076029	1.604393	0.595625
8	1	0	-0.315482	1.546751	1.333792
9	1	0	-0.097037	2.757423	0.079646
10	1	0	0.106682	-1.181382	-1.819873
11	1	0	-0.220803	-2.347542	-0.515008
12	1	0	-1.032686	1.194733	-1.638998
13	1	0	-2.160872	1.478597	-0.315437
14	15	0	1.346415	-0.639540	0.150886
15	9	0	-1.487791	-0.697677	1.038316
16	1	0	-2.197899	-0.888962	-0.840779
17	1	0	2.530542	-1.205765	-0.322075
18	1	0	1.256930	-0.982271	1.498552

**3equatorial**

Standard orientation:

Center Number	Atomic Number	Atomic Type	Coordinates (Angstroms)		
			X	Y	Z
1	6	0	0.566789	1.671418	0.266254
2	6	0	1.674921	0.779498	-0.333253
3	6	0	-0.405429	-1.244745	-0.228073
4	6	0	-1.262559	-0.093894	0.323526
5	6	0	-0.841777	1.272747	-0.194425
6	1	0	1.674082	0.841464	-1.427493
7	1	0	2.670139	1.060266	0.024326
8	1	0	0.624712	1.654873	1.362058
9	1	0	0.773336	2.700134	-0.039321
10	1	0	-0.530055	-1.292145	-1.316328
11	1	0	-0.711082	-2.205046	0.197817
12	1	0	-0.903429	1.273621	-1.289640
13	1	0	-1.565831	2.005627	0.171515
14	15	0	1.339796	-0.935635	0.112354
15	9	0	-2.557325	-0.359977	-0.077984
16	1	0	-1.252624	-0.105548	1.420807
17	1	0	2.152991	-1.846519	-0.562989
18	1	0	1.595080	-1.122544	1.471609

**4axial**

Standard orientation:

Center Number	Atomic Number	Atomic Type	Coordinates (Angstroms)		
			X	Y	Z
1	6	0	-1.210546	1.468457	0.622384
2	6	0	0.281196	1.614117	0.262916
3	6	0	-0.116055	-0.866073	-1.125553
4	6	0	-1.566801	-0.712779	-0.654501
5	6	0	-2.013876	0.727348	-0.452493
6	1	0	0.396175	2.193688	-0.661798
7	1	0	0.839331	2.132466	1.050276
8	1	0	-1.320561	0.957571	1.584206
9	1	0	-1.623245	2.472468	0.753028
10	1	0	-0.008193	-0.430859	-2.126390
11	1	0	0.153493	-1.925654	-1.183998
12	1	0	-1.943543	1.251553	-1.414291
13	1	0	-3.070426	0.714945	-0.169948
14	15	0	1.035410	-0.002627	-0.022805
15	6	0	1.240768	-0.890878	1.529373
16	1	0	1.651203	-1.884117	1.327652
17	1	0	1.933414	-0.338235	2.170168
18	1	0	0.275944	-1.001787	2.026434
19	6	0	2.640867	0.160327	-0.821718
20	1	0	3.324314	0.703078	-0.162971
21	1	0	3.054260	-0.831329	-1.024991
22	1	0	2.536612	0.707537	-1.761781
23	9	0	-1.671076	-1.384084	0.570425
24	1	0	-2.223565	-1.228277	-1.359784

**4equatorial**

Standard orientation:

Center Number	Atomic Number	Atomic Type	Coordinates (Angstroms)		
			X	Y	Z
1	6	0	-0.751657	1.883969	0.110189
2	6	0	0.614735	1.526505	-0.508809
3	6	0	-0.352526	-1.164976	-0.280482
4	6	0	-1.611085	-0.498506	0.288588
5	6	0	-1.856936	0.891903	-0.274232
6	1	0	0.550031	1.543282	-1.603813
7	1	0	1.395013	2.235181	-0.210424
8	1	0	-0.667216	1.950535	1.201845
9	1	0	-1.024280	2.883886	-0.237534
10	1	0	-0.486577	-1.296183	-1.361393
11	1	0	-0.200615	-2.153979	0.164939
12	1	0	-1.945895	0.821864	-1.365560
13	1	0	-2.818526	1.245956	0.107823
14	15	0	1.114505	-0.140363	-0.024497
15	9	0	-2.672914	-1.323179	-0.045810
16	1	0	-1.566807	-0.464037	1.384168
17	6	0	1.591980	-0.166344	1.713226
18	1	0	1.830072	-1.190935	2.011750
19	1	0	2.473610	0.463799	1.859182
20	1	0	0.778803	0.207423	2.339395
21	6	0	2.485549	-0.744093	-1.021359
22	1	0	3.358432	-0.102598	-0.872924
23	1	0	2.736159	-1.765612	-0.722645
24	1	0	2.206084	-0.735272	-2.077790

(2-fluoroethyl)triphenylphosphonium anti  
Standard orientation:

Center Number	Atomic Number	Atomic Type	Coordinates (Angstroms)		
			X	Y	Z
1	15	0	0.035407	0.007350	0.411878
2	6	0	-1.037190	-1.226685	-0.320019
3	6	0	-1.345333	-2.394985	0.403095
4	6	0	-1.471138	-1.071733	-1.650313
5	6	0	-2.107781	-3.397425	-0.204242
6	1	0	-0.998705	-2.531490	1.424701
7	6	0	-2.227936	-2.086148	-2.246462
8	1	0	-1.221378	-0.174379	-2.210992
9	6	0	-2.548434	-3.243595	-1.525603
10	1	0	-2.355914	-4.296064	0.353150
11	1	0	-2.568093	-1.970354	-3.271584
12	1	0	-3.140595	-4.025503	-1.992476
13	6	0	-0.269117	1.589386	-0.376400
14	6	0	0.809416	2.383663	-0.804682
15	6	0	-1.596527	2.041025	-0.521519
16	6	0	0.553469	3.637413	-1.371985
17	1	0	1.831245	2.025820	-0.708659
18	6	0	-1.835489	3.296389	-1.087414
19	1	0	-2.433718	1.415115	-0.219710
20	6	0	-0.762614	4.095332	-1.507009
21	1	0	1.382385	4.253168	-1.708873
22	1	0	-2.856558	3.648500	-1.203478
23	1	0	-0.954455	5.069608	-1.947390
24	6	0	1.748741	-0.475005	0.201372
25	6	0	2.750290	0.079994	1.021600
26	6	0	2.081448	-1.373865	-0.829091
27	6	0	4.086194	-0.273372	0.806001
28	1	0	2.503495	0.777843	1.817816
29	6	0	3.422472	-1.713298	-1.034988
30	1	0	1.305759	-1.808012	-1.455153
31	6	0	4.421900	-1.165477	-0.220783
32	1	0	4.861634	0.146291	1.440360
33	1	0	3.684437	-2.410159	-1.825902
34	1	0	5.461164	-1.437050	-0.382269
35	6	0	-0.301147	0.128804	2.193281
36	1	0	-0.046324	-0.837099	2.643959
37	1	0	0.384166	0.877482	2.605110
38	6	0	-1.739120	0.502165	2.545313
39	1	0	-1.972809	1.524936	2.240340
40	1	0	-2.458436	-0.193515	2.103435
41	9	0	-1.859004	0.426568	3.922061

(2-fluoroethyl)triphenylphosphonium *gauche*

Standard orientation:

Center Number	Atomic Number	Atomic Type	Coordinates (Angstroms)		
			X	Y	Z
1	15	0	0.081464	0.016159	0.532251
2	6	0	-0.828432	-1.360304	-0.161874
3	6	0	-0.973430	-2.556412	0.563460
4	6	0	-1.282674	-1.268100	-1.491224
5	6	0	-1.595381	-3.653326	-0.039896
6	1	0	-0.621491	-2.640255	1.587761
7	6	0	-1.898869	-2.375685	-2.083155
8	1	0	-1.159549	-0.346424	-2.054512
9	6	0	-2.055726	-3.564901	-1.360280
10	1	0	-1.720984	-4.574823	0.521155
11	1	0	-2.256701	-2.307540	-3.106520
12	1	0	-2.540164	-4.420117	-1.822771
13	6	0	-0.481467	1.531214	-0.246612
14	6	0	0.443273	2.452972	-0.769693
15	6	0	-1.867846	1.778804	-0.322013
16	6	0	-0.025402	3.634696	-1.355364
17	1	0	1.509829	2.248052	-0.734360
18	6	0	-2.317595	2.966012	-0.906940
19	1	0	-2.581169	1.053134	0.061361
20	6	0	-1.399877	3.893020	-1.420512
21	1	0	0.683813	4.347900	-1.765491
22	1	0	-3.384249	3.162411	-0.968856
23	1	0	-1.757007	4.811515	-1.877579
24	6	0	1.835455	-0.224511	0.231943
25	6	0	2.788358	0.562445	0.908884
26	6	0	2.244423	-1.173672	-0.723254
27	6	0	4.147532	0.392344	0.627975
28	1	0	2.485778	1.307131	1.641461
29	6	0	3.607451	-1.331601	-0.995101
30	1	0	1.510450	-1.785595	-1.241268
31	6	0	4.556667	-0.552394	-0.322292
32	1	0	4.884004	0.994781	1.151976
33	1	0	3.926316	-2.067205	-1.727897
34	1	0	5.613906	-0.682351	-0.535073
35	6	0	-0.151332	0.128517	2.340163
36	1	0	0.038040	-0.863536	2.763187
37	1	0	0.626322	0.801184	2.719635
38	6	0	-1.514935	0.657301	2.761875
39	1	0	-1.666552	1.686409	2.426787
40	9	0	-2.508227	-0.132235	2.190319
41	1	0	-1.619667	0.604544	3.847834

*7-cis-g\_s*

Standard orientation:

Center Number	Atomic Number	Atomic Type	Coordinates (Angstroms)		
			X	Y	Z
1	6	0	-1.082092	1.554667	0.455173
2	6	0	0.401505	1.581065	0.051069
3	6	0	-0.103080	-1.034645	-0.888153
4	6	0	-1.558640	-0.751228	-0.523324
5	6	0	-1.927985	0.725845	-0.517516
6	1	0	0.518141	1.974858	-0.965789
7	1	0	0.991859	2.207195	0.727903
8	1	0	-1.183530	1.143939	1.465414
9	1	0	-1.467310	2.578831	0.483599
10	1	0	0.058237	-0.766361	-1.938841
11	1	0	0.111027	-2.101549	-0.771295
12	1	0	-2.216297	-1.299820	-1.205894
13	1	0	-1.816300	1.113298	-1.539168
14	1	0	-2.987346	0.805865	-0.252277
15	15	0	1.088166	-0.088832	0.106816
16	8	0	1.410194	-0.618356	1.460529
17	9	0	-1.803177	-1.264739	0.756009
18	8	0	2.384067	-0.014218	-0.891573
19	1	0	3.165282	-0.334761	-0.425128

***7-cis-g\_a***

Standard orientation:

Center Number	Atomic Number	Atomic Type	Coordinates (Angstroms)		
			X	Y	Z
1	6	0	-1.054588	1.561709	0.462937
2	6	0	0.431197	1.576088	0.064535
3	6	0	-0.097343	-1.025739	-0.901469
4	6	0	-1.554227	-0.729615	-0.543134
5	6	0	-1.906487	0.751701	-0.520237
6	1	0	0.543345	1.988823	-0.947031
7	1	0	1.023173	2.192581	0.748878
8	1	0	-1.159945	1.141145	1.468572
9	1	0	-1.429516	2.589436	0.501744
10	1	0	0.053231	-0.757306	-1.955049
11	1	0	0.101183	-2.096687	-0.793466
12	1	0	-2.211689	-1.259705	-1.240785
13	1	0	-1.790246	1.150269	-1.537526
14	1	0	-2.965607	0.839746	-0.256747
15	15	0	1.096853	-0.108508	0.128531
16	8	0	1.336219	-0.646825	1.487852
17	9	0	-1.816930	-1.258831	0.723658
18	8	0	2.471492	-0.089405	-0.757224
19	1	0	2.362655	0.253771	-1.650288

***7-trans-g\_s***

Standard orientation:

Center Number	Atomic Number	Atomic Type	Coordinates (Angstroms)		
			X	Y	Z
1	6	0	-1.023042	1.551842	0.463765
2	6	0	0.438520	1.601420	-0.010552
3	6	0	-0.107480	-1.022793	-0.943025
4	6	0	-1.547857	-0.737800	-0.521870
5	6	0	-1.909864	0.740058	-0.486037
6	1	0	0.503558	2.044248	-1.011935
7	1	0	1.058889	2.205095	0.659834
8	1	0	-1.071021	1.116020	1.466866
9	1	0	-1.412488	2.572586	0.535108
10	1	0	-0.001909	-0.792053	-2.010320
11	1	0	0.117777	-2.085605	-0.812045
12	1	0	-2.230022	-1.275581	-1.189133
13	1	0	-1.834124	1.138962	-1.506588
14	1	0	-2.958395	0.821698	-0.181416
15	15	0	1.171828	-0.046096	-0.100544
16	9	0	-1.754581	-1.267870	0.757601
17	8	0	2.530416	-0.154985	-0.703212
18	8	0	1.091782	-0.544880	1.451073
19	1	0	1.962304	-0.840544	1.742807

**7-trans-g\_a**

Standard orientation:

Center Number	Atomic Number	Atomic Type	Coordinates (Angstroms)		
			X	Y	Z
1	6	0	-1.039405	1.555669	0.477830
2	6	0	0.440366	1.604689	0.066169
3	6	0	-0.064867	-0.952764	-1.041223
4	6	0	-1.498904	-0.723937	-0.578375
5	6	0	-1.902888	0.738864	-0.490959
6	1	0	0.553867	2.092268	-0.909652
7	1	0	1.033751	2.175584	0.788146
8	1	0	-1.131391	1.140287	1.487072
9	1	0	-1.434030	2.575775	0.525520
10	1	0	0.032941	-0.613104	-2.078586
11	1	0	0.177065	-2.020392	-1.019950
12	1	0	-2.196179	-1.280673	-1.210607
13	1	0	-1.837509	1.163167	-1.501623
14	1	0	-2.953354	0.787694	-0.185730
15	15	0	1.181751	-0.041904	-0.069137
16	9	0	-1.631236	-1.290185	0.717098
17	8	0	2.561280	-0.083334	-0.612324
18	8	0	1.053429	-0.672967	1.424435
19	1	0	0.186223	-1.065100	1.591040

**7-trans-g\_s'**

Standard orientation:

Center Number	Atomic Number	Atomic Type	Coordinates (Angstroms)		
			X	Y	Z
1	6	0	-1.019081	1.561592	0.430605
2	6	0	0.444982	1.601012	-0.037936
3	6	0	-0.101580	-1.041547	-0.925271
4	6	0	-1.543046	-0.749038	-0.514766
5	6	0	-1.903616	0.729387	-0.503487
6	1	0	0.514717	2.021998	-1.048266
7	1	0	1.063850	2.217072	0.622136
8	1	0	-1.071745	1.150407	1.443478
9	1	0	-1.408212	2.584041	0.474630
10	1	0	0.009616	-0.833455	-1.996577
11	1	0	0.120431	-2.103599	-0.778349
12	1	0	-2.223910	-1.294849	-1.176907
13	1	0	-1.827452	1.108474	-1.531629
14	1	0	-2.952568	0.817033	-0.201809
15	15	0	1.176372	-0.046265	-0.094511
16	9	0	-1.756403	-1.262428	0.771446
17	8	0	2.526863	-0.201082	-0.703388
18	8	0	1.090432	-0.436428	1.486248
19	1	0	1.733002	-1.119659	1.710202

**7-trans-a\_s**

Standard orientation:

Center Number	Atomic Number	Atomic Type	Coordinates (Angstroms)		
			X	Y	Z
1	6	0	-0.619089	1.884966	0.166229
2	6	0	0.722849	1.469542	-0.462337
3	6	0	-0.325784	-1.137777	-0.313395
4	6	0	-1.557141	-0.470797	0.283720
5	6	0	-1.770356	0.946274	-0.223154
6	1	0	0.653595	1.463829	-1.556468
7	1	0	1.527351	2.153088	-0.173278
8	1	0	-0.516724	1.909376	1.258029
9	1	0	-0.865608	2.901892	-0.153405
10	1	0	-0.427568	-1.185617	-1.403408
11	1	0	-0.212900	-2.154687	0.074340
12	1	0	-1.878417	0.913264	-1.315003
13	1	0	-2.712570	1.320442	0.189521
14	15	0	1.159811	-0.187835	0.104981
15	8	0	1.590168	-0.286762	1.529591
16	8	0	2.268650	-0.713097	-0.970126
17	1	0	3.056919	-1.016390	-0.503760
18	1	0	-1.498203	-0.477732	1.377812
19	9	0	-2.677384	-1.240480	-0.061245

**7-trans-a\_a**

Standard orientation:

Center Number	Atomic Number	Atomic Type	Coordinates (Angstroms)		
			X	Y	Z
1	6	0	-0.589037	1.889903	0.144470
2	6	0	0.749431	1.453079	-0.477716
3	6	0	-0.326646	-1.142821	-0.307092
4	6	0	-1.553176	-0.458020	0.281255
5	6	0	-1.749832	0.958576	-0.234022
6	1	0	0.671985	1.449550	-1.572823
7	1	0	1.559296	2.132953	-0.194499
8	1	0	-0.483442	1.924832	1.235304
9	1	0	-0.825739	2.905642	-0.186561
10	1	0	-0.443344	-1.200760	-1.396461
11	1	0	-0.228677	-2.158090	0.089256
12	1	0	-1.861971	0.918712	-1.325619
13	1	0	-2.687417	1.345867	0.176945
14	15	0	1.167542	-0.202512	0.126982
15	8	0	1.534222	-0.265598	1.563770
16	8	0	2.351263	-0.775686	-0.835620
17	1	0	2.143325	-0.748187	-1.775860
18	1	0	-1.496714	-0.462509	1.375046
19	9	0	-2.680973	-1.216040	-0.066225

**7-cis-a\_s**

Standard orientation:

Center Number	Atomic Number	Atomic Type	Coordinates (Angstroms)		
			X	Y	Z
1	6	0	-0.546903	1.877245	0.176121
2	6	0	0.766165	1.459485	-0.506833
3	6	0	-0.339304	-1.141771	-0.392840
4	6	0	-1.527691	-0.457145	0.267164
5	6	0	-1.727881	0.973259	-0.203422
6	1	0	0.673271	1.529304	-1.597378
7	1	0	1.597502	2.103417	-0.202568
8	1	0	-0.410064	1.865930	1.263492
9	1	0	-0.782489	2.907921	-0.106537
10	1	0	-0.505524	-1.192609	-1.475169
11	1	0	-0.223066	-2.163000	-0.017367
12	1	0	-1.867206	0.967839	-1.292255
13	1	0	-2.650119	1.356503	0.244382
14	15	0	1.211440	-0.246517	-0.114437
15	8	0	2.427160	-0.809230	-0.762731
16	8	0	1.280799	-0.207575	1.523344
17	1	0	2.123252	-0.565554	1.827550
18	9	0	-2.679219	-1.195217	-0.045617
19	1	0	-1.424182	-0.487042	1.356903

**8-cis-g**

Standard orientation:

Center Number	Atomic Number	Atomic Type	Coordinates (Angstroms)		
			X	Y	Z
1	6	0	0.682637	1.558726	-0.540293
2	6	0	-0.682217	1.564116	0.165370
3	6	0	0.057400	-1.018498	1.016472
4	6	0	1.400029	-0.719773	0.353730
5	6	0	1.731032	0.762042	0.243085
6	1	0	-0.585329	1.970753	1.181313
7	1	0	-1.407847	2.178402	-0.377536
8	1	0	0.579157	1.133887	-1.544452
9	1	0	1.031407	2.589250	-0.661484
10	1	0	0.117520	-0.726261	2.073451
11	1	0	-0.145005	-2.093196	0.972398
12	1	0	2.195292	-1.240634	0.897962
13	1	0	1.833513	1.169579	1.258117
14	1	0	2.708029	0.851222	-0.243047
15	15	0	-1.352507	-0.123365	0.269424
16	8	0	-1.925710	-0.684343	-0.992476
17	9	0	1.388285	-1.258794	-0.937554
18	1	0	-2.261296	-0.058321	1.349531

**8-trans-g**

Standard orientation:

Center Number	Atomic Number	Atomic Type	Coordinates (Angstroms)		
			X	Y	Z
1	6	0	0.899176	1.597426	-0.276404
2	6	0	-0.605361	1.523923	0.030851
3	6	0	-0.057751	-1.174756	0.655831
4	6	0	1.398672	-0.809815	0.390177
5	6	0	1.726848	0.659224	0.607922
6	1	0	-0.801585	1.785491	1.078049
7	1	0	-1.174871	2.223031	-0.590591
8	1	0	1.080024	1.350209	-1.328501
9	1	0	1.245722	2.625822	-0.131654
10	1	0	-0.276359	-1.048085	1.723254
11	1	0	-0.232821	-2.226288	0.408266
12	1	0	2.056204	-1.439313	0.998393
13	1	0	1.559684	0.894058	1.667432
14	1	0	2.793534	0.802635	0.406472
15	15	0	-1.269426	-0.144690	-0.239197
16	9	0	1.686780	-1.125672	-0.950306
17	1	0	-0.956054	-0.376695	-1.593370
18	8	0	-2.700327	-0.383185	0.131587

***8-trans-a***

Standard orientation:

Center Number	Atomic Number	Atomic Type	Coordinates (Angstroms)		
			X	Y	Z
1	6	0	0.014798	1.802801	0.358638
2	6	0	1.145100	1.266004	-0.535691
3	6	0	-0.355670	-1.104969	-0.571478
4	6	0	-1.339377	-0.345374	0.306556
5	6	0	-1.339994	1.151887	0.045354
6	1	0	0.914692	1.444124	-1.594263
7	1	0	2.096230	1.756396	-0.304978
8	1	0	0.271965	1.632561	1.411103
9	1	0	-0.069280	2.885446	0.223066
10	1	0	-0.611459	-0.943424	-1.626245
11	1	0	-0.406687	-2.176787	-0.357515
12	1	0	-1.606241	1.321157	-1.006193
13	1	0	-2.123989	1.606615	0.659059
14	15	0	1.343166	-0.519340	-0.261706
15	8	0	1.917601	-0.907846	1.066010
16	1	0	2.061869	-0.976671	-1.386755
17	9	0	-2.625222	-0.841268	0.043985
18	1	0	-1.137550	-0.547224	1.364102

***8-cis-a***

Standard orientation:

Center Number	Atomic Number	Atomic Type	Coordinates (Angstroms)		
			X	Y	Z
1	6	0	-0.386919	1.867951	0.214521
2	6	0	0.982195	1.394393	-0.299399
3	6	0	-0.192190	-1.169512	-0.171557
4	6	0	-1.433921	-0.430534	0.302841
5	6	0	-1.543237	0.976816	-0.256925
6	1	0	1.006020	1.397727	-1.395745
7	1	0	1.787077	2.051015	0.046800
8	1	0	-0.380455	1.906050	1.312115
9	1	0	-0.560961	2.892588	-0.127908
10	1	0	-0.223862	-1.271495	-1.262682
11	1	0	-0.155154	-2.176037	0.256863
12	1	0	-1.555930	0.919832	-1.352594
13	1	0	-2.499635	1.402531	0.062489
14	15	0	1.354913	-0.298504	0.242305
15	1	0	1.264477	-0.179166	1.648777
16	8	0	2.616303	-0.927280	-0.257916
17	9	0	-2.558183	-1.164870	-0.099456
18	1	0	-1.467615	-0.398092	1.398860

**9-cis-g**

Standard orientation:

Center Number	Atomic Number	Atomic Type	Coordinates (Angstroms)		
			X	Y	Z
1	6	0	-1.104203	1.563391	0.424834
2	6	0	0.386955	1.582060	0.055077
3	6	0	-0.102125	-1.033790	-0.876927
4	6	0	-1.568742	-0.741213	-0.567004
5	6	0	-1.928632	0.738174	-0.568607
6	1	0	0.520946	1.972731	-0.962484
7	1	0	0.956352	2.218338	0.741538
8	1	0	-1.227928	1.150471	1.431750
9	1	0	-1.488245	2.588532	0.445655
10	1	0	0.083447	-0.777852	-1.928247
11	1	0	0.092103	-2.103918	-0.748176
12	1	0	-2.202961	-1.279141	-1.280546
13	1	0	-1.788817	1.125644	-1.587249
14	1	0	-2.994559	0.823020	-0.332281
15	15	0	1.080666	-0.098579	0.165253
16	8	0	1.262292	-0.607198	1.563114
17	9	0	-1.871804	-1.261186	0.695647
18	6	0	2.613232	-0.075263	-0.809016
19	1	0	3.348993	0.539106	-0.283110
20	1	0	3.003480	-1.094384	-0.876917
21	1	0	2.456181	0.324248	-1.814602

**9-trans-g**

Standard orientation:

Center Number	Atomic Number	Atomic Type	Coordinates (Angstroms)		
			X	Y	Z
1	6	0	-1.078975	1.496624	0.609919
2	6	0	0.386566	1.601641	0.160880
3	6	0	-0.112754	-0.897599	-1.071872
4	6	0	-1.547041	-0.699115	-0.595198
5	6	0	-1.950718	0.754951	-0.408133
6	1	0	0.455032	2.151941	-0.786103
7	1	0	0.990914	2.150512	0.892076
8	1	0	-1.146360	0.990934	1.579145
9	1	0	-1.482336	2.504409	0.756122
10	1	0	-0.029729	-0.525050	-2.100548
11	1	0	0.130324	-1.965225	-1.096600
12	1	0	-2.236071	-1.196106	-1.285981
13	1	0	-1.892563	1.253165	-1.384980
14	1	0	-2.999008	0.779724	-0.092075
15	15	0	1.183125	-0.009273	-0.132263
16	9	0	-1.703842	-1.355825	0.641216
17	8	0	2.497018	0.055299	-0.854066
18	6	0	1.279588	-0.808764	1.490980
19	1	0	1.676450	-1.818267	1.354727
20	1	0	1.979625	-0.242368	2.111331
21	1	0	0.305289	-0.870972	1.978966

**9-trans-a**

Standard orientation:

Center Number	Atomic Number	Atomic Type	Coordinates (Angstroms)		
			X	Y	Z
1	6	0	-0.683241	1.883421	0.091829
2	6	0	0.676188	1.473008	-0.498448
3	6	0	-0.309636	-1.145118	-0.290051
4	6	0	-1.565987	-0.492098	0.265293
5	6	0	-1.804367	0.904437	-0.285414
6	1	0	0.618388	1.426254	-1.593631
7	1	0	1.454660	2.194188	-0.226622
8	1	0	-0.597979	1.944213	1.183423
9	1	0	-0.947997	2.883557	-0.265578
10	1	0	-0.394049	-1.218385	-1.381306
11	1	0	-0.194898	-2.152511	0.123254
12	1	0	-1.895007	0.836615	-1.377619
13	1	0	-2.762521	1.266494	0.100962
14	15	0	1.155499	-0.153277	0.164070
15	8	0	1.448618	-0.150072	1.636783
16	9	0	-2.664240	-1.296689	-0.079603
17	1	0	-1.526505	-0.468781	1.359506
18	6	0	2.507712	-0.766836	-0.874205
19	1	0	3.389183	-0.141747	-0.708693
20	1	0	2.747602	-1.789637	-0.572002
21	1	0	2.241848	-0.751221	-1.934602

**9-cis-a**

Standard orientation:

Center Number	Atomic Number	Atomic Type	Coordinates (Angstroms)		
			X	Y	Z
1	6	0	-0.601178	1.880797	0.192376
2	6	0	0.718723	1.481626	-0.485966
3	6	0	-0.352183	-1.133176	-0.377168
4	6	0	-1.548396	-0.464289	0.279763
5	6	0	-1.768628	0.962349	-0.190925
6	1	0	0.623270	1.565219	-1.575693
7	1	0	1.538681	2.143552	-0.185603
8	1	0	-0.481422	1.884954	1.283172
9	1	0	-0.850154	2.908276	-0.092027
10	1	0	-0.525974	-1.191104	-1.458339
11	1	0	-0.230520	-2.157198	-0.008357
12	1	0	-1.900162	0.954504	-1.280386
13	1	0	-2.699318	1.332822	0.250675
14	15	0	1.224335	-0.236022	-0.154556
15	8	0	2.351392	-0.749707	-0.998284
16	9	0	-2.691919	-1.217700	-0.027779
17	1	0	-1.458223	-0.488649	1.372503
18	6	0	1.563777	-0.305431	1.628382
19	1	0	1.755294	-1.345822	1.904505
20	1	0	2.466547	0.277005	1.831605
21	1	0	0.740412	0.082470	2.233809

**PFgauche**

Standard orientation:

Center Number	Atomic Number	Atomic Type	Coordinates (Angstroms)		
			X	Y	Z
1	6	0	1.352425	0.417425	0.269911
2	1	0	2.192904	0.977702	-0.139742
3	1	0	1.403504	0.407783	1.360827
4	6	0	0.025933	0.988110	-0.233707
5	1	0	0.059177	1.176410	-1.311116
6	1	0	-0.229739	1.922029	0.276726
7	1	0	-1.293577	-0.666895	1.367740
8	1	0	-2.548459	0.359234	-0.185544
9	1	0	-1.181499	-1.320509	-0.780394
10	15	0	-1.301501	-0.213132	0.051085
11	9	0	1.427783	-0.899109	-0.174666

**PFanti**

Standard orientation:

Center Number	Atomic Number	Atomic Type	Coordinates (Angstroms)		
			X	Y	Z
1	6	0	-1.136085	-0.512187	0.000003
2	1	0	-1.077161	-1.137049	-0.895520
3	1	0	-1.077180	-1.137026	0.895543
4	6	0	-0.056179	0.579244	-0.000002
5	1	0	-0.163928	1.212396	0.886764
6	1	0	-0.163966	1.212369	-0.886773
7	1	0	1.876100	-0.858350	-1.120466
8	1	0	2.562513	0.962625	-0.000556
9	1	0	1.876434	-0.857439	1.121018
10	15	0	1.627880	-0.069258	0.000000
11	9	0	-2.344159	0.137667	-0.000002

**PPanti**

Standard orientation:

Center Number	Atomic Number	Atomic Type	Coordinates (Angstroms)		
			X	Y	Z
1	6	0	0.529551	0.562179	0.000013
2	1	0	0.441306	1.203928	-0.884349
3	1	0	0.441502	1.204099	0.884268
4	6	0	-0.529551	-0.562179	0.000013
5	1	0	-0.441502	-1.204100	0.884268
6	1	0	-0.441307	-1.203927	-0.884349
7	1	0	-2.497332	0.834344	-1.130833
8	1	0	-3.126954	-1.030161	-0.000869
9	1	0	-2.497729	0.832807	1.131481
10	1	0	3.126953	1.030162	-0.000868
11	1	0	2.497728	-0.832807	1.131481
12	1	0	2.497334	-0.834344	-1.130833
13	15	0	2.253136	-0.056414	0.000015
14	15	0	-2.253136	0.056414	0.000015

## Standard coordinates of the compounds in implicit DMSO

***1-cis-g***

Standard orientation:

Center Number	Atomic Number	Atomic Type	Coordinates (Angstroms)		
			X	Y	Z
1	6	0	-0.031420	1.656950	-0.303993
2	6	0	-1.389627	1.049218	0.056423
3	6	0	0.095675	-1.247651	0.712950
4	6	0	1.313364	-0.403315	0.373416
5	6	0	1.112002	1.092168	0.542935
6	1	0	-1.636975	1.274906	1.101836
7	1	0	-2.181796	1.491607	-0.557777
8	1	0	0.179815	1.476995	-1.364433
9	1	0	-0.066817	2.743938	-0.164316
10	1	0	-0.082649	-1.166247	1.792026
11	1	0	0.316455	-2.300132	0.506366
12	1	0	0.918428	1.282064	1.606867
13	1	0	2.051078	1.595924	0.290194
14	15	0	-1.485858	-0.790771	-0.147257
15	9	0	1.667766	-0.649343	-0.976489
16	1	0	2.171659	-0.737948	0.965042
17	1	0	-0.991185	-0.839671	-1.468928

***1-trans-g***

Standard orientation:

Center Number	Atomic Number	Atomic Type	Coordinates (Angstroms)		
			X	Y	Z
1	6	0	-0.023528	1.657029	-0.314881
2	6	0	-1.375698	1.057347	0.096228
3	6	0	0.065096	-1.215460	0.751451
4	6	0	1.305450	-0.415216	0.382285
5	6	0	1.139614	1.090221	0.506170
6	1	0	-1.537754	1.213176	1.169241
7	1	0	-2.188301	1.551500	-0.445818
8	1	0	0.157352	1.472580	-1.380873
9	1	0	-0.048994	2.743942	-0.181552
10	1	0	-0.154713	-1.017267	1.806341
11	1	0	0.279405	-2.283015	0.643002
12	1	0	0.987842	1.317614	1.569162
13	1	0	2.079748	1.564169	0.204708
14	15	0	-1.388415	-0.752182	-0.320311
15	1	0	-2.398446	-1.174767	0.570156
16	9	0	1.647478	-0.710973	-0.962122
17	1	0	2.157170	-0.749960	0.981872

***1-trans-a***

Standard orientation:

Center Number	Atomic Number	Atomic Type	Coordinates (Angstroms)		
			X	Y	Z
1	6	0	0.579951	1.664915	0.255287
2	6	0	1.652691	0.745176	-0.334017
3	6	0	-0.357477	-1.224960	-0.283564
4	6	0	-1.205207	-0.121984	0.310590
5	6	0	-0.836024	1.265616	-0.174985
6	1	0	1.652313	0.821322	-1.428744
7	1	0	2.648072	1.054881	0.003598
8	1	0	0.644224	1.646200	1.350809
9	1	0	0.767323	2.698491	-0.058391
10	1	0	-0.476790	-1.227874	-1.373469
11	1	0	-0.692258	-2.197754	0.090999
12	1	0	-0.916460	1.288379	-1.269411
13	1	0	-1.562595	1.978634	0.228545
14	15	0	1.455362	-1.048030	0.089169
15	1	0	1.318173	-0.876450	1.486627
16	1	0	-1.175709	-0.163660	1.404961
17	9	0	-2.560037	-0.363810	-0.045881

**1-cis-a**

Standard orientation:

Center Number	Atomic Number	Atomic Type	Coordinates (Angstroms)		
			X	Y	Z
1	6	0	-0.565996	1.664527	-0.246967
2	6	0	-1.627719	0.751362	0.382063
3	6	0	0.327272	-1.210476	0.308828
4	6	0	1.208039	-0.143581	-0.309798
5	6	0	0.862123	1.262039	0.145941
6	1	0	-1.525305	0.762838	1.473085
7	1	0	-2.629815	1.112651	0.129817
8	1	0	-0.661423	1.648082	-1.340880
9	1	0	-0.738742	2.698421	0.069468
10	1	0	0.387947	-1.137268	1.399933
11	1	0	0.678309	-2.199723	-0.000800
12	1	0	0.974611	1.309848	1.236385
13	1	0	1.580703	1.960068	-0.295879
14	15	0	-1.425028	-0.969388	-0.283241
15	9	0	2.551498	-0.406877	0.061201
16	1	0	1.185261	-0.207648	-1.403689
17	1	0	-2.061932	-1.687779	0.749963

**2-cis-g**

Standard orientation:

Center Number	Atomic Number	Atomic Type	Coordinates (Angstroms)		
			X	Y	Z
1	6	0	-0.624771	1.522482	0.665715
2	6	0	0.694070	1.593626	-0.110129
3	6	0	-0.105614	-0.898237	-1.161842
4	6	0	-1.396801	-0.667641	-0.391076
5	6	0	-1.718988	0.789898	-0.114386
6	1	0	0.538465	2.156206	-1.040033
7	1	0	1.451468	2.141437	0.463507
8	1	0	-0.475378	1.031058	1.632970
9	1	0	-0.970659	2.539769	0.883365
10	1	0	-0.281736	-0.560688	-2.191490
11	1	0	0.095232	-1.974243	-1.218719
12	1	0	-1.879189	1.283181	-1.082388
13	1	0	-2.667716	0.833366	0.431347
14	15	0	1.435431	-0.039204	-0.579556
15	6	0	1.711245	-0.797096	1.081691
16	1	0	1.962904	-1.853737	0.947794
17	1	0	2.573917	-0.305771	1.542433
18	1	0	0.853448	-0.725436	1.751285
19	9	0	-1.317580	-1.343977	0.853091
20	1	0	-2.228847	-1.139472	-0.924404

**2-trans-g**

Standard orientation:

Center Number	Atomic Number	Atomic Type	Coordinates (Angstroms)		
			X	Y	Z
1	6	0	0.936243	1.622470	-0.227148
2	6	0	-0.579960	1.490213	-0.024830
3	6	0	-0.075331	-1.147283	0.588310
4	6	0	1.399882	-0.803602	0.442968
5	6	0	1.725652	0.663220	0.669764
6	1	0	-0.825767	1.634281	1.036746
7	1	0	-1.109391	2.257063	-0.600935
8	1	0	1.189941	1.434856	-1.277441
9	1	0	1.249998	2.648099	-0.003952
10	1	0	-0.367225	-0.925020	1.623666
11	1	0	-0.215147	-2.220516	0.421239
12	1	0	1.516691	0.886387	1.724063
13	1	0	2.801343	0.802401	0.517417
14	15	0	-1.147795	-0.180909	-0.582907
15	9	0	1.815547	-1.151344	-0.867999
16	1	0	1.997735	-1.427481	1.114399
17	6	0	-2.754462	-0.318634	0.310376
18	1	0	-3.491372	0.336774	-0.163139
19	1	0	-3.125205	-1.345643	0.240922
20	1	0	-2.656743	-0.043784	1.365963

**2-trans-a**

Standard orientation:

Center Number	Atomic Number	Atomic Type	Coordinates (Angstroms)		
			X	Y	Z
1	6	0	0.039691	1.787966	0.409370
2	6	0	1.138933	1.290440	-0.535125
3	6	0	-0.390463	-1.069588	-0.663462
4	6	0	-1.309399	-0.342327	0.294054
5	6	0	-1.324154	1.160310	0.097862
6	1	0	0.908127	1.609377	-1.559864
7	1	0	2.103035	1.744831	-0.276431
8	1	0	0.306662	1.580270	1.452255
9	1	0	-0.044711	2.877384	0.322912
10	1	0	-0.742562	-0.892539	-1.687237
11	1	0	-0.435334	-2.149366	-0.482419
12	1	0	-1.607278	1.376421	-0.940673
13	1	0	-2.091364	1.589957	0.750594
14	15	0	1.391671	-0.544609	-0.592435
15	9	0	-2.630783	-0.825420	0.083050
16	1	0	-1.076202	-0.589510	1.334070
17	6	0	1.802302	-0.913992	1.171078
18	1	0	1.766390	-1.998013	1.317107
19	1	0	2.828737	-0.586880	1.362333
20	1	0	1.145022	-0.440872	1.903763

**2-cis-a**

Standard orientation:

Center Number	Atomic Number	Atomic Type	Coordinates (Angstroms)		
			X	Y	Z
1	6	0	0.511902	1.882936	-0.125408
2	6	0	-0.894086	1.405791	0.265664
3	6	0	0.139594	-1.141750	0.081199
4	6	0	1.442333	-0.466121	-0.295823
5	6	0	1.606926	0.907620	0.327405
6	1	0	-0.945185	1.257795	1.353127
7	1	0	-1.638955	2.160867	-0.008512
8	1	0	0.570773	2.017844	-1.213468
9	1	0	0.706119	2.861925	0.325244
10	1	0	0.067967	-1.198637	1.175249
11	1	0	0.119650	-2.157668	-0.327478
12	1	0	1.578747	0.797965	1.418940
13	1	0	2.592280	1.300548	0.055917
14	15	0	-1.295467	-0.177586	-0.604598
15	6	0	-2.642941	-0.838903	0.463858
16	1	0	-3.553116	-0.254190	0.302176
17	1	0	-2.854645	-1.875318	0.185385
18	1	0	-2.374132	-0.798977	1.524355
19	9	0	2.514466	-1.281963	0.151262
20	1	0	1.549932	-0.408145	-1.384702

**3axial**

Standard orientation:

Center Number	Atomic Number	Atomic Type	Coordinates (Angstroms)		
			X	Y	Z
1	6	0	0.045552	1.674447	-0.280697
2	6	0	-1.354476	1.120550	0.041739
3	6	0	0.106933	-1.286860	0.710951
4	6	0	1.330484	-0.441534	0.357283
5	6	0	1.155410	1.053188	0.575438
6	1	0	-1.627467	1.326745	1.081795
7	1	0	-2.122219	1.548184	-0.607540
8	1	0	0.269141	1.526596	-1.341859
9	1	0	0.022042	2.753090	-0.106842
10	1	0	-0.092904	-1.213819	1.784495
11	1	0	0.272078	-2.335970	0.456168
12	1	0	0.954774	1.219605	1.640622
13	1	0	2.106073	1.540988	0.342904
14	15	0	-1.354687	-0.671237	-0.157327
15	9	0	1.603738	-0.659179	-1.008264
16	1	0	2.189972	-0.817824	0.915316
17	1	0	-2.508105	-1.262391	0.346947
18	1	0	-1.280139	-1.002771	-1.506008

**3equatorial**

Standard orientation:

Center Number	Atomic Number	Atomic Type	Coordinates (Angstroms)		
			X	Y	Z
1	6	0	0.554428	1.675989	0.264301
2	6	0	1.666771	0.789361	-0.325156
3	6	0	-0.396129	-1.242516	-0.226730
4	6	0	-1.252593	-0.101930	0.322958
5	6	0	-0.850753	1.266718	-0.198344
6	1	0	1.676690	0.851054	-1.417903
7	1	0	2.654753	1.072606	0.046527
8	1	0	0.606000	1.663002	1.359213
9	1	0	0.750044	2.703980	-0.049746
10	1	0	-0.511062	-1.294043	-1.314450
11	1	0	-0.685733	-2.202555	0.207306
12	1	0	-0.903791	1.261412	-1.293671
13	1	0	-1.578220	1.995340	0.169673
14	15	0	1.352150	-0.931433	0.110896
15	9	0	-2.569743	-0.370819	-0.075164
16	1	0	-1.251333	-0.112028	1.417526
17	1	0	2.148880	-1.824340	-0.597713
18	1	0	1.608850	-1.131286	1.464099

**4axial**

Standard orientation:

Center Number	Atomic Number	Atomic Type	Coordinates (Angstroms)		
			X	Y	Z
1	6	0	-1.181666	1.485410	0.609360
2	6	0	0.307222	1.616461	0.242809
3	6	0	-0.121860	-0.888440	-1.092264
4	6	0	-1.573617	-0.698224	-0.655656
5	6	0	-1.993913	0.749281	-0.461467
6	1	0	0.422853	2.179527	-0.690398
7	1	0	0.873559	2.135580	1.022156
8	1	0	-1.291522	0.979413	1.573899
9	1	0	-1.586455	2.493156	0.735270
10	1	0	-0.001924	-0.484971	-2.103705
11	1	0	0.134446	-1.951525	-1.120136
12	1	0	-1.899630	1.260990	-1.427077
13	1	0	-3.053457	0.759718	-0.189470
14	15	0	1.046095	-0.009732	-0.020189
15	6	0	1.235982	-0.868713	1.548931
16	1	0	1.622171	-1.873202	1.361968
17	1	0	1.941054	-0.315537	2.173381
18	1	0	0.269693	-0.940592	2.049424
19	6	0	2.642906	0.114607	-0.834209
20	1	0	3.331132	0.667683	-0.191131
21	1	0	3.035697	-0.889080	-1.011581
22	1	0	2.526140	0.637919	-1.785333
23	9	0	-1.742238	-1.375503	0.570846
24	1	0	-2.225364	-1.195860	-1.377075

**4equatorial**

Standard orientation:

Center Number	Atomic Number	Atomic Type	Coordinates (Angstroms)		
			X	Y	Z
1	6	0	-0.747280	1.882857	0.109018
2	6	0	0.617100	1.526088	-0.508151
3	6	0	-0.351889	-1.162205	-0.278563
4	6	0	-1.601611	-0.492682	0.287693
5	6	0	-1.853548	0.892878	-0.278727
6	1	0	0.556894	1.541074	-1.602384
7	1	0	1.396136	2.230786	-0.201760
8	1	0	-0.666618	1.943777	1.200505
9	1	0	-1.021584	2.881707	-0.239909
10	1	0	-0.474013	-1.292740	-1.359873
11	1	0	-0.190613	-2.144336	0.175802
12	1	0	-1.932818	0.823168	-1.370239
13	1	0	-2.813025	1.249798	0.106407
14	15	0	1.119893	-0.138500	-0.022759
15	9	0	-2.686005	-1.322353	-0.041849
16	1	0	-1.565232	-0.459079	1.381245
17	6	0	1.591097	-0.166438	1.713219
18	1	0	1.828764	-1.193139	2.000572
19	1	0	2.469858	0.466995	1.854342
20	1	0	0.773986	0.203832	2.335225
21	6	0	2.475017	-0.754009	-1.025817
22	1	0	3.350971	-0.120331	-0.871375
23	1	0	2.705340	-1.778448	-0.724799
24	1	0	2.184295	-0.733322	-2.077762

(2-fluoroethyl)triphenylphosphonium anti  
Standard orientation:

Center Number	Atomic Number	Atomic Type	Coordinates (Angstroms)		
			X	Y	Z
1	15	0	0.029468	0.003461	0.425154
2	6	0	-1.078665	-1.193089	-0.318802
3	6	0	-1.439656	-2.344456	0.405883
4	6	0	-1.492865	-1.024664	-1.653207
5	6	0	-2.235456	-3.317507	-0.206407
6	1	0	-1.108250	-2.491333	1.430371
7	6	0	-2.282882	-2.010489	-2.253958
8	1	0	-1.199561	-0.142898	-2.216635
9	6	0	-2.657524	-3.151136	-1.532327
10	1	0	-2.523990	-4.202856	0.352575
11	1	0	-2.606077	-1.884240	-3.283145
12	1	0	-3.275439	-3.910756	-2.002640
13	6	0	-0.210837	1.594104	-0.372163
14	6	0	0.903903	2.352362	-0.770871
15	6	0	-1.518498	2.084397	-0.557318
16	6	0	0.703907	3.610514	-1.350300
17	1	0	1.911259	1.967274	-0.637496
18	6	0	-1.701478	3.343957	-1.135302
19	1	0	-2.384579	1.490313	-0.275790
20	6	0	-0.593268	4.107158	-1.528435
21	1	0	1.561929	4.198160	-1.663481
22	1	0	-2.707946	3.724864	-1.282107
23	1	0	-0.742178	5.084036	-1.979627
24	6	0	1.726349	-0.538550	0.212232
25	6	0	2.735780	-0.086982	1.082730
26	6	0	2.034359	-1.377289	-0.874670
27	6	0	4.058518	-0.483170	0.858400
28	1	0	2.505733	0.564038	1.921332
29	6	0	3.362475	-1.759430	-1.088308
30	1	0	1.251748	-1.730214	-1.541426
31	6	0	4.372200	-1.314361	-0.224898
32	1	0	4.840685	-0.141498	1.529965
33	1	0	3.605226	-2.408822	-1.924385
34	1	0	5.401459	-1.618135	-0.393355
35	6	0	-0.308563	0.135977	2.205072
36	1	0	-0.079591	-0.835309	2.656755
37	1	0	0.393807	0.872653	2.607969
38	6	0	-1.735438	0.552111	2.538352
39	1	0	-1.953240	1.564523	2.194355
40	1	0	-2.471890	-0.149423	2.141132
41	9	0	-1.857253	0.546773	3.930455

(2-fluoroethyl)triphenylphosphonium *gauche*

Standard orientation:

Center Number	Atomic Number	Atomic Type	Coordinates (Angstroms)		
			X	Y	Z
1	15	0	0.080259	0.017058	0.543760
2	6	0	-0.834461	-1.351885	-0.166657
3	6	0	-0.955643	-2.559139	0.544632
4	6	0	-1.316962	-1.243101	-1.484079
5	6	0	-1.583491	-3.651438	-0.061911
6	1	0	-0.571815	-2.657188	1.555901
7	6	0	-1.938999	-2.345941	-2.078962
8	1	0	-1.205301	-0.316020	-2.039891
9	6	0	-2.074443	-3.546551	-1.370433
10	1	0	-1.686719	-4.582780	0.487314
11	1	0	-2.315741	-2.264871	-3.094491
12	1	0	-2.561548	-4.398595	-1.836166
13	6	0	-0.464132	1.535161	-0.245683
14	6	0	0.474455	2.448962	-0.755640
15	6	0	-1.846157	1.796920	-0.332684
16	6	0	0.023091	3.636641	-1.342737
17	1	0	1.538864	2.238126	-0.702722
18	6	0	-2.279978	2.989638	-0.918473
19	1	0	-2.570970	1.079673	0.043881
20	6	0	-1.348446	3.908461	-1.421763
21	1	0	0.744149	4.344578	-1.741012
22	1	0	-3.344061	3.196384	-0.987826
23	1	0	-1.692039	4.831992	-1.879166
24	6	0	1.832656	-0.239681	0.241874
25	6	0	2.794339	0.505836	0.950711
26	6	0	2.226882	-1.155942	-0.750668
27	6	0	4.150961	0.327065	0.661030
28	1	0	2.503815	1.223959	1.712675
29	6	0	3.587340	-1.321823	-1.030432
30	1	0	1.485246	-1.733782	-1.295683
31	6	0	4.547689	-0.583646	-0.327011
32	1	0	4.894512	0.898887	1.208542
33	1	0	3.894473	-2.030954	-1.793657
34	1	0	5.603006	-0.718494	-0.546514
35	6	0	-0.175472	0.126727	2.344075
36	1	0	0.009704	-0.863652	2.770575
37	1	0	0.592887	0.803877	2.733050
38	6	0	-1.537159	0.661101	2.754239
39	1	0	-1.693048	1.683892	2.406230
40	9	0	-2.542421	-0.137055	2.194053
41	1	0	-1.639935	0.618413	3.839511

*7-cis-g\_s*

Standard orientation:

Center Number	Atomic Number	Atomic Type	Coordinates (Angstroms)		
			X	Y	Z
1	6	0	-1.069803	1.558332	0.470139
2	6	0	0.419257	1.580101	0.082249
3	6	0	-0.100687	-1.017315	-0.921119
4	6	0	-1.553284	-0.734678	-0.545565
5	6	0	-1.917583	0.740922	-0.510707
6	1	0	0.545669	1.994836	-0.924158
7	1	0	1.006918	2.187029	0.778245
8	1	0	-1.185592	1.154636	1.481734
9	1	0	-1.443486	2.586008	0.493479
10	1	0	0.047870	-0.717288	-1.964358
11	1	0	0.110121	-2.088128	-0.841028
12	1	0	-2.215432	-1.273819	-1.227941
13	1	0	-1.804479	1.138728	-1.527008
14	1	0	-2.976331	0.822953	-0.245226
15	15	0	1.081915	-0.091957	0.098063
16	8	0	1.339493	-0.688880	1.449401
17	9	0	-1.792204	-1.276583	0.737266
18	8	0	2.420289	0.055111	-0.819894
19	1	0	3.070193	-0.630358	-0.616107

***7-cis-g\_a***

Standard orientation:

Center Number	Atomic Number	Atomic Type	Coordinates (Angstroms)		
			X	Y	Z
1	6	0	-1.066418	1.564290	0.457442
2	6	0	0.423337	1.581597	0.069424
3	6	0	-0.092987	-1.021410	-0.915525
4	6	0	-1.547454	-0.734946	-0.546100
5	6	0	-1.913092	0.740426	-0.518669
6	1	0	0.541470	1.993629	-0.939921
7	1	0	1.010173	2.196989	0.758815
8	1	0	-1.181655	1.168029	1.471901
9	1	0	-1.439122	2.592585	0.472991
10	1	0	0.050241	-0.735674	-1.964220
11	1	0	0.115698	-2.091825	-0.826082
12	1	0	-2.206603	-1.277203	-1.228887
13	1	0	-1.801176	1.133466	-1.537042
14	1	0	-2.971981	0.821994	-0.253619
15	15	0	1.084636	-0.095640	0.108814
16	8	0	1.318491	-0.652554	1.477325
17	9	0	-1.790112	-1.272175	0.737227
18	8	0	2.490140	-0.091374	-0.713224
19	1	0	2.435049	0.253873	-1.613433

***7-cis-g\_s'***

Standard orientation:

Center Number	Atomic Number	Atomic Type	Coordinates (Angstroms)		
			X	Y	Z
1	6	0	-1.084499	1.568201	0.421525
2	6	0	0.402948	1.589755	0.025625
3	6	0	-0.089317	-1.043393	-0.888308
4	6	0	-1.543212	-0.761551	-0.519715
5	6	0	-1.925561	0.709851	-0.529626
6	1	0	0.517593	1.966452	-0.996971
7	1	0	0.986731	2.230404	0.694325
8	1	0	-1.192483	1.196599	1.446133
9	1	0	-1.468616	2.592392	0.411384
10	1	0	0.061453	-0.775676	-1.940053
11	1	0	0.131509	-2.108760	-0.773420
12	1	0	-2.201563	-1.329858	-1.181528
13	1	0	-1.821528	1.076683	-1.558574
14	1	0	-2.984453	0.786196	-0.262900
15	15	0	1.080766	-0.080127	0.099701
16	8	0	1.350800	-0.572462	1.490213
17	9	0	-1.769600	-1.265343	0.781272
18	8	0	2.389021	-0.107678	-0.871657
19	1	0	3.205540	0.019497	-0.370809

**7-trans-g\_g**

Standard orientation:

Center Number	Atomic Number	Atomic Type	Coordinates (Angstroms)		
			X	Y	Z
1	6	0	-0.997829	1.575344	0.455954
2	6	0	0.477316	1.595298	0.023574
3	6	0	-0.108478	-1.037710	-0.925370
4	6	0	-1.548425	-0.711134	-0.534946
5	6	0	-1.876414	0.772512	-0.508630
6	1	0	0.577688	2.054495	-0.966916
7	1	0	1.091663	2.177623	0.719179
8	1	0	-1.084784	1.159513	1.464786
9	1	0	-1.365464	2.604961	0.499959
10	1	0	0.008910	-0.827020	-1.994675
11	1	0	0.093688	-2.102877	-0.776841
12	1	0	-2.226816	-1.237151	-1.212056
13	1	0	-1.765483	1.160505	-1.529195
14	1	0	-2.930224	0.880493	-0.232916
15	15	0	1.168676	-0.067099	-0.091165
16	9	0	-1.797811	-1.240407	0.748806
17	8	0	2.527512	-0.147537	-0.719625
18	8	0	1.084670	-0.681946	1.414896
19	1	0	1.676521	-0.230384	2.031229

**7-trans-g\_a**

Standard orientation:

Center Number	Atomic Number	Atomic Type	Coordinates (Angstroms)		
			X	Y	Z
1	6	0	-1.041578	1.553169	0.484060
2	6	0	0.437010	1.611435	0.061851
3	6	0	-0.064372	-0.949500	-1.052219
4	6	0	-1.496275	-0.726426	-0.575360
5	6	0	-1.907656	0.731877	-0.477921
6	1	0	0.535920	2.095532	-0.916798
7	1	0	1.031650	2.185057	0.780428
8	1	0	-1.123524	1.143798	1.496613
9	1	0	-1.434466	2.573118	0.527625
10	1	0	0.018117	-0.600896	-2.087508
11	1	0	0.181261	-2.015929	-1.035736
12	1	0	-2.191372	-1.287797	-1.202716
13	1	0	-1.855939	1.156609	-1.488180
14	1	0	-2.954471	0.773054	-0.161368
15	15	0	1.161267	-0.032658	-0.079719
16	9	0	-1.606188	-1.301639	0.724677
17	8	0	2.563026	-0.082603	-0.598224
18	8	0	1.069323	-0.675131	1.413966
19	1	0	0.207937	-1.079373	1.592930

**7-trans-g\_g'**

Standard orientation:

Center Number	Atomic Number	Atomic Type	Coordinates (Angstroms)		
			X	Y	Z
1	6	0	-1.011759	1.573141	0.433475
2	6	0	0.462526	1.601220	-0.004582
3	6	0	-0.095130	-1.037101	-0.937224
4	6	0	-1.535162	-0.735450	-0.530909
5	6	0	-1.888286	0.742569	-0.509449
6	1	0	0.554232	2.038017	-1.005784
7	1	0	1.074054	2.200678	0.677639
8	1	0	-1.087537	1.178177	1.451093
9	1	0	-1.390121	2.599527	0.456812
10	1	0	0.014789	-0.813296	-2.004828
11	1	0	0.118476	-2.102800	-0.805439
12	1	0	-2.215121	-1.276304	-1.194718
13	1	0	-1.799928	1.121654	-1.535545
14	1	0	-2.939785	0.835599	-0.219573
15	15	0	1.167838	-0.050719	-0.086159
16	9	0	-1.753675	-1.264892	0.759781
17	8	0	2.526571	-0.185797	-0.704973
18	8	0	1.097100	-0.455600	1.488758
19	1	0	1.353950	-1.371530	1.656547

**7-trans-a\_s**

Standard orientation:

Center Number	Atomic Number	Atomic Type	Coordinates (Angstroms)		
			X	Y	Z
1	6	0	-0.610282	1.883682	0.184828
2	6	0	0.740821	1.474026	-0.429222
3	6	0	-0.330214	-1.138497	-0.316121
4	6	0	-1.558578	-0.462852	0.276162
5	6	0	-1.760841	0.954426	-0.229213
6	1	0	0.685430	1.489898	-1.523294
7	1	0	1.542397	2.149551	-0.115204
8	1	0	-0.529377	1.903279	1.278274
9	1	0	-0.846641	2.902254	-0.134313
10	1	0	-0.428595	-1.179095	-1.406344
11	1	0	-0.221669	-2.156494	0.070324
12	1	0	-1.848645	0.929913	-1.322548
13	1	0	-2.703415	1.335466	0.175546
14	15	0	1.159732	-0.192078	0.101493
15	8	0	1.566626	-0.340579	1.537399
16	8	0	2.295770	-0.640302	-0.970605
17	1	0	2.864654	-1.339817	-0.622454
18	1	0	-1.518439	-0.476804	1.370104
19	9	0	-2.686253	-1.232737	-0.082828

**7-trans-a\_a**

Standard orientation:

Center Number	Atomic Number	Atomic Type	Coordinates (Angstroms)		
			X	Y	Z
1	6	0	-0.605110	1.888742	0.155076
2	6	0	0.745548	1.466377	-0.452477
3	6	0	-0.327744	-1.143344	-0.292963
4	6	0	-1.556412	-0.453877	0.284067
5	6	0	-1.756624	0.954830	-0.244726
6	1	0	0.685136	1.476140	-1.546984
7	1	0	1.547664	2.146074	-0.148514
8	1	0	-0.523350	1.925448	1.247853
9	1	0	-0.839277	2.902583	-0.180718
10	1	0	-0.434105	-1.212002	-1.381731
11	1	0	-0.221345	-2.152696	0.115918
12	1	0	-1.844092	0.912847	-1.337574
13	1	0	-2.699007	1.343227	0.153325
14	15	0	1.163845	-0.194602	0.111017
15	8	0	1.570809	-0.285272	1.548027
16	8	0	2.351635	-0.769874	-0.835948
17	1	0	2.164232	-0.745378	-1.783337
18	1	0	-1.517809	-0.450247	1.378062
19	9	0	-2.683692	-1.229128	-0.063560

**7-trans-a\_s'**

Standard orientation:

Center Number	Atomic Number	Atomic Type	Coordinates (Angstroms)		
			X	Y	Z
1	6	0	-0.618304	1.890192	0.142841
2	6	0	0.730883	1.469576	-0.468375
3	6	0	-0.323853	-1.145078	-0.282123
4	6	0	-1.554098	-0.457232	0.292826
5	6	0	-1.764874	0.945902	-0.246920
6	1	0	0.666504	1.457759	-1.562103
7	1	0	1.531045	2.157590	-0.178056
8	1	0	-0.533230	1.934110	1.235206
9	1	0	-0.860290	2.900228	-0.198929
10	1	0	-0.422851	-1.219247	-1.370590
11	1	0	-0.209403	-2.150090	0.134653
12	1	0	-1.854214	0.894499	-1.339169
13	1	0	-2.709230	1.330640	0.150201
14	15	0	1.160458	-0.186444	0.101942
15	8	0	1.602081	-0.242793	1.534312
16	8	0	2.227535	-0.806988	-0.956124
17	1	0	3.138175	-0.707736	-0.648000
18	1	0	-1.512365	-0.442485	1.386796
19	9	0	-2.677385	-1.242280	-0.043793

***7-cis-a\_g***

Standard orientation:

Center Number	Atomic Number	Atomic Type	Coordinates (Angstroms)		
			X	Y	Z
1	6	0	-0.524045	1.887160	0.171787
2	6	0	0.799477	1.456169	-0.481713
3	6	0	-0.344514	-1.148781	-0.365607
4	6	0	-1.529940	-0.434127	0.266879
5	6	0	-1.705193	0.990710	-0.224798
6	1	0	0.732278	1.535596	-1.572932
7	1	0	1.629727	2.091911	-0.155689
8	1	0	-0.415142	1.889019	1.262056
9	1	0	-0.744656	2.915051	-0.129848
10	1	0	-0.497439	-1.213336	-1.448642
11	1	0	-0.240195	-2.162923	0.031690
12	1	0	-1.816629	0.977087	-1.316291
13	1	0	-2.629579	1.391743	0.202012
14	15	0	1.206575	-0.260171	-0.100687
15	8	0	2.405287	-0.812267	-0.807918
16	8	0	1.266587	-0.339043	1.526776
17	1	0	2.012701	0.145008	1.904674
18	9	0	-2.691457	-1.167174	-0.063854
19	1	0	-1.456282	-0.458338	1.357807

***7-cis-a\_g'***

Standard orientation:

Center Number	Atomic Number	Atomic Type	Coordinates (Angstroms)		
			X	Y	Z
1	6	0	-0.536834	1.884171	0.160313
2	6	0	0.792008	1.455755	-0.484605
3	6	0	-0.342120	-1.153704	-0.357280
4	6	0	-1.529876	-0.440046	0.271124
5	6	0	-1.712423	0.979104	-0.233496
6	1	0	0.727181	1.527624	-1.576309
7	1	0	1.619210	2.093257	-0.156813
8	1	0	-0.430593	1.894927	1.250405
9	1	0	-0.761156	2.908152	-0.151547
10	1	0	-0.496572	-1.230470	-1.439534
11	1	0	-0.237290	-2.166397	0.045564
12	1	0	-1.820954	0.955778	-1.325105
13	1	0	-2.639746	1.379196	0.187809
14	15	0	1.209613	-0.251244	-0.100659
15	8	0	2.385214	-0.846409	-0.811375
16	8	0	1.367370	-0.136126	1.517575
17	1	0	1.502657	-0.989720	1.949896
18	9	0	-2.688636	-1.182725	-0.047004
19	1	0	-1.454405	-0.450575	1.362613

**8-cis-g**

Standard orientation:

Center Number	Atomic Number	Atomic Type	Coordinates (Angstroms)		
			X	Y	Z
1	6	0	0.679548	1.565467	-0.539846
2	6	0	-0.692101	1.565453	0.153771
3	6	0	0.053168	-1.013277	1.028338
4	6	0	1.392320	-0.715736	0.362386
5	6	0	1.725216	0.762417	0.240886
6	1	0	-0.605046	1.973446	1.168686
7	1	0	-1.418000	2.174535	-0.393948
8	1	0	0.587139	1.161460	-1.553824
9	1	0	1.026274	2.598180	-0.640363
10	1	0	0.114466	-0.705346	2.079719
11	1	0	-0.149474	-2.088107	1.005178
12	1	0	2.188177	-1.240397	0.897529
13	1	0	1.828278	1.167797	1.255404
14	1	0	2.702348	0.850289	-0.244568
15	15	0	-1.344991	-0.119543	0.277509
16	8	0	-1.885646	-0.700302	-1.008535
17	9	0	1.370371	-1.267732	-0.939125
18	1	0	-2.296387	-0.072653	1.310747

**8-trans-g**

Standard orientation:

Center Number	Atomic Number	Atomic Type	Coordinates (Angstroms)		
			X	Y	Z
1	6	0	0.883696	1.603388	-0.279526
2	6	0	-0.620389	1.525441	0.035728
3	6	0	-0.055997	-1.174818	0.662014
4	6	0	1.399173	-0.801743	0.395424
5	6	0	1.721542	0.668851	0.598778
6	1	0	-0.808541	1.781764	1.085247
7	1	0	-1.193498	2.219927	-0.586823
8	1	0	1.056759	1.366430	-1.335256
9	1	0	1.222311	2.632865	-0.129842
10	1	0	-0.265408	-1.041740	1.729952
11	1	0	-0.226293	-2.227603	0.417836
12	1	0	2.056498	-1.425060	1.007041
13	1	0	1.561914	0.903801	1.658356
14	1	0	2.785734	0.816411	0.389313
15	15	0	-1.253480	-0.145545	-0.238112
16	9	0	1.688379	-1.133041	-0.949581
17	1	0	-0.966274	-0.383238	-1.592769
18	8	0	-2.698072	-0.398717	0.125043

**8-trans-a**

Standard orientation:

Center Number	Atomic Number	Atomic Type	Coordinates (Angstroms)		
			X	Y	Z
1	6	0	0.001591	1.805367	0.361067
2	6	0	1.147567	1.272605	-0.515555
3	6	0	-0.352127	-1.111489	-0.553122
4	6	0	-1.339692	-0.341702	0.309532
5	6	0	-1.347243	1.150270	0.030473
6	1	0	0.935340	1.455387	-1.576275
7	1	0	2.095453	1.761354	-0.269835
8	1	0	0.237771	1.646019	1.420123
9	1	0	-0.083566	2.885820	0.215044
10	1	0	-0.601591	-0.967220	-1.611272
11	1	0	-0.390189	-2.180718	-0.324979
12	1	0	-1.592723	1.309696	-1.026927
13	1	0	-2.137528	1.610649	0.631391
14	15	0	1.343017	-0.510833	-0.272145
15	8	0	1.936056	-0.915694	1.057661
16	1	0	2.064176	-0.974596	-1.384651
17	9	0	-2.629416	-0.853117	0.042413
18	1	0	-1.156673	-0.530598	1.372173

**8-cis-a**

Standard orientation:

Center Number	Atomic Number	Atomic Type	Coordinates (Angstroms)		
			X	Y	Z
1	6	0	-0.375308	1.867425	0.214249
2	6	0	0.994117	1.391583	-0.300315
3	6	0	-0.195032	-1.172150	-0.156416
4	6	0	-1.433377	-0.420207	0.307393
5	6	0	-1.534354	0.981953	-0.261792
6	1	0	1.013393	1.391508	-1.396299
7	1	0	1.797402	2.046857	0.050464
8	1	0	-0.370369	1.906237	1.310903
9	1	0	-0.542201	2.890552	-0.133585
10	1	0	-0.223726	-1.280299	-1.246966
11	1	0	-0.159509	-2.170947	0.289422
12	1	0	-1.539194	0.922446	-1.357028
13	1	0	-2.486155	1.418220	0.056117
14	15	0	1.345736	-0.294920	0.249506
15	1	0	1.305374	-0.193501	1.652296
16	8	0	2.602616	-0.945185	-0.275953
17	9	0	-2.561642	-1.160900	-0.108867
18	1	0	-1.483488	-0.389317	1.400795

**9-cis-g**

Standard orientation:

Center Number	Atomic Number	Atomic Type	Coordinates (Angstroms)		
			X	Y	Z
1	6	0	-1.111642	1.566932	0.422988
2	6	0	0.383980	1.583862	0.070045
3	6	0	-0.096878	-1.029182	-0.888300
4	6	0	-1.561247	-0.741365	-0.574154
5	6	0	-1.929572	0.733497	-0.569104
6	1	0	0.527119	1.979259	-0.943138
7	1	0	0.950527	2.215740	0.762479
8	1	0	-1.251731	1.174816	1.436164
9	1	0	-1.491043	2.593320	0.423356
10	1	0	0.083568	-0.758631	-1.935827
11	1	0	0.106659	-2.099535	-0.780013
12	1	0	-2.197137	-1.286723	-1.277023
13	1	0	-1.787911	1.118015	-1.587354
14	1	0	-2.996390	0.815096	-0.336933
15	15	0	1.076873	-0.091490	0.148407
16	8	0	1.234998	-0.623469	1.558001
17	9	0	-1.855650	-1.270875	0.703079
18	6	0	2.627995	-0.070808	-0.779294
19	1	0	3.352120	0.543821	-0.238068
20	1	0	3.013231	-1.091267	-0.851754
21	1	0	2.482942	0.336453	-1.782777

**9-trans-g**

Standard orientation:

Center Number	Atomic Number	Atomic Type	Coordinates (Angstroms)		
			X	Y	Z
1	6	0	-1.067902	1.502017	0.610023
2	6	0	0.394971	1.607336	0.147980
3	6	0	-0.114792	-0.898068	-1.074795
4	6	0	-1.547776	-0.695204	-0.593964
5	6	0	-1.948623	0.756599	-0.397219
6	1	0	0.448792	2.147233	-0.805566
7	1	0	1.002908	2.159505	0.873090
8	1	0	-1.123613	1.007244	1.585505
9	1	0	-1.465731	2.511977	0.749959
10	1	0	-0.043235	-0.519873	-2.101744
11	1	0	0.125845	-1.965909	-1.102325
12	1	0	-2.236076	-1.189993	-1.284420
13	1	0	-1.902454	1.252546	-1.375066
14	1	0	-2.993219	0.780713	-0.070325
15	15	0	1.166879	-0.009829	-0.129819
16	9	0	-1.699288	-1.364603	0.644712
17	8	0	2.495498	0.043432	-0.856147
18	6	0	1.288898	-0.804735	1.488667
19	1	0	1.656866	-1.824940	1.351481
20	1	0	2.005814	-0.246077	2.096255
21	1	0	0.321862	-0.838694	1.993053

**9-trans-a**

Standard orientation:

Center Number	Atomic Number	Atomic Type	Coordinates (Angstroms)		
			X	Y	Z
1	6	0	-0.694290	1.884118	0.097589
2	6	0	0.675426	1.482494	-0.474380
3	6	0	-0.309997	-1.145382	-0.275245
4	6	0	-1.567167	-0.486349	0.267220
5	6	0	-1.807296	0.902374	-0.296620
6	1	0	0.633342	1.446488	-1.569738
7	1	0	1.449835	2.201995	-0.188004
8	1	0	-0.633814	1.950655	1.190493
9	1	0	-0.955801	2.881319	-0.268128
10	1	0	-0.385737	-1.226829	-1.365911
11	1	0	-0.187694	-2.148139	0.146578
12	1	0	-1.875137	0.831825	-1.389566
13	1	0	-2.769705	1.266415	0.076610
14	15	0	1.157803	-0.150583	0.151042
15	8	0	1.468695	-0.164085	1.634048
16	9	0	-2.667381	-1.305182	-0.078604
17	1	0	-1.547485	-0.456504	1.361276
18	6	0	2.504674	-0.763927	-0.881759
19	1	0	3.384738	-0.135639	-0.722348
20	1	0	2.740199	-1.788799	-0.583776
21	1	0	2.228986	-0.744689	-1.938890

**9-cis-a**

Standard orientation:

Center Number	Atomic Number	Atomic Type	Coordinates (Angstroms)		
			X	Y	Z
1	6	0	-0.592373	1.879768	0.194843
2	6	0	0.722606	1.480090	-0.494827
3	6	0	-0.355307	-1.134044	-0.372557
4	6	0	-1.546069	-0.457672	0.287633
5	6	0	-1.765927	0.966907	-0.184077
6	1	0	0.613293	1.557862	-1.583352
7	1	0	1.542577	2.142421	-0.197331
8	1	0	-0.464888	1.883353	1.283826
9	1	0	-0.837798	2.906659	-0.091483
10	1	0	-0.531242	-1.185968	-1.453642
11	1	0	-0.231924	-2.154896	0.003429
12	1	0	-1.901421	0.962170	-1.272826
13	1	0	-2.688341	1.344554	0.267895
14	15	0	1.212686	-0.231072	-0.147635
15	8	0	2.334784	-0.761106	-1.013438
16	9	0	-2.695846	-1.217365	-0.027815
17	1	0	-1.462585	-0.489873	1.378849
18	6	0	1.589410	-0.311058	1.619300
19	1	0	1.774945	-1.353271	1.891575
20	1	0	2.492845	0.274121	1.810250
21	1	0	0.774555	0.080129	2.233285

**PFgauche**

Standard orientation:

Center Number	Atomic Number	Atomic Type	Coordinates (Angstroms)		
			X	Y	Z
1	6	0	1.318919	0.438778	0.316899
2	1	0	2.123117	1.111757	0.020769
3	1	0	1.274488	0.362217	1.404064
4	6	0	0.003085	0.914152	-0.278670
5	1	0	0.080437	1.020928	-1.363206
6	1	0	-0.268661	1.883529	0.148400
7	1	0	-1.486948	-0.456888	1.417333
8	1	0	-2.556117	0.304547	-0.411347
9	1	0	-1.159374	-1.447069	-0.573295
10	15	0	-1.360862	-0.225843	0.053726
11	9	0	1.608218	-0.834328	-0.186443

**PFanti**

Standard orientation:

Center Number	Atomic Number	Atomic Type	Coordinates (Angstroms)		
			X	Y	Z
1	6	0	-1.123535	-0.507595	0.000013
2	1	0	-1.073229	-1.129694	-0.894447
3	1	0	-1.073287	-1.129486	0.894645
4	6	0	-0.053234	0.577396	-0.000027
5	1	0	-0.149254	1.207089	0.888209
6	1	0	-0.149376	1.207163	-0.888170
7	1	0	1.871094	-0.850333	-1.124108
8	1	0	2.535809	0.981589	-0.000558
9	1	0	1.871639	-0.849199	1.124748
10	15	0	1.631941	-0.071288	-0.000012
11	9	0	-2.361321	0.134820	-0.000007

**PPgauche**

Standard orientation:

Center Number	Atomic Number	Atomic Type	Coordinates (Angstroms)		
			X	Y	Z
1	6	0	0.638059	0.801610	0.431619
2	1	0	1.099552	1.790197	0.358232
3	1	0	0.433328	0.628762	1.491193
4	6	0	-0.638072	0.801624	-0.431621
5	1	0	-0.433356	0.628757	-1.491194
6	1	0	-1.099584	1.790197	-0.358211
7	1	0	-2.301825	-0.139486	1.389455
8	1	0	-3.062035	-0.128182	-0.733571
9	1	0	-1.568758	-1.679892	-0.078978
10	1	0	3.061902	-0.128449	0.733854
11	1	0	1.568651	-1.679910	0.078562
12	1	0	2.302129	-0.139168	-1.389333
13	15	0	1.948332	-0.352071	-0.063792
14	15	0	-1.948327	-0.352077	0.063792

**PPanti**

Standard orientation:

Center Number	Atomic Number	Atomic Type	Coordinates (Angstroms)		
			X	Y	Z
1	6	0	0.516167	-0.567641	0.000004
2	1	0	0.424198	-1.202052	0.885752
3	1	0	0.424177	-1.201972	-0.885782
4	6	0	-0.516176	0.567752	-0.000007
5	1	0	-0.424258	1.202179	-0.885765
6	1	0	-0.424309	1.202173	0.885738
7	1	0	-2.458477	-0.829729	1.127168
8	1	0	-3.099813	1.016061	0.000074
9	1	0	-2.458663	-0.829714	-1.127159
10	1	0	3.099608	-1.016250	-0.000404
11	1	0	2.458708	0.829987	-1.126957
12	1	0	2.458765	0.829325	1.127430
13	15	0	2.217121	0.055547	-0.000002
14	15	0	-2.217113	-0.055592	-0.000003

**Table S1.**Relative Gibbs free energies (kcal mol<sup>-1</sup>) and conformational populations (%) obtained in the gas phase and implicit DMSO (IEFPCM) at the B3LYP-D3BJ/6-311++g(d,p) theory level.

Compound	Relative energy(gas phase)	Population (gas phase)	Relative energy(Implicit DMSO)	Population (Implicit DMSO)
<b>1-cis-g</b>	1.25	11	1.37	9
<b>1-trans-g</b>	3.72	0	3.46	0
<b>1-trans-a</b>	0.00	88	0.00	90
<b>1-cis-a</b>	2.35	1	2.48	1
<b>2-cis-g</b>	0.98	10	1.48	5
<b>2-trans-g</b>	1.74	3	1.52	5
<b>2-trans-a</b>	0.00	54	0.00	63
<b>2-cis-a</b>	0.28	33	0.49	27
<b>3axial</b>	0.00	100	0.00	72
<b>3equatorial</b>	3.41	0	0.57	28
<b>4axial</b>	0.00	100	0.00	82
<b>4equatorial</b>	3.25	0	0.91	18
<b>5anti</b>	1.90	4	0.39	34
<b>5gauche</b>	0.00	96	0.00	66
<b>7-cis-g_s</b>	2.82	1	1.12	4
<b>7-cis-g_a</b>	7.74	0	2.65	0
<b>7-cis-g_s'</b>	---	---	1.03	5
<b>7-trans-g_s</b>	1.30	7	---	---
<b>7-trans-g_g</b>	---	---	1.00	5
<b>7-trans-g_a</b>	2.55	1	0.47	12
<b>7-trans-g_g'</b>	---	---	0.65	9
<b>7-trans-g_s'</b>	1.94	3	---	---
<b>7-trans-a_s</b>	0.66	22	0.71	8
<b>7-trans-a_a</b>	4.94	0	2.03	1
<b>7-trans-a_s'</b>	---	---	0.53	11
<b>7-cis-a_s</b>	0.00	66	---	---
<b>7-cis-a_g</b>	---	---	0.00	26
<b>7-cis-a_g'</b>	---	---	0.18	19
<b>8-cis-g</b>	2.72	0	1.48	4
<b>8-trans-g</b>	0.00	37	0.22	33
<b>8-trans-a</b>	0.08	32	0.64	16
<b>8-cis-a</b>	0.10	31	0.00	47
<b>9-cis-g</b>	3.35	0	1.34	4
<b>9-trans-g</b>	0.42	27	0.51	18
<b>9-trans-a</b>	0.00	55	0.11	35
<b>9-cis-a</b>	0.64	18	0.00	43

**Table S2.** Relative full energies ( $E_{\text{FULL}}$ ), non-Lewis ( $E_{\text{NL}}$ ) and Lewis-type ( $E_{\text{L}}$ ) contributions, and the main electron delocalization energies obtained for the gas phase compounds at the B3LYP-D3BJ/6-311++g(d,p) theory level (in kcal mol<sup>-1</sup>).

Conf.	$E_{\text{FULL}}$	$E_{\text{NL}}$	$E_{\text{L}}$	$\sigma_{\text{ClH}} \rightarrow \sigma^*_{\text{CF}}$	$\sigma_{\text{ClH}} \rightarrow \sigma^*_{\text{C}_2\text{H}}$	$\sigma_{\text{ClH}} \rightarrow \sigma^*_{\text{C}_2\text{C}_3}$	$\sigma_{\text{CF}} \rightarrow \sigma^*_{\text{CP}}$	$\sigma_{\text{ClH}} \rightarrow \sigma^*_{\text{PH/C}}$	$\sigma_{\text{CH}} \rightarrow \sigma^*_{\text{PO}}$	$\sigma_{\text{CH}} \rightarrow \pi^*_{\text{PO}}$	$\sigma_{\text{CP}} \rightarrow \sigma^*_{\text{CF}}$
<b>1-cis-g</b>	1.30	-7.04	8.34	5.12	-	3.03	-	0.96	-	-	-
<b>1-trans-g</b>	3.84	0.00	3.84	5.19	-	3.04	-	-	-	-	-
<b>1-trans-a</b>	0.00	-8.16	8.16	0.77	2.81	2.90	1.66	0.98	-	-	4.58
<b>1-cis-a</b>	2.41	-0.23	2.64	0.93	2.79	2.84	1.48	-	-	-	5.20
<b>2-cis-g</b>	0.93	-9.26	10.19	5.29	-	3.06	-	1.27	-	-	-
<b>2-trans-g</b>	1.93	0.00	1.93	5.18	-	3.04	-	-	-	-	-
<b>2-trans-a</b>	0.00	-8.36	8.36	0.89	2.95	2.88	1.51	1.28	-	-	4.31
<b>2-cis-a</b>	0.30	-0.15	0.45	0.93	2.78	2.83	1.33	-	-	-	5.16
<b>3axial</b>	0.00	0.00	0.00	3.83	-	2.45	-	1.85	-	-	-
<b>3equatorial</b>	3.57	-2.95	6.52	1.08	2.18	2.20	1.78	2.08	-	-	2.85
<b>4 axial</b>	0.00	0.00	0.00	4.19	-	2.52	-	2.25	-	-	-
<b>4equatorial</b>	3.60	-0.95	4.55	1.05	2.35	2.28	1.57	2.45	-	-	2.75
<b>5anti</b>	2.39	0.00	2.39	1.15	2.10	-	1.83	2.49	-	-	2.30
<b>5gauche</b>	0.00	-3.68	3.68	4.22	2.03	-	-	2.29	-	-	-
<b>7-cis-g_s</b>	2.72	-23.18	25.90	4.73	-	2.84	-	-	1.62	-	-
<b>7-cis-g_a</b>	7.84	0.00	7.84	4.60	-	2.84	-	-	1.76	-	-
<b>7-trans-g_s</b>	2.09	-34.35	36.44	4.76	-	2.81	-	-	0.74	2.43	-
<b>7-trans-g_a*</b>	1.69	-2.74	4.43	5.18	-	2.92	-	-	0.56	3.02	2.96
<b>7-trans-g_s'</b>	1.99	-34.31	36.30	4.77	-	2.81	-	-	0.91	1.86	-
<b>7-trans-a_s</b>	0.53	-18.58	19.11	0.75	2.53	2.63	1.14	-	1.91	-	4.18
<b>7-trans-a_a</b>	4.89	-0.98	5.87	0.73	2.46	2.64	1.12	-	1.91	-	4.23
<b>7-cis-a_s</b>	0.00	-29.09	29.09	0.85	2.57	2.65	1.14	-	0.73	2.32	4.23
<b>8-cis-g</b>	2.85	-8.08	10.93	4.70	-	2.88	-	-	2.02	-	-
<b>8-trans-g</b>	0.00	0.00	0.00	4.85	-	2.91	-	1.42	-	-	-
<b>8-trans-a</b>	0.18	-1.22	1.40	0.77	2.49	2.66	1.31	-	2.14	-	4.39
<b>8-cis-a</b>	0.14	-5.06	5.20	0.83	2.68	2.70	1.34	1.45	-	-	4.10
<b>9-cis-g</b>	3.39	-6.12	9.51	4.68	-	2.89	-	-	2.02	-	-
<b>9-trans-g</b>	0.00	-0.16	0.16	5.14	-	2.92	-	1.56	-	-	-
<b>9-trans-a</b>	0.13	0.00	0.13	0.78	2.48	2.67	1.21	-	2.17	-	4.48
<b>9-cis-a</b>	0.60	-2.42	3.02	0.89	2.84	2.73	1.26	1.63	-	-	4.02

\* The conformer which is prone to establish an intramolecular hydrogen bond possesses an  $n_{\text{F}} \rightarrow \sigma^*_{\text{HO}}$  interaction of 2.96 kcal mol<sup>-1</sup>.

**Table S3.** Relative full energies (E<sub>FULL</sub>), non-Lewis (E<sub>NL</sub>) and Lewis-type (E<sub>L</sub>) contributions, and the main electron delocalization energies obtained for compounds in implicit DMSO at the B3LYP-D3BJ/6-311++g(d,p) theory level (in kcal mol<sup>-1</sup>).

Conf	E <sub>FULL</sub>	E <sub>NL</sub>	E <sub>L</sub>	$\sigma_{\text{CIH} \rightarrow \sigma^*_{\text{C2F}}}$	$\sigma_{\text{CIH} \rightarrow \sigma^*_{\text{C2H}}}$	$\sigma_{\text{CIH} \rightarrow \sigma^*_{\text{C2C3}}}$	$\sigma_{\text{CF} \rightarrow \sigma^*_{\text{CP}}}$	$\sigma_{\text{CIH} \rightarrow \sigma^*_{\text{PH/C}}}$	$\sigma_{\text{CH} \rightarrow \sigma^*_{\text{PO}}}$	$\sigma_{\text{CH} \rightarrow \pi^*_{\text{PO}}}$	$\sigma_{\text{CP} \rightarrow \sigma^*_{\text{CF}}}$
<b>1-cis-g</b>	1.44	-7.47	8.91	5.44	-	3.05	-	1.05	-	-	-
<b>1-trans-g</b>	3.58	0.00	3.58	5.54	-	3.05	-	-	-	-	-
<b>1-trans-a</b>	0.00	-7.65	7.65	0.79	2.82	2.93	1.67	0.97	-	-	4.93
<b>1-cis-a</b>	2.58	-0.10	2.68	0.94	2.84	2.86	1.50	-	-	-	5.53
<b>2-cis-g</b>	1.50	-9.61	11.11	5.58	-	3.05	-	1.36	-	-	-
<b>2-trans-g</b>	1.70	-0.03	1.73	5.55	-	3.06	-	-	-	-	-
<b>2-trans-a</b>	0.00	-7.80	7.80	0.90	2.94	2.91	1.52	1.27	-	-	4.64
<b>2-cis-a</b>	0.57	0.00	0.57	0.94	2.84	2.86	1.35	-	-	-	5.53
<b>3axial</b>	0.00	-1.37	1.37	4.56	-	2.64	-	1.83	-	-	-
<b>3equatorial</b>	0.84	0.00	0.84	1.08	2.33	2.41	1.68	1.87	-	-	3.48
<b>4 axial</b>	0.00	-1.88	1.88	4.79	-	2.69	-	2.23	-	-	-
<b>4equatorial</b>	0.88	0.00	0.88	1.05	2.47	2.47	1.50	2.32	-	-	3.36
<b>5anti</b>	1.04	0.00	1.04	1.04	2.14	-	1.80	2.50	-	-	2.58
<b>5gauche</b>	0.00	-4.77	4.77	4.68	2.08	-	-	2.36	-	-	-
<b>7-cis-g_s</b>	1.74	-2.23	3.97	5.08	-	2.79	-	-	2.03	-	-
<b>7-cis-g_a</b>	2.77	-0.38	3.15	4.99	-	2.79	-	-	2.07	-	-
<b>7-cis-g_s'</b>	1.78	-2.05	3.83	5.02	-	2.81	-	-	2.21	-	-
<b>7-trans-g_g</b>	1.18	-3.79	4.97	4.96	-	2.76	-	-	1.94	-	-
<b>7-trans-g_a*</b>	0.18	-5.32	5.50	5.20	-	2.83	-	-	2.03	-	-
<b>7-trans-g_g'</b>	0.95	-3.99	4.94	5.00	-	2.78	-	-	2.28	-	-
<b>7-trans-a_s</b>	1.08	-2.10	3.18	0.79	2.60	2.61	1.19	-	2.09	-	4.57
<b>7-trans-a_a</b>	2.06	0.00	2.06	0.80	2.56	2.61	1.19	-	2.13	-	4.53
<b>7-trans-a_g'</b>	1.23	-1.74	2.97	0.81	2.57	2.62	1.18	-	2.27	-	4.50
<b>7-cis-a_g</b>	0.00	-4.88	4.88	0.94	2.56	2.63	1.25	-	1.92	-	4.01
<b>7-cis-a_g'</b>	0.04	-4.97	5.01	0.88	2.58	2.62	1.24	-	2.23	-	4.14
<b>8-cis-g</b>	1.34	-2.15	3.49	5.10	-	2.86	-	-	2.25	-	-
<b>8-trans-g</b>	0.18	0.00	0.18	5.00	-	2.85	-	1.52	-	-	-
<b>8-trans-a</b>	0.62	-0.24	0.86	0.81	2.60	2.65	1.35	-	2.26	-	4.50
<b>8-cis-a</b>	0.00	-0.96	0.96	0.89	2.60	2.65	1.38	1.47	-	-	4.14
<b>9-cis-g</b>	1.28	-1.63	2.91	5.12	-	2.87	-	-	2.28	-	-
<b>9-trans-g</b>	0.12	0.00	0.12	5.24	-	2.86	-	1.67	-	-	-
<b>9-trans-a</b>	0.19	-0.34	0.53	0.79	2.61	2.68	1.25	-	2.32	-	4.62
<b>9-cis-a</b>	0.00	-0.03	0.03	0.95	2.74	2.68	1.30	1.68	-	-	4.08

\* The conformer which is prone to establish an intramolecular hydrogen bond possesses an  $n_F \rightarrow \sigma^*_{\text{HO}}$  interaction of 3.21 kcal mol<sup>-1</sup>.

**Table S4.** Electron density and the Laplacian of electron density at the BCP, bond ellipticity, average number of electrons, net charge, intratomic dipole moment contribution, volume obtained at 0.001 isodensity surface, and interacting quantum atoms (IQA) intratomic energy component in the hydrogen atom (in au).<sup>a</sup>

Conformer	$\rho$	$\nabla^2\rho$	$\epsilon$	N(H)	Q(H)	$ \mu(H) $	V(H)	E(H)
<b>2-cis-g</b>	0.011	0.041	0.1615	0.974 (0.984)	0.026 (0.016)	0.133 (0.151)	43.12 (50.41)	-0.453 (-0.460)
<b>4ax</b>	0.011	0.039	0.2300	0.878 (0.921)	0.1221 (0.084)	0.116 (0.134)	40.23 (46.39)	-0.446 (-0.454)
<b>9-trans-g</b>	0.011	0.038	0.1760	0.964 (0.918)	0.0361 (0.083)	0.149 (0.147)	44.51 (47.20)	-0.451 (-0.452)

<sup>a</sup> The values for the hydrogen ( $\text{CH}_3$ ) not involved in hydrogen bond with the fluorine atom are in parenthesis.

**Table S5.** NEDA energies in kcal mol<sup>-1</sup> for **PF**: energy of interaction ( $E_{\text{int}}$ ), electrical interaction ( $E_{\text{EL}}$ ), charge transfer ( $E_{\text{CT}}$ ), Core repulsion ( $E_{\text{CORE}}$ ), classical electrostatic interaction ( $E_{\text{ES}}$ ), polarization contribution ( $E_{\text{POL}}$ ), the penalty of polarization ( $E_{\text{SE}}$ ), deformation cost ( $E_{\text{DEF}}$ ), and exchange interaction ( $E_{\text{XC}}$ ). The energies for **PF** in the gas phase are presented for the C–C equilibrium distance in the *gauche* conformer (1.53 Å), as well as with -0.5 Å and +0.5 Å.

C–C Bond distance (Å)	$\phi_{\text{PCCF}}$ (deg.)	$E_{\text{int}}$	$E_{\text{EL}}$	$E_{\text{CT}}$	$E_{\text{CORE}}$	$E_{\text{ES}}$	$E_{\text{POL}}$	$E_{\text{SE}}$	$E_{\text{DEF}}$	$E_{\text{XC}}$
1.53	0	1.79	-11.11	-4.18	17.08	-10.12	-2.98	1.99	19.07	0.00
	30	0.00	-8.38	-4.35	12.73	-7.76	-2.17	1.55	20.24	-5.96
	60	0.26	-4.72	-3.69	8.67	-4.60	-1.25	1.13	21.46	-11.66
	90	4.15	-3.12	-1.16	8.43	-3.36	-0.69	0.93	21.62	-12.26
	120	7.03	-1.93	0.00	8.96	-2.51	0.00	0.58	21.62	-12.08
	150	6.10	-0.54	-2.08	8.72	-0.94	-0.10	0.50	21.94	-12.72
	180	5.15	0.00	-3.62	8.77	0.00	-0.72	0.72	22.07	-12.58
	0	26.17	-37.46	-31.89	95.52	-33.25	-14.62	10.41	105.93	0.00
1.03	30	9.95	-24.55	-35.12	69.62	-21.57	-10.56	7.58	110.69	-33.49
	60	0.00	-9.51	-32.88	42.39	-9.29	-4.36	4.14	116.23	-69.70
	90	13.57	-6.86	-13.70	34.13	-9.35	-0.62	3.11	116.76	-79.52
	120	26.02	-6.89	0.00	32.91	-10.18	0.00	3.29	116.01	-79.81
	150	16.25	-2.64	-18.08	36.97	-4.31	-0.01	1.68	117.59	-78.94
	180	8.16	0.00	-32.48	40.64	0.00	-0.88	0.88	118.61	-77.09
	0	0.00	-5.41	-0.17	5.58	-5.06	-0.62	0.27	5.85	0.00
	30	0.25	-4.50	-0.15	4.90	-4.33	-0.29	0.12	6.08	-1.06
2.03	60	1.21	-3.05	-0.15	4.41	-2.99	-0.12	0.06	6.33	-1.86
	90	2.75	-2.00	0.00	4.75	-1.89	-0.26	0.15	6.39	-1.49
	120	3.92	-1.11	-0.11	5.14	-1.04	-0.18	0.11	6.42	-1.17
	150	4.25	-0.33	-0.34	4.92	-0.33	-0.02	0.02	6.49	-1.55
	180	4.31	0.00	-0.32	4.63	0.00	0.00	0.00	6.53	-1.90

**Table S6.** NEDA energies in kcal mol<sup>-1</sup> for **PP**: energy of interaction ( $E_{\text{int}}$ ), electrical interaction ( $E_{\text{EL}}$ ), charge transfer ( $E_{\text{CT}}$ ), Core repulsion ( $E_{\text{CORE}}$ ), classical electrostatic interaction ( $E_{\text{ES}}$ ), polarization contribution ( $E_{\text{POL}}$ ), the penalty of polarization ( $E_{\text{SE}}$ ), deformation cost ( $E_{\text{DEF}}$ ), and exchange interaction ( $E_{\text{EXC}}$ ). The energies for **PP** in the gas phase are presented for the C–C equilibrium distance in the *gauche* conformer (1.53 Å), as well as with -0.5 Å and +0.5 Å.

C–C Bond distance (Å)	$\phi_{\text{PCCP}}$ (deg.)	$E_{\text{int}}$	$E_{\text{EL}}$	$E_{\text{CT}}$	$E_{\text{CORE}}$	$E_{\text{ES}}$	$E_{\text{POL}}$	$E_{\text{SE}}$	$E_{\text{DEF}}$	$E_{\text{EXC}}$
1.54	0	23.45	0.00	-5.62	29.07	0.00	-5.19	5.19	34.26	0.00
	30	17.57	-0.95	-5.23	23.75	-2.03	-3.29	4.37	35.35	-7.23
	60	10.53	-3.98	-2.77	17.28	-6.13	-1.59	3.74	36.93	-15.91
	90	6.52	-8.02	-0.61	15.15	-10.75	-0.90	3.63	38.12	-19.34
	120	4.82	-10.56	0.00	15.38	-13.89	0.00	3.33	38.66	-19.95
	150	1.85	-11.81	-1.96	15.62	-15.17	-0.03	3.39	38.99	-19.98
	180	0.00	-12.41	-3.24	15.65	-15.43	-0.72	3.74	39.09	-19.70
	0	70.85	0.00	-43.97	114.82	0.00	0.00	0.00	114.82	0.00
1.04	30	43.16	-0.71	-49.59	93.46	-0.34	-2.77	2.40	118.18	-22.32
	60	19.37	-1.55	-31.97	52.89	-0.75	-12.31	11.51	122.17	-57.77
	90	15.40	-7.49	-12.31	35.20	-6.30	-16.60	15.41	124.25	-73.64
	120	20.62	-11.87	0.00	32.49	-10.97	-17.61	16.71	124.44	-75.24
	150	9.40	-12.25	-13.77	35.42	-10.63	-17.98	16.36	125.22	-73.44
	180	0.00	-11.32	-26.83	38.15	-9.19	-18.08	15.95	125.77	-71.67
	0	12.95	0.00	-0.35	13.30	0.00	-3.87	3.87	17.17	0.00
	30	11.00	-0.86	-0.31	12.17	-1.59	-2.46	3.19	17.62	-2.26
2.04	60	7.56	-3.35	0.00	10.91	-5.11	-0.47	2.23	18.40	-5.26
	90	4.45	-6.70	-0.08	11.23	-8.73	0.00	2.03	18.97	-5.71
	120	2.23	-9.42	-0.24	11.89	-11.29	-0.38	2.25	19.22	-5.08
	150	0.65	-10.86	-0.19	11.70	-12.68	-0.51	2.33	19.38	-5.35
	180	0.00	-11.27	-0.15	11.42	-13.12	-0.44	2.29	19.43	-5.72

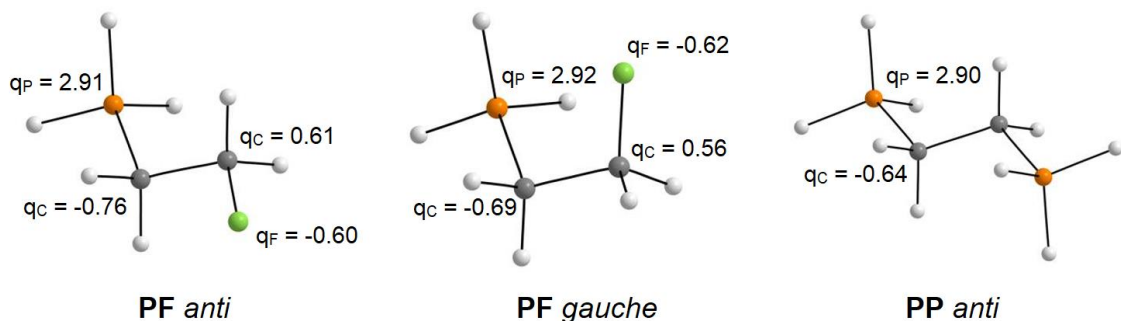


**Figure S1.** QTAIM plots for **PF** and **PP** in the gas phase (the P and F atomic charges, in a.u., are shown).

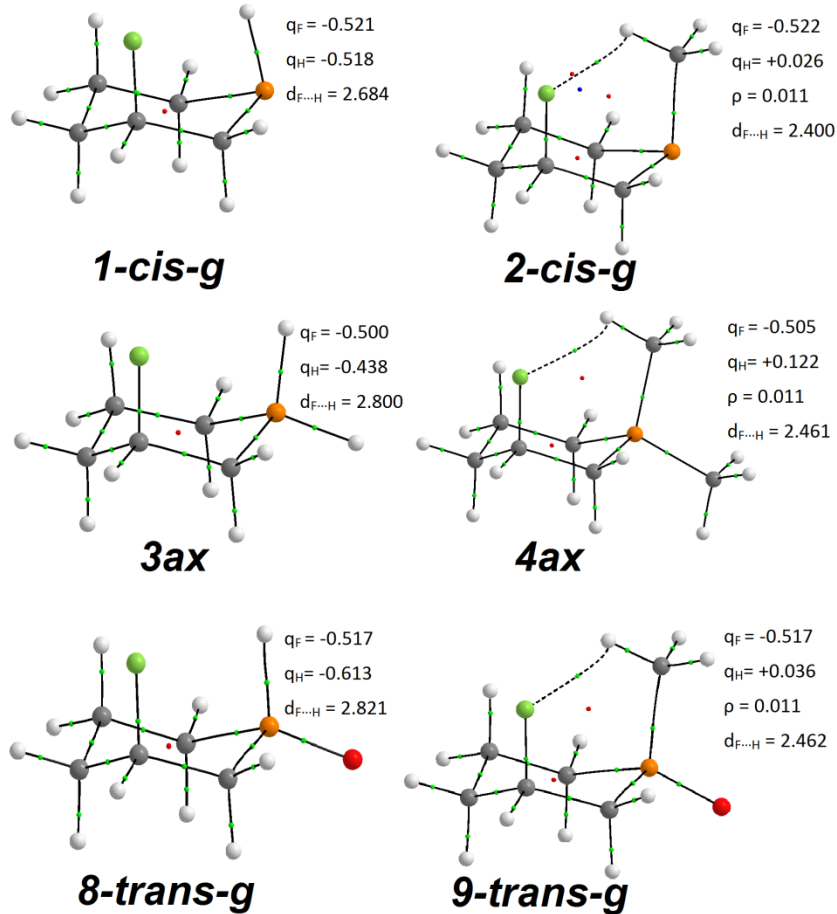


**Figure S2.** QTAIM plots indicating bond paths between interacting atoms for **1-cis-g**, **2-cis-g**, **3ax**, **4ax**, **8-trans-g** and **9-trans-g**. The atomic charges ( $q$ , in a.u.), electron densities at the bond critical point ( $\rho$ ), and the distances between interacting atoms ( $r$ , in angstroms) are also depicted. (H = white, C = gray, F = green, P = orange, O = red, bond-critical point = green dot, ring-critical point = red dot, cage-critical point = blue dot).

### X-ray diffraction

The crystal data were obtained on Oxford-Rigaku GEMINI diffractometer with MoK $\alpha$  ( $\lambda = 0.71073 \text{ \AA}$ ) radiation at room temperature (298K). The data collection, cell refinements and data reduction were performed using the CRYSTALISPRO software.<sup>S1</sup> The structures were solved by direct methods and refined using SHELXL-2018/3.<sup>S2</sup> All non-hydrogen atoms were refined with anisotropic thermal parameters. H atoms were placed in idealized positions and treated by a rigid model, with  $U_{iso}(H) = 1.2U_{eq}(C)$ . CCDC 1971685 contains the supplementary crystallographic data. The figures were drawn using ORTEP-3 for Windows<sup>S3</sup> and Mercury.<sup>S4</sup>

## Crystal structure discussion

The crystal analysis indicates that the compound crystallizes in a non-centrosymmetric tetragonal space group P4<sub>1</sub>2<sub>1</sub>2. The compound is a triphenylphosphoniumiodine salt, as can be seen in Figure S1. In the solid state is observed the two-fold axis in the middle of C-C bond of ethane residue reducing the asymmetric unit for this crystal to half of the molecule. Crystal data and selected geometrical parameters are listed in Tables S5 and S6, respectively.

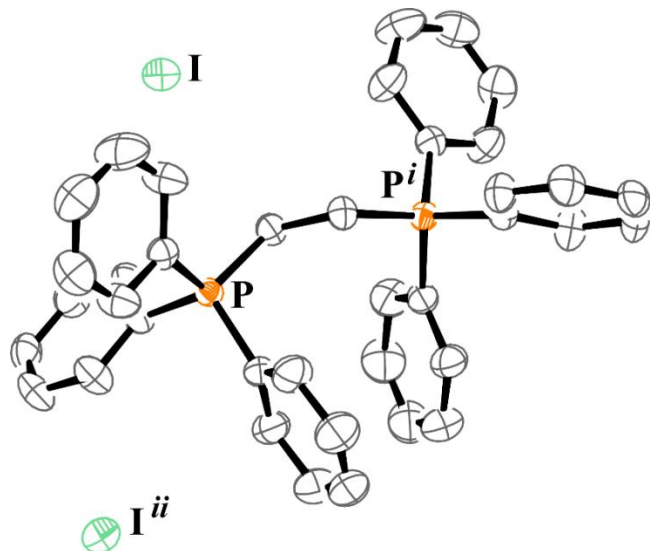


**Figure S1.** Molecular representation of the crystal with displacement ellipsoids at the 50% probability level. The H atoms were omitted for clarity. Symmetry codes: *i* (*y*, *x*, -*z*) *ii* (*y*, -1 + *y*, -*z*).

**Table S5.** Crystal data and structure refinement results for the crystal.

Empirical formula	C <sub>38</sub> H <sub>34</sub> I <sub>2</sub> P <sub>2</sub>
Formula weight (g.mol <sup>-1</sup> )	806.39
Wavelength ( $\lambda$ )	0.71073
Crystal system	Tetragonal
Space group	P4 <sub>1</sub> 2 <sub>1</sub> 2
Temperature (K)	298(2)
<i>a</i> (Å)	9.9016(2)
<i>b</i> (Å)	9.9016(2)
<i>c</i> (Å)	35.0282(8)
$\alpha = \beta = \gamma$ (°)	90.00
V (Å <sup>3</sup> )	3434.2(2)
<i>Z</i>	4
Density (calculated) (g cm <sup>-3</sup> )	1.560
Crystal size (mm <sup>3</sup> )	0.15 x0.19 x0.32
F(000)	1592
Absorption coefficient (mm <sup>-1</sup> )	1.95
T <sub>min</sub> /T <sub>máx</sub>	0.773 /1
2θ range for data collection (°)	2.38 to 25.02
Reflections collected	32408
Independent / observed reflections	4508 / 3465
R <sub>int</sub>	0.0604
Number of parameters	190
Final R indexes [I>2σ(I)]	R <sub>1</sub> =0.0389 wR <sub>2</sub> = 0.0555
Final R indexes (all data)	R <sub>1</sub> =0.0670 wR <sub>2</sub> = 0.0628
Goodness-of-fit on F <sup>2</sup>	1.055
Δρ <sub>max</sub> and Δρ <sub>min</sub> .	0.469 and -0.457

The average of P-C bond distance is 1.801(5) Å, which is similar to the periodate (1.797(6) Å)<sup>S5</sup> and tribromide (1.801(4) Å)<sup>S6</sup> salts. The torsion angle P-C-C-P is 134.8(3) ° which is very close to observed in periodate salt (136.1(2) °) but different to tribromide (average of 162.3(3) °). The P(C<sub>6</sub>H<sub>5</sub>)<sub>3</sub> groups are in eclipsed conformation to each other. The geometry of P atom is tetrahedral slightly distorted with average of C-P-C bond angles of 109.5(2)° (range of 107.7(2) to 113.5(2)°). The torsion angles among aromatic rings are 70.6(5), 72.2(6) and 76.7(5)° and the average deviation of P atom to aromatic ring planes are 0.143, 0.164 and 0.176 Å. The supramolecular arrangement of this crystal is formed by non-classical hydrogen bonds C-H···I interactions that gives rise to a bi-dimensional network in the *ab* crystallographic plane,

as can be seen in Figure S2. The average C···I distance is 3.918(5) Å. All geometrical parameters of non-classical hydrogen bonds are displayed in Table S7.

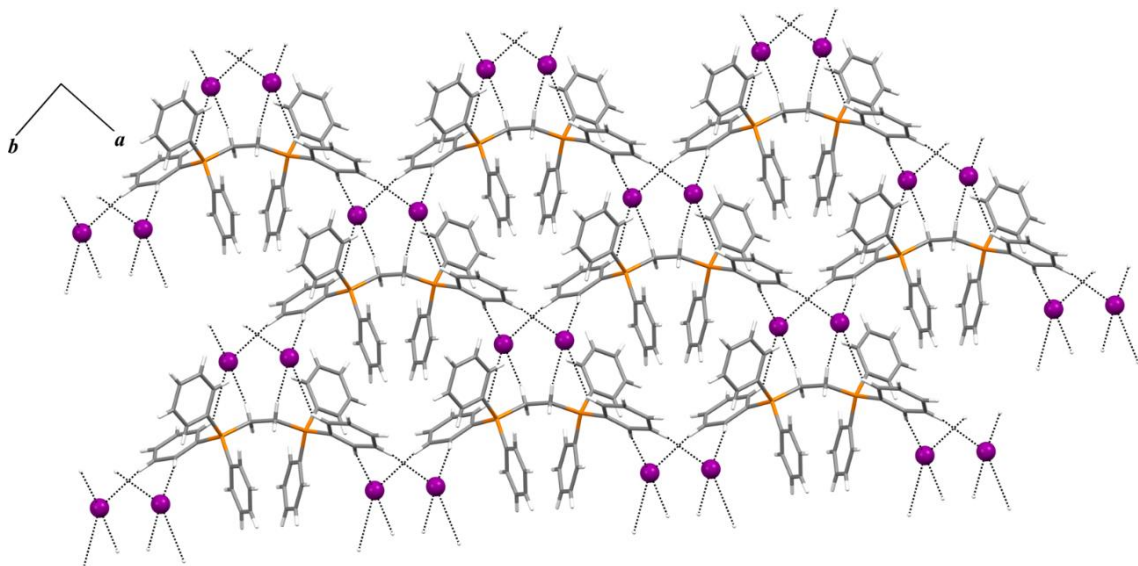


**Figure S2.** 2-D network of the crystal in *ab* crystallographic plane. The pink sphere represents the iodine anion.

**Table S6.** Selected geometrical parameters of the crystal.

Bond distance / Å			
P-C1	1.797(5)	P-C19	1.815(5)
P-C7	1.791(5)	C19-C19 <sup>i</sup>	1.542(9)
P-C13	1.800(5)		
Bond angle / °			
C1-P-C7	109.8(2)	C7-P-C19	108.0(2)
C1-P-C13	107.7(2)	C13-P-C19	113.5(2)
C1-P-C19	109.2(2)	P-C19-C19 <sup>i</sup>	115.2(4)
C7-P-C13	108.6(2)		

Symmetry code: *i* (*y*, *x*, -*z*)

**Table S7.** Geometrical parameters of non-classical hydrogen bonds.

D-H···A	D-H / Å	H···A / Å	D···A / Å	D-H···A / °
C2-H2···I <sup>ii</sup>	0.93	3.13	3.874(5)	138.0
C19-H19a···I <sup>ii</sup>	0.94	3.00	3.906(5)	161.0
C6-H6···I	0.93	3.12	4.009(5)	161.0
C5-H5···I <sup>iii</sup>	0.93	3.16	3.883(5)	136.0

Symmetry code: *ii* (*y*, -1 + *y*, -*z*), *iii* (1 + *y*, -1 + *y*, -*z*)

## References

- (S1) Rigaku Oxford Diffraction, *CrysAlis Pro*. Rigaku Corporation, Tokyo (Japan) **2015**.
- (S2) Sheldrick, G. M. Crystal structure refinement with SHELXL. *Acta Cryst. C***2015**, *71*, 3-8.
- (S3) Farrugia, L. J. *J. Appl. Cryst.* **1997**, *30*, 565.
- (S4) Macrae, C. F.; Bruno, I. J.; Chisholm, J. A.; Edgington, P. R.; McCabe, P.; Pidcock, E.; Rodriguez-Monge, L.; Taylor, R.; Streck, J.; Wood, P. A. Mercury CSD 2.0 – new features for the visualization and investigation of crystal structures. *J. Appl. Cryst.* **2008**, *41*, 466-470.
- (S5) Gholizadeh, M.; Zonoz, F. M.; Pourayoubi, M.; Ebrahimpour, M.; Salehabadi, M. *Acta Cryst.* **2011**, *E67*, 0863.
- (S6) Salmasi, R.; Gholizadeh, M.; Salimi, A.; Garrison, J. C. *J. Iran. Chem. Soc.* **2016**, *13*, 2019-2028.

**APPENDIX C**

Supporting Information for:

**Theoretical study of fluorinated bioisosteres of organochlorine compounds  
as effective and eco-friendly pesticides****INDEX**

Standard Orientation	196
<b>Table S1.</b> Interacting Residues	200

## Aldrin:

## Standard orientation:

Center Number	Atomic Number	Atomic Type	Coordinates (Angstroms)		
			X	Y	Z
1	6	0	-1.080292	0.785837	-0.889054
2	6	0	0.296074	1.132168	-0.229112
3	6	0	0.295995	-1.132306	-0.228498
4	6	0	-1.080329	-0.786243	-0.888666
5	6	0	1.201107	-0.000268	-0.845435
6	6	0	0.318455	0.668680	1.223891
7	6	0	0.318372	-0.668023	1.224253
8	6	0	-2.452547	1.132961	-0.213980
9	6	0	-2.452621	-1.132965	-0.213466
10	6	0	-2.659000	0.000240	0.823033
11	1	0	-3.681087	0.000360	1.203796
12	1	0	-1.977934	0.000407	1.665974
13	6	0	-3.465529	0.668809	-1.264847
14	6	0	-3.465558	-0.669217	-1.264558
15	1	0	-2.549272	2.161604	0.129277
16	1	0	-2.549424	-2.161445	0.130258
17	17	0	0.203148	1.715783	2.575178
18	17	0	0.202941	-1.714376	2.576111
19	17	0	2.893783	-0.000167	-0.249681
20	17	0	1.274727	-0.000760	-2.639524
21	17	0	0.836423	2.804847	-0.509706
22	17	0	0.836239	-2.805173	-0.508168
23	1	0	-3.994967	-1.326217	-1.942904
24	1	0	-3.994904	1.325539	-1.943480
25	1	0	-1.050319	-1.191881	-1.897635
26	1	0	-1.050297	1.190976	-1.898224

## Diieldrin:

## Standard orientation:

Center Number	Atomic Number	Atomic Type	Coordinates (Angstroms)		
			X	Y	Z
1	6	0	-0.990460	0.777249	0.733517
2	6	0	0.455823	0.325035	1.113087
3	6	0	0.456705	0.160727	-1.148693
4	6	0	-0.990110	0.665056	-0.839783
5	6	0	1.276892	0.964905	-0.069757
6	6	0	0.657505	-1.143942	0.753583
7	6	0	0.657637	-1.240627	-0.579904
8	6	0	-2.251760	-0.037242	1.145372
9	6	0	-2.254034	-0.196253	-1.132642
10	6	0	-2.359218	-1.148665	0.078463
11	1	0	-3.327461	-1.643071	0.114401
12	1	0	-1.588046	-1.905555	0.129732
13	6	0	-3.373808	0.911490	0.673540
14	1	0	-3.606670	1.821588	1.216196
15	6	0	-3.374316	0.809244	-0.795128
16	1	0	-3.607822	1.634821	-1.459160
17	1	0	-2.292144	-0.341144	2.190633
18	1	0	-2.296830	-0.642363	-2.125504
19	17	0	1.126401	2.750257	-0.198724
20	17	0	3.027503	0.584066	-0.041272
21	17	0	0.959785	0.383445	-2.840735
22	17	0	0.957065	0.791034	2.755478
23	17	0	0.704335	-2.420325	1.894838
24	17	0	0.705801	-2.668536	-1.524642
25	8	0	-4.469284	0.299661	-0.021318
26	1	0	-1.085390	1.813022	1.059449
27	1	0	-1.081638	1.644539	-1.309175

$\alpha$ -Chlordane: Standard orientation:

Center Number	Atomic Number	Atomic Type	Coordinates (Angstroms)		
			X	Y	Z
1	6	0	0.783787	0.975884	0.975503
2	6	0	0.278492	1.002519	-0.468335
3	6	0	1.233400	-0.258152	1.227283
4	6	0	-1.016919	0.132895	-0.547101
5	6	0	1.041204	-1.091107	-0.040792
6	6	0	-0.485726	-1.317688	-0.255462
7	6	0	1.331172	0.023615	-1.109245
8	1	0	-1.435173	0.204233	-1.548950
9	17	0	1.845772	-0.867473	2.708131
10	17	0	0.686755	2.298024	2.061876
11	17	0	3.011014	0.639493	-1.090958
12	17	0	0.946762	-0.457294	-2.794607
13	17	0	2.024003	-2.567330	-0.152173
14	17	0	0.155584	2.607501	-1.214562
15	6	0	-2.115229	0.363965	0.502161
16	6	0	-1.324843	-1.854475	0.922736
17	6	0	-2.624497	-1.044140	0.850399
18	1	0	-0.617671	-1.947038	-1.132858
19	17	0	-3.380880	1.543896	0.005084
20	17	0	-3.717534	-1.725770	-0.440234
21	1	0	-3.214038	-1.061174	1.763690
22	1	0	-1.700382	0.774594	1.423161
23	1	0	-1.504301	-2.926697	0.862559
24	1	0	-0.848568	-1.651614	1.886047

 $\beta$ -Chlordane: Standard orientation:

Center Number	Atomic Number	Atomic Type	Coordinates (Angstroms)		
			X	Y	Z
1	6	0	-0.427523	-0.071991	1.364324
2	6	0	-0.460308	-1.091499	0.224613
3	6	0	-0.807998	1.109576	0.866060
4	6	0	0.693436	-0.747807	-0.770795
5	6	0	-1.100922	0.913370	-0.621533
6	6	0	0.249075	0.643983	-1.356824
7	6	0	-1.704531	-0.535084	-0.561295
8	1	0	0.722671	-1.507396	-1.549652
9	17	0	-0.892249	2.612734	1.683396
10	17	0	0.090023	-0.419408	2.959941
11	17	0	-3.248536	-0.652021	0.332941
12	17	0	-1.949998	-1.294534	-2.170502
13	17	0	-2.111131	2.159709	-1.384310
14	17	0	-0.543381	-2.795267	0.711662
15	6	0	2.104822	-0.524225	-0.201508
16	6	0	1.420881	1.612296	-1.107824
17	6	0	2.628525	0.672781	-1.004507
18	1	0	0.040923	0.552952	-2.421720
19	17	0	3.161397	-1.983307	-0.344752
20	1	0	2.093516	-0.276203	0.858060
21	1	0	1.540752	2.346334	-1.904195
22	1	0	1.309773	2.156274	-0.168434
23	17	0	4.067858	1.460178	-0.247784
24	1	0	2.961921	0.342218	-1.988402

## F-aldrin:

## Standard orientation:

Center Number	Atomic Number	Atomic Type	Coordinates (Angstroms)		
			X	Y	Z
1	6	0	-0.768688	0.790426	-0.686573
2	6	0	0.686011	1.125834	-0.238757
3	6	0	0.685947	-1.126189	-0.237186
4	6	0	-0.768717	-0.791337	-0.685536
5	6	0	1.448720	-0.000726	-0.996377
6	6	0	0.965505	0.665821	1.178367
7	6	0	0.965388	-0.664195	1.179309
8	6	0	-2.019315	1.133671	0.193210
9	6	0	-2.019405	-1.133387	0.194614
10	6	0	-2.046591	0.000802	1.249593
11	1	0	-2.986447	0.001187	1.802809
12	1	0	-1.228966	0.001196	1.964514
13	6	0	-3.189603	0.668627	-0.677472
14	6	0	-3.189634	-0.669331	-0.676663
15	1	0	-2.061616	2.161431	0.550258
16	1	0	-2.061790	-2.160694	0.552953
17	9	0	1.084073	-2.409771	-0.500572
18	9	0	1.232097	-0.001655	-2.338543
19	9	0	2.789658	-0.000648	-0.829493
20	9	0	0.974225	-1.499013	2.212468
21	9	0	0.974469	1.502103	2.210338
22	9	0	1.084190	2.409026	-0.503962
23	1	0	-0.880972	-1.198553	-1.690513
24	1	0	-0.880991	1.196321	-1.692079
25	1	0	-3.822704	-1.326793	-1.258817
26	1	0	-3.822629	1.325414	-1.260434

## F-dieldrin:

## Standard orientation:

Center Number	Atomic Number	Atomic Type	Coordinates (Angstroms)		
			X	Y	Z
1	6	0	0.552308	0.652544	-0.793726
2	6	0	-0.911892	0.240609	-1.127591
3	6	0	-0.912064	0.240357	1.127554
4	6	0	0.552240	0.652093	0.793943
5	6	0	-1.655377	1.016245	0.000035
6	6	0	-1.221804	-1.169021	-0.665356
7	6	0	-1.222197	-1.169085	0.665078
8	6	0	1.767855	-0.252331	-1.142813
9	6	0	1.767537	-0.253404	1.142586
10	6	0	1.804923	-1.291742	-0.000556
11	1	0	2.736149	-1.853562	-0.000668
12	1	0	0.983644	-1.998920	-0.001092
13	6	0	2.946310	0.655039	-0.735501
14	1	0	3.233872	1.508522	-1.340312
15	6	0	2.946240	0.654310	0.736446
16	1	0	3.233811	1.507193	1.342088
17	1	0	1.789885	-0.633092	-2.163330
18	1	0	1.789231	-0.634950	2.162810
19	8	0	4.003391	0.024003	0.000190
20	9	0	-1.405693	2.352989	0.000259
21	9	0	-2.998162	0.880216	-0.000122
22	9	0	-1.304842	0.514898	2.409548
23	9	0	-1.304570	0.515270	-2.409566
24	9	0	-1.251076	-2.201632	-1.499453
25	9	0	-1.251915	-2.201762	1.499068
26	1	0	0.684181	1.659280	1.194783
27	1	0	0.683947	1.660013	-1.193984

$\alpha$ -Fluordane:

## Standard orientation:

Center Number	Atomic Number	Atomic Type	Coordinates (Angstroms)		
			X	Y	Z
1	6	0	0.937369	0.744248	1.183561
2	6	0	0.549911	1.135994	-0.233777
3	6	0	1.221609	-0.555661	1.180425
4	6	0	-0.815016	0.489955	-0.604551
5	6	0	1.031283	-1.065195	-0.238101
6	6	0	-0.476794	-1.052177	-0.611451
7	6	0	1.511973	0.194099	-1.013846
8	1	0	-1.122843	0.840078	-1.590280
9	6	0	-1.982576	0.640791	0.379680
10	6	0	-1.479735	-1.708640	0.363418
11	6	0	-2.655778	-0.737249	0.390545
12	1	0	-0.580140	-1.459320	-1.616870
13	1	0	-1.641595	0.870350	1.394495
14	1	0	-1.797965	-2.700965	0.044182
15	1	0	-1.066561	-1.802972	1.372386
16	9	0	0.842008	1.584609	2.206362
17	9	0	1.486763	-1.363897	2.199647
18	9	0	1.682951	-2.234928	-0.510245
19	9	0	0.657685	2.469274	-0.500366
20	9	0	2.823181	0.481909	-0.883883
21	9	0	1.253489	0.140150	-2.346483
22	9	0	-2.854230	1.651706	0.007434
23	9	0	-3.390966	-0.882924	-0.794426
24	1	0	-3.352303	-0.877265	1.218302

 $\beta$ -Fluordane:

## Standard orientation:

Center Number	Atomic Number	Atomic Type	Coordinates (Angstroms)		
			X	Y	Z
1	6	0	-0.675479	-0.265075	1.414916
2	6	0	-0.637032	-1.135846	0.169141
3	6	0	-0.938806	0.981309	1.029154
4	6	0	0.610017	-0.780442	-0.688281
5	6	0	-1.077733	0.974734	-0.483491
6	6	0	0.303806	0.701455	-1.144039
7	6	0	-1.742441	-0.419469	-0.659018
8	1	0	0.656623	-1.463349	-1.537932
9	6	0	1.978410	-0.733745	-0.000836
10	6	0	1.504742	1.547190	-0.680280
11	6	0	2.639941	0.529221	-0.552588
12	1	0	0.170196	0.748375	-2.225330
13	1	0	1.916415	-0.665796	1.088903
14	1	0	1.746700	2.355660	-1.369420
15	1	0	1.334324	1.992589	0.304232
16	1	0	3.106229	0.301401	-1.516154
17	9	0	-0.357886	-0.728227	2.616096
18	9	0	-0.954764	2.100145	1.740870
19	9	0	-1.756661	2.043729	-0.995073
20	9	0	-0.820360	-2.466585	0.403708
21	9	0	-2.990110	-0.527788	-0.161004
22	9	0	-1.800132	-0.831726	-1.953517
23	9	0	2.726215	-1.872875	-0.292808
24	9	0	3.651138	0.987231	0.289243

PCP:					
Center Number	Atomic Number	Atomic Type	Standard orientation:		
			X	Y	Z
1	6	0	1.199227	-0.923776	-0.000088
2	6	0	1.223282	0.474422	-0.000125
3	6	0	-0.022445	-1.609811	-0.000096
4	6	0	0.023952	1.204064	-0.000129
5	6	0	-1.213014	-0.873445	-0.000105
6	6	0	-1.200314	0.523349	-0.000106
7	17	0	-2.711438	-1.774909	0.000005
8	17	0	-2.698360	1.399248	0.000086
9	17	0	0.054769	2.940982	0.000030
10	17	0	2.745841	1.305640	0.000000
11	17	0	2.659028	-1.860959	0.000094
12	8	0	-0.000308	-2.956161	0.000025
13	1	0	-0.908933	-3.289569	0.000059

PFP:					
Center Number	Atomic Number	Atomic Type	Standard orientation:		
			X	Y	Z
1	6	0	-0.246365	1.365538	0.000029
2	6	0	1.063211	0.900298	0.000004
3	6	0	-1.321112	0.474973	0.000019
4	6	0	1.326359	-0.465891	0.000016
5	6	0	-1.034296	-0.888993	0.000010
6	6	0	0.268234	-1.366729	0.000045
7	8	0	-2.584433	0.958092	-0.000019
8	1	0	-3.211823	0.224038	-0.000035
9	9	0	-2.072937	-1.751410	-0.000073
10	9	0	0.502633	-2.681403	0.000050
11	9	0	2.587326	-0.908633	-0.000023
12	9	0	2.076264	1.769983	-0.000069
13	9	0	-0.476496	2.682135	0.000053

**Table S1.** Number of hydrogen bonds, halogen interactions, hydrophobic interactions and destabilizing interactions between ligands and residues (specific residues in parenthesis).

Ligand	H-bond	Halogen interaction	Hydrophobic interaction	destabilizing interactions
Picrotoxin	3 (THR256, THR271, SER267)	-	4	-
Aldrin	-	1 (ALA252)	12	-
Dieldrin	1 (SER267)	-	9	-
$\alpha$ -Chlordane	-	1 (ALA252)	16	-
$\beta$ -Chlordane	-	1 (ALA252)	14	-
F-Aldrin	2 (SER267, THR256)	1 (ALA252)	1	-
F-Dieldrin	1 (SER267)	1 (THR256)	1	-
$\alpha$ -Fluordane	2 (SER267, THR256)	1 (ALA252)	1	-
$\beta$ -Fluordane	1 (THR256)	1 (THR256)	1	-

## APPENDIX D

Supporting Information for:

### **Theoretical exploitation of 1,2,3,4,5,6-hexachloro- and 1,2,3,4,5,6-hexafluorocyclohexane isomers as biological compounds**

#### INDEX

Standard Orientation of the optimized structures in the gas phase	202
Standard Orientation of the optimized structures in water implicit solvent	211
<b>Table S1.</b> Relative Gibbs energy for all isomers, Grel, in kcal mol <sup>-1</sup> . Relative Gibbs energy from the conformational ring flip isomerism, ΔGrel, in kcal mol <sup>-1</sup> , and the conformational population, in parenthesis. Nuclear-electronic relative energy, Erel, in kcal mol <sup>-1</sup> . Dipole moment, μ, Debye. The data were acquired in gas phase and implicit water at the MP2/6-311++g(d,p) level of theory.	220
<b>Table S2.</b> Relative full energy (E <sub>Full</sub> ), Lewis energy (E <sub>Lewis</sub> ), and non-Lewis energy (E <sub>non-Lewis</sub> ), in kcal mol <sup>-1</sup> , obtained through Natural Bond Orbital (NBO) analysis at the B3LYP/6-311++g(d,p) level.	220
<b>Table S3.</b> Docking score (D <sub>score</sub> ), in kcal mol <sup>-1</sup> , and the ligand efficiency SA (surface area) of HCH and HFH isomers in the picrotoxin and barbiturate sites of GABA <sub>A</sub> receptor, and InsP <sub>3</sub> receptor	221
<b>Table S4.</b> Docking score (D <sub>score</sub> ), in kcal mol <sup>-1</sup> , and the ligand efficiency SA (surface area) of HCH and HFH isomers in three predicted sites of ryanodine receptor.	222
<b>Table S5.</b> Number and types of interactions of HCHs and HFHs in the picrotoxin site of GABA <sub>A</sub> receptor.	223
<b>Table S6.</b> Number and types of interactions of HCHs and HFHs in the barbiturate site of GABA <sub>A</sub> receptor.	224
<b>Table S7.</b> Number and types of interactions of HCHs and HFHs in the site 1 of ryanodine receptor.	225

### Standard Orientation of the optimized structures in the gas phase

 $\alpha\epsilon$ -HCH

Standard orientation:

Center Number	Atomic Number	Atomic Type	Coordinates (Angstroms)		
			X	Y	Z
1	6	0	-0.754103	-1.540602	-0.115583
2	6	0	0.754574	-1.540682	0.116004
3	6	0	1.392230	-0.282311	-0.463679
4	6	0	0.762064	0.993868	0.086186
5	6	0	-0.762488	0.993861	-0.086101
6	6	0	-1.392591	-0.282414	0.463695
7	1	0	1.198409	-2.418389	-0.356876
8	1	0	-1.197781	-2.418443	0.357184
9	1	0	1.014806	1.111955	1.143307
10	1	0	-1.015136	1.111969	-1.143237
11	1	0	-1.250297	-0.311504	1.546652
12	1	0	1.249490	-0.311642	-1.546582
13	17	0	-3.149431	-0.308282	0.196308
14	17	0	-1.051543	-1.707124	-1.871388
15	17	0	-1.440424	2.402794	0.767184
16	17	0	1.440132	2.402636	-0.767107
17	17	0	3.149138	-0.307588	-0.197028
18	17	0	1.052270	-1.706805	1.871821

 $\alpha\alpha$ -HCH

Standard orientation:

Center Number	Atomic Number	Atomic Type	Coordinates (Angstroms)		
			X	Y	Z
1	6	0	0.983839	0.410745	-0.642064
2	6	0	0.983894	-0.410468	0.641996
3	6	0	-0.236900	-1.330715	0.675818
4	6	0	-1.547330	-0.548423	0.537039
5	6	0	-1.547380	0.548093	-0.537130
6	6	0	-0.237170	1.330668	-0.675820
7	1	0	-0.251007	-1.863617	1.627485
8	1	0	-2.358197	-1.245670	0.325370
9	1	0	-2.358393	1.245200	-0.325546
10	1	0	-0.251465	1.863680	-1.627424
11	1	0	0.923874	-0.259706	-1.503840
12	1	0	0.923727	0.259994	1.503752
13	17	0	-0.151357	2.599228	0.582551
14	17	0	2.464623	1.365234	-0.859835
15	17	0	2.464866	-1.364658	0.859884
16	17	0	-0.150640	-2.599437	-0.582356
17	17	0	-1.931957	-0.165418	-2.138069
18	17	0	-1.932139	0.165094	2.137893

 $\beta\epsilon$ -HCH

Standard orientation:

Center Number	Atomic Number	Atomic Type	Coordinates (Angstroms)		
			X	Y	Z
1	6	0	0.983716	1.078356	-0.222982
2	6	0	-0.442035	1.391099	0.223075
3	6	0	-1.425722	0.312745	-0.223046
4	6	0	-0.983711	-1.078321	0.223038
5	6	0	0.442038	-1.391136	-0.223045
6	6	0	1.425783	-0.312781	0.222951
7	1	0	-0.474730	1.493798	1.312544
8	1	0	1.056345	1.158077	-1.312445
9	1	0	-1.056333	-1.157879	1.312518
10	1	0	-1.530916	0.335821	-1.312530
11	1	0	1.531130	-0.335935	1.312413
12	1	0	0.474647	-1.493917	-1.312510
13	17	0	2.091326	2.292419	0.462586
14	17	0	3.031016	-0.664853	-0.462644
15	17	0	0.939833	-2.957327	0.462501
16	17	0	-2.091471	-2.292321	-0.462344
17	17	0	-3.031047	0.664750	0.462307
18	17	0	-0.939691	2.957347	-0.462403

$\beta$ -HCH

## Standard orientation:

Center Number	Atomic Number	Atomic Type	Coordinates (Angstroms)		
			X	Y	Z
1	6	0	0.160430	0.767796	1.285721
2	6	0	-0.160234	1.497386	-0.022043
3	6	0	0.160158	0.729512	-1.307806
4	6	0	-0.160176	-0.767954	-1.285619
5	6	0	0.160349	-1.497376	0.022282
6	6	0	-0.160522	-0.729483	1.307865
7	1	0	-0.396520	-2.434026	0.036096
8	1	0	0.396875	-1.248217	-2.089764
9	1	0	0.396136	-1.185878	2.126056
10	1	0	-0.396956	1.185761	-2.125773
11	1	0	-0.396326	1.248196	2.089986
12	1	0	0.396761	2.433960	-0.035927
13	17	0	1.887370	-1.984601	0.029880
14	17	0	1.887525	1.017269	1.704001
15	17	0	-1.887682	-0.966559	1.733037
16	17	0	1.886969	0.967301	-1.733918
17	17	0	-1.887035	-1.018340	-1.704287
18	17	0	-1.887147	1.984985	-0.028895

 $\gamma$ -HCH

## Standard orientation:

Center Number	Atomic Number	Atomic Type	Coordinates (Angstroms)		
			X	Y	Z
1	6	0	-1.239131	0.474944	0.424798
2	6	0	-0.001234	1.146833	-0.171355
3	6	0	1.238046	0.477154	0.424746
4	6	0	1.293891	-1.022800	0.135580
5	6	0	0.001626	-1.725996	0.560287
6	6	0	-1.291895	-1.025018	0.135393
7	1	0	1.199272	0.599444	1.511970
8	1	0	0.002535	-2.750942	0.188009
9	1	0	2.121744	-1.452143	0.702555
10	1	0	-2.119088	-1.456079	0.702024
11	1	0	-0.001186	1.080655	-1.262646
12	1	0	-1.200695	0.597257	1.512027
13	17	0	-0.002706	2.873861	0.257327
14	17	0	-2.751883	1.248301	-0.093794
15	17	0	-1.652902	-1.372456	-1.577600
16	17	0	0.001574	-1.843286	2.354882
17	17	0	1.656004	-1.369934	-1.577233
18	17	0	2.749302	1.253580	-0.093619

 $\delta$ e-HCH

## Standard orientation:

Center Number	Atomic Number	Atomic Type	Coordinates (Angstroms)		
			X	Y	Z
1	6	0	0.000693	-1.586755	-0.249689
2	6	0	-1.238596	-0.787180	-0.638726
3	6	0	-1.288242	0.548640	0.093462
4	6	0	-0.000763	1.347222	-0.137320
5	6	0	1.287418	0.549148	0.093078
6	6	0	1.239291	-0.786639	-0.639302
7	1	0	1.195209	-0.604928	-1.719111
8	1	0	-1.449855	0.384353	1.160602
9	1	0	0.000701	-2.539130	-0.784196
10	1	0	-1.194676	-0.605301	-1.718536
11	1	0	-0.000958	1.722744	-1.165779
12	1	0	1.449013	0.384753	1.160211
13	17	0	0.001065	-1.980548	1.489589
14	17	0	2.709236	-1.743081	-0.357680
15	17	0	2.664551	1.510993	-0.499448
16	17	0	-0.000955	2.775178	0.926843
17	17	0	-2.666089	1.509058	-0.499643
18	17	0	-2.707705	-1.745077	-0.357438

$\delta\alpha$ -HCH

## Standard orientation:

Center Number	Atomic Number	Atomic Type	Coordinates (Angstroms)		
			X	Y	Z
1	6	0	0.940890	0.178599	-1.301127
2	6	0	-0.498130	-0.349899	-1.293450
3	6	0	-0.786065	-1.101423	0.000131
4	6	0	-0.497880	-0.349674	1.293575
5	6	0	0.941136	0.178895	1.300959
6	6	0	1.411502	0.841865	-0.000207
7	1	0	-0.094651	-1.951472	0.000128
8	1	0	1.056141	0.892161	2.117059
9	1	0	-0.600008	-1.057150	2.117879
10	1	0	2.501572	0.856631	-0.000317
11	1	0	-0.600378	-1.057524	-2.117611
12	1	0	1.055839	0.891657	-2.117420
13	17	0	0.921239	2.565858	-0.000338
14	17	0	2.029002	-1.193626	-1.706776
15	17	0	2.029390	-1.193175	1.706787
16	17	0	-1.647553	0.962773	1.662524
17	17	0	-2.412881	-1.808082	0.000334
18	17	0	-1.647858	0.962459	-1.662472

 $\epsilon e$ -HCH

## Standard orientation:

Center Number	Atomic Number	Atomic Type	Coordinates (Angstroms)		
			X	Y	Z
1	6	0	-1.255837	0.509621	0.566826
2	6	0	-1.256092	-0.509691	-0.566998
3	6	0	-0.000130	-1.384193	-0.494981
4	6	0	1.255456	-0.509346	-0.567232
5	6	0	1.255717	0.509309	0.567035
6	6	0	0.000090	1.384341	0.495111
7	1	0	0.000058	-2.079535	-1.337117
8	1	0	0.000006	2.079425	1.337452
9	1	0	-1.248234	-0.014458	1.526491
10	1	0	-1.248492	0.014339	-1.526703
11	1	0	1.247752	-0.015161	1.526498
12	1	0	1.247408	0.015058	-1.526728
13	17	0	2.714100	1.521799	0.571100
14	17	0	2.713612	-1.522201	-0.571309
15	17	0	0.000376	-2.394444	0.979199
16	17	0	-2.714192	-1.522690	-0.570280
17	17	0	-2.713801	1.522767	0.570358
18	17	0	0.000274	2.394773	-0.978976

 $\epsilon a$ -HCH

## Standard orientation:

Center Number	Atomic Number	Atomic Type	Coordinates (Angstroms)		
			X	Y	Z
1	6	0	0.748158	1.297813	0.169872
2	6	0	-0.747827	1.297787	-0.169922
3	6	0	-1.140548	0.000009	-0.868853
4	6	0	-0.748110	-1.297702	-0.169850
5	6	0	0.747840	-1.297826	0.169874
6	6	0	1.140622	-0.000046	0.868869
7	1	0	-0.955447	-2.125953	-0.849049
8	1	0	0.955021	-2.126136	0.849052
9	1	0	0.574340	0.000003	1.807383
10	1	0	-0.574263	-0.000097	-1.807361
11	1	0	0.955518	2.126115	0.849023
12	1	0	-0.955131	2.126048	-0.849116
13	17	0	2.852212	-0.000162	1.336333
14	17	0	1.674732	1.655178	-1.315987
15	17	0	1.674343	-1.655380	-1.315942
16	17	0	-1.674733	-1.655177	1.315933
17	17	0	-2.852181	0.000076	-1.336158
18	17	0	-1.674424	1.655454	1.315828

$\zeta$ -HCH

## Standard orientation:

Center Number	Atomic Number	Atomic Type	Coordinates (Angstroms)		
			X	Y	Z
1	6	0	0.778635	-1.199298	-0.924059
2	6	0	-0.680841	-1.335842	-0.479142
3	6	0	-1.428030	-0.074793	-0.924180
4	6	0	-0.816669	1.257429	-0.479258
5	6	0	0.649135	1.273998	-0.924096
6	6	0	1.497361	0.078368	-0.479538
7	1	0	-1.332438	2.051687	-1.025767
8	1	0	2.442852	0.127867	-1.026467
9	1	0	-1.364334	-0.071505	-2.020137
10	1	0	0.743823	-1.146002	-2.020022
11	1	0	-1.110862	-2.179668	-1.025563
12	1	0	0.620136	1.217355	-2.020059
13	17	0	1.723804	-2.654879	-0.561720
14	17	0	1.948138	0.102010	1.235850
15	17	0	-0.885515	-1.736843	1.236558
16	17	0	1.437118	2.820310	-0.561698
17	17	0	-1.062164	1.635013	1.236400
18	17	0	-3.161189	-0.165546	-0.561881

 $\eta$ -HCH

## Standard orientation:

Center Number	Atomic Number	Atomic Type	Coordinates (Angstroms)		
			X	Y	Z
1	6	0	-1.242535	-0.169700	0.515698
2	6	0	-0.941357	0.803926	-0.618776
3	6	0	0.563480	1.100228	-0.685497
4	6	0	1.322090	-0.218633	-0.843635
5	6	0	1.001192	-1.299107	0.187069
6	6	0	-0.512528	-1.495739	0.298849
7	1	0	1.455206	-2.233630	-0.146888
8	1	0	-0.729277	-2.166434	1.131362
9	1	0	-1.237357	0.353126	-1.570506
10	1	0	-0.890240	0.253057	1.460581
11	1	0	0.993097	-0.630723	-1.803760
12	1	0	0.756947	1.709751	-1.571697
13	17	0	-1.079426	-2.340698	-1.177192
14	17	0	1.655980	-1.001921	1.819334
15	17	0	3.070261	0.031863	-1.011817
16	17	0	1.112613	2.078101	0.697368
17	17	0	-1.865506	2.313701	-0.490845
18	17	0	-2.981595	-0.469928	0.714838

 $\theta\epsilon$ -HCH

## Standard orientation:

Center Number	Atomic Number	Atomic Type	Coordinates (Angstroms)		
			X	Y	Z
1	6	0	-0.709373	1.242070	-0.566621
2	6	0	-1.320357	0.000022	0.086152
3	6	0	-0.709572	-1.242057	-0.566671
4	6	0	0.815167	-1.292593	-0.425204
5	6	0	1.397860	-0.000014	-0.997822
6	6	0	0.815355	1.292570	-0.425114
7	1	0	1.186320	-2.126212	-1.026755
8	1	0	1.186534	2.126181	-1.026661
9	1	0	1.121483	0.000035	-2.060193
10	1	0	-0.938099	-1.207322	-1.638732
11	1	0	-0.937838	1.207309	-1.638695
12	1	0	-1.149302	0.000006	1.165604
13	17	0	-1.433890	2.749872	0.028417
14	17	0	1.323597	1.641645	1.241803
15	17	0	3.171398	-0.000160	-0.973250
16	17	0	1.323396	-1.641719	1.241731
17	17	0	-1.434124	-2.749775	0.028505
18	17	0	-3.079998	0.000137	-0.179142

$\theta\alpha$ -HCH

## Standard orientation:

Center Number	Atomic Number	Atomic Type	Coordinates (Angstroms)		
			X	Y	Z
1	6	0	1.234813	-0.142383	-0.888702
2	6	0	0.000501	-1.046372	-0.885892
3	6	0	-1.234519	-0.143154	-0.888539
4	6	0	-1.299823	0.903058	0.222112
5	6	0	-0.000802	1.716039	0.287653
6	6	0	1.298900	0.904030	0.221921
7	1	0	-2.112140	1.590967	-0.019273
8	1	0	2.110619	1.592652	-0.019452
9	1	0	-1.174597	0.428311	-1.821794
10	1	0	1.174542	0.428913	-1.822040
11	1	0	-0.000980	2.330075	1.188573
12	1	0	0.000638	-1.604224	-1.826187
13	17	0	1.705573	0.249631	1.828197
14	17	0	2.742343	-1.068959	-1.006926
15	17	0	0.001011	-2.280859	0.390301
16	17	0	-1.705838	0.248233	1.828380
17	17	0	-2.741299	-1.070878	-1.007183
18	17	0	-0.001349	2.869067	-1.096954

 $\alpha\epsilon$ -HFH

## Standard orientation:

Center Number	Atomic Number	Atomic Type	Coordinates (Angstroms)		
			X	Y	Z
1	6	0	-0.746537	-1.439429	-0.152879
2	6	0	0.746555	-1.439429	0.152840
3	6	0	1.399571	-0.195189	-0.420509
4	6	0	0.752600	1.071532	0.110274
5	6	0	-0.752620	1.071521	-0.110271
6	6	0	-1.399556	-0.195212	0.420518
7	1	0	1.233578	-2.337100	-0.234746
8	1	0	-1.233554	-2.337116	0.234679
9	1	0	0.977569	1.194858	1.173624
10	1	0	-0.977594	1.194840	-1.173619
11	1	0	-1.321219	-0.216206	1.511883
12	1	0	1.321275	-0.216163	-1.511877
13	9	0	-0.882314	-1.434506	-1.538192
14	9	0	0.882328	-1.434555	1.538156
15	9	0	2.743176	-0.196753	-0.089253
16	9	0	1.294068	2.157654	-0.559972
17	9	0	-1.294099	2.157637	0.559974
18	9	0	-2.743174	-0.196795	0.089312

 $\alpha\alpha$ -HFH

## Standard orientation:

Center Number	Atomic Number	Atomic Type	Coordinates (Angstroms)		
			X	Y	Z
1	6	0	-1.081566	-0.572198	-0.497010
2	6	0	-1.081539	0.572233	0.497023
3	6	0	0.143344	1.445880	0.284605
4	6	0	1.443799	0.655496	0.393451
5	6	0	1.443768	-0.655546	-0.393466
6	6	0	0.143282	-1.445884	-0.284599
7	9	0	0.089557	-1.985602	0.994586
8	9	0	1.639729	-0.355354	-1.735944
9	9	0	1.639774	0.355304	1.735932
10	9	0	0.089628	1.985591	-0.994585
11	1	0	0.147657	2.270306	1.002363
12	1	0	2.273306	1.276536	0.044763
13	1	0	2.273261	-1.276609	-0.044789
14	1	0	0.147545	-2.270314	-1.002353
15	1	0	-1.089866	-0.182914	-1.519007
16	1	0	-1.089855	0.182954	1.519021
17	9	0	-2.214294	-1.347607	-0.320596
18	9	0	-2.214235	1.347687	0.320605

$\beta\text{-HFH}$ 

## Standard orientation:

Center Number	Atomic Number	Atomic Type	Coordinates (Angstroms)		
			X	Y	Z
1	6	0	-1.216513	-0.790191	-0.222974
2	6	0	0.076064	-1.448639	0.222986
3	6	0	1.292579	-0.658441	-0.222970
4	6	0	1.216517	0.790191	0.222970
5	6	0	-0.076064	1.448640	-0.222984
6	6	0	-1.292574	0.658439	0.222966
7	1	0	0.082253	-1.566494	1.312331
8	1	0	-1.315474	-0.854487	-1.312319
9	9	0	0.142591	-2.715528	-0.330467
10	9	0	-2.280435	-1.481229	0.330473
11	1	0	1.315475	0.854479	1.312318
12	9	0	2.280432	1.481232	-0.330470
13	1	0	1.397721	-0.712010	-1.312319
14	1	0	-1.397725	0.712012	1.312312
15	1	0	-0.082247	1.566508	-1.312328
16	9	0	-0.142593	2.715526	0.330482
17	9	0	-2.423016	1.234263	-0.330478
18	9	0	2.423015	-1.234265	0.330464

 $\beta\text{a-HFH}$ 

## Standard orientation:

Center Number	Atomic Number	Atomic Type	Coordinates (Angstroms)		
			X	Y	Z
1	6	0	1.262681	-0.780195	0.175084
2	6	0	-0.044368	-1.483636	-0.174739
3	6	0	-1.307029	-0.703355	0.175155
4	6	0	-1.262679	0.780188	-0.175083
5	6	0	0.044369	1.483636	0.174736
6	6	0	1.307033	0.703355	-0.175154
7	9	0	0.051287	1.713885	1.543101
8	9	0	-1.458484	0.900898	-1.543504
9	9	0	1.509619	0.812155	-1.543579
10	9	0	-1.509605	-0.812150	1.543589
11	9	0	1.458473	-0.900905	1.543501
12	9	0	-0.051297	-1.713877	-1.543107
13	1	0	0.073100	2.444716	-0.346821
14	1	0	-2.080700	1.285741	0.346250
15	1	0	2.153828	1.159121	0.346138
16	1	0	-2.153825	-1.159131	-0.346129
17	1	0	2.080708	-1.285737	-0.346249
18	1	0	-0.073093	-2.444721	0.346808

 $\gamma\text{-HFH}$ 

## Standard orientation:

Center Number	Atomic Number	Atomic Type	Coordinates (Angstroms)		
			X	Y	Z
1	6	0	-1.239414	0.540613	0.373813
2	6	0	0.000072	1.244746	-0.150105
3	6	0	1.239479	0.540477	0.373814
4	6	0	1.275921	-0.924961	-0.024518
5	6	0	-0.000091	-1.651167	0.394196
6	6	0	-1.276024	-0.924820	-0.024523
7	1	0	1.259426	0.618054	1.466648
8	1	0	-0.000146	-2.664553	-0.013619
9	1	0	2.145455	-1.411692	0.425934
10	1	0	-2.145606	-1.411452	0.425942
11	9	0	2.372919	1.164847	-0.112727
12	9	0	1.392321	-1.020590	-1.401272
13	9	0	-0.000101	-1.721623	1.786962
14	9	0	-1.392445	-1.020438	-1.401270
15	1	0	0.000075	1.288168	-1.241752
16	1	0	-1.259349	0.618187	1.466647
17	9	0	0.000143	2.545354	0.331492
18	9	0	-2.372784	1.165113	-0.112724

$\delta e$ -HFH

## Standard orientation:

Center Number	Atomic Number	Atomic Type	Coordinates (Angstroms)		
			X	Y	Z
1	6	0	-0.000014	-1.540015	-0.103270
2	6	0	-1.241290	-0.773563	-0.518677
3	6	0	-1.272655	0.588411	0.151037
4	6	0	0.000017	1.371887	-0.131801
5	6	0	1.272669	0.588387	0.151060
6	6	0	1.241264	-0.773571	-0.518685
7	1	0	1.260429	-0.651604	-1.608268
8	1	0	-1.420666	0.475480	1.227968
9	1	0	-0.000016	-2.549138	-0.522191
10	9	0	-0.000017	-1.656213	1.282834
11	9	0	-2.346282	1.308063	-0.350139
12	9	0	2.366626	-1.489892	-0.158088
13	1	0	-1.260480	-0.651628	-1.608263
14	1	0	0.000035	1.699836	-1.177667
15	1	0	1.420652	0.475437	1.227992
16	9	0	-2.366653	-1.489853	-0.158029
17	9	0	0.000017	2.512365	0.653777
18	9	0	2.346320	1.308020	-0.350083

 $\delta a$ -HFH

## Standard orientation:

Center Number	Atomic Number	Atomic Type	Coordinates (Angstroms)		
			X	Y	Z
1	6	0	-0.867958	-1.289586	-0.060768
2	6	0	0.658345	-1.269895	-0.109511
3	6	0	1.150270	0.000000	-0.775939
4	6	0	0.658356	1.269894	-0.109502
5	6	0	-0.867947	1.289597	-0.060771
6	6	0	-1.505709	0.000009	0.454016
7	1	0	0.766771	0.000004	-1.803101
8	1	0	-1.201364	2.121527	0.564802
9	1	0	1.010825	2.137916	-0.674724
10	1	0	-2.562253	0.000009	0.169326
11	1	0	1.010796	-2.137918	-0.674743
12	1	0	-1.201371	-2.121502	0.564827
13	9	0	2.532903	-0.000003	-0.828338
14	9	0	1.136887	-1.373303	1.182303
15	9	0	1.136888	1.373281	1.182315
16	9	0	-1.316846	1.496376	-1.362866
17	9	0	-1.414689	0.000010	1.837044
18	9	0	-1.316871	-1.496378	-1.362851

 $\epsilon e$ -HFH

## Standard orientation:

Center Number	Atomic Number	Atomic Type	Coordinates (Angstroms)		
			X	Y	Z
1	6	0	-1.255699	0.567017	0.505325
2	6	0	-1.255707	-0.567009	-0.505329
3	6	0	-0.000002	-1.407442	-0.335606
4	6	0	1.255705	-0.567014	-0.505323
5	6	0	1.255702	0.567016	0.505328
6	6	0	0.000001	1.407450	0.335590
7	9	0	0.000005	1.924068	-0.958641
8	9	0	-0.000007	-1.924079	0.958621
9	1	0	0.000001	-2.253627	-1.026506
10	1	0	-0.000003	2.253643	1.026481
11	1	0	-1.309989	0.160707	1.519551
12	1	0	-1.310015	-0.160704	-1.519555
13	9	0	-2.363966	1.369584	0.305304
14	9	0	-2.363966	-1.369579	-0.305287
15	1	0	1.309996	0.160713	1.519556
16	1	0	1.310018	-0.160705	-1.519548
17	9	0	2.363970	1.369578	0.305295
18	9	0	2.363962	-1.369587	-0.305280

$\epsilon\text{-HFH}$ 

## Standard orientation:

Center Number	Atomic Number	Atomic Type	Coordinates (Angstroms)		
			X	Y	Z
1	6	0	0.761959	1.275108	0.058843
2	6	0	-0.761940	1.275114	-0.058854
3	6	0	-1.235367	0.000002	-0.735156
4	6	0	-0.761967	-1.275111	-0.058831
5	6	0	0.761933	-1.275127	0.058838
6	6	0	1.235366	-0.000019	0.735152
7	1	0	-1.093752	-2.141894	-0.636617
8	1	0	1.093708	-2.141918	0.636615
9	1	0	0.821551	-0.000020	1.750003
10	1	0	-0.821540	-0.000011	-1.750005
11	1	0	1.093704	2.141880	0.636668
12	1	0	-1.093705	2.141898	-0.636649
13	9	0	1.283256	1.385408	-1.221319
14	9	0	-1.283202	1.385394	1.221338
15	9	0	1.283182	-1.385398	-1.221362
16	9	0	-1.283222	-1.385361	1.221355
17	9	0	-2.615800	0.000016	-0.823759
18	9	0	2.615802	-0.000030	0.823751

 $\zeta\text{-HFH}$ 

## Standard orientation:

Center Number	Atomic Number	Atomic Type	Coordinates (Angstroms)		
			X	Y	Z
1	6	0	1.086141	0.930135	-0.689102
2	6	0	1.387847	-0.489403	-0.223634
3	6	0	0.262440	-1.405682	-0.689095
4	6	0	-1.117765	-0.957211	-0.223596
5	6	0	-1.348580	0.475549	-0.689094
6	6	0	-0.270093	1.446609	-0.223603
7	9	0	-1.219430	-1.044269	1.144502
8	9	0	-0.294655	1.578180	1.144494
9	1	0	-1.882835	-1.612390	-0.653555
10	1	0	-0.454978	2.436767	-0.653554
11	1	0	0.263392	-1.410897	-1.788099
12	1	0	1.090176	0.933610	-1.788102
13	9	0	0.503308	-2.695687	-0.264719
14	9	0	2.082906	1.783709	-0.264708
15	9	0	1.514086	-0.533912	1.144478
16	1	0	2.337780	-0.824398	-0.653584
17	1	0	-1.353569	0.477302	-1.788094
18	9	0	-2.586205	0.911981	-0.264742

 $\eta\text{-HFH}$ 

## Standard orientation:

Center Number	Atomic Number	Atomic Type	Coordinates (Angstroms)		
			X	Y	Z
1	6	0	-1.281247	-0.231503	0.475748
2	6	0	-0.962836	0.889661	-0.496554
3	6	0	0.518067	1.238828	-0.425877
4	6	0	1.355606	0.004667	-0.720036
5	6	0	1.041215	-1.170390	0.194950
6	6	0	-0.455335	-1.466941	0.156445
7	1	0	1.608761	-2.048477	-0.124756
8	1	0	-0.707942	-2.277533	0.843350
9	9	0	1.382397	-0.891397	1.506437
10	9	0	-0.752496	-1.888080	-1.139768
11	1	0	-1.236271	0.590292	-1.513157
12	1	0	-1.073446	0.094672	1.498514
13	9	0	-1.703334	2.010984	-0.171743
14	9	0	-2.623419	-0.558756	0.385425
15	1	0	1.140778	-0.314149	-1.746853
16	1	0	0.757405	2.036268	-1.135104
17	9	0	2.698696	0.317188	-0.638216
18	9	0	0.800145	1.713728	0.843415

$\theta_{e-HFH}$ 

Standard orientation:

Center Number	Atomic Number	Atomic Type	Coordinates (Angstroms)		
			X	Y	Z
1	6	0	-0.693803	1.244929	-0.435866
2	6	0	-1.336717	0.000010	0.154211
3	6	0	-0.693828	-1.244923	-0.435866
4	6	0	0.810293	-1.267973	-0.205870
5	6	0	1.427810	-0.000014	-0.777479
6	6	0	0.810319	1.267961	-0.205870
7	9	0	1.053675	-1.353283	1.150461
8	9	0	1.053714	1.353280	1.150450
9	1	0	1.253424	-2.150517	-0.676647
10	1	0	1.253456	2.150491	-0.676666
11	1	0	1.260131	-0.000012	-1.863201
12	1	0	-0.905270	-1.281801	-1.512051
13	1	0	-0.905241	1.281810	-1.512051
14	1	0	-1.257844	0.000007	1.243813
15	9	0	2.790267	-0.000028	-0.560120
16	9	0	-1.254935	-2.370233	0.134444
17	9	0	-1.254894	2.370250	0.134442
18	9	0	-2.681506	0.000023	-0.183316

 $\theta_{a-HFH}$ 

Standard orientation:

Center Number	Atomic Number	Atomic Type	Coordinates (Angstroms)		
			X	Y	Z
1	6	0	1.232923	-0.430513	-0.711909
2	6	0	0.000013	-1.290049	-0.478664
3	6	0	-1.232905	-0.430533	-0.711907
4	6	0	-1.285973	0.808346	0.168340
5	6	0	-0.000021	1.624696	0.034924
6	6	0	1.285950	0.808370	0.168351
7	9	0	-1.448511	0.465429	1.494160
8	9	0	1.448487	0.465447	1.494164
9	1	0	-2.136327	1.429566	-0.130101
10	1	0	2.136293	1.429611	-0.130075
11	1	0	-1.216064	-0.091053	-1.755165
12	1	0	1.216091	-0.091042	-1.755165
13	9	0	-2.376584	-1.183324	-0.528339
14	9	0	2.376617	-1.183279	-0.528327
15	9	0	0.000016	-1.806614	0.797876
16	9	0	-0.000014	2.185309	-1.245356
17	1	0	-0.000037	2.428466	0.774466
18	1	0	0.000012	-2.134159	-1.176377

### Standard Orientation of the optimized structures in water implicit solvent

 $\alpha\epsilon$ -HCH

Standard orientation:

Center Number	Atomic Number	Atomic Type	Coordinates (Angstroms)		
			X	Y	Z
1	6	0	-0.755700	-1.545055	-0.112156
2	6	0	0.754658	-1.545054	0.113553
3	6	0	1.390177	-0.286563	-0.468820
4	6	0	0.762363	0.988409	0.086635
5	6	0	-0.761413	0.989099	-0.087266
6	6	0	-1.390465	-0.285377	0.468656
7	1	0	1.193915	-2.424739	-0.358512
8	1	0	-1.195339	-2.423770	0.361431
9	1	0	1.016705	1.106143	1.142911
10	1	0	-1.015582	1.106616	-1.143627
11	1	0	-1.251788	-0.316085	1.551693
12	1	0	1.251052	-0.317973	-1.551750
13	17	0	-3.150865	-0.303531	0.201011
14	17	0	-1.059780	-1.708029	-1.868363
15	17	0	-1.440271	2.405592	0.760861
16	17	0	1.442003	2.404097	-0.762153
17	17	0	3.150776	-0.305950	-0.201665
18	17	0	1.058333	-1.705293	1.869970

 $\alpha\alpha$ -HCH

Standard orientation:

Center Number	Atomic Number	Atomic Type	Coordinates (Angstroms)		
			X	Y	Z
1	6	0	0.979799	0.408271	-0.643676
2	6	0	0.980171	-0.407629	0.643732
3	6	0	-0.240620	-1.327212	0.686541
4	6	0	-1.550431	-0.544667	0.540827
5	6	0	-1.550717	0.543741	-0.541045
6	6	0	-0.241528	1.327098	-0.686486
7	1	0	-0.255565	-1.855536	1.640088
8	1	0	-2.364545	-1.241210	0.342394
9	1	0	-2.365342	1.239729	-0.342756
10	1	0	-0.256724	1.855540	-1.639964
11	1	0	0.926478	-0.260973	-1.506283
12	1	0	0.926391	0.261601	1.506326
13	17	0	-0.153469	2.605384	0.565740
14	17	0	2.464672	1.364283	-0.859518
15	17	0	2.465696	-1.362640	0.859547
16	17	0	-0.151525	-2.605697	-0.565411
17	17	0	-1.926284	-0.186419	-2.137980
18	17	0	-1.926780	0.185278	2.137671

 $\beta\epsilon$ -HCH

Standard orientation:

Center Number	Atomic Number	Atomic Type	Coordinates (Angstroms)		
			X	Y	Z
1	6	0	0.126751	-1.449949	-0.227877
2	6	0	1.320184	-0.615505	0.229281
3	6	0	1.193420	0.834697	-0.228900
4	6	0	-0.126736	1.449975	0.227813
5	6	0	-1.320236	0.615525	-0.229212
6	6	0	-1.193413	-0.834717	0.228865
7	1	0	1.412565	-0.657190	1.318011
8	1	0	0.135645	-1.548030	-1.317141
9	1	0	-0.135582	1.548144	1.317069
10	1	0	1.277140	0.890947	-1.317717
11	1	0	-1.277121	-0.891052	1.317678
12	1	0	-1.412738	0.657251	-1.317929
13	17	0	0.270320	-3.096289	0.445283
14	17	0	-2.546536	-1.783095	-0.445426
15	17	0	-2.817263	1.314604	0.445540
16	17	0	-0.270335	3.096265	-0.445462
17	17	0	2.546532	1.783117	0.445345
18	17	0	2.817297	-1.314615	-0.445268

$\beta$ -HCH Standard orientation:						
Center Number	Atomic Number	Atomic Type	Coordinates (Angstroms)			
			X	Y	Z	
1	6	0	0.158581	0.705475	-1.321802	
2	6	0	-0.158664	-0.792041	-1.271898	
3	6	0	0.158298	-1.497507	0.049972	
4	6	0	-0.158498	-0.705409	1.321868	
5	6	0	0.158712	0.792111	1.271818	
6	6	0	-0.158487	1.497561	-0.049983	
7	1	0	-0.391745	1.289011	2.069786	
8	1	0	0.392124	-1.148020	2.151069	
9	1	0	0.392461	2.436793	-0.081376	
10	1	0	-0.392832	-2.436633	0.081370	
11	1	0	-0.391910	1.148090	-2.151082	
12	1	0	0.391899	-1.288949	-2.069794	
13	17	0	1.888666	1.049494	1.684518	
14	17	0	1.888510	0.934799	-1.750798	
15	17	0	-1.888148	1.984609	-0.066135	
16	17	0	1.887820	-1.984999	0.066077	
17	17	0	-1.888292	-0.934691	1.751363	
18	17	0	-1.888535	-1.049297	-1.685015	

$\gamma$ -HCH Standard orientation:						
Center Number	Atomic Number	Atomic Type	Coordinates (Angstroms)			
			X	Y	Z	
1	6	0	-1.238588	0.469590	0.433110	
2	6	0	-0.000316	1.140990	-0.162454	
3	6	0	1.238315	0.470521	0.433478	
4	6	0	1.293658	-1.027608	0.136248	
5	6	0	0.000331	-1.732475	0.555452	
6	6	0	-1.293213	-1.028461	0.135497	
7	1	0	1.207266	0.588306	1.520716	
8	1	0	0.000745	-2.756280	0.181323	
9	1	0	2.121685	-1.463743	0.696252	
10	1	0	-2.121308	-1.465162	0.694963	
11	1	0	-0.000143	1.078191	-1.253655	
12	1	0	-1.207839	0.587078	1.520381	
13	17	0	-0.001085	2.873043	0.260840	
14	17	0	-2.749666	1.252526	-0.089503	
15	17	0	-1.652863	-1.361041	-1.584850	
16	17	0	-0.000188	-1.853849	2.348332	
17	17	0	1.654632	-1.360291	-1.583789	
18	17	0	2.749081	1.254099	-0.089145	

$\delta$ e-HCH Standard orientation:						
Center Number	Atomic Number	Atomic Type	Coordinates (Angstroms)			
			X	Y	Z	
1	6	0	0.000471	-1.588692	-0.266573	
2	6	0	-1.238376	-0.784596	-0.647548	
3	6	0	-1.283200	0.547678	0.091496	
4	6	0	-0.000541	1.348981	-0.152136	
5	6	0	1.282812	0.548266	0.091025	
6	6	0	1.239244	-0.784527	-0.647472	
7	1	0	1.204896	-0.609704	-1.727208	
8	1	0	-1.432753	0.381732	1.160037	
9	1	0	0.000431	-2.533944	-0.811944	
10	1	0	-1.203685	-0.609252	-1.727187	
11	1	0	-0.000822	1.720986	-1.180751	
12	1	0	1.432764	0.382761	1.159577	
13	17	0	0.000316	-1.999833	1.472846	
14	17	0	2.711598	-1.739481	-0.348553	
15	17	0	2.672720	1.510987	-0.479580	
16	17	0	-0.000563	2.785476	0.907967	
17	17	0	-2.673870	1.509538	-0.478580	
18	17	0	-2.710396	-1.740525	-0.349704	

$\delta\alpha$ -HCH

## Standard orientation:

Center Number	Atomic Number	Atomic Type	Coordinates (Angstroms)		
			X	Y	Z
1	6	0	0.944003	0.184116	-1.301325
2	6	0	-0.490870	-0.356060	-1.294836
3	6	0	-0.779805	-1.104806	-0.000201
4	6	0	-0.491177	-0.356451	1.294770
5	6	0	0.943692	0.183884	1.301453
6	6	0	1.409475	0.849123	0.000162
7	1	0	-0.094487	-1.959254	-0.000267
8	1	0	1.058268	0.892744	2.120978
9	1	0	-0.590979	-1.061733	2.120344
10	1	0	2.498619	0.881203	0.000310
11	1	0	-0.590659	-1.061095	-2.120624
12	1	0	1.058696	0.893118	-2.120707
13	17	0	0.900134	2.571030	0.000236
14	17	0	2.038801	-1.184613	-1.701930
15	17	0	2.038523	-1.184838	1.702033
16	17	0	-1.652666	0.951360	1.667571
17	17	0	-2.410932	-1.809859	-0.000532
18	17	0	-1.652176	0.951990	-1.667388

 $\epsilon\epsilon$ -HCH

## Standard orientation:

Center Number	Atomic Number	Atomic Type	Coordinates (Angstroms)		
			X	Y	Z
1	6	0	-1.253129	0.508285	0.567913
2	6	0	-1.253088	-0.508406	-0.568120
3	6	0	0.000020	-1.386088	-0.501274
4	6	0	1.253317	-0.508578	-0.567981
5	6	0	1.253227	0.508492	0.567794
6	6	0	0.000036	1.386052	0.501425
7	1	0	0.000042	-2.074527	-1.348054
8	1	0	-0.000004	2.074231	1.348409
9	1	0	-1.248060	-0.008393	1.531005
10	1	0	-1.247922	0.008167	-1.531265
11	1	0	1.248398	-0.007962	1.531008
12	1	0	1.248334	0.007804	-1.531236
13	17	0	2.715081	1.522531	0.565157
14	17	0	2.715172	-1.522541	-0.565293
15	17	0	-0.000120	-2.403450	0.971217
16	17	0	-2.715016	-1.522283	-0.565856
17	17	0	-2.715115	1.522109	0.565695
18	17	0	-0.000185	2.403760	-0.970827

 $\epsilon\alpha$ -HCH

## Standard orientation:

Center Number	Atomic Number	Atomic Type	Coordinates (Angstroms)		
			X	Y	Z
1	6	0	0.747242	1.298685	0.173967
2	6	0	-0.746966	1.298778	-0.173414
3	6	0	-1.139125	0.000015	-0.870803
4	6	0	-0.747227	-1.298643	-0.173400
5	6	0	0.746686	-1.298678	0.173638
6	6	0	1.139637	-0.000171	0.871026
7	1	0	-0.952329	-2.128187	-0.850651
8	1	0	0.951785	-2.128408	0.850689
9	1	0	0.582646	-0.000188	1.814042
10	1	0	-0.581553	-0.000091	-1.813481
11	1	0	0.952324	2.128182	0.851300
12	1	0	-0.951976	2.128321	-0.850705
13	17	0	2.855867	-0.000602	1.331893
14	17	0	1.679580	1.657434	-1.310697
15	17	0	1.678612	-1.657199	-1.311311
16	17	0	-1.679627	-1.657049	1.311270
17	17	0	-2.855065	0.000145	-1.332756
18	17	0	-1.679507	1.657298	1.311173

$\zeta$ -HCH

## Standard orientation:

Center Number	Atomic Number	Atomic Type	Coordinates (Angstroms)		
			X	Y	Z
1	6	0	-1.105121	-0.907813	-0.930760
2	6	0	-1.403731	0.527935	-0.492425
3	6	0	-0.233084	1.410990	-0.931415
4	6	0	1.159274	0.951165	-0.492371
5	6	0	1.338521	-0.504315	-0.930668
6	6	0	0.244417	-1.479826	-0.490413
7	1	0	1.891503	1.551804	-1.036091
8	1	0	0.398587	-2.414790	-1.033191
9	1	0	-0.225420	1.362121	-2.026280
10	1	0	-1.064641	-0.876486	-2.025611
11	1	0	-2.289960	0.861380	-1.036417
12	1	0	1.290696	-0.487133	-2.025395
13	17	0	-2.446567	-2.009183	-0.550109
14	17	0	0.318316	-1.926574	1.233563
15	17	0	-1.829989	0.688553	1.231000
16	17	0	2.963080	-1.115299	-0.549860
17	17	0	1.510729	1.240138	1.231172
18	17	0	-0.515711	3.123206	-0.549219

 $\eta$ -HCH

## Standard orientation:

Center Number	Atomic Number	Atomic Type	Coordinates (Angstroms)		
			X	Y	Z
1	6	0	-1.240878	-0.168344	0.515948
2	6	0	-0.937984	0.803060	-0.619985
3	6	0	0.566574	1.094705	-0.694845
4	6	0	1.321268	-0.226767	-0.846001
5	6	0	0.995887	-1.306433	0.183730
6	6	0	-0.518227	-1.498373	0.300388
7	1	0	1.447013	-2.243551	-0.144638
8	1	0	-0.734055	-2.168454	1.133058
9	1	0	-1.238329	0.362297	-1.574335
10	1	0	-0.893063	0.250347	1.463911
11	1	0	1.001769	-0.635959	-1.809698
12	1	0	0.759093	1.700255	-1.582736
13	17	0	-1.092430	-2.338421	-1.175363
14	17	0	1.652922	-1.005113	1.818567
15	17	0	3.073546	0.023342	-1.003477
16	17	0	1.122070	2.080031	0.687792
17	17	0	-1.856851	2.320197	-0.483265
18	17	0	-2.985273	-0.459567	0.713336

 $\theta\epsilon$ -HCH

## Standard orientation:

Center Number	Atomic Number	Atomic Type	Coordinates (Angstroms)		
			X	Y	Z
1	6	0	-0.708321	1.241250	-0.577091
2	6	0	-1.315861	-0.000008	0.079424
3	6	0	-0.708367	-1.241216	-0.577153
4	6	0	0.815493	-1.293536	-0.435866
5	6	0	1.399502	0.000090	-1.002979
6	6	0	0.815510	1.293597	-0.435708
7	1	0	1.187263	-2.126579	-1.035743
8	1	0	1.187325	2.126712	-1.035461
9	1	0	1.137027	0.000162	-2.067362
10	1	0	-0.934304	-1.215081	-1.648302
11	1	0	-0.934188	1.215155	-1.648253
12	1	0	-1.143418	-0.000044	1.158546
13	17	0	-1.435566	2.748287	0.029753
14	17	0	1.320909	1.644936	1.238867
15	17	0	3.176050	0.000131	-0.956484
16	17	0	1.320960	-1.645159	1.238624
17	17	0	-1.435509	-2.748271	0.029772
18	17	0	-3.081399	-0.000006	-0.170367

$\theta\alpha$ -HCH

## Standard orientation:

Center Number	Atomic Number	Atomic Type	Coordinates (Angstroms)		
			X	Y	Z
1	6	0	1.235262	-0.138215	-0.889721
2	6	0	0.000021	-1.039573	-0.895182
3	6	0	-1.235166	-0.138172	-0.889952
4	6	0	-1.299055	0.909369	0.218591
5	6	0	0.000188	1.721607	0.286605
6	6	0	1.299179	0.909123	0.218896
7	1	0	-2.112394	1.597058	-0.015864
8	1	0	2.112786	1.596592	-0.015278
9	1	0	-1.184288	0.427779	-1.826176
10	1	0	1.184554	0.427830	-1.825897
11	1	0	0.000120	2.337931	1.185484
12	1	0	0.000094	-1.596129	-1.834824
13	17	0	1.705309	0.248930	1.829432
14	17	0	2.742024	-1.074080	-0.998015
15	17	0	-0.000136	-2.285315	0.381169
16	17	0	-1.705860	0.249514	1.829088
17	17	0	-2.742009	-1.073893	-0.998273
18	17	0	0.000468	2.868026	-1.100042

 $\alpha e$ -HFH

## Standard orientation:

Center Number	Atomic Number	Atomic Type	Coordinates (Angstroms)		
			X	Y	Z
1	6	0	-0.749660	-1.443912	-0.139860
2	6	0	0.749674	-1.443913	0.139821
3	6	0	1.395018	-0.195242	-0.432679
4	6	0	0.750928	1.065075	0.114239
5	6	0	-0.750942	1.065065	-0.114237
6	6	0	-1.395001	-0.195262	0.432688
7	1	0	1.225960	-2.340646	-0.259420
8	1	0	-1.225939	-2.340660	0.259358
9	1	0	0.974820	1.180744	1.177975
10	1	0	-0.974841	1.180728	-1.177972
11	1	0	-1.319648	-0.212493	1.523189
12	1	0	1.319704	-0.212456	-1.523184
13	9	0	-0.910049	-1.441583	-1.525208
14	9	0	0.910056	-1.441629	1.525175
15	9	0	2.745055	-0.188917	-0.101223
16	9	0	1.296158	2.165764	-0.542874
17	9	0	-1.296182	2.165749	0.542874
18	9	0	-2.745052	-0.188949	0.101280

 $\alpha a$ -HFH

## Standard orientation:

Center Number	Atomic Number	Atomic Type	Coordinates (Angstroms)		
			X	Y	Z
1	6	0	-1.075622	-0.566629	-0.502433
2	6	0	-1.075598	0.566664	0.502446
3	6	0	0.149904	1.442981	0.313668
4	6	0	1.447193	0.644878	0.410275
5	6	0	1.447165	-0.644922	-0.410283
6	6	0	0.149847	-1.442984	-0.313667
7	9	0	0.096776	-2.005977	0.960916
8	9	0	1.620316	-0.301281	-1.748644
9	9	0	1.620344	0.301237	1.748642
10	9	0	0.096846	2.005955	-0.960925
11	1	0	0.154256	2.255470	1.042905
12	1	0	2.285080	1.271045	0.096514
13	1	0	2.285037	-1.271111	-0.096524
14	1	0	0.154155	-2.255471	-1.042908
15	1	0	-1.099540	-0.174888	-1.522244
16	1	0	-1.099531	0.174931	1.522259
17	9	0	-2.213657	-1.345477	-0.318285
18	9	0	-2.213602	1.345553	0.318292

$\beta\text{-HFH}$ 

## Standard orientation:

Center Number	Atomic Number	Atomic Type	Coordinates (Angstroms)		
			X	Y	Z
1	6	0	0.637692	1.300271	-0.225991
2	6	0	-0.807257	1.202627	0.226385
3	6	0	-1.445012	-0.097692	-0.225616
4	6	0	-0.637692	-1.300272	0.225991
5	6	0	0.807257	-1.202627	-0.226385
6	6	0	1.445012	0.097692	0.225616
7	1	0	-0.874613	1.304260	1.313465
8	1	0	0.690810	1.409678	-1.313097
9	9	0	-1.517994	2.261289	-0.329275
10	9	0	1.199483	2.445192	0.329130
11	1	0	-0.690810	-1.409678	1.313097
12	9	0	-1.199483	-2.445192	-0.329130
13	1	0	-1.566184	-0.105442	-1.312745
14	1	0	1.566184	0.105442	1.312745
15	1	0	0.874613	-1.304260	-1.313465
16	9	0	1.517994	-2.261289	0.329275
17	9	0	2.717582	0.184053	-0.328996
18	9	0	-2.717582	-0.184053	0.328996

 $\beta\text{a-HFH}$ 

## Standard orientation:

Center Number	Atomic Number	Atomic Type	Coordinates (Angstroms)		
			X	Y	Z
1	6	0	-0.538804	-1.381398	0.181118
2	6	0	-1.467688	-0.222968	-0.167079
3	6	0	-0.925142	1.158456	0.183763
4	6	0	0.538803	1.381401	-0.181118
5	6	0	1.467686	0.222971	0.167080
6	6	0	0.925140	-1.158454	-0.183764
7	9	0	1.682823	0.254295	1.543083
8	9	0	0.604527	1.574327	-1.559142
9	9	0	1.044945	-1.320125	-1.562169
10	9	0	-1.044943	1.320122	1.562171
11	9	0	-0.604527	-1.574329	1.559140
12	9	0	-1.682821	-0.254296	-1.543084
13	1	0	2.424314	0.369084	-0.339964
14	1	0	0.895888	2.286177	0.316300
15	1	0	1.535373	-1.917225	0.311807
16	1	0	-1.535376	1.917230	-0.311800
17	1	0	-0.895890	-2.286171	-0.316305
18	1	0	-2.424317	-0.369081	0.339962

 $\gamma\text{-HFH}$ 

## Standard orientation:

Center Number	Atomic Number	Atomic Type	Coordinates (Angstroms)		
			X	Y	Z
1	6	0	-1.239510	0.533043	0.385691
2	6	0	-0.000028	1.235137	-0.136578
3	6	0	1.239486	0.533096	0.385693
4	6	0	1.277369	-0.928458	-0.023731
5	6	0	0.000031	-1.658912	0.385400
6	6	0	-1.277331	-0.928509	-0.023739
7	1	0	1.272843	0.607196	1.476689
8	1	0	0.000052	-2.668947	-0.028050
9	1	0	2.146971	-1.422053	0.414917
10	1	0	-2.146921	-1.422139	0.414891
11	9	0	2.369108	1.170411	-0.113656
12	9	0	1.390964	-1.002370	-1.408808
13	9	0	0.000028	-1.736036	1.777380
14	9	0	-1.390902	-1.002419	-1.408820
15	1	0	-0.000029	1.281914	-1.227723
16	1	0	-1.272875	0.607136	1.476686
17	9	0	-0.000052	2.545050	0.338251
18	9	0	-2.369162	1.170310	-0.113662

$\delta e$ -HFH

## Standard orientation:

Center Number	Atomic Number	Atomic Type	Coordinates (Angstroms)		
			X	Y	Z
1	6	0	-0.000002	-1.544674	-0.133055
2	6	0	-1.242433	-0.769759	-0.528621
3	6	0	-1.263833	0.587602	0.150068
4	6	0	0.000004	1.375338	-0.150126
5	6	0	1.263835	0.587597	0.150073
6	6	0	1.242426	-0.769757	-0.528626
7	1	0	1.284194	-0.657065	-1.616158
8	1	0	-1.393058	0.470761	1.228556
9	1	0	-0.000002	-2.542823	-0.573833
10	9	0	-0.000004	-1.691408	1.256205
11	9	0	-2.355102	1.311357	-0.322115
12	9	0	2.368171	-1.482721	-0.136049
13	1	0	-1.284204	-0.657075	-1.616155
14	1	0	0.000007	1.703659	-1.193735
15	1	0	1.393048	0.470749	1.228562
16	9	0	-2.368173	-1.482713	-0.136030
17	9	0	0.000004	2.524549	0.636140
18	9	0	2.355108	1.311349	-0.322096

 $\delta a$ -HFH

## Standard orientation:

Center Number	Atomic Number	Atomic Type	Coordinates (Angstroms)		
			X	Y	Z
1	6	0	-0.878729	-1.287441	-0.045739
2	6	0	0.645452	-1.272162	-0.139462
3	6	0	1.131737	-0.000010	-0.804722
4	6	0	0.645472	1.272155	-0.139470
5	6	0	-0.878708	1.287453	-0.045752
6	6	0	-1.492354	0.000014	0.500869
7	1	0	0.761219	-0.000009	-1.835170
8	1	0	-1.200377	2.129596	0.570518
9	1	0	0.983880	2.141543	-0.707954
10	1	0	-2.563623	0.000023	0.285288
11	1	0	0.983847	-2.141559	-0.707939
12	1	0	-1.200402	-2.129570	0.570548
13	9	0	2.521290	-0.000022	-0.843108
14	9	0	1.160108	-1.376872	1.147953
15	9	0	1.160131	1.376869	1.147943
16	9	0	-1.362597	1.468279	-1.341063
17	9	0	-1.316501	0.000019	1.881579
18	9	0	-1.362627	-1.468282	-1.341042

 $\epsilon e$ -HFH

## Standard orientation:

Center Number	Atomic Number	Atomic Type	Coordinates (Angstroms)		
			X	Y	Z
1	6	0	-1.253004	0.565533	0.506206
2	6	0	-1.253012	-0.565527	-0.506211
3	6	0	-0.000003	-1.410637	-0.349559
4	6	0	1.253009	-0.565533	-0.506205
5	6	0	1.253008	0.565530	0.506209
6	6	0	0.000003	1.410642	0.349549
7	9	0	0.000007	1.948946	-0.940778
8	9	0	-0.000009	-1.948949	0.940767
9	1	0	-0.000002	-2.243791	-1.054136
10	1	0	0.000001	2.243799	1.054123
11	1	0	-1.317120	0.168869	1.522501
12	1	0	-1.317137	-0.168866	-1.522507
13	9	0	-2.366076	1.369828	0.293165
14	9	0	-2.366081	-1.369819	-0.293155
15	1	0	1.317126	0.168873	1.522506
16	1	0	1.317140	-0.168870	-1.522500
17	9	0	2.366083	1.369818	0.293158
18	9	0	2.366074	-1.369830	-0.293149

$\epsilon$ -HFH

## Standard orientation:

Center Number	Atomic Number	Atomic Type	Coordinates (Angstroms)		
			X	Y	Z
1	6	0	0.760661	1.276066	0.072458
2	6	0	-0.760660	1.276067	-0.072458
3	6	0	-1.232052	0.000001	-0.747362
4	6	0	-0.760661	-1.276066	-0.072458
5	6	0	0.760660	-1.276067	0.072458
6	6	0	1.232052	-0.000000	0.747362
7	1	0	-1.083472	-2.145347	-0.648899
8	1	0	1.083470	-2.145347	0.648898
9	1	0	0.837992	-0.000000	1.768588
10	1	0	-0.837992	0.000000	-1.768588
11	1	0	1.083472	2.145347	0.648899
12	1	0	-1.083470	2.145348	-0.648898
13	9	0	1.303399	1.382253	-1.205156
14	9	0	-1.303398	1.382252	1.205156
15	9	0	1.303398	-1.382253	-1.205156
16	9	0	-1.303399	-1.382253	1.205155
17	9	0	-2.619666	0.000001	-0.814355
18	9	0	2.619666	-0.000001	0.814355

 $\zeta$ -HFH

## Standard orientation:

Center Number	Atomic Number	Atomic Type	Coordinates (Angstroms)		
			X	Y	Z
1	6	0	-1.344604	-0.497190	-0.701841
2	6	0	-1.132326	0.939955	-0.248551
3	6	0	0.241529	1.412441	-0.701477
4	6	0	1.380388	0.510443	-0.248408
5	6	0	1.102861	-0.915517	-0.701713
6	6	0	-0.248039	-1.450270	-0.248888
7	9	0	1.506392	0.556789	1.133632
8	9	0	-0.270535	-1.581419	1.133356
9	1	0	2.325472	0.860309	-0.670864
10	1	0	-0.417785	-2.443946	-0.670477
11	1	0	0.248687	1.452670	-1.796189
12	1	0	-1.384324	-0.511464	-1.796458
13	9	0	0.461010	2.697277	-0.226386
14	9	0	-2.566586	-0.949518	-0.225460
15	9	0	-1.235395	1.025201	1.133572
16	1	0	-1.907410	1.584293	-0.670566
17	1	0	1.135363	-0.941603	-1.796344
18	9	0	2.105240	-1.748267	-0.225808

 $\eta$ -HFH

## Standard orientation:

Center Number	Atomic Number	Atomic Type	Coordinates (Angstroms)		
			X	Y	Z
1	6	0	-1.279464	-0.220674	0.478465
2	6	0	-0.953690	0.892797	-0.498305
3	6	0	0.529257	1.227701	-0.448936
4	6	0	1.355649	-0.016604	-0.728502
5	6	0	1.027988	-1.185650	0.187935
6	6	0	-0.471912	-1.468187	0.163453
7	1	0	1.585807	-2.072205	-0.119569
8	1	0	-0.725329	-2.272207	0.856068
9	9	0	1.377253	-0.891875	1.501377
10	9	0	-0.787374	-1.889697	-1.129747
11	1	0	-1.242721	0.607397	-1.512956
12	1	0	-1.075109	0.100282	1.502725
13	9	0	-1.679605	2.027778	-0.156010
14	9	0	-2.632819	-0.527794	0.386580
15	1	0	1.163697	-0.331848	-1.759064
16	1	0	0.770056	2.015064	-1.166167
17	9	0	2.703601	0.294103	-0.614794
18	9	0	0.827459	1.718287	0.820850

$\theta_{e-HFH}$ 

Standard orientation:

Center Number	Atomic Number	Atomic Type	Coordinates (Angstroms)		
			X	Y	Z
1	6	0	-0.695979	1.245813	-0.451547
2	6	0	-1.328390	0.000000	0.143696
3	6	0	-0.695980	-1.245813	-0.451547
4	6	0	0.808139	-1.270029	-0.230175
5	6	0	1.433165	-0.000000	-0.786821
6	6	0	0.808140	1.270029	-0.230175
7	9	0	1.051563	-1.359960	1.136940
8	9	0	1.051564	1.359960	1.136940
9	1	0	1.250623	-2.151351	-0.699100
10	1	0	1.250623	2.151351	-0.699099
11	1	0	1.310405	0.000000	-1.875308
12	1	0	-0.917491	-1.303822	-1.521948
13	1	0	-0.917490	1.303822	-1.521948
14	1	0	-1.237526	0.000000	1.232238
15	9	0	2.791755	-0.000001	-0.508459
16	9	0	-1.255077	-2.365627	0.150819
17	9	0	-1.255076	2.365627	0.150818
18	9	0	-2.686254	0.000001	-0.164326

 $\theta_{a-HFH}$ 

Standard orientation:

Center Number	Atomic Number	Atomic Type	Coordinates (Angstroms)		
			X	Y	Z
1	6	0	1.236671	-0.415645	-0.720813
2	6	0	0.000041	-1.274849	-0.518628
3	6	0	-1.236629	-0.415710	-0.720821
4	6	0	-1.284388	0.814549	0.169346
5	6	0	-0.000046	1.633813	0.043085
6	6	0	1.284332	0.814606	0.169385
7	9	0	-1.433796	0.444603	1.499729
8	9	0	1.433709	0.444639	1.499760
9	1	0	-2.139661	1.437049	-0.104374
10	1	0	2.139587	1.437151	-0.104288
11	1	0	-1.251977	-0.077438	-1.762217
12	1	0	1.252017	-0.077369	-1.762203
13	9	0	-2.371971	-1.185460	-0.503226
14	9	0	2.372057	-1.185332	-0.503207
15	9	0	0.000054	-1.825537	0.757550
16	9	0	-0.000036	2.197166	-1.234122
17	1	0	-0.000081	2.434824	0.784340
18	1	0	0.000060	-2.105502	-1.228929

**Table S1.** Relative Gibbs energy for all isomers, G<sub>rel</sub>, in kcal mol<sup>-1</sup>. Relative Gibbs energy from the conformational ring flip isomerism, ΔG<sub>rel</sub>, in kcal mol<sup>-1</sup>, and the conformational population, in parenthesis. Nuclear-electronic relative energy, E<sub>rel</sub>, in kcal mol<sup>-1</sup>. Dipole moment, μ, Debye. The data were acquired in gas phase and implicit water at the MP2/6-311++g(d,p) level of theory.

Isomer	Gas Phase				Implicit Water			
	G <sub>rel</sub>	ΔG <sub>rel</sub>	E <sub>rel</sub>	μ	G <sub>rel</sub>	ΔG <sub>rel</sub>	E <sub>rel</sub>	μ
<b>α<sub>e</sub>-HCH</b>	0.00	0.00 (100%)	0.00	2.37	0.00	0.00 (100%)	0.00	3.31
<b>α<sub>a</sub>-HCH</b>	4.06	4.06 (0%)	3.76	2.28	4.36	4.36 (0%)	4.08	3.20
<b>β<sub>e</sub>-HCH</b>	3.43	0.00 (100%)	3.95	0.00	2.25	0.00 (100%)	2.38	0.00
<b>β<sub>a</sub>-HCH</b>	11.29	7.86 (0%)	10.71	0.00	11.67	9.42 (0%)	11.12	0.00
<b>γ-HCH</b>	3.47	-	3.38	3.04	3.34	-	3.16	4.42
<b>δ<sub>e</sub>-HCH</b>	1.99	0.00 (100%)	2.23	2.16	0.66	0.00 (100%)	1.01	3.23
<b>δ<sub>a</sub>-HCH</b>	7.72	5.73 (0%)	7.23	2.07	7.76	7.10 (0%)	7.28	3.17
<b>ε<sub>e</sub>-HCH</b>	2.04	0.00 (96%)	1.96	0.00	1.24	0.00 (99%)	1.13	0.00
<b>ε<sub>a</sub>-HCH</b>	3.86	1.82 (4%)	3.46	0.00	3.94	2.70 (1%)	3.64	0.00
<b>ζ-HCH</b>	11.71	-	11.48	5.19	7.87	-	7.37	8.07
<b>η-HCH</b>	3.35	-	3.10	2.22	2.74	-	2.48	3.35
<b>θ<sub>e</sub>-HCH</b>	6.73	0.00 (87%)	6.84	3.68	4.44	0.00 (97%)	4.40	5.61
<b>θ<sub>a</sub>-HCH</b>	7.85	1.12 (13%)	7.42	3.58	6.45	2.01 (3%)	6.05	5.59
<b>α<sub>e</sub>-HFH</b>	0.00	0.00 (97%)	0.18	3.30	0.69	0.00 (99%)	0.97	4.17
<b>α<sub>a</sub>-HFH</b>	2.12	2.12 (3%)	2.29	3.04	3.27	2.58 (1%)	3.40	3.87
<b>β<sub>e</sub>-HFH</b>	1.90	0.00 (100%)	2.66	0.00	0.88	0.00 (100%)	1.43	0.00
<b>β<sub>a</sub>-HFH</b>	6.58	4.68 (0%)	7.03	0.00	7.49	6.61 (0%)	7.79	0.00
<b>γ-HFH</b>	1.97	-	2.20	4.30	2.35	-	2.65	5.59
<b>δ<sub>e</sub>-HFH</b>	1.02	0.00 (100%)	1.39	3.03	0.21	0.00 (100%)	0.65	4.10
<b>δ<sub>a</sub>-HFH</b>	4.93	3.91 (0%)	5.15	2.86	5.38	5.17 (0%)	5.55	3.82
<b>ε<sub>e</sub>-HFH</b>	0.04	0.00 (99%)	0.00	0.00	0.00	0.00 (100%)	0.00	0.00
<b>ε<sub>a</sub>-HFH</b>	2.94	2.90 (1%)	2.92	0.00	3.45	3.45 (0%)	3.46	0.0
<b>ζ-HFH</b>	8.94	-	8.97	7.23	3.89	-	3.82	9.90
<b>η-HFH</b>	2.00	-	1.99	3.08	1.86	-	1.87	4.11
<b>θ<sub>e</sub>-HFH</b>	4.09	0.00 (95%)	4.33	5.16	1.68	0.00 (99%)	1.91	7.08
<b>θ<sub>a</sub>-HFH</b>	5.85	1.76 (5%)	5.89	5.05	4.31	2.63 (1%)	4.30	6.85

**Table S2.** Relative full energy (E<sub>Full</sub>), Lewis energy (E<sub>Lewis</sub>), and non-Lewis energy (E<sub>non-Lewis</sub>), in kcal mol<sup>-1</sup>, obtained through Natural Bond Orbital (NBO) analysis at the B3LYP/6-311++g(d,p) level.

Isomers	HCH			HFH		
	E <sub>Full</sub>	E <sub>Lewis</sub>	E <sub>non-Lewis</sub>	E <sub>Full</sub>	E <sub>Lewis</sub>	E <sub>non-Lewis</sub>
<b>α<sub>e</sub></b>	0.00	15.34	-15.34	0.00	19.91	-19.91
<b>α<sub>a</sub></b>	3.67	21.03	-17.36	2.20	16.22	-14.02
<b>β<sub>e</sub></b>	2.75	2.75	0.00	1.60	27.30	-25.70
<b>β<sub>a</sub></b>	8.83	18.43	-9.60	6.30	6.30	0.00
<b>γ</b>	3.41	20.06	-16.65	2.07	23.14	-21.07
<b>δ<sub>e</sub></b>	2.05	16.63	-14.58	1.05	29.15	-28.10
<b>δ<sub>a</sub></b>	6.65	40.70	-34.05	4.91	21.92	-17.01
<b>ε<sub>e</sub></b>	2.23	27.45	-25.22	0.21	30.36	-30.15
<b>ε<sub>a</sub></b>	3.90	32.91	-29.01	3.10	35.95	-32.85
<b>ζ</b>	12.53	76.53	-64.00	9.48	72.85	-63.37
<b>η</b>	3.59	30.17	-26.58	2.22	33.15	-30.93
<b>θ<sub>e</sub></b>	7.32	30.28	-22.96	4.38	45.75	-41.37
<b>θ<sub>a</sub></b>	7.72	58.64	-50.92	6.10	44.48	-38.38

**Table S3.** Docking score ( $D_{\text{score}}$ ), in kcal mol<sup>-1</sup>, and the ligand efficiency SA (surface area) of HCH and HFH isomers in the picrotoxin and barbiturate sites of GABA<sub>A</sub> receptor and InsP<sub>3</sub> receptor.

Isomer	Picrotoxin site		Barbiturate site		InsP <sub>3</sub> receptor	
	$D_{\text{score}}$	Efficiency SA	$D_{\text{score}}$	Efficiency SA	$D_{\text{score}}$	Efficiency SA
<b><math>\alpha_e\text{-HCH}</math></b>	-3.72	-0.711	-4.39	-0.838	-0.68	-0.129
<b><math>\alpha_a\text{-HCH}</math></b>	-3.94	-0.753	-4.65	-0.887	-0.89	-0.171
<b><math>\beta_e\text{-HCH}</math></b>	-3.82	-0.728	-3.39	-0.648	-0.56	-0.107
<b><math>\beta_a\text{-HCH}</math></b>	-3.70	-0.706	-4.41	-0.841	-0.53	-0.101
<b><math>\gamma\text{-HCH}</math></b>	-3.86	-0.737	-4.14	-0.790	-1.05	-0.201
<b><math>\delta_e\text{-HCH}</math></b>	-3.96	-0.756	-4.10	-0.782	-1.29	-0.247
<b><math>\delta_a\text{-HCH}</math></b>	-3.98	-0.760	-3.99	-0.761	-0.60	-0.114
<b><math>\varepsilon_e\text{-HCH}</math></b>	-3.73	-0.711	-3.94	-0.751	-0.41	-0.078
<b><math>\varepsilon_a\text{-HCH}</math></b>	-4.09	-0.779	-4.33	-0.826	-0.35	-0.066
<b><math>\zeta\text{-HCH}</math></b>	-2.99	-0.570	-4.07	-0.777	-0.57	-0.108
<b><math>\eta\text{-HCH}</math></b>	-3.52	-0.672	-4.09	-0.781	-0.92	-0.175
<b><math>\theta_e\text{-HCH}</math></b>	-3.91	-0.746	-4.34	-0.827	-0.65	-0.124
<b><math>\theta_a\text{-HCH}</math></b>	-3.94	-0.751	-4.18	-0.798	-0.16	-0.031
<b><math>\alpha_e\text{-HFH}</math></b>	-3.80	-0.726	-4.50	-0.859	-0.04	-0.007
<b><math>\alpha_a\text{-HFH}</math></b>	-3.74	-0.714	-4.34	-0.827	-0.46	-0.088
<b><math>\beta_e\text{-HFH}</math></b>	-3.95	-0.754	-4.69	-0.894	-0.80	-0.153
<b><math>\beta_a\text{-HFH}</math></b>	-4.20	-0.801	-4.42	-0.844	-1.12	-0.213
<b><math>\gamma\text{-HFH}</math></b>	-3.87	-0.738	-4.54	-0.866	-0.46	-0.088
<b><math>\delta_e\text{-HFH}</math></b>	-3.86	-0.736	-4.61	-0.879	-0.69	-0.131
<b><math>\delta_a\text{-HFH}</math></b>	-3.90	-0.745	-4.34	-0.829	0.01	0.002
<b><math>\varepsilon_e\text{-HFH}</math></b>	-3.47	-0.662	-3.95	-0.753	0.16	0.031
<b><math>\varepsilon_a\text{-HFH}</math></b>	-3.94	-0.752	-4.38	-0.836	-0.34	-0.064
<b><math>\zeta\text{-HFH}</math></b>	-4.02	-0.768	-4.57	-0.872	-0.60	-0.114
<b><math>\eta\text{-HFH}</math></b>	-3.83	-0.731	-4.39	-0.838	-0.24	-0.046
<b><math>\theta_e\text{-HFH}</math></b>	-3.95	-0.754	-4.73	-0.903	-0.15	-0.028
<b><math>\theta_a\text{-HFH}</math></b>	-3.86	-0.737	-4.48	-0.854	-0.29	-0.056

**Table S4.** Docking score ( $D_{\text{score}}$ ), in kcal mol<sup>-1</sup>, and the ligand efficiency SA (surface area) of HCH and HFH isomers in three predicted sites of ryanodine receptor.

Isomer	RyR site 1		RyR site 2		RyR site 3	
	$D_{\text{score}}$	Efficiency SA	$D_{\text{score}}$	Efficiency SA	$D_{\text{score}}$	Efficiency SA
<b><math>\alpha_e\text{-HCH}</math></b>	-3.21	-0.612	-1.52	-0.289	-1.51	-0.289
<b><math>\alpha_a\text{-HCH}</math></b>	-3.52	-0.672	-1.77	-0.338	-0.85	-0.162
<b><math>\beta_e\text{-HCH}</math></b>	-2.62	-0.500	-1.08	-0.206	-0.23	-0.044
<b><math>\beta_a\text{-HCH}</math></b>	-3.42	-0.652	-1.12	-0.214	-1.37	-0.260
<b><math>\gamma\text{-HCH}</math></b>	-3.63	-0.692	-2.12	-0.405	-0.49	-0.093
<b><math>\delta_e\text{-HCH}</math></b>	-3.01	-0.573	-1.99	-0.381	-1.78	-0.339
<b><math>\delta_a\text{-HCH}</math></b>	-3.40	-0.648	-1.99	-0.382	-1.60	-0.305
<b><math>\varepsilon_e\text{-HCH}</math></b>	-3.00	-0.573	-2.24	-0.428	-1.48	-0.283
<b><math>\varepsilon_a\text{-HCH}</math></b>	-3.38	-0.646	-1.66	-0.318	-0.26	-0.050
<b><math>\zeta\text{-HCH}</math></b>	-3.08	-0.588	-1.81	-0.346	-1.17	-0.224
<b><math>\eta\text{-HCH}</math></b>	-3.23	-0.616	-1.60	-0.306	-1.28	-0.244
<b><math>\theta_e\text{-HCH}</math></b>	-3.11	-0.593	-1.99	-0.381	-1.16	-0.222
<b><math>\theta_a\text{-HCH}</math></b>	-3.59	-0.685	-1.66	-0.317	-0.32	-0.061
<b><math>\alpha_e\text{-HFH}</math></b>	-3.64	-0.695	-1.31	-0.251	-0.29	-0.055
<b><math>\alpha_a\text{-HFH}</math></b>	-3.58	-0.684	-1.54	-0.293	-0.19	-0.037
<b><math>\beta_e\text{-HFH}</math></b>	-2.93	-0.558	-0.49	-0.094	0.22	0.041
<b><math>\beta_a\text{-HFH}</math></b>	-3.55	-0.677	-0.90	-0.172	-0.66	-0.125
<b><math>\gamma\text{-HFH}</math></b>	-3.50	-0.668	-1.34	-0.256	0.36	0.069
<b><math>\delta_e\text{-HFH}</math></b>	-3.54	-0.675	-1.59	-0.304	-0.01	-0.001
<b><math>\delta_a\text{-HFH}</math></b>	-3.48	-0.665	-1.22	-0.232	0.24	0.045
<b><math>\varepsilon_e\text{-HFH}</math></b>	-3.68	-0.702	-1.52	-0.290	0.68	0.130
<b><math>\varepsilon_a\text{-HFH}</math></b>	-3.70	-0.706	-1.24	-0.237	-0.70	-0.133
<b><math>\zeta\text{-HFH}</math></b>	-3.11	-0.595	-1.67	-0.319	-0.66	-0.127
<b><math>\eta\text{-HFH}</math></b>	-3.08	-0.588	-1.17	-0.222	0.37	0.070
<b><math>\theta_e\text{-HFH}</math></b>	-3.67	-0.701	-1.86	-0.355	0.29	0.055
<b><math>\theta_a\text{-HFH}</math></b>	-3.52	-0.671	-1.26	-0.240	0.46	0.087

**Table S5.** Number and types of interactions of HCHs and HFHs in the picrotoxin site of GABA<sub>A</sub> receptor.

Isomer	X•••HO	X•••HC	X•••π <sub>CO/N</sub>	R•••π <sub>Ar</sub>	R•••R
<b>α<sub>e</sub>-HCH</b>	-	-	-	-	-
<b>α<sub>a</sub>-HCH</b>	-	1	-	-	-
<b>β<sub>e</sub>-HCH</b>	-	-	-	-	-
<b>β<sub>a</sub>-HCH</b>	-	-	-	-	-
<b>γ-HCH</b>	-	2	-	-	-
<b>δ<sub>e</sub>-HCH</b>	-	3	-	-	-
<b>δ<sub>a</sub>-HCH</b>	-	-	-	-	-
<b>ε<sub>e</sub>-HCH</b>	-	-	-	-	-
<b>ε<sub>a</sub>-HCH</b>	-	-	-	-	-
<b>ζ-HCH</b>	-	-	-	-	-
<b>η-HCH</b>	-	-	-	-	-
<b>θ<sub>e</sub>-HCH</b>	-	1	-	-	-
<b>θ<sub>a</sub>-HCH</b>	-	2	-	-	-
<b>α<sub>e</sub>-HFH</b>	1	-	1	-	-
<b>α<sub>a</sub>-HFH</b>	-	-	-	-	-
<b>β<sub>e</sub>-HFH</b>	-	-	-	-	-
<b>β<sub>a</sub>-HFH</b>	-	-	-	-	-
<b>γ-HFH</b>	-	-	-	-	-
<b>δ<sub>e</sub>-HFH</b>	-	-	-	-	-
<b>δ<sub>a</sub>-HFH</b>	-	1	-	-	-
<b>ε<sub>e</sub>-HFH</b>	-	-	-	-	-
<b>ε<sub>a</sub>-HFH</b>	-	-	-	-	-
<b>ζ-HFH</b>	-	-	-	-	-
<b>η-HFH</b>	1	1	2	-	-
<b>θ<sub>e</sub>-HFH</b>	-	-	-	-	-
<b>θ<sub>a</sub>-HFH</b>	-	-	-	-	-

**Table S6.** Number and types of interactions of HCHs and HFHs in the barbiturate site of GABA<sub>A</sub> receptor.

Isomer	X•••HO	X•••HC	X•••π <sub>CO/N</sub>	R•••π <sub>Ar</sub>	R•••R
<b>α<sub>e</sub>-HCH</b>	-	4	2	1	-
<b>α<sub>a</sub>-HCH</b>	-	4	2	1	-
<b>β<sub>e</sub>-HCH</b>	-	-	1	-	-
<b>β<sub>a</sub>-HCH</b>	-	1	1	-	-
<b>γ-HCH</b>	-	4	1	1	-
<b>δ<sub>e</sub>-HCH</b>	-	2	-	-	-
<b>δ<sub>a</sub>-HCH</b>	-	4	2	1	-
<b>ε<sub>e</sub>-HCH</b>	-	4	2	1	-
<b>ε<sub>a</sub>-HCH</b>	-	1	2	-	-
<b>ζ-HCH</b>	-	3	1	1	-
<b>η-HCH</b>	-	4	2	1	-
<b>θ<sub>e</sub>-HCH</b>	-	3	-	-	-
<b>θ<sub>a</sub>-HCH</b>	-	4	1	1	-
<b>α<sub>e</sub>-HFH</b>	-	3	2	-	-
<b>α<sub>a</sub>-HFH</b>	-	5	3	1	-
<b>β<sub>e</sub>-HFH</b>	-	2	5	-	-
<b>β<sub>a</sub>-HFH</b>	-	3	3	1	-
<b>γ-HFH</b>	-	3	3	1	-
<b>δ<sub>e</sub>-HFH</b>	2	-	1	-	-
<b>δ<sub>a</sub>-HFH</b>	-	3	3	1	-
<b>ε<sub>e</sub>-HFH</b>	-	3	1	1	-
<b>ε<sub>a</sub>-HFH</b>	-	4	2	1	-
<b>ζ-HFH</b>	-	2	2	-	-
<b>η-HFH</b>	-	3	1	-	-
<b>θ<sub>e</sub>-HFH</b>	-	2	2	-	-
<b>θ<sub>a</sub>-HFH</b>	-	3	2	1	-

**Table S7.** Number and types of interactions of HCHs and HFHs in the site 1 of ryanodine receptor.

Isomer	X•••HO	X•••HC	X•••π <sub>CO/N</sub>	R•••π <sub>Ar</sub>	R•••R
<b>α<sub>e</sub>-HCH</b>	-	4	2	-	-
<b>α<sub>a</sub>-HCH</b>	1	5	2	-	-
<b>β<sub>e</sub>-HCH</b>	1	3	4	-	-
<b>β<sub>a</sub>-HCH</b>	-	3	-	-	-
<b>γ-HCH</b>	-	3	1	-	-
<b>δ<sub>e</sub>-HCH</b>	1	4	3	-	-
<b>δ<sub>a</sub>-HCH</b>	-	2	-	-	-
<b>ε<sub>e</sub>-HCH</b>	-	4	2	-	-
<b>ε<sub>a</sub>-HCH</b>	-	3	-	-	-
<b>ζ-HCH</b>	-	5	2	-	1
<b>η-HCH</b>	-	2	1	-	-
<b>θ<sub>e</sub>-HCH</b>	-	4	2	-	-
<b>θ<sub>a</sub>-HCH</b>	-	6	3	-	-
<b>α<sub>e</sub>-HFH</b>	2	4	4	-	-
<b>α<sub>a</sub>-HFH</b>	2	3	4	-	-
<b>β<sub>e</sub>-HFH</b>	2	3	5	-	-
<b>β<sub>a</sub>-HFH</b>	2	3	3	-	-
<b>γ-HFH</b>	2	4	4	-	-
<b>δ<sub>e</sub>-HFH</b>	1	3	4	-	-
<b>δ<sub>a</sub>-HFH</b>	2	3	5	-	-
<b>ε<sub>e</sub>-HFH</b>	1	2	5	-	-
<b>ε<sub>a</sub>-HFH</b>	2	3	4	-	-
<b>ζ-HFH</b>	1	4	4	-	1
<b>η-HFH</b>	-	4	2	-	-
<b>θ<sub>e</sub>-HFH</b>	2	3	4	-	1
<b>θ<sub>a</sub>-HFH</b>	3	4	7	-	-

## APPENDIX E

Supporting Information for:

### An examination of the relationship between molecular dipole moment and blood-gas partition for common anaesthetic gases

## INDEX

Standard coordinates for the optimized geometries of the fluorinated anaesthetics	227
<b>Table S1.</b> Weighted dipole moment (Db), blood-gas partition coefficient ( $K_{bg}$ ), and MAC (%) for the studied fluorinated anaesthetics	241
<b>Table S2.</b> Conformational Gibbs free energies (in kcal mol <sup>-1</sup> ) and population (%), in parenthesis), molecular dipole moments ( $\mu$ , in Db), bond lengths (in Å), and dihedral angles (degrees) obtained for the main conformers of the studied fluorinated anesthetics	242
<b>Table S3.</b> Important electron delocalization interactions obtained through NBO analysis (in kcal mol <sup>-1</sup> ) in the gas phase at the B3LYP/aug-cc-pVTZ level.	243

## STANDARD COORDINATES

**H**

Standard orientation:  
 Free Gibbs Energy (Hartree) = -3408.289718

Center Number	Atomic Number	Atomic Type	Coordinates (Angstroms)		
			X	Y	Z
1	6	0	-0.102819	0.360968	-0.523301
2	1	0	-0.135755	0.348512	-1.607686
3	6	0	-1.204364	-0.558340	-0.000622
4	9	0	-1.231299	-0.615950	1.327592
5	9	0	-2.395775	-0.124076	-0.427818
6	9	0	-1.029610	-1.795946	-0.476669
7	17	0	-0.382846	2.006750	0.029356
8	35	0	1.611354	-0.298722	0.012692

**Esag**

Standard orientation:  
 Free Gibbs Energy (Hartree) = -1148.792883

Center Number	Atomic Number	Atomic Type	Coordinates (Angstroms)		
			X	Y	Z
1	6	0	1.529131	0.199256	-0.525229
2	1	0	1.472187	0.321875	-1.603815
3	6	0	0.186844	0.577409	0.101733
4	6	0	-2.068720	-0.009704	0.039353
5	1	0	-2.171127	0.907693	0.612752
6	8	0	-0.787041	-0.185033	-0.475259
7	9	0	2.475122	1.031637	-0.018689
8	17	0	1.932380	-1.468933	-0.163139
9	9	0	0.207967	0.432362	1.439770
10	9	0	-0.037839	1.895216	-0.131574
11	9	0	-2.907932	-0.003759	-1.002672
12	9	0	-2.374954	-1.064255	0.809983

**Es'a'g**

Standard orientation:  
 Free Gibbs Energy (Hartree) = -1148.792795

Center Number	Atomic Number	Atomic Type	Coordinates (Angstroms)		
			X	Y	Z
1	6	0	1.500772	0.224555	-0.534985
2	1	0	1.372075	0.318041	-1.610257
3	6	0	0.171973	0.515264	0.163015
4	6	0	-2.064911	-0.142512	0.136663
5	1	0	-2.102834	0.449488	1.047081
6	8	0	-0.765894	-0.352980	-0.316831
7	9	0	2.407288	1.137851	-0.100970
8	17	0	2.052357	-1.399617	-0.167157
9	9	0	0.291927	0.420781	1.502550
10	9	0	-0.178100	1.798113	-0.094732
11	9	0	-2.770753	0.466028	-0.830726
12	9	0	-2.603603	-1.348778	0.340691

**Esag'**

Standard orientation:  
 Free Gibbs Energy (Hartree) = -1148.792552

Center Number	Atomic Number	Atomic Type	Coordinates (Angstroms)		
			X	Y	Z
1	6	0	1.354135	0.387545	-0.589719
2	1	0	1.249949	0.201450	-1.655604
3	6	0	0.153145	-0.205302	0.148901
4	6	0	-2.177315	-0.066060	0.152969
5	1	0	-2.067258	-0.586544	1.100474
6	8	0	-0.966859	0.401381	-0.350305
7	9	0	1.382051	1.724314	-0.358349
8	17	0	2.841156	-0.356401	-0.026037
9	9	0	0.108099	-1.541037	-0.048862
10	9	0	0.253428	-0.013900	1.479718
11	9	0	-2.974463	0.997506	0.293831
12	9	0	-2.738811	-0.885129	-0.752194

**Es'a'g'**

Standard orientation:  
 Free Gibbs Energy (Hartree) = -1148.792553

Center Number	Atomic Number	Atomic Type	Coordinates (Angstroms)		
			X	Y	Z
1	6	0	1.357959	0.366116	-0.612400
2	1	0	1.319671	0.149492	-1.676971
3	6	0	0.158389	-0.280363	0.082091
4	6	0	-2.172736	-0.170985	0.072421
5	1	0	-2.069364	-1.051478	0.700980
6	8	0	-0.968929	0.226112	-0.503419
7	9	0	1.294530	1.706860	-0.414982
8	17	0	2.856165	-0.272325	0.043647
9	9	0	0.212315	-1.624086	-0.073881
10	9	0	0.169348	-0.044720	1.407252
11	9	0	-2.667216	0.846481	0.793204
12	9	0	-3.021794	-0.414089	-0.932851

**Es'a'a'**

Standard orientation:  
 Free Gibbs Energy (Hartree) = -1148.792488

Center Number	Atomic Number	Atomic Type	Coordinates (Angstroms)		
			X	Y	Z
1	6	0	-1.633563	0.419341	0.004013
2	1	0	-2.278489	0.869888	0.754889
3	6	0	-0.185984	0.503600	0.486337
4	6	0	1.995659	-0.084504	-0.073623
5	1	0	2.241589	0.622719	0.714072
6	8	0	0.650464	-0.050984	-0.429968
7	9	0	-1.740365	1.108058	-1.160500
8	17	0	-2.115808	-1.251377	-0.224158
9	9	0	0.116407	1.811809	0.691107
10	9	0	-0.077346	-0.094640	1.693907
11	9	0	2.311105	-1.328840	0.319551
12	9	0	2.695227	0.187842	-1.179497

**Esaa**

Standard orientation:

Free Gibbs Energy (Hartree) = -1148.792427

Center Number	Atomic Number	Atomic Type	Coordinates (Angstroms)		
			X	Y	Z
1	6	0	-1.599792	0.487120	-0.070567
2	1	0	-2.226272	1.084555	0.587721
3	6	0	-0.176640	0.473714	0.485432
4	6	0	1.982069	-0.271828	0.036645
5	1	0	2.159402	0.062788	1.055377
6	8	0	0.631423	-0.285383	-0.300404
7	9	0	-1.573747	1.046846	-1.306181
8	17	0	-2.253037	-1.139251	-0.147192
9	9	0	0.266720	1.752239	0.558598
10	9	0	-0.200275	0.015960	1.760550
11	9	0	2.433503	-1.519305	-0.128895
12	9	0	2.638610	0.523033	-0.822589

**Es'g'g'**

Standard orientation:

Free Gibbs Energy (Hartree) = -1148.790414

Center Number	Atomic Number	Atomic Type	Coordinates (Angstroms)		
			X	Y	Z
1	6	0	-1.090682	-0.552274	-0.402712
2	1	0	-1.075599	-0.768339	-1.467771
3	6	0	-0.234305	0.688436	-0.123072
4	6	0	1.933326	-0.227435	0.201011
5	1	0	1.513551	-0.534400	1.152738
6	8	0	1.061213	0.534344	-0.565564
7	9	0	-0.542135	-1.600048	0.279657
8	17	0	-2.748731	-0.306494	0.109168
9	9	0	-0.732335	1.721131	-0.806646
10	9	0	-0.260163	0.985255	1.190931
11	9	0	2.293265	-1.306218	-0.515045
12	9	0	3.035894	0.509438	0.399141

**Eg'gg**

Standard orientation:

Free Gibbs Energy (Hartree) = -1148.790265

Center Number	Atomic Number	Atomic Type	Coordinates (Angstroms)		
			X	Y	Z
1	6	0	-1.509275	0.082208	-0.464964
2	1	0	-1.585083	0.170655	-1.545825
3	6	0	-0.300151	-0.788561	-0.110872
4	6	0	1.779093	0.332265	0.133961
5	1	0	1.331502	0.851892	0.974614
6	8	0	0.845259	-0.288128	-0.686295
7	9	0	-2.630528	-0.495790	0.031647
8	17	0	-1.312178	1.696613	0.214547
9	9	0	-0.182846	-0.916141	1.222471
10	9	0	-0.510356	-2.009020	-0.626827
11	9	0	2.657603	-0.580959	0.585163
12	9	0	2.441743	1.189086	-0.649620

**Esga**

Standard orientation:  
 Free Gibbs Energ (Hartree) = -1148.790018

Center Number	Atomic Number	Atomic Type	Coordinates (Angstroms)		
			X	Y	Z
1	6	0	1.318727	0.065154	0.578502
2	1	0	2.123562	0.677365	0.977331
3	6	0	0.260439	0.972065	-0.064118
4	6	0	-1.698013	-0.343579	0.101438
5	1	0	-1.661335	-0.052924	1.146412
6	8	0	-0.778906	0.336918	-0.688140
7	9	0	0.725739	-0.618766	1.600708
8	17	0	1.976631	-1.051418	-0.597469
9	9	0	-0.199213	1.795073	0.913172
10	9	0	0.850780	1.726619	-0.993756
11	9	0	-2.907525	-0.083600	-0.411361
12	9	0	-1.483184	-1.664606	-0.015049

**Eg'g'g**

Standard orientation:  
 Free Gibbs Energy (Hartree) = -1148.789663

Center Number	Atomic Number	Atomic Type	Coordinates (Angstroms)		
			X	Y	Z
1	6	0	-1.150554	-0.132535	0.572762
2	1	0	-0.646158	-0.473057	1.471861
3	6	0	-0.216805	0.761695	-0.254381
4	6	0	1.987602	0.021076	0.165138
5	1	0	2.302123	0.980871	0.562761
6	8	0	0.914961	0.113594	-0.703663
7	9	0	-2.239553	0.606657	0.914469
8	17	0	-1.637055	-1.533397	-0.365729
9	9	0	-0.847282	1.215729	-1.334536
10	9	0	0.117128	1.827560	0.516340
11	9	0	1.681196	-0.798562	1.203504
12	9	0	2.969936	-0.545853	-0.531892

**Egg'a**

Standard orientation:  
 Free Gibbs Energy (Hartree) = -1148.789659

Center Number	Atomic Number	Atomic Type	Coordinates (Angstroms)		
			X	Y	Z
1	6	0	1.624323	-0.162124	-0.018011
2	1	0	2.376428	-0.674232	0.577287
3	6	0	0.274958	-0.878234	0.118078
4	6	0	-1.673716	0.468511	0.016888
5	1	0	-1.288567	0.983823	0.890340
6	8	0	-0.718022	-0.303785	-0.631075
7	9	0	1.985698	-0.172162	-1.323365
8	17	0	1.490649	1.497898	0.556607
9	9	0	0.438836	-2.134156	-0.323591
10	9	0	-0.048265	-0.939567	1.428334
11	9	0	-2.114996	1.344982	-0.889561
12	9	0	-2.709952	-0.311598	0.376732

**Egg'**

Standard orientation:

Free Gibbs Energy (Hartree) = -1148.789422

Center Number	Atomic Number	Atomic Type	Coordinates (Angstroms)		
			X	Y	Z
1	6	0	-0.993422	-0.642604	0.035019
2	1	0	-0.564055	-1.325488	-0.691381
3	6	0	-0.159819	0.644427	0.111096
4	6	0	2.074894	0.006520	-0.333049
5	1	0	2.156381	0.666047	-1.191328
6	8	0	1.119772	0.413347	0.580784
7	9	0	-0.985869	-1.218667	1.264087
8	17	0	-2.642053	-0.272921	-0.451654
9	9	0	-0.122325	1.210728	-1.117686
10	9	0	-0.711215	1.507738	0.960301
11	9	0	3.223418	-0.036606	0.339273
12	9	0	1.799822	-1.247385	-0.775291

**Eaaa**

Standard orientation:

Free Gibbs Energy (Hartree) = -1148.789353

Center Number	Atomic Number	Atomic Type	Coordinates (Angstroms)		
			X	Y	Z
1	6	0	-1.493005	0.397823	0.440318
2	1	0	-1.948931	0.322606	1.424701
3	6	0	-0.061811	-0.137775	0.519562
4	6	0	1.893670	-0.105677	-0.839101
5	1	0	2.119936	-0.354185	-1.870405
6	8	0	0.512808	-0.088132	-0.724290
7	9	0	-1.446293	1.699396	0.058402
8	17	0	-2.452010	-0.536634	-0.695606
9	9	0	0.613510	0.601813	1.421176
10	9	0	-0.096550	-1.399205	0.991981
11	9	0	2.413499	1.096677	-0.537087
12	9	0	2.446674	-1.006105	-0.007733

**Eaag**

Standard orientation:

Free Gibbs Energy (Hartree) = -1148.789194

Center Number	Atomic Number	Atomic Type	Coordinates (Angstroms)		
			X	Y	Z
1	6	0	1.526015	0.299965	-0.428484
2	1	0	1.652138	0.473679	-1.494080
3	6	0	0.070698	0.569636	-0.034119
4	6	0	-2.025450	-0.488236	-0.461405
5	1	0	-2.542771	-0.857497	-1.340492
6	8	0	-0.724418	-0.208202	-0.847221
7	9	0	2.316490	1.153633	0.270892
8	17	0	1.966248	-1.361627	-0.069068
9	9	0	-0.132297	0.332972	1.267120
10	9	0	-0.181467	1.878145	-0.247417
11	9	0	-2.045523	-1.423826	0.503617
12	9	0	-2.642516	0.604510	0.020292

**Ea'a'g'**

Standard orientation:  
 Free Gibbs Energy (Hartree) = -1148.789031

Center Number	Atomic Number	Atomic Type	Coordinates (Angstroms)		
			X	Y	Z
1	6	0	1.370581	0.409306	-0.549884
2	1	0	1.494261	0.300283	-1.624328
3	6	0	0.073655	-0.277548	-0.111564
4	6	0	-2.247084	0.220506	-0.378759
5	1	0	-2.890034	0.494894	-1.208328
6	8	0	-0.941102	0.319875	-0.832199
7	9	0	1.288168	1.726546	-0.230445
8	17	0	2.749023	-0.320880	0.255867
9	9	0	0.146963	-1.588988	-0.408440
10	9	0	-0.111878	-0.166960	1.209151
11	9	0	-2.529798	-1.025376	0.040049
12	9	0	-2.459200	1.053358	0.654325

**Eag'g**

Standard orientation:  
 Free Gibbs Energy (Hartree) = -1148.788386

Center Number	Atomic Number	Atomic Type	Coordinates (Angstroms)		
			X	Y	Z
1	6	0	-1.115640	-0.036098	0.605499
2	1	0	-0.650160	-0.557603	1.435000
3	6	0	-0.049688	0.664093	-0.251349
4	6	0	1.884811	-0.748064	-0.241910
5	1	0	2.253621	-1.570685	-0.844574
6	8	0	0.801106	-0.216514	-0.902681
7	9	0	-1.952798	0.921594	1.084735
8	17	0	-2.015448	-1.196265	-0.360431
9	9	0	-0.636549	1.377086	-1.212718
10	9	0	0.629600	1.507432	0.548296
11	9	0	2.856530	0.162159	-0.066804
12	9	0	1.540263	-1.199682	0.989260

**Eg'ga**

Standard orientation:  
 Free Gibbs Energy (Hartree) = -1148.788315

Center Number	Atomic Number	Atomic Type	Coordinates (Angstroms)		
			X	Y	Z
1	6	0	1.312261	0.142436	0.555269
2	1	0	2.173705	0.783286	0.723426
3	6	0	0.300996	0.900453	-0.320771
4	6	0	-1.517095	-0.598117	0.029000
5	1	0	-0.925898	-1.307281	0.600051
6	8	0	-0.756224	0.192780	-0.826186
7	9	0	0.736834	-0.159911	1.754325
8	17	0	1.847900	-1.327506	-0.242991
9	9	0	-0.123425	1.959665	0.399997
10	9	0	0.962405	1.371799	-1.387043
11	9	0	-2.227164	0.171689	0.872237
12	9	0	-2.369681	-1.245385	-0.768864

**Eagg'**

Standard orientation:  
 Free Gibbs Energy (Hartree) = -1148.787568

Center Number	Atomic Number	Atomic Type	Coordinates (Angstroms)		
			X	Y	Z
1	6	0	-0.762122	-0.606644	-0.162151
2	1	0	-0.218088	-0.994763	-1.018195
3	6	0	-0.115988	0.687921	0.354707
4	6	0	2.138044	-0.086302	0.052228
5	1	0	3.102109	0.126549	0.500270
6	8	0	1.184229	0.536021	0.822493
7	9	0	-0.750490	-1.516305	0.845211
8	17	0	-2.417429	-0.287837	-0.662597
9	9	0	-0.150949	1.613692	-0.619058
10	9	0	-0.796526	1.155894	1.401312
11	9	0	1.941455	-1.424212	0.014932
12	9	0	2.109715	0.337979	-1.227571

**Egg'a'**

Standard orientation:  
 Free Gibbs Energy (Hartree) = -1148.786243

Center Number	Atomic Number	Atomic Type	Coordinates (Angstroms)		
			X	Y	Z
1	6	0	1.413121	-0.041834	-0.386637
2	1	0	2.396715	-0.461975	-0.194331
3	6	0	0.362971	-0.945965	0.288847
4	6	0	-1.537614	0.398887	-0.254447
5	1	0	-0.970055	1.110342	-0.846376
6	8	0	-0.928133	-0.845620	-0.154567
7	9	0	1.173661	-0.039936	-1.725945
8	17	0	1.400943	1.607455	0.230908
9	9	0	0.722987	-2.213355	0.016750
10	9	0	0.444028	-0.781180	1.621583
11	9	0	-2.718268	0.159173	-0.829933
12	9	0	-1.761131	0.911224	0.969236

**Eg'gg'**

Standard orientation:  
 Free Gibbs Energy (Hartree) = -1148.786186

Center Number	Atomic Number	Atomic Type	Coordinates (Angstroms)		
			X	Y	Z
1	6	0	0.912187	0.629072	-0.147080
2	1	0	0.504535	1.048764	-1.063506
3	6	0	0.180232	-0.674073	0.213284
4	6	0	-1.900627	0.456224	-0.036548
5	1	0	-1.566215	1.470917	0.167630
6	8	0	-1.133713	-0.506100	0.597813
7	9	0	0.739308	1.515289	0.876999
8	17	0	2.617298	0.323398	-0.402101
9	9	0	0.250850	-1.491828	-0.855104
10	9	0	0.775585	-1.281695	1.240844
11	9	0	-1.905338	0.257724	-1.375214
12	9	0	-3.139675	0.285400	0.420380

**Egg'g**

Standard orientation:  
 Free Gibbs Energy (Hartree) = -1148.785920

Center Number	Atomic Number	Atomic Type	Coordinates (Angstroms)		
			X	Y	Z
1	6	0	-1.095954	0.098285	-0.602338
2	1	0	-0.574046	0.247704	-1.544429
3	6	0	-0.255366	-0.762862	0.355387
4	6	0	1.703347	0.491922	-0.145671
5	1	0	1.242034	1.429929	-0.448323
6	8	0	0.939321	-0.216645	0.767040
7	9	0	-2.255951	-0.560700	-0.841555
8	17	0	-1.434292	1.669726	0.117370
9	9	0	-0.945845	-0.012387	1.469037
10	9	0	-0.039667	-1.940783	-0.266692
11	9	0	2.860629	0.733061	0.467364
12	9	0	1.946195	-0.251845	-1.248502

**Eaga**

Standard orientation:  
 Free Gibbs Energy (Hartree) = -1148.785292

Center Number	Atomic Number	Atomic Type	Coordinates (Angstroms)		
			X	Y	Z
1	6	0	1.057884	0.120169	0.714660
2	1	0	1.741937	0.780576	1.242699
3	6	0	0.119315	1.000989	-0.124449
4	6	0	-1.663212	-0.556450	-0.639396
5	1	0	-2.355638	-0.652806	-1.468858
6	8	0	-0.731755	0.392705	-1.021351
7	9	0	0.337337	-0.591412	1.617816
8	17	0	2.002409	-0.947359	-0.309867
9	9	0	-0.567138	1.782738	0.733617
10	9	0	0.887250	1.803603	-0.875639
11	9	0	-1.077674	-1.744404	-0.401453
12	9	0	-2.319455	-0.200808	0.476748

**Ea'g'g'**

Standard orientation:  
 Free Gibbs Energy (Hartree) = -1148.784915

Center Number	Atomic Number	Atomic Type	Coordinates (Angstroms)		
			X	Y	Z
1	6	0	-0.808617	-0.576516	-0.342399
2	1	0	-0.641868	-0.833264	-1.385100
3	6	0	-0.183056	0.796593	-0.032129
4	6	0	2.130357	0.086160	-0.240012
5	1	0	3.054453	0.578280	-0.523661
6	8	0	1.113173	0.978662	-0.498452
7	9	0	-0.242465	-1.512845	0.459851
8	17	0	-2.541468	-0.527178	-0.044600
9	9	0	-0.883271	1.744420	-0.667137
10	9	0	-0.243873	1.036598	1.284288
11	9	0	2.173508	-0.279443	1.049579
12	9	0	1.979975	-1.038697	-0.977492

**Ea'g'a'**

Standard orientation:  
 Free Gibbs Energy (Hartree) = -1148.783418

Center Number	Atomic Number	Atomic Type	Coordinates (Angstroms)		
			X	Y	Z
1	6	0	-1.294652	0.332954	0.176751
2	1	0	-2.319363	0.166200	-0.146944
3	6	0	-0.501676	-0.944576	-0.159332
4	6	0	1.781070	-0.301710	0.371062
5	1	0	2.636673	-0.843072	0.760364
6	8	0	0.702099	-1.156570	0.477496
7	9	0	-1.272713	0.509610	1.522517
8	17	0	-0.704029	1.764290	-0.650263
9	9	0	-1.267023	-1.973248	0.252969
10	9	0	-0.376506	-1.045483	-1.492671
11	9	0	2.007637	0.071496	-0.900069
12	9	0	1.589264	0.817236	1.093942

**Eagg**

Standard orientation:  
 Free Gibbs Energy (Hartree) = -1148.782879

Center Number	Atomic Number	Atomic Type	Coordinates (Angstroms)		
			X	Y	Z
1	6	0	-1.056053	0.358690	-0.536428
2	1	0	-0.765957	0.437573	-1.580645
3	6	0	-0.416492	-0.904228	0.088410
4	6	0	1.926862	-0.346733	-0.261950
5	1	0	2.818498	-0.922605	-0.485234
6	8	0	0.864723	-1.216474	-0.346538
7	9	0	-2.406229	0.214020	-0.451681
8	17	0	-0.590194	1.829284	0.299415
9	9	0	-0.467240	-0.855399	1.425179
10	9	0	-1.145320	-1.955921	-0.310930
11	9	0	1.803515	0.652667	-1.167541
12	9	0	2.030504	0.219368	0.950299

**Iag**

Standard orientation:  
 Free Gibbs Energy (Hartree) = -1148.799883

Center Number	Atomic Number	Atomic Type	Coordinates (Angstroms)		
			X	Y	Z
1	6	0	-0.089969	0.246587	-0.205939
2	1	0	0.296773	0.039396	-1.201098
3	6	0	-1.395659	-0.525761	-0.023955
4	9	0	-1.927166	-0.328923	1.179324
5	9	0	-2.284156	-0.161691	-0.951043
6	9	0	-1.154698	-1.833352	-0.170402
7	17	0	-0.400228	1.982172	-0.085534
8	8	0	0.781493	-0.187418	0.803218
9	6	0	2.069384	-0.414319	0.395199
10	1	0	2.653524	-0.694663	1.264564
11	9	0	2.114373	-1.399827	-0.532866
12	9	0	2.595991	0.681421	-0.194676

**Iga**

Standard orientation:

Free Gibbs Energy (Hartree) = -1148.799253

Center Number	Atomic Number	Atomic Type	Coordinates (Angstroms)		
			X	Y	Z
1	6	0	-0.211771	0.223925	-0.334333
2	1	0	-0.030556	0.178297	-1.406538
3	6	0	-1.489066	-0.552510	-0.017919
4	9	0	-1.780343	-0.524619	1.278482
5	9	0	-2.515165	-0.039391	-0.700763
6	9	0	-1.335482	-1.825645	-0.392265
7	17	0	-0.435404	1.939431	0.091586
8	8	0	0.803153	-0.376018	0.401335
9	6	0	2.074309	0.048370	0.066875
10	1	0	2.215309	1.117729	0.211411
11	9	0	2.910970	-0.645516	0.837106
12	9	0	2.336804	-0.251154	-1.229255

**Ig'a**

Standard orientation:

Free Gibbs Energy (Hartree) = -1148.797772

Center Number	Atomic Number	Atomic Type	Coordinates (Angstroms)		
			X	Y	Z
1	6	0	-0.240217	0.209529	-0.389237
2	1	0	-0.127651	0.155691	-1.473084
3	6	0	-1.533831	-0.512235	-0.008890
4	9	0	-1.750485	-0.489677	1.300903
5	9	0	-2.573614	0.049443	-0.629152
6	9	0	-1.455591	-1.787970	-0.405529
7	17	0	-0.365922	1.924922	0.043329
8	8	0	0.787593	-0.445278	0.277991
9	6	0	2.028851	-0.341521	-0.314921
10	1	0	1.975383	-0.376594	-1.404266
11	9	0	2.638413	0.802936	0.052656
12	9	0	2.757207	-1.360863	0.147246

**Is'g'**

Standard orientation:

Free Gibbs Energy (Hartree) = -1148.795881

Center Number	Atomic Number	Atomic Type	Coordinates (Angstroms)		
			X	Y	Z
1	6	0	-0.416341	0.491188	-0.702818
2	1	0	-0.838338	0.657281	-1.689205
3	6	0	-1.236396	-0.616760	-0.028275
4	9	0	-0.871968	-0.818285	1.240629
5	9	0	-2.532239	-0.296230	-0.048882
6	9	0	-1.075988	-1.758146	-0.698777
7	17	0	-0.618875	1.998838	0.222258
8	8	0	0.914937	0.151922	-0.909464
9	6	0	1.711584	-0.071271	0.201423
10	1	0	1.349648	0.430436	1.094936
11	9	0	1.803825	-1.396100	0.431308
12	9	0	2.936034	0.368507	-0.116542

**Ia'g'**

Standard orientation:  
 Free Gibbs Energy (Hartree) = -1148.790664

Center Number	Atomic Number	Atomic Type	Coordinates (Angstroms)		
			X	Y	Z
1	6	0	0.419849	0.424075	0.766278
2	1	0	0.977343	0.452852	1.697672
3	6	0	1.021570	-0.722856	-0.059763
4	9	0	0.556498	-0.788131	-1.302210
5	9	0	2.348142	-0.554363	-0.116371
6	9	0	0.783080	-1.886725	0.552418
7	17	0	0.731986	1.963467	-0.059365
8	8	0	-0.911966	0.259924	1.160899
9	6	0	-1.923191	-0.022378	0.266342
10	1	0	-2.857082	0.148974	0.791876
11	9	0	-1.861842	0.743972	-0.836649
12	9	0	-1.867842	-1.307331	-0.142152

**Dag**

Standard orientation:  
 Free Gibbs Energy (Hartree) = -788.819857

Center Number	Atomic Number	Atomic Type	Coordinates (Angstroms)		
			X	Y	Z
1	6	0	0.102359	-0.420753	-0.248139
2	1	0	-0.267280	-0.151653	-1.236684
3	6	0	1.478986	0.203166	-0.024264
4	9	0	1.955575	-0.083075	1.183865
5	9	0	2.334977	-0.254839	-0.941165
6	9	0	1.395713	1.530251	-0.151218
7	8	0	-0.727160	0.035430	0.771809
8	6	0	-2.027015	0.272171	0.402961
9	1	0	-2.589881	0.533164	1.291860
10	9	0	-2.090915	1.279748	-0.499128
11	9	0	-2.566612	-0.809341	-0.198462
12	9	0	0.232202	-1.773016	-0.173113

**Dga**

Standard orientation:  
 Free Gibbs Energy (Hartree) = -788.818501

Center Number	Atomic Number	Atomic Type	Coordinates (Angstroms)		
			X	Y	Z
1	6	0	0.236492	0.499303	0.241313
2	1	0	0.053323	0.651926	1.304826
3	6	0	1.554991	-0.246714	0.042731
4	9	0	1.812499	-0.450570	-1.244788
5	9	0	2.550739	0.470692	0.570164
6	9	0	1.506905	-1.424752	0.667091
7	8	0	-0.749422	-0.253158	-0.367002
8	6	0	-2.036009	0.176188	-0.096139
9	1	0	-2.210081	1.209805	-0.387380
10	9	0	-2.847954	-0.640769	-0.764591
11	9	0	-2.296013	0.049348	1.227743
12	9	0	0.342634	1.728371	-0.356605

**Dg'a**

Standard orientation:

Free Gibbs Energy (Hartree) = -788.817401

Center Number	Atomic Number	Atomic Type	Coordinates (Angstroms)		
			X	Y	Z
1	6	0	-0.253162	0.433741	-0.366110
2	1	0	-0.140207	0.453485	-1.452993
3	6	0	-1.588856	-0.218112	-0.006336
4	9	0	-1.767198	-0.279032	1.307809
5	9	0	-2.587097	0.487153	-0.544010
6	9	0	-1.631911	-1.456375	-0.507566
7	8	0	0.738576	-0.300441	0.251628
8	6	0	1.990622	-0.182559	-0.318707
9	1	0	1.953667	-0.192967	-1.408984
10	9	0	2.588864	0.955354	0.083646
11	9	0	2.711711	-1.211452	0.130664
12	9	0	-0.271447	1.720417	0.084553

**Ds'g'**

Standard orientation:

Free Gibbs Energy (Hartree) = -788.815255

Center Number	Atomic Number	Atomic Type	Coordinates (Angstroms)		
			X	Y	Z
1	6	0	0.409973	0.859343	0.533083
2	1	0	0.819250	1.254582	1.459507
3	6	0	1.338264	-0.250984	0.020559
4	9	0	0.963397	-0.697532	-1.181373
5	9	0	2.581321	0.227366	-0.079786
6	9	0	1.343954	-1.271959	0.874998
7	8	0	-0.874056	0.442108	0.823129
8	6	0	-1.645039	-0.045352	-0.221223
9	1	0	-1.321519	0.308072	-1.195843
10	9	0	-1.629736	-1.392308	-0.198976
11	9	0	-2.901717	0.348337	0.021183
12	9	0	0.406729	1.844144	-0.418624

**Dgg'**

Standard orientation:

Free Gibbs Energy (Hartree) = -788.813402

Center Number	Atomic Number	Atomic Type	Coordinates (Angstroms)		
			X	Y	Z
1	6	0	-0.416271	0.546315	-0.805838
2	1	0	-0.838916	0.581751	-1.807296
3	6	0	-1.344187	-0.299384	0.080428
4	9	0	-1.034598	-0.199771	1.376524
5	9	0	-2.602262	0.110308	-0.081163
6	9	0	-1.268428	-1.587133	-0.271995
7	8	0	0.862385	0.043999	-0.955581
8	6	0	1.592277	-0.310892	0.170605
9	1	0	1.080047	-1.019842	0.815357
10	9	0	2.717795	-0.856238	-0.300971
11	9	0	1.919825	0.779809	0.887350
12	9	0	-0.413568	1.805232	-0.280254

**Da'g'**

Standard orientation:  
 Free Gibbs Energy (Hartree) = -788.811079

Center Number	Atomic Number	Atomic Type	Coordinates (Angstroms)		
			X	Y	Z
1	6	0	0.359030	0.793841	0.682728
2	1	0	0.901782	1.050415	1.589858
3	6	0	1.180013	-0.274571	-0.057472
4	9	0	0.720261	-0.542214	-1.273747
5	9	0	2.433248	0.183764	-0.176685
6	9	0	1.217156	-1.400661	0.657503
7	8	0	-0.905921	0.416100	1.118639
8	6	0	-1.842050	-0.126938	0.261788
9	1	0	-2.797065	-0.084507	0.774925
10	9	0	-1.909441	0.539873	-0.903203
11	9	0	-1.545916	-1.410556	-0.029297
12	9	0	0.302547	1.891049	-0.123032

**Sgg**

Standard orientation:  
 Free Gibbs Energy (Hartree) = -927.165191

Center Number	Atomic Number	Atomic Type	Coordinates (Angstroms)		
			X	Y	Z
1	6	0	0.138325	0.066696	-0.212311
2	1	0	0.521900	0.150787	-1.231005
3	6	0	-0.245030	-1.398367	-0.006157
4	9	0	-0.639684	-1.640512	1.242436
5	9	0	-1.232524	-1.752566	-0.837083
6	9	0	0.812346	-2.170512	-0.266331
7	8	0	1.110128	0.378833	0.754759
8	6	0	2.208851	1.070400	0.253962
9	1	0	2.821078	1.329627	1.111169
10	9	0	2.939831	0.254113	-0.583006
11	6	0	-1.036331	1.036857	-0.079454
12	9	0	-0.572861	2.294045	-0.187497
13	9	0	-1.656740	0.931034	1.092915
14	9	0	-1.931324	0.850408	-1.053266
15	1	0	1.909712	1.941301	-0.327974

**Ssg**

Standard orientation:  
 Free Gibbs Energy (Hartree) = -927.158997

Center Number	Atomic Number	Atomic Type	Coordinates (Angstroms)		
			X	Y	Z
1	6	0	0.187479	-0.004332	-0.701369
2	1	0	0.471437	-0.361067	-1.691419
3	6	0	1.508731	0.317814	0.010601
4	9	0	1.346156	0.640598	1.301716
5	9	0	2.346371	-0.720124	-0.050667
6	9	0	2.091162	1.356352	-0.594502
7	8	0	-0.575072	1.152479	-0.925848
8	6	0	-1.247852	1.753001	0.143547
9	1	0	-1.357387	2.798307	-0.127166
10	9	0	-2.506553	1.215706	0.269894
11	6	0	-0.592407	-1.157412	-0.058143
12	9	0	0.150779	-2.271232	-0.065742
13	9	0	-0.942113	-0.907283	1.207387
14	9	0	-1.698709	-1.395103	-0.760639
15	1	0	-0.733020	1.618271	1.090525

**Mgaa**

Standard orientation:

Free Gibbs Energy (Hartree) = -1310.466432

Center Number	Atomic Number	Atomic Type	Coordinates (Angstroms)		
			X	Y	Z
1	6	0	-0.845395	-0.000000	0.472341
2	1	0	-1.120270	0.000001	1.522287
3	6	0	0.681512	0.000001	0.382291
4	8	0	1.094003	-0.000000	-0.891801
5	6	0	2.522663	-0.000001	-1.062281
6	1	0	2.956013	-0.893505	-0.619784
7	1	0	2.679107	-0.000000	-2.134358
8	1	0	2.956015	0.893500	-0.619782
9	17	0	-1.500971	-1.458371	-0.267193
10	17	0	-1.500974	1.458369	-0.267195
11	9	0	1.147637	1.081245	1.073139
12	9	0	1.147639	-1.081239	1.073143

**Mgag**

Standard orientation:

Free Gibbs Energy (Hartree) = -1310.466116

Center Number	Atomic Number	Atomic Type	Coordinates (Angstroms)		
			X	Y	Z
1	6	0	-0.736649	0.107999	-0.516555
2	1	0	-0.708058	0.115244	-1.601124
3	6	0	0.644222	-0.306917	-0.001786
4	8	0	1.555690	0.556765	-0.489185
5	6	0	2.908404	0.299593	-0.067066
6	1	0	3.219194	-0.695951	-0.374715
7	1	0	3.508832	1.050158	-0.567206
8	1	0	2.992984	0.408627	1.011039
9	17	0	-1.128616	1.734532	0.036717
10	17	0	-1.954959	-1.056747	-0.001984
11	9	0	0.663698	-0.360376	1.352093
12	9	0	0.898439	-1.579468	-0.422375

**Mgg'g**

Standard orientation:

Free Gibbs Energy (Hartree) = -1310.461402

Center Number	Atomic Number	Atomic Type	Coordinates (Angstroms)		
			X	Y	Z
1	6	0	-0.498458	0.202629	-0.451891
2	1	0	-0.218974	0.312053	-1.494563
3	6	0	0.617033	-0.547061	0.298400
4	8	0	1.788909	0.126956	0.396134
5	6	0	2.368793	0.535049	-0.848338
6	1	0	1.826450	1.383687	-1.265178
7	1	0	3.381331	0.839789	-0.609398
8	1	0	2.394168	-0.292812	-1.554831
9	17	0	-0.700558	1.815918	0.232121
10	17	0	-1.999517	-0.718047	-0.404620
11	9	0	0.235398	-0.830902	1.547279
12	9	0	0.796027	-1.731972	-0.358573

**Mgga**  
Standard orientation:  
Free Gibbs Energy (Hartree) = -1310.460963

Center Number	Atomic Number	Atomic Type	Coordinates (Angstroms)		
			X	Y	Z
1	6	0	0.633429	-0.145761	-0.582698
2	1	0	0.833704	-0.400568	-1.618280
3	6	0	-0.894532	-0.243180	-0.369480
4	8	0	-1.361918	-0.322401	0.891400
5	6	0	-1.093570	0.791174	1.757176
6	1	0	-1.317518	1.731255	1.258260
7	1	0	-1.756329	0.653273	2.604230
8	1	0	-0.058047	0.775535	2.089052
9	17	0	1.448642	-1.327156	0.438336
10	17	0	1.261422	1.485994	-0.319595
11	9	0	-1.463408	0.790516	-1.051290
12	9	0	-1.286539	-1.378730	-0.983492

**Table S1.** Weighted dipole moment (Db), blood-gas partition coefficient ( $K_{bg}$ ), and MAC(%) for the studied fluorinated anaesthetics.

Molecule	Dipole moment	$K_{bg}$	MAC (%)
Halothane	1.49	2.40	0.74
Enflurane	1.51	1.90	1.58
Isoflurane	1.93	1.40	1.15
Sevoflurane	2.56	0.65	2.00
Desflurane	1.97	0.45	5.80
Methoxyflurane	2.04	12.00	0.20

**Table S2.** Conformational Gibbs free energies (in kcal mol<sup>-1</sup>) and population (%), in parenthesis, molecular dipole moments ( $\mu$ , in Db), bond lengths (in Å), and dihedral angles (degrees) obtained for the main conformers of the studied fluorinated anesthetics.<sup>a</sup>

C $\phi_1\phi_2\phi_3$	G <sup>0</sup> <sub>rel</sub> (%)	$\mu$	O–C <sub>1</sub>	C <sub>2</sub> –O	C <sub>1</sub> –Fatorial	C <sub>2</sub> –R <sup>2</sup>	$\Phi_1$	$\Phi_2$	$\Phi_3$
<b>H</b>	--(100)	1.49	-	-	-	-	-	-	58.29
<b>Esag</b>	0.0(21)	1.26	1.39	1.36	1.34	1.36	17.26	176.77	56.14
<b>Es'a'g</b>	0.1(19)	0.45	1.39	1.37	1.34	1.35	340.46	185.33	57.62
<b>Esag'</b>	0.2(14)	1.06	1.39	1.37	1.34	1.35	20.12	176.57	300.55
<b>Es'a'g'</b>	0.2(14)	1.81	1.39	1.37	1.34	1.35	342.37	184.84	301.67
<b>Es'a'a'</b>	0.3(13)	2.37	1.39	1.36	1.34	1.36	340.40	182.66	180.03
<b>Esaa</b>	0.3(13)	2.51	1.39	1.36	1.34	1.36	19.33	174.25	178.90
<b>Es'g'g'</b>	1.6(2)	1.48	1.39	1.38	1.34	1.35	353.25	282.10	302.91
<b>Eg'gg</b>	1.6(1)	1.78	1.39	1.38	1.35	1.35	327.29	107.34	55.14
<b>Ega</b>	1.8(1)	2.52	1.39	1.37	1.34	1.36	17.39	69.43	175.99
<b>Eg'g'g</b>	2.0(1)	2.06	1.38	1.38	1.36	1.36	306.15	276.46	62.44
<b>Egg'a</b>	2.0(1)	2.97	1.39	1.37	1.35	1.35	31.72	255.70	180.00
<b>Egg'</b>	2.2(0)	2.39	1.38	1.39	1.36	1.35	53.48	84.38	295.59
<b>Eaaa</b>	2.2(0)	1.11	1.39	1.37	1.34	1.35	163.58	159.42	178.13
<b>Eaag</b>	2.3(0)	3.25	1.39	1.38	1.34	1.35	164.43	160.17	54.65
<b>Ea'a'g'</b>	2.4(0)	2.95	1.39	1.38	1.34	1.35	195.91	199.90	302.19
<b>Eag'g</b>	2.8(0)	2.78	1.38	1.39	1.36	1.35	166.53	277.08	66.14
<b>Eg'ga</b>	2.9(0)	2.74	1.39	1.37	1.34	1.35	306.06	49.93	169.72
<b>Eagg'</b>	3.3(0)	2.28	1.37	1.39	1.35	1.34	166.27	51.31	297.27
<b>Egg'a'</b>	4.2(0)	2.69	1.39	1.37	1.35	1.35	53.86	309.42	199.45
<b>Eg'gg'</b>	4.2(0)	2.45	1.38	1.38	1.35	1.35	293.20	37.14	291.53
<b>Egg'g</b>	4.4(0)	2.77	1.39	1.38	1.35	1.35	68.27	320.62	64.09
<b>Eaga</b>	4.8(0)	0.80	1.38	1.38	1.35	1.35	164.80	58.03	171.75
<b>Ea'g'g'</b>	5.0(0)	2.46	1.38	1.39	1.35	1.34	192.38	308.32	313.10
<b>Ea'g'a'</b>	5.9(0)	0.57	1.38	1.38	1.35	1.35	193.94	299.14	198.47
<b>Eagg</b>	6.3(0)	2.84	1.38	1.39	1.35	1.34	168.88	56.53	36.67
<b>Iag</b>	0.0(61)	1.72	1.37	1.40	1.35	1.77	177.22	136.85	58.40
<b>Iga</b>	0.4(31)	2.11	1.38	1.39	1.36	1.78	60.05	169.45	59.41
<b>Ig'a</b>	1.3(7)	2.91	1.38	1.39	1.35	1.77	322.35	154.39	59.46
<b>Is'g'</b>	2.5(1)	1.84	1.39	1.39	1.35	1.78	335.79	295.71	68.55
<b>Ia'g'</b>	5.8(0)	2.48	1.38	1.40	1.35	1.77	193.80	306.44	72.24
<b>Dag</b>	0.0(76)	1.89	1.37	1.39	1.35	1.36	174.93	143.71	56.48
<b>Dga</b>	0.9(18)	2.02	1.38	1.38	1.36	1.37	57.98	170.26	57.35
<b>Dg'a</b>	1.5(5)	3.13	1.38	1.38	1.35	1.36	318.43	157.60	57.24
<b>Ds'g'</b>	2.9(1)	1.59	1.39	1.38	1.35	1.37	336.92	296.68	67.23
<b>Dgg'</b>	4.1(0)	1.86	1.39	1.38	1.35	1.36	54.79	309.10	73.28
<b>Da'g'</b>	5.5(0)	2.61	1.38	1.39	1.35	1.36	194.64	306.13	71.52
<b>Sgg</b>	0.0(100)	2.56	1.39	1.41	1.38	1.53	51.09	133.73	54.89
<b>Sgg'</b>	3.9(0)	1.71	1.40	1.40	1.37	1.54	30.89	285.23	72.63
<b>Mgaa</b>	0.00(58)	1.62	1.44	1.34	-	1.37	61.22	180.00	180.00
<b>Mgag</b>	0.20(42)	2.62	1.44	1.35	-	1.36	59.25	179.07	57.60
<b>Mgg'g</b>	3.16(0)	3.60	1.43	1.36	-	1.37	74.78	303.19	66.44
<b>Mgga</b>	3.43(0)	1.73	1.44	1.35	-	1.36	46.81	62.13	162.67

**Table S3.** Important electron delocalization interactions obtained through NBO analysis (in kcal mol<sup>-1</sup>) in the gas phase at the B3LYP/aug-cc-pVTZ level.

	C <sub>Φ</sub>  Φ <sub>2</sub> Φ <sub>3</sub>	σ <sub>C3H→ σ<sup>*</sup><sub>C4F</sub></sub>	σ <sub>C3F/Cl→ σ<sup>*</sup><sub>C4F</sub></sub>	σ <sub>C3F/Cl→ σ<sup>*</sup><sub>C4X</sub></sub>	σ <sub>C3O→ σ<sup>*</sup><sub>C4F</sub></sub>	σ <sub>C4H→ σ<sup>*</sup><sub>C3F</sub></sub>	σ <sub>C4H→ σ<sup>*</sup><sub>C3O</sub></sub>	σ <sub>C4F→ σ<sup>*</sup><sub>C3F/Cl</sub></sub>	σ <sub>C4F→ σ<sup>*</sup><sub>C3O</sub></sub>	σ <sub>C4X→ σ<sup>*</sup><sub>C3F</sub></sub>	σ <sub>C4X→ σ<sup>*</sup><sub>C3O</sub></sub>
<b>H</b>	-	1.57	1.75	-	3.80	-	2.39	-	3.01	-	
<b>Esag</b>	-	-	1.26	0.93	3.79	-	-	1.25	2.59	-	
<b>Es'a'g</b>	-	-	1.26	0.93	3.79	-	-	1.26	2.59	-	
<b>Esag'</b>	-	0.91	-	-	3.79	-	1.30	-	-	2.37	
<b>Es'a'g'</b>	-	0.91	-	-	3.79	-	1.31	-	-	2.38	
<b>Es'a'a'</b>	-	0.93	1.28	-	-	3.34	1.30	-	2.59	-	
<b>Esaa</b>	-	0.94	1.27	-	-	3.35	1.29	-	2.60	-	
<b>Es'g'g'</b>	-	0.99	-	-	3.46	-	1.16	-	-	2.29	
<b>Eg'gg</b>	-	-	1.29	0.99	3.55	-	-	1.09	2.41		
<b>Esga</b>	-	1.00	1.35	-	-	3.43	1.14	-	2.33	-	
<b>Eg'g'g</b>	-	-	1.30	0.86	3.34	-	-	1.23	2.46	-	
<b>Egg'a</b>	-	0.96	1.29	-	-	3.23	1.17	-	2.35	-	
<b>Iag</b>	3.29	2.28	-	1.24	-	-	1.42	0.97	-	-	
<b>Iga</b>	3.23	2.29	-	1.18	-	-	1.47	0.93	-	-	
<b>Ig'a</b>	3.24	2.29	-	1.16	-	-	1.43	0.93	-	-	
<b>Is'g'</b>	3.67	2.42	-	0.89	-	-	1.37	1.14	-	-	
<b>Dag</b>	2.99	1.03	-	1.12	-	-	0.76	0.71	-	-	
<b>Dga</b>	2.94	1.02	-	1.08	-	-	0.79	0.70	-	-	
<b>Dg'a</b>	2.95	1.02	-	1.06	-	-	0.77	0.69	-	-	
<b>Ds'g'</b>	3.33	1.11	-	0.83	-	-	0.73	0.85	-	-	
<b>Sgg</b>	7.66	-	-	2.44	-	-	-	1.74	-	-	
<b>Mgaa</b>	-	-	3.40	-	-	3.46	-	-	5.22	-	
<b>Mgag</b>	-	-	1.66	-	4.09	-	-	-	2.62	2.26	